ERDC/CHL TR-09-8

Coastal and Hydraulics Laboratory

US Army Corps
of Engineers®
Engineer Research and
Development Center

Coastal Inlets Research Program

Barrier Island Migration Over a Consolidating Substrate

Julie Dean Rosati

September 2009

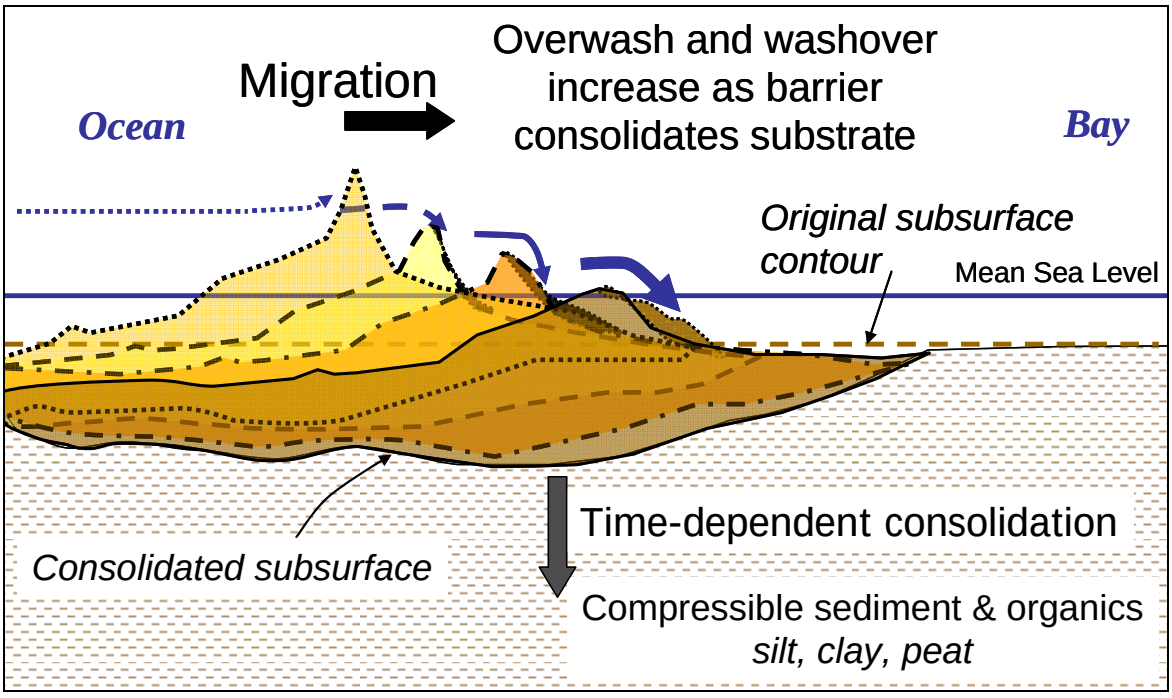

Approved for public release; distribution is unlimited.

Coastal Inlets Research Program

ERDC/CHL TR-09-8
September 2009

Barrier Islaind Migration Over a Consolidating Substrate

Julie Dean Rosati

U.S. Army Engineer Research and Development Center
Coastal and Hydraulics Laboratory
3909 Halls Ferry Road
Vicksburg, MS 39180-6199

Final Report
Approved for public release; distribution is unlimited.

Prepared for U.S. Army Corps of Engineers
Washington, DC 20314-1000

Monitored by Coastal and Hydraulics Laboratory
U.S. Army Engineer Research and Development Center
3909 Halls Ferry Road, Vicksburg, MS 39180-6199

Abstract: Barrier islands that overlie a compressible substrate load and consolidate the underlying subsurface. Through time, the elevation and aerial extent of these islands are reduced, making them more susceptible to inundation and overwash. Sand washed over the island and onto back-barrier marsh or into the bay or estuary begins the consolidation process on a previously non-loaded substrate, with time-dependent consolidation a function of the magnitude of the load, duration of load, and characteristics of the substrate. The result is an increase in the overwash, migration, breaching, and segmentation of these islands.

This research determined the degree to which consolidation affects the evolution of barrier island systems overlying a poorly-consolidated substrate, both for natural islands and those that have been restored with an infusion of sand from an external source. A two-dimensional (cross-shore) mathematical model was developed, tested with field data, and then applied to evaluate how a compressible substrate modifies long-term barrier island evolution. The model spans time durations of years to decades and represents cross-shore evolution of a sandy barrier island due to erosion, runup, overwash, migration, and time-dependent consolidation of the underlying substrate due to loading by the island. The implications of two strategies for restoring these islands (a one-time "Initial" large-scale infusion of sand from an external source versus traditional "Incremental" beach nourishment and subsequent smaller maintenance volumes) were tested.

Barrier islands overlying a compressible substrate are more likely to have reduced dune elevations due to consolidation, incur overall volumetric adjustment of the profile to fill in compressed regions outside the immediate footprint of the island, and experience increased overwash and migration when the dune reaches a critical elevation with respect to the prevalent storm conditions. Initial large-scale infusion of sand from an external source decreased the cross-shore migration rate, consolidation rate, and rate of dune lowering for barrier islands overlying a compressible substrate as compared to the Incremental restoration. The reduction in the migration and consolidation processes for the Initial Method resulted in more stability of the island as compared to the Incremental Method.

DISCLAIMER: The contents of this report are not to be used for advertising, publication, or promotional purposes. Citation of trade names does not constitute an official endorsement or approval of the use of such commercial products. All product names and trademarks cited are the property of their respective owners. The findings of this report are not to be construed as an official Department of the Army position unless so designated by other authorized documents.

DESTROY THIS REPORT WHEN NO LONGER NEEDED. DO NOT RETURN IT TO THE ORIGINATOR.

Contents

Contents ... iii

Figures and Tables ... v

Preface ... ix

1 Introduction and Significance ... 1

Forcing processes ... 1
Statement of problem ... 3
Research plan ... 4
Objectives of this research and hypotheses ... 6
Overview ... 6

2 Barrier Island Morphologic Evolution ... 7

Introduction ... 7
Review of literature ... 10
Overview ... *10*
Previous summaries ... *10*
NGOM literature ... 14
Synthesis ... *23*
Conceptual model of barrier island evolution ... 25
Implications for coastal restoration and engineering design ... 32
Conclusions ... 35

3 Review: Barrier Island Modeling and Consolidation ... 37

Overview ... 37
Previous studies ... 38
Modeling ... *38*
Consolidation ... *45*
Conclusions ... 55

4 Development of 2D Numerical Model ... 57

Purpose and scope ... 57
Theory ... 58
Wave transformation ... *58*
Erosion ... *59*
Runup overwash and inundation overwash ... *62*
Consolidation ... *64*
Bay processes ... *71*
Sensitivity analysis ... 71
Overview ... *71*
Discussion ... *82*
Comparison, calibration, and validation ... 86
Overview ... *86*

Data from Virginia (Gayes 1983) *87*
Implications of a consolidating substrate 99
Conclusions 100

5 Long-Term Processes in Barrier Island Evolution 101
Overview 101
Theory and conceptual development of sub-modules 102
Gradient in longshore sand transport *102*
Post-storm recovery *103*
Wind-blown (eolian) sand transport *106*
Erosion of fine-grained sediment *109*
Regional sources and sinks of sand *113*
Data 122
Overview *122*
Fine-grained sediment erosion *130*
Regional sources and sinks *131*
Conclusions 135

6 Evaluation of Hypotheses 137
Introduction 137
Hypothesis 1 137
Overview *137*
Analysis *138*
Hypothesis 2 143
Overview *143*
Analysis *144*
Hypothesis 3 147
Overview *147*
Analysis *152*
Implications for functional restoration in deltaic environments 163
Summary 166

7 Conclusions 168

References 172

Appendix A: Selected Figures From 2D MCO Sensitivity Analysis With Triangular Barrier Island 185

Appendix B: Barrier Island Consolidation Data From Virginia 198

Appendix C: Data Needs and Recommendations for Future Research 201

Report Documentation Page

Figures and Tables

Figures

Figure 1. Consequence of consolidation on barrier island migration and overwash. 3
Figure 2. Temporal and spatial scales associated with 2D MCO and sub-modules (modified from Larson and Kraus 1995). 5
Figure 3. Location map for studies reviewed in literature summary. 7
Figure 4. Conceptual model of barrier island evolution (Continued). 28
Figure 4. (Concluded). 29
Figure 5. Conceptual designs of barrier island restoration. 34
Figure 6. Regional design providing future sources of sediment for migrating barrier island. 35
Figure 7. Bruun Rule modified for barrier island migration due to sea level rise (adapted from Dean and Maurmeyer 1983; Dean et al. 2002). 39
Figure 8. Definition of soil settlement and consolidation regimes. 46
Figure 9. Location map for Virginia barrier island data (from Gayes 1983). 50
Figure 10. Assawoman Island, VA, Cross-Section #1 (adapted from Gayes 1983). 51
Figure 11. Assawoman Island, VA, Cross-Section #2 (adapted from Gayes 1983). 52
Figure 12. Metomkin Island, VA (adapted from Gayes 1983). 53
Figure 13. Wallops Island, VA (adapted from Gayes 1983). 54
Figure 14. Hypothesis about deformation of bay prodelta muds in Louisiana (Kuecher 1994) 55
Figure 15. Flowchart for 2D MCO Model. 58
Figure 16. Terminology for erosion and overwash calculations. 60
Figure 17. Parameters associated with consolidation testing 66
Figure 18. Example consolidation test from sediment sample taken at Chaland Headland, LA. 67
Figure 19. Definition sketch for consolidation relationship. 68
Figure 20. 2D MCO consolidation routine. 70
Figure 21. Comparison of consolidation routine (shown in (a)) to calculations from Blum et al. (2008) (reproduced in (b) and (c), their Figure 3b and c). 71
Figure 22. 2D MCO hydrodynamic and morphologic change summary (Table 6, Analysis 2c). 78
Figure 23. 2D MCO erosion and overwash summary (Table 6, Analysis 2c) 79
Figure 24. 2D MCO profile and consolidated subsurface (Table 6, Analysis 2c). 80
Figure 25. 2D MCO volume change summary (Table 6, Analysis 2c). 81
Figure 26. Sensitivity Analysis 1 (Table 6) 83
Figure 27. Sensitivity Analysis 6 (Table 6). 84
Figure 28. Sensitivity Analysis 7 (Table 6) 85

Figure 29. 2D MCO comparison with Assawoman 1, VA, for 150-year simulation: Evolution of profile (top) and consolidation magnitude (bottom). 93
Figure 30. 2D MCO comparison with Assawoman 1, VA: Profiles (top) and consolidation magnitude (bottom) after 150 year simulation. 94
Figure 31. 2D MCO comparison with Assawoman 2, VA, for 150-year simulation: Evolution of profile (top) and consolidation magnitude (bottom). 95
Figure 32. 2D MCO comparison with Assawoman 2, VA: Profiles (top) and consolidation magnitude (bottom) after 150 year simulation. 96
Figure 33. 2D MCO comparison with Metomkin, VA, for 150-year simulation: Evolution of profile (top) and consolidation magnitude (bottom). 97
Figure 34. 2D MCO comparison with Metomkin, VA: Profiles (top) and consolidation magnitude (bottom) after 150 year simulation. 98
Figure 35. Comparison of consolidating and non-consolidating substrate (Sensitivity Analyses 2 and 3). 99
Figure 36. Definition of terms for incorporating a gradient in LST. 103
Figure 37. Plot of Equation 28 for initial V_b = 100 m^3/m and various k_1 values. 105
Figure 38. Recovery and eolian transport sub-modules. 107
Figure 39. Example application of eolian transport sub-module. 109
Figure 40. Characterization of stratigraphy for deltaic barrier islands in Louisiana. 111
Figure 41. Pre-(top) and post-(bottom) Hurricane Katrina images of Chandeleur Islands, LA, showing removal of sand beach, followed by exposure and erosion of back-barrier marsh sediment (USGS 2007). 112
Figure 42. Example application of fine-grained sediment erosion sub-module. 114
Figure 43. Terminology used in development of regional sources and sinks of sand sub-module. 116
Figure 44. Influence of bay area on barrier island and delta volumes (Test 1). 121
Figure 45. Infilling bay (area decreasing at 0.02 percent/year) with and without dredged channel and placement of dredged sand on adjacent islands (Test 2). 122
Figure 46. Location of data sets. 123
Figure 47. Example of rapid dune growth and migration gulfward (Profile H, adapted from Ritchie and Penland 1988, p. 116). 124
Figure 48. Example of continuously accreting dune ridge (Profile I, adapted from Ritchie and Penland 1988, p. 118). 125
Figure 49. Retreating dune ridge (Profile G, adapted from Ritchie and Penland 1988, p. 115). 125
Figure 50. Dune erosion and recovery (Profile J, adapted from Ritchie and Penland 1988, p. 119). 126
Figure 51. Beach profile data and sand-mud interface for Trinity Island, Isle Dernieres (adapted from Dingler and Reiss 1989, 1990, and 1995). 128
Figure 52. Profile evolution from September 1988 to September 1990 showing erosion of berm and dune migration towards gulf. 128
Figure 53. Erosion of fine-grained sediment from November 1992 to November 1993. 130
Figure 54. Application of fine-grained sediment erosion sub-module with wave information for 2003 from sta CSI-5. 131
Figure 55. Location map for Barataria Bay, LA. 132

Figure 56. Coefficients for ebb delta volume and cross-sectional area relationships (Equations 48 and 51, respectively) derived for data from 1880s through 2000 for Barataria Bay Passes (ebb volumes from List et al. 1991, cross-sectional areas from FitzGerald et al. 2007). 134

Figure 57. Comparison of regional sub-module with measurements, Barataria Bay, LA (B= Barataria, C = Caminada, QB = Quatre Bayou, PA = Pass Abel). 135

Figure 58. Percentage of total barrier island sand consolidated. 139

Figure 59. Lifetime of BIC compared to BIS as function of initial fill volume. 145

Figure 60. Duration of simulation as function of initial dune crest elevation and substrate. 146

Figure 61. Influence of barrier island width on duration for BIC and BIS. 147

Figure 62. Duration of simulation as function of fill volumes, for incremental and initial methods of fill placement and various substrate characteristics. 153

Figure 63. Migration rates as function of fill volumes, for incremental and initial methods of fill placement and various substrate characteristics. 155

Figure 64. Consolidation rates as function of fill volumes, for incremental and initial methods of fill placement and various substrate characteristics. 156

Figure 65. Rate of dune lowering (due to consolidation, erosion, and overwash processes) as function of fill volumes, for incremental and initial methods of fill placement and various substrate characteristics. 156

Figure 66. Comparison of total cost for incremental and initial barrier island restoration projects, for various substrate conditions. 162

Figure 67. Conceptual design of large-scale stable restoration: Plan and front views. 165

Figure 68. Conceptual design of large-scale stable restoration: Cross-sections. 166

Figure 69. 2D MCO hydrodynamic and morphologic change summary (Table 6, Analysis 1b). 186

Figure 70. 2D MCO erosion and overwash summary (Table 6, Analysis 1b). 187

Figure 71. 2D MCO profile and consolidated subsurface (Table 6, Analysis 1b). 188

Figure 72. 2D MCO volume change summary (Table 6, Analysis 1b). 189

Figure 73. 2D MCO hydrodynamic and morphologic change summary (Table 6, Analysis 1c). 190

Figure 74. 2D MCO erosion and overwash summary (Table 6, Analysis 1c). 191

Figure 75. 2D MCO profile and consolidated subsurface (Table 6, Analysis 1c). 192

Figure 76. 2D MCO volume change summary (Table 6, Analysis 1c). 193

Figure 77. 2D MCO hydrodynamic and morphologic change summary (Table 6, Analysis 1d). 194

Figure 78. 2D MCO erosion and overwash summary (Table 6, Analysis 1d). 195

Figure 79. 2D MCO profile and consolidated subsurface (Table 6, Analysis 1d). 196

Figure 80. 2D MCO volume change summary (Table 6, Analysis 1d). 197

Figure 81. Example design for settlement plates and sediment cores. 202

Tables

Table 1. Summary of concepts in previous reviews. 13

Table 2. Processes of morphologic change in NGOM. 24

Table 3. Barrier and storm conditions for conceptual model. 26

Table 4. Representative processes along NGOM. 30
Table 5. Processes of potential importance in modeling barrier island evolution in deltaic settings. 37
Table 6. 2D MCO Sensitivity analysis with triangular Barrier Island[1]. 74
Table 7. Data from Virginia applied in comparison with 2D MCO (summarized from Gayes 1983). 90
Table 8. Application of 2D MCO in comparison with Virginia Barrier Islands.[1] 91
Table 9. Equations for regional sources and sinks of sand sub-module (Figure 43 for notation). 120
Table 10. Volumetric change for Trinity Island, LA (Dingler 2008). 127
Table 11. Summary of average wind speed exceeding threshold1, percent occurrence, sta CSI-52 (Coastal Studies Institute 2008), and results from eolian sand transport sub-module. 129
Table 12. Evaluation of Metric 1a – volume sequestered through consolidation is greater than 10 percent of total barrier island volume*. 138
Table 13. Evaluation of metric 1a for Virginia barrier islands. 140
Table 14. Evaluation of Metric 1b. 141
Table 15. Evaluation of Metric 1c – migration rates of BIC are greater than migration of BIS if sufficient sand source is available. 142
Table 16. Evaluation of Metric 1d, lifetime of BIC is reduced as compared to BIS. 143
Table 17. Incremental method versus initial method of beach fill restoration – Hypothesis 3, application of 2D MCO. 149
Table 18. Approximate costs for barrier island restoration projects in Louisiana (Thomson 2008)*. 158
Table 19. Calculation of decadal-rate of inflation (Financial Trend Forecasters 2008). 159
Table 20. Comparison of incremental and initial fill simulations: Total cost in 2009 dollars. 160
Table 21. Summary of hypotheses and associated metrics. 167
Table 22. Elevation and facies data from Metomkin and Assawoman Islands, VA (digitized from Gayes 1983, his Figures 5, 6, and 7). 199

Preface

This study was funded by several programs of the U.S. Army Corps of Engineers: the Coastal Inlets Research Program (CIRP), Internal Research and Investment Program (IRIP), and System-Wide Water Resources Program (SWWRP), all funded through the Coastal and Hydraulics Laboratory, Engineering Research and Development Center (ERDC). Headquarters, USACE, provided funding for these R&D programs.

This report was prepared by Dr. Julie Dean Rosati, Coastal Processes Branch, (HF-CI), CHL, and edited by Holley J. Messing, Coastal Engineering Branch, (HN-C), CHL. This report was reviewed by Dr. Nicholas C. Kraus, Senior Scientist Group, CHL, and professors from Louisiana State University: Drs. Jaye E. Cable, Patrick A. Hesp, Dubravko Justic, Harry H. Roberts, Gregory W. Stone, Robert R. Twilley, and Michael W. Wascom. Work was performed under the general administrative supervision of Ty V. Wamsley, Chief, Coastal Processes Branch; Bruce A. Ebersole, Chief, Flood and Storm Damage Division; Thomas W. Richardson, former Director, CHL; Dr. William D. Martin, former Deputy Director and present Director, CHL; and Dr. Rose M. Kress, acting Deputy Director, CHL.

COL Gary E. Johnston was Commander and Executive Director of ERDC. Dr. James R. Houston was Director.

1 Introduction and Significance

Forcing processes

The formation and evolution of coastal Louisiana has been dominated by the Mississippi River system. The present-day barrier islands were created as abandoned Mississippi River delta lobes were reworked by coastal processes (Penland and Boyd 1981). These islands are composed of a thin layer of sand overlying thick sequences of deltaic sediment and organics (Kuecher 1994, Roberts et al. 1994, Kulp et al. 2002). Because of the antecedent geology and a combination of other factors, the Louisiana coastline has been retreating at nearly 10 m/year for the past 30 years (Penland et al. 2005). This research is the first to quantify one of the reasons for rapid retreat of Louisiana's barrier islands: compaction of the deltaic substrate as a function of the weight and long-term morphologic evolution of the overlying barrier island. This research indicates that between 20 and 40 percent of the total sand volume can be sequestered, and lost from the sandy barrier island through the consolidation process. A new numerical model developed as a part of this research incorporates time-dependent consolidation of the subsurface with cross-shore morphology change of the island, and is applied to evaluate options for large-scale restoration.

The morphology of barrier islands evolves in response to sediment transport processes acting across-shore and alongshore. In the cross-shore, storm surge and wave runup exceeding the crest of the island can overwash the barrier island and transport sand to the back-barrier and bay. Lower surge and wave conditions can erode the foreshore, depositing beach sand offshore and suspending fine sediment (silt, clay, and mud) that is then transported out of the barrier island system. Wind of sufficient speed and duration can transport sand from dry, unvegetated beaches to deposit in the dune system or adjacent waters. Storm passage into the bay may create wind-waves and surge on the bay, resulting in erosion of the bayshore or overwash from the bay to the ocean shore. These processes are episodic and relatively short term, occurring within hours to days. Barrier islands may recover from some cross-shore storm losses through constructive across-shore and alongshore processes acting on longer temporal scales ranging from weeks to years. After a storm, vegetation can return to dunes, enhancing capture of wind-blown (eolian) sand and subsequent dune building.

Along the shore, currents produced by obliquely incident waves as well as by the tide and wind at some locations transport sand parallel to the barrier beach and operate on temporal scales ranging from years to decades. Beaches adjacent to inlets transport sediment from inlet deltas, channels, and bars in response to tidal currents and waves transformed over nearshore bathymetry. On ultra-long time scales ranging from decades to centuries, processes in the vertical dimension such as eustatic sea level change, regional down-warping or uplift, and consolidation of sediment may contribute to the evolution of coastal morphology. For barrier islands overlying poorly-consolidated sediment, such as deltaic, bay, estuarine, and peat deposits, consolidation of the underlying substrate due to the weight of the island can accelerate long-term morphologic response.

Deltaic, bay, estuarine, and peat deposits compress, or consolidate as a function of the load that is applied, duration of loading, and characteristics of the substrate itself. River deltas experience consolidation wherever the river deposits organics and fine sediments, such as silt and clay. Deltaic systems that experience accelerated subsidence include the Mississippi River (Coleman et al. 1998); Rhine-Meuse River, The Netherlands (Berendsen 1998); Ebro River, Spain (Sanchez-Arcilla et al. 1998); Nile River, Egypt (Stanley and Warne 1998), the Ganges-Brahmaputra Rivers, Bangladesh, India (Allison 1998); and the Yangtze River, China (Xiqing 1998). Compaction of the subsurface can also occur for bays and estuaries with fine sediment, organic material, and peat deposits. For barrier islands overlying this type of substrate, the weight of the island compresses the subsurface resulting in a reduction of island elevation. The net result is an increased propensity for overwash of the island and subsequent migration. New washover deposits begin to consolidate previously non-loaded sediment, thus exacerbating the morphologic change process. This research concerns how local compaction or consolidation of a compressible substrate beneath a barrier island modifies the morphologic evolution and migration of the island.

Primary consolidation occurs as fluid or gas that is trapped in the voids between sediment grains is expelled and the grains shift due to loading. Secondary consolidation continues indefinitely after the fluid and gas have been expelled as sediment grains deform (Wu 1966). The rate of consolidation decreases with time. Poorly-consolidated substrates can occur where rivers deposit fine-grained sediment and organics, or where organic deposits from a buried marsh system decompose such as a bay or estuary.

Statement of problem

Barrier islands overlying poorly-consolidated sediment experience rapid rise in relative sea level because of the decrease in island elevation as a function of consolidation of the substrate. Lowering of a barrier island by consolidation is compounded as barrier sand migrates into the bay by overwash during storms. The existing barrier elevation is reduced, making future overwash more likely, and the overwash deposit (called "washover") begins to load the previously unconsolidated substrate (Figure 1). The newly loaded sediment base then begins the primary consolidation process. Over long periods of time, these barrier islands are eroded and distorted by successive storms, potentially migrating into the bay and breaching. They ultimately may become submerged, such as Ship Island Shoal in Louisiana (Penland et al. 1988).

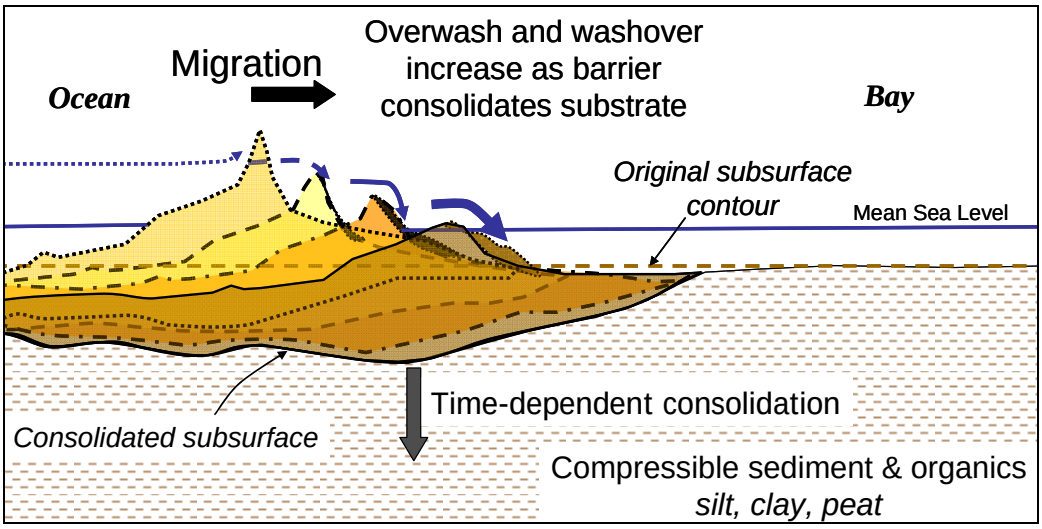

Figure 1. Consequence of consolidation on barrier island migration and overwash.

Based on shoreline position data spanning at least an 80-year period, McBride et al. (1995) found that morphology change of barrier islands in Louisiana was best characterized by landward rollover, retreat, and breakup. Penland et al. (2005) documented long-term (greater than 100 years) and short-term (less than 30 years) shoreline change in Louisiana as -6.1 and -9.4 m/year, respectively. Each kilometer of barrier island shoreline in Louisiana is estimated to protect estuarine habitat with area 30 km^2 (McBride and Byrnes 1997). If the Isle Dernieres island chain in Louisiana were to become submerged shoals, Stone and McBride (1998) estimated that fair-weather conditions would result in a seven-fold increase in wave height in the bays. The rapid erosion of Louisiana's coast is attributed to the predominance of muddy sediment, rapid rate of

subsidence, and frequency of hurricanes (Penland et al. 2005). However, the links between the loading by the islands on the deltaic substrate, the magnitude of time-dependent consolidation as a function of the load, and the subsequent morphologic change and evolution of the islands have not been previously quantified.

In a study of Virginia barrier islands, Gayes (1983) surveyed the barrier and beach profile, and collected sediment cores across three migrating barrier island systems that overlie a compressible peat and bay sediment substrate: Assawoman Island, Metomkin Island, and Wallops Island. Based on the measurements and island migration rates, these barrier island systems experienced consolidation between 0.1 and 3.5 m over 35 to 40 years. The elevations of these islands were approximately 0.8 to 2.6 m relative to mean high water (MHW), with the maximum thickness of sand overlying the substrate ranging from 1.4 to 3.5 m. The magnitudes of consolidation with sand thicknesses of this magnitude within such time periods considered make this process of concern on human time scales.

Research plan

This research is the first to quantify the magnitude to which consolidation modifies the migration and morphologic evolution for barrier island systems overlying a poorly-consolidated substrate. The research is accomplished through conceptual development, and computational, quantitative, and systematic analysis. A two-dimensional (2D) cross-shore mathematical model for Migration, Consolidation, and Overwash (2D MCO) is developed to calculate barrier island erosion, overwash, and migration due to storms, together with consolidation of the underlying substrate. Model predictions are compared with field data, and then applied to evaluate the effects of time-dependent consolidation on barrier island erosion, overwash, and migration. Five sub-modules are developed to characterize long-term processes, and are applied in conjunction with the two-dimensional model to represent evolution of the island in the non-storm period. The relative significance of consolidation to overall morphologic evolution of the barrier is evaluated under various sequences of storms and initial geologic settings.

The 2D MCO represents storm processes over periods of hours to days and the subsequent consolidation associated with barrier island migration over periods of years to a century. The five sub-modules of 2D MCO developed herein represent processes other than storms that may contribute to morphologic change of the barrier island, such as a gradient in longshore

sand transport; post-storm recovery; eolian sand transport; erosion of fine-grained "core" sediment that underlies the veneer of sand on Louisiana barrier islands, and erosion of fine-grained sediment on the bayside of these islands that may be exposed after a storm; and changes in regional sources and sinks of sand due to regional processes such as a change in tidal prism due to increasing bay area. Figure 2 shows how the temporal and spatial scales of the 2D MCO and sub-modules relate to each other.

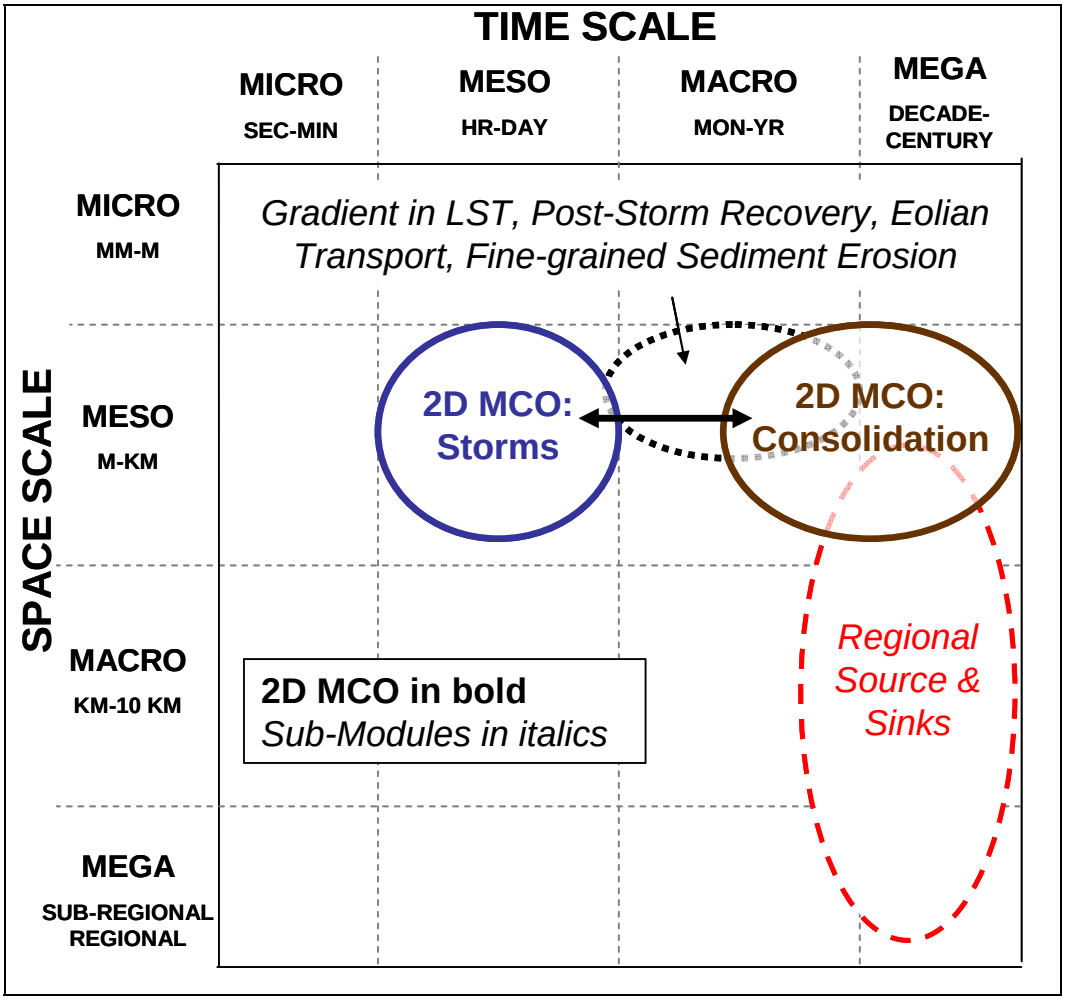

Figure 2. Temporal and spatial scales associated with 2D MCO and sub-modules (modified from Larson and Kraus 1995).

The 2D MCO calculates morphology change due to storms in a given year, then consolidates the subsurface based on the morphology of the island. The first four sub-modules operate on temporal scales of days to years and spatial scales of meters, with the Regional Sources and Sinks sub-module representing periods of years to multiple decades and spatial scales extending to tens of kilometers.

Objectives of this research and hypotheses

Through analysis of geotechnical and geomorphic data, positing of theories to represent the controlling physical processes, and mathematical representation of this information within a 2D mathematical model and five sub-modules developed in this study, three hypotheses are tested:

1. Consolidation is a dominant process governing morphologic evolution and migration for barrier island systems overlying poorly-consolidated sediment.
2. Given similar forcing conditions, barrier islands overlying poorly-consolidated sediment require a greater volume of sand, greater dune elevation, and greater width to maintain functioning as compared to islands residing on a non-compressible substrate.
3. To preserve barrier islands that overlie a compressible substrate, it is best to initially infuse a large volume of sand from an external source, rather than smaller quantities that are placed incrementally in time.

Overview

This technical report is organized in seven chapters and three appendices. Chapter 1 introduces the problem and objectives of the research. Chapter 2 reviews the literature for barrier island morphologic evolution and concludes with a conceptual model of barrier island evolution and implications for coastal preservation and restoration (published as Rosati and Stone 2009). Chapter 3 is a review of the state of conceptual and mathematical model applications for barrier island evolution and of consolidation as it applies to barrier islands. The goals of the literature reviews in Chapters 2 and 3 are to demonstrate that the topic of this technical report is original and establish the background for model development. Chapter 4 presents development, comparison with available field data, and sensitivity testing of 2D MCO (Rosati et al. 2007, and Rosati et al. 2009). Five sub-modules that represent long-term processes are developed and tested with available data in Chapter 5 (portions published as Rosati and Kraus 2008). Chapter 6 evaluates the hypotheses and applies this research to develop recommendations for preservation and restoration of barrier islands that overlie a compressible substrate. Chapter 7 is a concluding chapter that summarizes the research and discusses questions and data needs to be addressed in future study. Three appendices document the sensitivity testing, data that were analyzed and derived for this study, and recommendations for future data collection and research.

2 Barrier Island Morphologic Evolution

Introduction

Barrier islands located in Louisiana, Mississippi, Alabama, and the panhandle of Florida differ in terms of their sediment source, the availability of littoral and inner shelf sediment, and the underlying substrate. Three general regions are defined as shown in Figure 3. The following discussion compares and contrasts each of these regions.

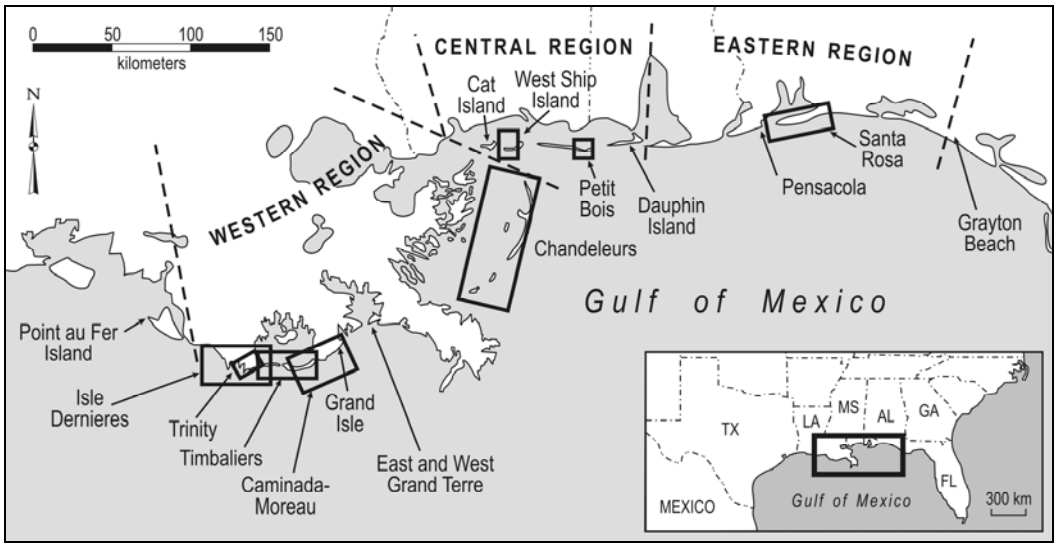

Figure 3. Location map for studies reviewed in literature summary.

Along the Western Region, barrier islands in Louisiana are intricately linked to abandoned deltaic lobes of the Mississippi River and subsequent reworking by littoral and inner shelf processes (for comprehensive reviews see Penland and Boyd 1981; Coleman et al. 1998). Penland and Boyd (1981) defined three stages of deltaic barrier island formation. After a mature active delta (e.g., the modern Bird's Foot delta) was abandoned by the river, Stage 1 began with an erosional headland that fed flanking barrier islands (e.g., Caminada-Moreau headland with flanking barriers, Timbalier Islands to the west, and Grand Isle to the east). Over time (millennia), subsidence and wave-induced erosion depleted the source of sediment. Stage 2 consists of a transgressive (retreating) barrier island arc (e.g., Chandeleur Islands). Finally, Stage 3 occurs when erosion and subsidence reduce the barrier island to a subaequeous inner shelf shoal (e.g., Ship Shoal). Until human intervention in the early 1900s (levee

construction and river diversion), this cycle repeated as the river occupied new locations or former deltas and provided a new source of sediment.

Because of this cycle of delta formation and abandonment, the Louisiana barrier islands are comprised of a relatively thin layer of fine sand that was reworked from the abandoned delta. The islands overlie a thick deltaic sequence of clay and silt that was deposited during the mid-to-late Holocene by the river, and eventually transgressed over back-barrier estuarine deposits (Coleman et al. 1998). During storms, surface sand can be eroded from these islands, exposing partially consolidated fine-grained clay, silt, and organics that comprise the "core" of the islands (Stone et al. 1995). Fine-grained sediment and organics on the bayside of the islands are deposited by tidal forcing and reverse flow from the estuaries to the Gulf following frontal passages. These bayside fines and organics can also be exposed when sand is removed from the islands. Barrier islands along Louisiana's coast were created from abandoned deltaic lobes of the river, so the original primary riverine source of sediment to the littoral system is no longer available. The present-day source of littoral sand is obtained from either erosion of adjacent islands or self-cannibalization (Penland and Boyd 1981). The islands are low in elevation, with vegetation including dune grasses on the primary and secondary dunes where they exist, and wetlands on the bayside/central portion of the islands. Some of the barrier islands are thinning in place (Penland et al. 2005), due to a combination of rapid relative sea level rise, a lack of littoral sediment, and erosion on both the Gulf and bay shores. Relative sea level rise (RSLR) for Grand Isle, (south-central Louisiana; see Figure 3) approximated 9.24 mm/year ± 0.59 mm/year from 1947-2006 (National Oceanographic and Atmospheric Administration (NOAA) 2008a).

In the Central Gulf Region, the Mississippi barrier islands along the west extending to Dauphin Island, Alabama, to the east, have migrated rapidly from east to west (McBride et al. 1995). The exception is the western-most island, Cat Island, which is primarily protected from offshore waves due to the incident wave sheltering of the Chandeleurs and Ship Island. Migration rates of the western termini of Dauphin, Horn, and Petit Bois Islands were approximately 55.3, 31.3, and 34.5 m/year from 1848 to 1986, respectively (McBride et al. 1995). Sediment is reworked from east to west (Cipriani and Stone 2001). Eastern Dauphin Island, with a Pleistocene core in the eastern section, is more stable than the other barriers although the eastern beaches have been eroding in response to the dominant westerly-directed transport. Based on grain size analysis, Cipriani and

Stone (2001) determined that offshore sources may also provide sediment to central Petit Bois Island (located just west of Dauphin Island); similarly, Otvos (1979) concluded that the primary source of sediment for these barrier islands is the shelf. These islands range from very well vegetated, with maritime forests on east Dauphin Island, to low elevation barriers that are overwashed and breached during hurricanes. From 1848 to 1986, long-term island area change rates were -2.5, -1.6, -1.7, and -2.0 ha/year for Cat, Ship, Horn, and Petit Bois Islands, respectively (Byrnes et al. 1991). Long-term RSLR for Dauphin Island, AL, was 2.98 mm/year ± 0.87 mm/year from 1966 to 2006 (NOAA 2008b).

The Eastern Region extends from Morgan Peninsula, AL, along the west to Grayton Beach, FL, to the east (Figure 3). Grayton Beach is a Pleistocene headland that supplies sediment to the Florida beaches to the west, with the source tapering in the vicinity of Santa Rosa Island. Research suggests that beaches west of Santa Rosa Island have derived a significant quantity of sand from offshore during the mid-to late Holocene. The mechanism for onshore sand transport is a direct function of a distinct decrease in the inner shelf slope and an increase in modal wave energy (Stone et al. 1992; Stone and Stapor 1996). Barrier islands in this region have the most plentiful source of littoral sediment for the Northern Gulf of Mexico (NGOM) barriers examined in this study. Sea level data examined over the period 1923 through 2006 indicate that this area underwent a rise in relative sea level approximating 2.10 mm/year ± 0.26 mm/year (NOAA 2008c). Based on radiocarbon dates (millennial time scales) of organic material extracted from the upper shoreface, Stone and Morgan (1993) also found that Santa Rosa Island, FL, was relatively stable and experienced a RSLR rate that approximated the eustatic (global) sea level rise of 2 mm/year as derived through the work of Douglas (1992) and Peltier (1998).

Comparing the RSLR rate for these three regions, it is evident that the Western Region experiences local subsidence and/or tectonic movement that increase the RSLR rate approximately 7.5 mm/year in addition to the eustatic rate. This phenomenon is greatly reduced for the Central Region, where the RSLR rate is approximately 0.5 mm/year greater than the eustatic rate. The Eastern Region appears stable, with the RSLR rate approximately equal to the eustatic rate. The increase in RSLR over the eustatic rate reflects the degree to which the substrate is an active factor in long-term barrier island response. For these three regions, it is evident

that the "substrate effect" is high along the Western Region, and low or virtually absent along the Western, Central, and Eastern Regions.

Based on discussion in this section, these three regions appear to be different. However, they share commonality through similarity in forcing processes that occur in the NGOM and how the barrier island morphology responds over short- to mid-term time scales (days to weeks to years). Through an understanding of how these islands respond to short- and mid-term forcing, we can anticipate and characterize long-term response by including knowledge of RSLR, geologic setting, and sediment availability for the region. Over longer time scales (decades to centuries), the morphologic response will be modified by regional constraints such as the underlying substrate and availability of littoral sediment.

Review of literature

Overview

In order to provide a contextual setting, three earlier compilations of barrier island literature are reviewed. These compilations are pertinent to understanding general concepts of morphologic change regardless of coastal setting. Next, the NGOM literature is synthesized and compared with the broader literature base to understand how the NGOM processes and barrier island responses differ from other coastal settings.

Previous summaries

Three summaries of barrier island literature have been reviewed, with focus on reviewing modes of barrier island formation and processes causing long-term morphologic change. The first summary was by Schwartz (1973), who compiled and published editorial commentary on 40 papers pertaining to barrier island evolution and morphological maintenance, literature that spanned a time period from 1845 to 1972. Schwart's compendium centered on delineating the mechanism(s) for barrier island formation, whether through bar emergence (de Beaumont 1845; Johnson 1919; Otvos 1970, 1979, 1981, 1985), spit formation and breaching (Gilbert 1885; Fisher 1968), or ridge engulfment (McGee 1890; Hoyt 1967). In an introduction, as well as in a separate paper (Schwartz 1971), Schwartz advocated "Multiple Causality" as opposed to a singular mode of formation for barriers, depending on sediment supply, coastal and geologic setting, and trends in relative sea level change.

Leatherman (1979) edited a collection of ten papers, the majority of which had been presented at a Coastal Research Symposium on barrier island research in March 1978. In the introduction, Leatherman emphasized substantial progress in the 1970s and he contended that three processes control landward barrier island migration: inlet dynamics, overwash, and dune migration (eolian processes). This collection included a landmark paper by Hayes (1979, see also follow-on paper by Davis and Hayes 1984), in which Hayes differentiated large-scale barrier island shape as tide- or wave-dominated based on tidal range and wave conditions.

An overall theme in Leatherman's (1979) review was the substantial role of inlets in determining morphologic response. Armon (1979) quantified the relative transport magnitude attributed to inlets, overwash, and eolian transport in transgression of the Malpeque barrier system in the Gulf of St. Lawrence, Canada. Over a 33-year period (1935-1968), 90 percent of the landward sediment movement in the barrier system occurred at existing or former inlets. Similar studies of landward transport along barrier island systems at Cape Hatteras, North Carolina (Pierce 1969) and Assateague Island, Maryland (Bartberger 1976) also concluded that the dominant contributions to migration were via existing tidal inlets (72 and 82 percent, respectively), followed by overwash (14 and 12 percent, respecttively) and eolian transport (13 and 6 percent, respectively). Considering a 36-year period for Rhode Island barrier beaches, Fisher and Simpson (1979) concluded that tidal inlet deltas contributed approximately 57 percent of the total sedimentation, with washover sedimentation providing 43 percent. Moslow and Heron (1979) investigated long-term migration of the Core Banks in North Carolina, which migrated landward approximately 6.7 km over a 7,000 year period. From 7,000 to 4,000 BP, overwash was identified as the dominant process of barrier migration, with rates ranging from 45 to 98 m/century. From 4,000 to 755 years BP, the rate of migration slowed as the rate of RSLR decreased, and inlet formation and migration were the dominant processes forcing barrier relocation onshore.

In the most recent summary of the literature, Leatherman (1985) presented a comprehensive annotated bibliography of the barrier island migration literature through 1980. Of the 71 studies reviewed, two primary theories of barrier island migration were documented: continuous migration and in-place drowning. The majority of the studies supported the concept of continuous migration or shoreface retreat forcing landward migration of the island by rising relative sea level. In this model of retreat,

the barrier island moves landward in response to rising sea level through "rolling over" itself. As with his 1979 compilation of studies, Leatherman concluded that the significant processes in shoreface retreat were, in the order of importance, inlets, overwash, and eolian processes. Eolian processes were found to be more significant for wide barrier beaches with arid and windy conditions (e.g., southern Texas).

A sub-set of the studies supported morphologic evolution through in-place drowning of the barrier island, in which the island responds to rising sea level by aggradation (through overwash or eolian deposition on the subaerial barrier) until it is drowned and later overstepped (e.g., possibly re-established at a landward position). This concept of superconstruction, in which the barrier increases elevation through overwash or eolian processes, was discussed in reference to both theories.

Another process of potential significance for barrier island migration is autocompaction, in which the barrier island decreases in elevation due to loading on the underlying sediments. This process was discussed with information from barrier islands in Virginia where sandy barrier islands have migrated over compressible peat and bay sediments. For the autocompaction process to be of significance, the underlying sediment sequences must be thick and compressible. Several papers in Leatherman's review supported the concept of neocatastrophism, in which low frequency, high-magnitude storms are shown to contribute more to long-term barrier island morphologic change as compared to high frequency, low magnitude storms.

Table 1 summarizes the more salient points that emerge from these earlier compilations. Most of these studies indicate that inlets dominate the processes responsible for barrier island migration. Inlets cause movement of the barrier island through cross-shore transfer of sediment, such as: (1) flood delta and ebb delta formation, (2) net longshore transport and subsequent inlet migration in the direction parallel to the barrier axis, and (3) welding of the ebb tidal delta onto the adjacent beach (FitzGerald 1988). Inlets influence migration processes even when closed, as recently closed inlets are lower in elevation, which increases the likelihood for overwash and possible superconstruction (vertical accretion). Newly deposited, non-vegetated washover fans provide a source for eolian transport which, if deposited within the subaerial barrier mass, can also increase barrier elevation.

Table 1. Summary of concepts in previous reviews.

Modes of Barrier Island Formation	
Bar emergence	de Beaumont (1845); Johnson (1919); Otvos (1970, 1979, 1981, 1985)
Spit formation and subsequent breaching	Gilbert (1885), Fisher (1968)
Ridge engulfment	McGee (1890), Hoyt (1967)
Combination of modes	Schwartz (1971, 1973)
Dominant Processes for Landward Migration	
1. Inlets (from 50 to 80% of total volume)	Armon (1979), Bartberger (1976), Fisher and Simpson (1979), Leatherman (1985), Pierce (1969), Rosen (1979)
2. Overwash (from 10 to 40% of total volume) - Occurs more frequently at former inlet sites	
3. Eolian (from 5 to 15% of total volume) - Overwash deposits provide conduits and source for eolian transport - Eolian transport has potential to increase elevation of barrier ("superconstruction") - Eolian more dominant for wide, arid barriers (e.g., TX)	
Modes of Migration	
1. Shoreface retreat - Via inlets, overwash, and eolian transport - Superconstruction (via overwash and eolian) - Autocompaction (compaction of underlying sediment due to loading by the island, discussed for islands in Virginia) 2. In-place drowning - Via overwash and eolian processes - Superconstruction (via overwash and eolian) - Autocompaction (discussed for islands in Virginia)	Leatherman (1985)
Aggradation and shoal growth	Otvos (1970, 1979, 1981, 1985)
Longshore processes - Spit growth and attachment - Inlet migration alongshore	Otvos (1970, 1979, 1981, 1985), Moslow and Heron (1979)
Barrier Characteristics and Processes	
Wave dominated barriers - Waves 0.6-1.5 m, tides < 2 m amplitude - Long, linear shape; frequent overwash Mixed energy barriers - Waves 0.6-1.5 m, tides 2-4 m amplitude - Short, "drumstick" shape	Hayes (1979), Davis and Hayes (1984)
Overwash is inversely proportional to barrier width Rate of beach erosion directly proportional to overwash	Fisher and Simpson (1979)
Significant sediment source reduces rate of migration	Oertel (1979)
Neocatastrophism - Storms are required for significant geomorphologic change	Leatherman (1985)

NGOM literature

In this section, studies pertinent to migration and morphologic change of barriers along the NGOM are reviewed, and knowledge considered essential to furthering our understanding of modeling past and future barrier island evolution as considered in this study is highlighted. The discussion is organized by region, from west to east, with study sites delineated in Figure 3.

Western Region

Regional Sediment Processes. In one of the earliest papers discussing evolution and potential for preservation of NGOM barrier islands, Peyronnin (1962) documented morphological response from 1890 to 1960 for Louisiana's barrier islands. He estimated that 1.9 million m^3/year of sediment was removed or sequestered from the barrier island system, including the nearshore above the 3.6-m contour, due to wave erosion and subsidence. The influence of autocompaction as discussed for Virginia barrier islands (Leatherman 1985) was also observed, with the weight of sandy beach ridges (1.8-2.4 m thick) compacting the underlying marsh and reducing marsh thickness by 1.0-1.2 m. Kuecher (1994) also concluded that the distribution and thickness of peaty marsh soils was a first-order cause of coastal land loss in Louisiana. Kuecher discussed the consolidation associated with loading by barrier islands, and hypothesized that Pelto Bay and Big Pelto Bay north of the Isle Dernieres were initiated due to loading of the prodelta muds by the barrier island chain (discussed later and shown in Figure 9). After the settlement began, deposition of bay muds continued loading the underlying sediment.

List et al. (1997) examined the applicability of the Bruun Rule to predict shoreline response due to RSLR for 150 km of Louisiana coastline west of the Mississippi River. The Bruun Rule translates a beach profile upwards and landwards due to RSLR, under the assumption that the profile shape remains constant (Bruun 1962). The authors eliminated approximately half of the profiles that did not maintain an equilibrium form over the 50- to 100-year period considered. For the remaining profiles tested, the authors assumed between 31 percent sand (for deltaic shorelines) and 100 percent sand (for sand spits) to calculate volumetric losses of fine sediment as the beach retreated. The Bruun Rule could not accurately predict shoreline response in a hindcast evaluation for the Louisiana coast. Long-term massive redistribution of sediment in the nearshore and on the shoreface was used as evidence of changes to the long-term regional

sediment budget that decreased applicability of the Bruun Rule. Also, RSLR has increased the size of the bays behind barrier islands, thus increasing the tidal prism of adjacent inlets and their associated ebb and flood tidal deltas. As the barrier retreats, the redistribution of sand into the deeper bay, in addition to deltas, suggested that the barrier islands cannot maintain their subaerial form.

These studies highlight the complexity of this region due to the rapid rate of RSLR, redistribution of sediment in the barrier island and nearshore system, and consolidation of the underlying substrate that has the potential to sequester sediment and effectively remove it from the active littoral system.

Morphology. Several researchers have characterized morphology and morphologic response for the Western Region. Ritchie and Penland (1988) monitored 13 cross-shore transects over a 10-year period along the barrier headland coast extending from Belle Pass to Caminada Pass (Figure 3). The coastal landforms and morphologic response were characterized as one of four types:

1. The Washover Flat consisted of a low elevation washover sheet with embryonic dunes that could reach 1 m in elevation during non-storm conditions. However, the dunes did not survive more than a year and vegetation could not grow due to the frequency of overwash, which exceeded 15 storms per year. The entire flat was inundated by unrestricted sheet flow.
2. The Washover Terrace was slightly higher in elevation, smooth and vegetated, or broken up with hummocky topography. Vegetation spread and recovered rapidly due to overwash, thereby promoting capture of eolian sediment.
3. The Dune Terrace had a surface 0.5 to 1.5 m higher than the washover terrace, and exhibited more varied relief. Topographically low points along the frontal dune along the barrier could be overwashed, resulting in washover deposits on the back barrier.
4. The Continuous Dune was characterized by two or more parallel dune ridges that were vegetated, with abundant backshore sand. During storms, the seaward facing dunes were scarped, with erosion creating a near-vertical slope and the foredunes could be completely removed. Washover fans were sparse due to the height and the morphological integrity of the vegetated dunes.

Data indicated that the overwash threshold for this coast was 1.42 m above mean sea level (MSL); consequently, approximately 75 percent of the Caminada-Moreau barrier headland would experience overwash. Un-vegetated sand surfaces, created through the overwash process, were then prone to eolian transport of sediment into the dune system. After analysis of weather statistics, the authors found that there were two dominant wind vectors in this location, from the north and northwest. Thus, eolian transport from washover flats towards the Gulf could result in deposition at the base of the dune system, assuming the dune had sufficient relief for capture. In a recent study of sand fences placed as part of beach nourishment projects for the Isle Dernieres, Khalil (2008) also noted the capacity of northern winds to build dunes if a non-vegetated source of sand was available for eolian transport. For both these studies, sand comprising washover flats was rarely transported further landward or into the bay (north) by eolian processes.

In the 10 years that Ritchie and Penland (1988) monitored the coast, a substantial amount of morphological change occurred in response to storms; for example, a dune terrace was reduced to a washover sheet after two minor washover events followed by a series of cold fronts (Ritchie and Penland's Profile D, p. 113). Eolian transport was observed to contribute significantly to dune building, with one profile increasing in elevation by approximately 1 m over a time period extending from April to December (1980) (Ritchie and Penland's Profile H, p. 116; discussed later and shown in Figure 47). Stability of morphologic features was noted for locations that were vegetated or rapidly revegetated after storms. Revegetation was directly linked to a minimum number of overwash events, above which vegetation could not be reestablished. Based on the 10 years of monitoring, the authors suggested that the dunes followed a 10-year cycle, increasing volume of supra-tidal sand storage for up to 10 years that was then rapidly removed during a major storm.

Campbell (2005) identified eight unique aspects of the Louisiana coast that should be considered in coastal engineering analysis and design:

1. For six coastal segments evaluated, the profile shape exhibited a distinct break in slope (at approximately the 2-3 m isobath, no datum given) above which it had the form of an equilibrium-type profile. Below this depth the profile was much flatter, and assumed to be a "passive depositional zone" with silts and clays.

2. Marsh sediments were observed to be more resistant to erosion as compared to sandy beaches.
3. The Louisiana barrier islands had low dunes and a high frequency of overwash.
4. The Louisiana barrier islands had rapid subsidence and a high rate of RSLR.
5. When actively exposed to wave attack, exposed marsh areas permanently lost fine sediment.
6. Longshore sand transport in the region was lower than observed or measured for exposed U.S. Atlantic and Pacific coasts, estimated to be 50,000 to 100,000 m^3/year for East and West Grand Terre.
7. Due to long-term RSLR and losses to the barrier-marsh systems, back-barrier bays were observed to increase in area, thus increasing the tidal prisms at inlets. Over time, the increasing tidal prism increased littoral system losses to larger ebb and flood tidal deltas.
8. High retreat rates on the Gulf shorelines were believed to be due to many interrelated factors, and "cannot be predicted by any one process independent of the others."

Based on this understanding, Campbell (2005) developed a four-stage conceptual dynamic morphosedimentary model for barrier island retreat in Louisiana. Stage 1 of the model showed an initial barrier with a thin sand layer with median grain size of 0.1 to 0.14 mm over mixed deltaic sediment (sand, silt, and clay), backed by a wide marsh system. During storms, the sand was eroded and marsh vegetation and deltaic sediment were exposed to wave attack (Stage 2). In Stage 3, sand and potentially marsh sediment, were eroded from the barrier as the beach retreated. Fine sediments were assumed to be lost to the passive depositional zone offshore of the observed break in profile slope, and sand was moved offshore or transported alongshore to inlets. Campbell observed that the barrier islands tended to retreat during the post-storm period, and this phenomenon was attributed to continuous wave action eroding the exposed marsh sediment. Sand eroded in Stage 3 partially returned to the barrier in the form of a sand cap on top of the deltaic sediments, which provided protection to the residual marsh (Stage 4). Overall, these processes narrow the barrier islands through time while increasing elevation (via overwash) and migrating them upslope and landward.

Based on shoreline position data spanning at least an 80-year period, McBride et al. (1995) characterized eight geomorphic response-types for barrier island systems in Louisiana, Mississippi, and Georgia/Northern

Florida. The authors found that barrier islands in Louisiana were best characterized by landward rollover, retreat, and breakup. Barrier island systems with a high rate of RSLR, such as Louisiana, were dominated by landward-directed, cross-shore processes with longshore transport having secondary importance.

These studies are valuable in their characterization of NGOM subaerial beach morphology, and responses, as a function of relative storm-to-beach elevation. Of the four types of beach morphologies characterized by Ritchie and Penland (1988), the first and fourth (washover flat and continuous dune) can be generally described as two-dimensional, whereas the intermediate types (washover terrace and dune terrace) have three-dimensional variation. This distinction has potentially significant implications from a numerical modeling perspective.

Storm Response. Five studies are discussed to review the response of barrier islands in the Western Region to hurricane and cold front passage. Kahn and Roberts (1982) described the morphologic response of the Chandeleur barrier islands to Hurricane Frederic, a powerful storm that made landfall east of the islands near Pascagoula, MS, on 12 September 1979. The barrier island system had two main morphologic zones: a more stable northern section with dunes from 2 to 4 m high (MSL), and a 19-km-long southern section with little or no dunes and elevations not exceeding 1.5 m (MSL). The southern section experienced Hurricane Frederic's waves for 24 hr prior to landfall, whereas the northern segment was more protected from initial storm waves.

Along the northern section, the beach width was eroded to less than 30 m, and the dunes survived the storm, although a 1.0-1.5 m scarp formed at the base. The southern section was most likely entirely inundated during Hurricane Frederic. Sheet flow over the barrier removed the entire sub-aerial beach and left washover fans extending up to several hundred meters into Chandeleur Sound. The authors attributed the differences in response observed during and after the storm to exposure of the barrier island to the storm (i.e., the southern portion received waves in advance of the storm, and the northern section benefited from northerly transport of sand prior to landfall of the hurricane), and the pre-storm morphology of the dunes. Breaching of the northern portion of the Chandeleurs in lower portions of the dune system initially caused sand to be washed into Chandeleur Sound as the storm passed; however, this sand washed back into the Gulf with return flow after the storm. These lobate sand features

were then a potential source of sand for longshore transport to facilitating infill of breaches during the post-storm recovery period.

Two studies compared how morphologic change differed for cold front passage and hurricanes along the Isle Dernieres. Dingler and Reiss (1990) documented morphologic change of a 400-m section of the Isle Dernieres from August 1986 to September 1987. During this period, tropical cyclones did not impact the area; thus, all morphologic change was due to cold fronts that frequent the area between October and May along the northern Gulf (Roberts et al. 2003; Pepper and Stone 2004; Stone et al. 2004). The profile was erosional in the "inshore-foreshore" portion of the barrier (defined as the area gulfward of the September 1987 berm crest), with losses ranging from 37 to 56 m^3/m. The "backshore" (remaining portion of barrier, landward of the September 1987 berm crest) was accretional, with gains ranging from 7 to 29 m^3/m. In total, 19,200 m^3 was eroded from the inshore-foreshore, and 5,600 m^3 was deposited on the backshore. Based on the thickness of sand and marsh, 13,600 m^3 of marsh deposits was considered eroded. The authors concluded that sand volume was conserved or accounted for during the study period, and that the eroded marsh deposits were replaced by sand. However, the authors did not develop a barrier island sediment budget that could be used to evaluate whether a longshore transport gradient may also have contributed to erosion of the inshore-foreshore. Further, erosional processes on the bayshore that occur after the passage of cold fronts were not considered as a possible mechanism of reduced accretion on the bayshore (Armbruster et al. 1995, Stone et al. 2004).

In a follow-on study, Dingler and Reiss (1995) studied this same 400-m section of the Isle Dernieres following Hurricane Andrew, a Category 3 hurricane which made landfall near Point Au Fer Island, LA, on 25 August 1992 (Stone and Finkl 1995). Hurricane Andrew eroded the subaerial beach resulting in a volumetric loss of 92 m^3/m, of which 85 m^3/m (92 percent) was sand. The authors noted that cold fronts have the propensity to maintain a constant beach-face slope whereas hurricanes reduce the slope. Both types of storms removed the coarser (sand) portion of the beach, thus exposing the muddy core. Where vegetation was not present, mud rapidly eroded. Rebuilding of the coast along the study area had not occurred 1 year after Hurricane Andrew, with the mud beach remaining submerged and exposed to waves and currents.

Penland et al. (2003a and b) documented the Gulf and bayside erosion and area change caused by Hurricane Andrew for the Timbalier and Isles Dernieres barrier island arcs, and compared these changes to long-term (1887/1906-1988) and short-term (1978-1988) erosion rates previously documented by McBride et al. (1992). In general, the maximum erosion rates caused by Hurricane Andrew were found to have occurred along the margins of existing inlets and newly-formed hurricane breaches. Bayside erosion occurred as a result of gulf-directed overwash scour and waves in the bay. During a 3-month period following the storm, erosion continued on the margins of all inlets and breaches that did not recover. Accretion was associated with breach closure and development of flood tidal deltas on the bayside. The average Gulf side erosion rate attributable to Hurricane Andrew was three times greater than the long-term erosion rate for Timbalier and East Timbalier Islands. The average bayside erosion rate due to Hurricane Andrew was 1.1 times greater than the average long-term rate. For Isles Dernieres, Hurricane Andrew resulted in more than 5 and 21 times the long-term Gulf side and bayside erosion rates, respectively.

In summary, cold front and tropical cyclone passage have significantly different morphologic signatures on these islands primarily due to variations in storm surge durations and magnitudes. Cold front passage was observed to erode the Gulf side sand and deposit it on the bayside marsh. In contrast, hurricanes tended to strip sand entirely from the islands and deposit it in the bay, which then could be transported back into the Gulf via return flow through breaches as the storm surge decreased. Once exposed, mud was rapidly eroded if not vegetated. Similar to Leatherman's (1979, 1985) findings, the greatest morphologic changes were observed at breaches and inlets.

Central Region

Regional Sediment Processes. Byrnes et al. (1991) and McBride et al. (1995) analyzed historical shoreline position and island area change from 1847/49 to 1986 along the Mississippi Sound barrier islands. For five of six islands studied (except Cat Island), Byrnes et al. (1991) found that lateral migration was typically an order of magnitude greater than cross-shore migration. Because the primary source of sand lies along the eastern portion of the region, migration rates decreased from Dauphin Island in the east to West Ship Island. Cat Island has responded differently over this time period due to the protection provided by the St. Bernard delta complex, which has been reworked into the present-day Chandeleur Islands. McBride et al. (1995) classified Cat Island as "retreating," and

Ship Island was undergoing counter-clockwise "rotational instability." Horn, Petit Bois, and Dauphin Island were characterized as "lateral movement." The eastern termini of the islands were moving more rapidly causing the inlets to widen between the barriers.

Cipriani and Stone (2001) quantified net annual estimates of potential net longshore sand transport rates for the Gulf side of East and West Ship, Petit Bois, and Horn Island, MS, and Dauphin Island, AL, based on a wave transformation modeling and granulometric study. The potential net longshore transport rates had maxima directed to the west approaching 65,000 m^3/year at West Ship Island and at Western Dauphin Island. Based on the sediment grain size analysis, the authors inferred that offshore sources of sediment may provide sediment to central Petit Bois Island.

Byrnes et al. (2009) developed historical (1917-1920 and 1960-1971) and calculated (based on wave transformation modeling) regional sediment budgets for the Central Region by incorporating shoreline position, bathymetric change, and maintenance dredging volumes for navigation channels in the study area. Pertinent findings from the study were that:

1. Net longshore sand transport is from east to west, and the barrier islands and adjacent passes are migrating laterally. The exception is Dauphin Island, which is anchored on the eastern end by a Pleistocene core. However, the western end continues to migrate west, elongating the island.
2. The source of sand for the region is the Mobile Pass ebb tidal delta and the sandy shelf and shoreline to the east of Mobile Pass.
3. Cat Island is not a part of the regional littoral system and does not receive sand from the adjacent barrier islands.

In summary, these studies emphasize the interconnectivity of sediment transport between the Eastern and Central Regions, the shelf as a potential source of littoral sediment, and the dominant direction of net longshore transport from east to west.

Morphology. In a study of geomorphic response, McBride et al. (1995) found that the Mississippi barrier islands were primarily evolving through lateral migration. The authors correlated the geomorphic response type with the rate of RSLR. The Mississippi barrier islands have a moderate rate of RSLR, and longshore transport processes dominate. In comparison,

a lower rate of RSLR in addition to a sufficient sediment supply result in a progradational barrier island system, such as near the Florida-Georgia border.

Storm Response. Nummedal et al. (1980) evaluated morphologic response of Dauphin Island, AL, and Chandeleur Islands, LA, 9 days and again 9 months after Hurricane Frederic. Two general conclusions postulated by the authors are pertinent for modeling NGOM barrier island morphologic response: (1) hurricanes are a "major, perhaps the dominant agents in the development of barrier island morphology along the northern and western shores of the Gulf of Mexico," and (2) "the surge height is the single most important factor" in determining the geological response to a hurricane because the surge elevation determines the extent of flooding and, to a great degree, the energy of breaking waves. Wave-induced turbulence is required in addition to sufficient water level to mobilize and rework sediment (e.g., Pepper and Stone 2004).

Eastern Region

Regional Sediment Processes, Morphology, and Storm Response. Stone et al. (2004) measured beach change at 11 locations on Santa Rosa Island, FL, over a 6.5-year period from February 1996 to July 2002. They documented barrier island change in response to six tropical cyclones and more than 200 cold front passages. The island conserved sediment during Hurricane Opal, a Category 3 storm that made landfall on 4 October 1995, through 40-m erosion of the Gulf shoreline and 40-m accretion of the bayshore. However, during the subsequent 2-year period, the bayshore eroded 20 m due to bayside waves generated during the passage of cold fronts. These losses on the bayshore are believed to be net losses to the subaerial barrier, as sediment is transported onto the bayside platform. The Gulf beaches did not begin to recover from Hurricane Opal until 6 years after landfall.

Armbruster et al. (1995) monitored the north (bay) shore of a 12 km stretch of Santa Rosa Island, FL, during the winter of 1995, documenting bayside erosion due to high frequency (2.5-3.3 sec), steep waves, generated by northerly winds during a series of cold front passages. Long-term erosion of the bayshore was evident from peat outcrops, exposed tree roots, and beach scarps. During the 3-week study, four cold fronts impacted the study area, resulting in high-frequency waves and elevated water level on the bayshore. Currents measured during a 14-hr period during one of the cold fronts were shown to be weaker than required for

transport of sand offshore, but sufficient for longshore transport. For the four storms that occurred during the study period, the overall result was a net loss of -1.92 m^3/m, which was measured between +0.5 m and -0.5 m (or deeper; -0.5 m was the extent of data) relative to National Geodetic Vertical Datum (NGVD). Because the profile surveys only extended offshore to -0.5 m NGVD, the erosion magnitude may have been greater. This order-of-magnitude estimate for bayshore erosion caused by cold front passage can be applied for developing storm response models for sandy NGOM barrier islands.

In summary, barrier islands in the Eastern Region have the capacity to conserve volume through hurricanes, although sand may be eroded from the bayshore of the islands during cold fronts if sufficient fetch is available for waves to develop in the bays. The low-gradient inner shelf may be a long-term source of sand for these islands.

Synthesis

Based on the 16 studies reviewed herein, several constraints and processes dominating the morphologic change of NGOM barrier islands can be summarized (Table 2). Forcing processes for morphologic change are organized in terms of time scale: short-term, representing tropical and extra tropical storms (hours to days); mid-term, for post-storm recovery processes extending to time periods of constructive processes (days to decades); and long-term, for processes in and constraints of the regional system (decades to centuries).

The studies reviewed herein identified several commonalities that span all barrier islands regardless of location. Over the short term, the relative elevation of the barrier island to storm elevation at the coast (surge plus wave setup) determines, to a large degree, geomorphologic response to the storm. In the post-storm recovery phase, longshore sand transport can weld ebb-tidal deltas onshore and mend breaches. Finally, the availability of littoral sediment (primarily sand) ultimately determines the long-term characteristics of barrier island morphology.

Table 2. Processes of morphologic change in NGOM.

Short-Term, Time Scale: Hours to Days
Minimum elevation of barrier island relative to storm surge elevation (including wave setup), and duration of the storm surge. - Lower elevations are most vulnerable to overwash and breaching.
Foredune elevation relative to elevation of breaking wave height - Foredune lower than breaking wave height results in more overwash and breaching
Composition of barrier (fine-grained silt, clay, and organic sediment vs. sand). - Fine-grained sediment is more resistant to erosion if vegetated and consolidated, but is finer than barrier sand, more readily transported offshore or into the bay, and not return to the littoral system. - Fine-grained sediment may erode during the post-storm phase if eroded barrier sand has not yet returned to the barrier.
Locations of previous breaches and washover fans. - Lower elevations and sparse vegetation more susceptible to new breaching and overwash. - Frequent overwash inhibits vegetation.
Vegetative cover. - Increased density of vegetation reduces erosion, decreases eolian transport from the site, and increases trapping of sand.
Bayshore erosion. - Relatively large bays and long fetches facilitate formation of high frequency, steep waves that erode the bayshore.
Storm surge ebb. - Elevated water in bay will result in flushing water and sediment from the bay into the Gulf, through inlets and breaches; may deepen channels and create/enlarge ebb deltas in Gulf.
Mid-Term, Time Scale: Days to Decades
Post-storm recovery. - Cross-shore movement of sediments onshore.* - Mending of breaches via longshore transport.* - Welding of ebb-tidal deltas onshore.* - Eolian transport towards Gulf via washover corridors.*
Eolian transport. - Sand fencing is effective at capturing sand; however, a dry beach, minimal vegetation, and sufficient sediment source are required.
Mid-Term, Time Scale: Days to Decades
Longshore transport. - If sufficient source is available, may create spits and close breaches. - Redistributes sand through gradients in transport rates; responsible for island migration alongshore (long-term).
Onshore transport - Cited as long-term source for some barrier islands with low-gradient shelf (central Petit Bois Island and between Pensacola, FL, and Morgan Point, AL).
Long-Term, Time Scale: Decades to Centuries
Regional geologic setting. - Littoral sediment supply. - Consolidation of underlying sediments due to loading.* - Tectonic and faulting.*
Relative sea level trends. - Rapid vs. gradual increase or decrease.
Bay area and inlet characteristics. - Increasing bay area and depth increases inlet tidal prism, thus increasing the potential sediment sink in ebb and flood tidal deltas.
Interrelationship between barrier islands, bays, regional geology, sediment supply, and redistribution of sediment to nearshore/inlet reservoirs/bays.

NOTE:

* Varying degrees to which these processes occur in the NGOM.

Unique aspects of the NGOM barrier islands as compared to knowledge summarized for other barrier types include: (1) storm paths, wind speeds, and large bays that create the potential for both Gulf and bayshore erosion; and (2) in the West and Central Regions, the potential for loading of the underlying substrate by the barrier island, which, through time, increases consolidation, RSLR, overwash, morphologic change, and migration.

In the Western Region, several other characteristics differentiate barrier island evolution:

1. During storm passage, the veneer of sand overlying core sediment and seaward of bayside sediment and organics can be removed, thus exposing fine sediments that may be rapidly eroded during and following the storm. Fine sediment is not returned to the barrier island system, thus reducing the overall long-term barrier volume.
2. The natural low elevation of these islands relative to MSL makes it less likely for beach sand to be mobilized by eolian transport processes, due to a potentially damp or saturated condition and adhesion to cohesive sediment. Thus, dunes are less likely to form naturally as compared to wider, higher, and sandy barrier island systems.
3. Finally, the rapid rate of RSLR for the Western Region has created an interconnected coastal system that has historically drowned barrier islands (e.g., Ship Shoal; Penland and Boyd 1981). Increasing bay areas result in larger tidal passes, which subsequently sequester more sand in tidal deltas. The result is a reduction in subaerial littoral sediment available to the regional barrier island system, which cannot keep pace with the rapid changes in RSL.

Conceptual model of barrier island evolution

Based on a synthesis of the literature discussed above, a conceptual model of barrier island evolution is developed and presented. The ultimate objective is to provide a general framework with which to develop and test numerical models for the NGOM. In addition to identifying and elucidating the geological complexity of this coast, the immediate implications associated with this work pertain to engineering and design of coastal restoration projects along this region.

Three barrier types have been conceptualized based on the coastal morphologies discussed by Ritchie and Penland (1988), with Ritchie and Penland's intermediate landforms (dune terrace and washover terrace)

combined into one barrier type (termed "dune-washover terrace") (Table 3; Figure 4). The three barrier types conceptualized herein are Continuous Dune, Dune-Washover Terrace, and Washover Flat. Response of each barrier island type to a tropical storm (TS) or weak hurricane (WH) (e.g., Category 1 or 2 on the Saffir-Simpson scale) is presented to illustrate how the initial morphology and existing vegetation modify the processes and determine ultimate, although possibly temporary, morphology.

As shown in Table 3, the relative elevation of the barrier island to storm surge (including wave setup) and the duration of the surge are primary factors in determining response. Many other types of storms occur in the NGOM, ranging from cold fronts, occurring 20-40 times each year, to severe and catastrophic hurricanes (Category 3 or higher), occurring on average every 10 to 30 years (Stone et al. 1997; Muller and Stone 2001; Keim et al. 2004; Stone and Orford 2004). The response to these different intensity storms will bracket the TS/WH storm, with the storm surge and wave setup elevations, duration of the storm, and storm path modifying response.

Table 3. Barrier and storm conditions for conceptual model.

Barrier Type	Description
Continuous dune	Continuous single or multiple dunes of approximately +2 m MSL; crests of dunes are vegetated; back barrier is vegetated wetland for the majority of the barrier system; spits exist on the flanks; system is sand-rich overlying fine-grained sediments (Figure 4).
Dune-washover terrace	Sparse dune system with maximum elevation of +1.5 m MSL; blowouts (breaks) have eroded sediment between dunes; blowouts consist of washover flats that become hummocky and vegetated during non-storm conditions; back barrier is a vegetated wetland or washover fan; spits may exist on flanks (Figure 4).
Washover flat	Sand-deficient system with maximum elevation of +1 m MSL that becomes frequently inundated and overwashed; vegetation exists only when enough time has elapsed between storms; vegetated bayside sediment may be exposed as slightly more erosion-resistant "islands" in the midst of the sandy barrier; back barrier is a vegetated wetland; spits may exist on flanks (Figure 4).

Table 4 compares these various types of storms so that the discussion for a TS/WH storm herein may be set in the appropriate contextual framework regarding other storms. The TS/WH storm is represented as both forcing from the Gulf as the storm approaches land, and from the bay as storm surge and waves are generated in the bay. Wave conditions and surge in

the bay can cause bayshore erosion. Long-term morphologic evolution of each barrier type is also hypothesized.

Characteristics of the barrier island that determine storm response include: (1) the minimum barrier elevations relative to the maximum storm elevation (storm surge, wave setup, and wave runup) and the duration of this maximum storm elevation, (2) the amount of sand and finer sediment in the system, and (3) the amount and type of vegetation coverage of the barrier. Lower elevations along the barrier island represent the weaker parts of the system and determine the barrier's propensity towards overwash and breaching. The quantity of additional sand and shell in barrier dunes and adjacent islands determines whether the island can rebuild and close breaches. Denser vegetation reduces the magnitude of erosion.

Barrier Morphology	Stage in Evolution		
	a. Initial Condition	b. Tropical Storm/Weak Hurricane in Gulf	c. TS/WH in Bay
Continuous Dune	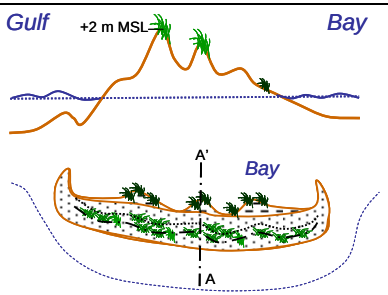	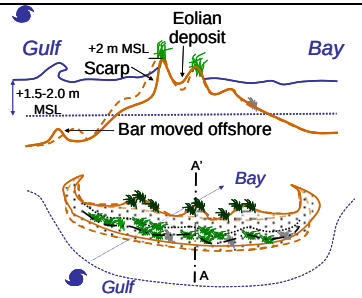	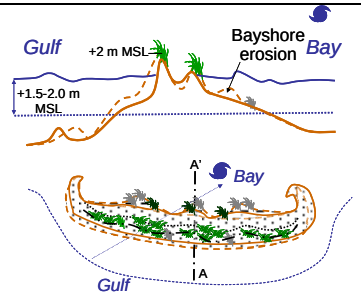
Dune-Washover Terrace	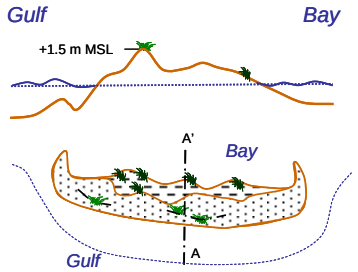	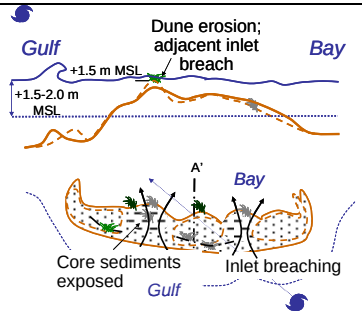	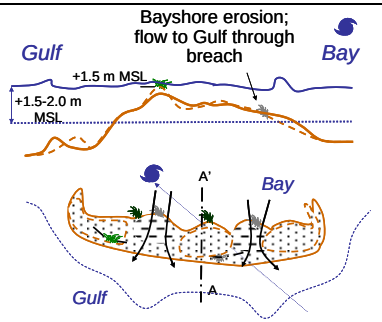
Washover Flat	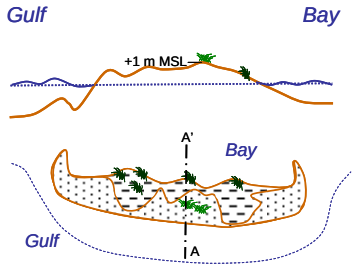	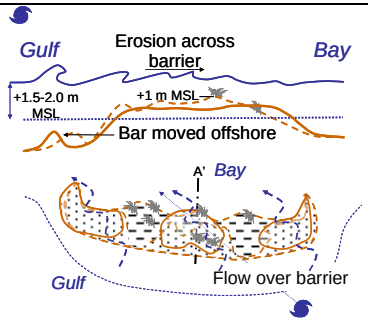	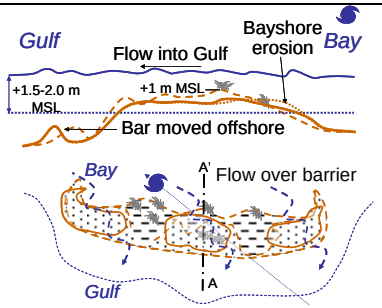

Figure 4. Conceptual model of barrier island evolution (Continued).

Barrier Morphology	Stage in Evolution	
	d. Post-Storm Recovery (days to weeks)	e. Long-term Evolution (years to decades)
Continuous Dune	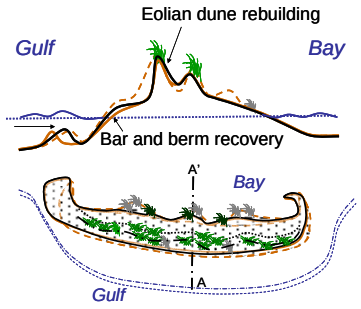	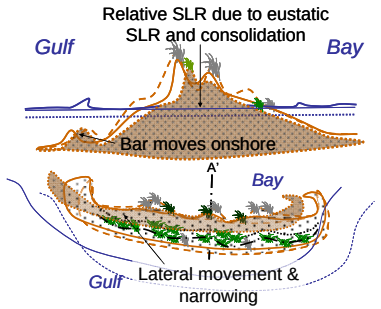
Dune-Washover Terrace	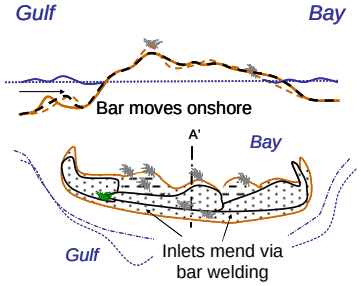	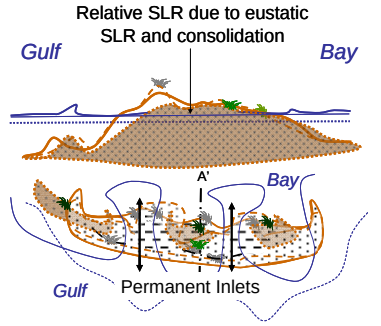
Washover Flat	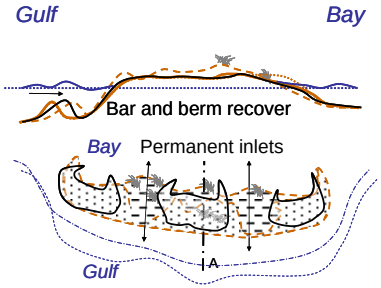	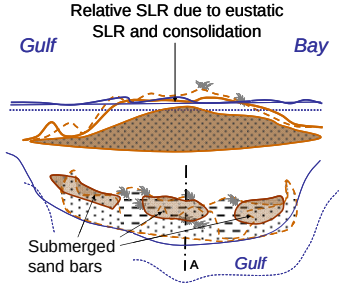

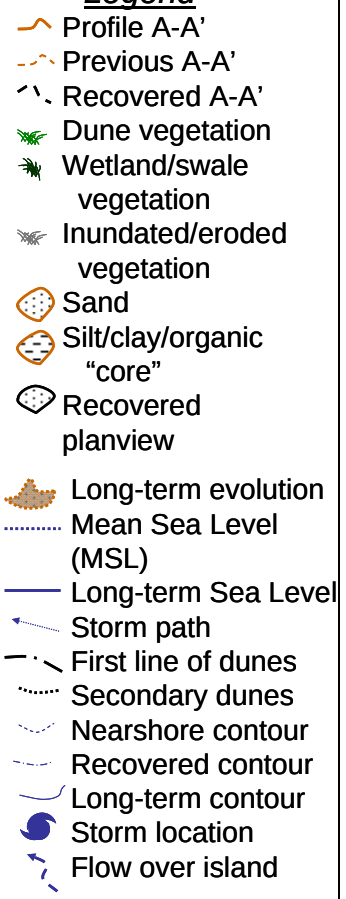

Figure 4. (Concluded).

Table 4. Representative processes along NGOM.

Storm	Frequency (events/year)	Description
Typical non-storm conditions	Majority of year	Microtidal climate with diurnal range = 0.15 (equatorial) to 1 m (tropic)[a]; 0.36 m (mean)[e]. Mean annual significant wave height = 0.8 to 1 m[a]. Associated wave period = 4.5 to 5.9 sec[a]. Winds most frequently from Southeast, but typically not of magnitude for eolian transport[e].
Cold front	20-40[a,e]	Fronts typically migrate northwest to southeast[a]. Pre-frontal conditions: significant deep water wave height 3 to 4 m; wind from south 13[c] to 36[a] km/hr. Frontal: Surge = 0.3 to 0.4 m[a]; winds from north 55 km/hr[c]. Post-frontal: Winds from north 65-85 km/hr; peak significant wave height = 2.7 m (for 5 hr) and 1.5 m (for 24 hr) [a]. Duration: 12-24 hr[a].
TS or WH (Cat. 1 or 2)	TS: 0.625 (once every 1.6 years)[f] WH (Cat. 1 or 2) 0.24 (once every 4.1 years)[f]	Peak occurrence Aug – Sep (TS); Sep (hurricane)[a]. Surge: 0.6 m (TS *Isidore*, Sep 2002); 2.2 m (Cat. 2 *Georges*, Sep 1998)[a]. Wind: 160 km/hr (*Georges*)[a]. Significant Wave Height: 2.3 m (*Isidore*), 2.8 m (Cat. 1 *Lili*, Oct 2002)[a]; 10 m (*Georges*)[b]; Wave period: 12-14 sec (*Georges*)[b].
Moderate to Severe Hurricane (Cat. 3+)	0.10 – 0.03 (once every 10 to 30 years)[d]	Peak in Sep.[a] Surge: 6.7 m (Cat. 5 Camille, Aug 1969)[a]; 1.2 m (Cat. 4 *Frederic*, Aug 1979)[g]; 2-4 m (Cat. 3 *Andrew*, Aug 1992)[h]; 8.5 m (Cat. 3 *Katrina*, Aug 2005)[i]; 1.3 m (Cat. 3 *Rita*, Sept 2005)[j]. Wind: 322 km/hr (*Camille*)[a]; 200 km/hr (*Frederic*)[g]; 210 km/hr (*Andrew*)[h]; 260 km/hr (*Katrina*)[i]; 160-220 km/hr (*Rita*)[k]. Offshore waves: 14 m (*Andrew*)[h];17 m (*Katrina*)[i]; 12 m (*Rita*)[k].

[a]Georgiou et al. (2005); [b]Stone et al. (2004); [c]Pepper and Stone (2004); [d]Ritchie and Penland (1988); [e]Dingler and Reiss (1990); [f]Dingler and Reiss (1995); [g]Kahn and Roberts (1982); [h]Penland et al. (2003a and b); [i]Interagency Performance Evaluation Team (2006); [j]URS, Inc. (2006); [k]http://www.ndbc.noaa.gov/hurricanes/2005/rita/.

Storm and nearshore bathymetry (offshore and bay) characteristics also modify response. Wave height and period, nearshore slope, maximum surge, duration of the storm, wind speed, and storm path (influencing the wave transformation and wind direction) determine storm severity for barrier island systems. Similarly, bay depth and area, as well as duration of wind-generated waves, are controlling factors in the magnitude of bay surge and waves in the bay. For simplicity, these storm and nearshore factors are not varied in the conceptual model. Figure 4 presents the hypothetical morphologic response.

A representative cross section and planview layout is presented for the initial condition of the barrier island prior to the TS/WH (Figure 4a). In the following section, response of each type of barrier is compared for each step of the storm and recovery sequence.

Figure 4b shows each type of barrier island as the storm approaches from the Gulf. The Continuous Dune is scarped near the mean water level and higher, and the dune may avalanche as the base is removed. Some eolian transport may remove sand from the dune due to winds blowing from the Gulf and deposit it in the center of the island. The offshore bar is moved further into the Gulf. Similarly, dunes on the Dune-Washover Terrace are scarped and potentially entirely removed, as lower parts of the island adjacent to the low dunes may result in the formation of breaches. Wash-over sand is deposited into the bay, underlying fine-grained sediment is exposed, and some vegetation is removed. The Washover Flat is completely inundated during the storm, with sheet flow transporting barrier sediment from the Gulf into the bay. Fine-grained sediment and organics are exposed in areas and all vegetation is removed; permanent inlets may form.

Storm surge and winds from the bayside generate waves in the bay, and bayshore erosion occurs for all barrier types. Larger and deeper bays have the potential to generate higher waves. Later in the storm cycle, resident storm surge in the bay may return to the Gulf via existing inlets at the barrier termini, overwash of the island, and return flow through new breaches (Figure 4c). Differences in response occur for the Dune-Washover Terrace and Washover Flat, which may transport barrier sand back into the Gulf through breaches or over the island proper. For the Dune-Washover Terrace, return flow through breaches may deepen them such that they subsequently capture the tidal prism and remain permanently open.

In the recovery process, offshore bars may return to their pre-storm position (Figure 4d), and sand that was transported offshore through breaches during the surge return flow in the Dune-Washover Terrace may weld back to the barrier through cross-shore and longshore processes. However, fine-grained sediment and organics that were eroded during the storm are most likely is lost from the littoral system. Breaches that deepened during the storm may remain open, especially for the Washover Flat with its limited sand supply. The Continuous Dune and Dune-Wash-over Terrace may increase in elevation due to vegetation growth and

vegetative trapping of eolian sediment. The Washover Flat may revegetate if the frequency of storms allows growth between events.

Over time, the cycles of storms and post-storm readjustment repeat with a net removal of sediment from the subaerial barrier island system by three phenomena: (1) offshore losses during storms (sand and fine-grained sediment and organics, if present and exposed); (2) losses to the bay through overwash, breaches, inlets, and erosion of the bayshore; and potentially (3) long-term RSLR due to consolidation of the underlying sediment, geologic faulting, anthropogenic factors, and eustatic sea level rise. Figure 4e represents the long-term loss of subaerial barrier island volume due to consolidation and eustatic sea level rise. A plentiful source of sand in the littoral system has the potential to fully mitigate these losses, although in the NGOM naturally supplied sources are minimal and many barrier islands are cannibalizing themselves as a result (Penland and Boyd 1981). Without an adequate source of sediment to replenish the islands, a Continuous Dune barrier will evolve into a Dune-Washover Terrace, which will then develop into a Washover Flat, and will finally be reduced to a submerged sand shoal as discussed by Penland and Boyd (1981). It seems likely that the morphologic change process from one barrier type to the next will accelerate through time due to the increasing number of processes that are able to act on the island as it changes form. For example, the Continuous Dune will respond to wave, wind, and inlet processes (at barrier termini); however, the Dune-Washover Terrace will have these processes as well as transport due to overwash and barrier breaching.

Implications for coastal restoration and engineering design

Design of restoration for the NGOM barrier islands should consider the forcing processes as listed in Table 4. For those locations with compressible substrates, such as the Western and Central Regions (Figure 3), the increased loading of the additional sediment must be integrated into the design. Native vegetation should be planted in the primary dune complex and on the bayshore to stabilize these regions at the time of the initial restoration. Vegetation should be carefully designed to meet short- and long-term project goals. If vegetation is not planted as part of the initial restoration, the beach can be rapidly eroded if a storm makes landfall near the site before native species are established. Sand fences should be placed such that eolian transport towards the Gulf and Bay will be captured within the subaerial barrier island. To provide more ecological habitat, it may be desirable to have areas of the island that overwash

occasionally. It should be accepted, however, that such a design may result in more rapid island disintegration through breakup. Alternatively, spits on the barrier termini could potentially allow overwash and unvegetated washover deposits. Figure 5 shows a conceptual design that incorporates some of these considerations.

In Figure 5a, the barrier island is wider opposite low areas in the dune to decrease the likelihood for breaching while permitting overwash during storms. A minimum or critical barrier width is one that will capture overwashed sediment over the project life, considering other forcing processes and response (Rosati and Stone 2007). If a breach occurs during a storm, there is sufficient littoral material in the barrier system for closure of the breach by longshore transport. In Figure 5b, a design is presented that minimizes overwash within the central part of the island, instead using low-elevation spits on the barrier termini to provide washover deposits. For both designs, active planting of vegetation common to the local area is recommended to stabilize the dune and bayshore. Planting of native species at the time of restoration is beneficial in providing partial stabilization of the new project prior to natural succession of the ecosystem. Sand fencing near the base of the dune, on the bay side, is recommended to capture eolian transport from the dunes and overwash fans.

For islands that are rapidly migrating onshore and alongshore, dredged material islands constructed in the migration path could provide future sources of sediment if these mounds would not interfere with navigation channels. These islands would provide additional ecological habitat as well as a source of sediment for the barrier islands to capture as they migrated landward or alongshore (Figure 6). The islands may also partially consolidate the underlying sediments prior to occupation of the site by the barrier island. For barrier systems that are not migrating rapidly but are eroding on the bayside, the islands could provide partial protection from waves generated in the bay. For barrier systems that readily receive sediment from sub-aqueous sources (e.g., Dauphin Island from the Mobile Bay ebb tidal delta and subaerial islands; Petit Bois Island from an offshore source), a nearshore berm or submerged feeder shoals may also provide a future source as well as wave protection.

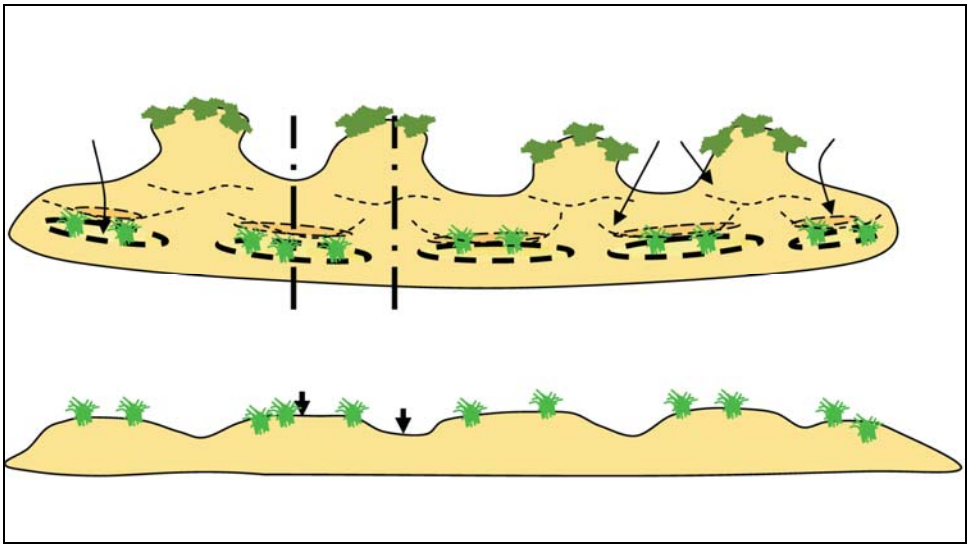

a. Design for overwash in middle of barrier island.

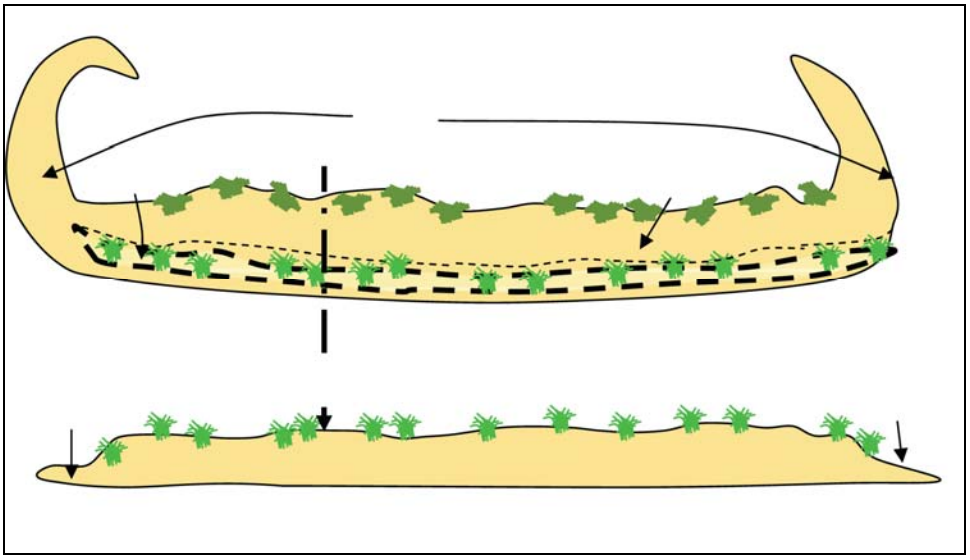

b. Design for overwash on termini of barrier island.

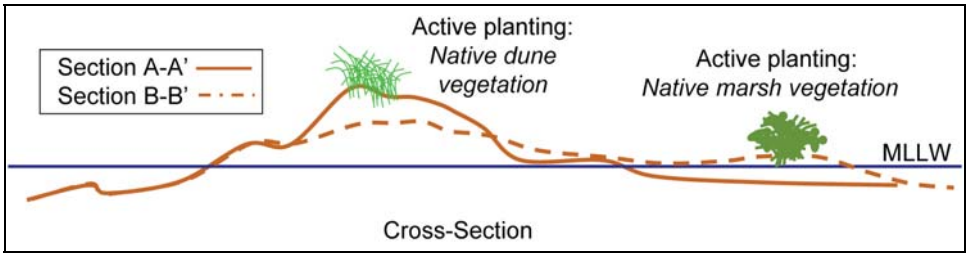

c. Cross section design.

Figure 5. Conceptual designs of barrier island restoration.

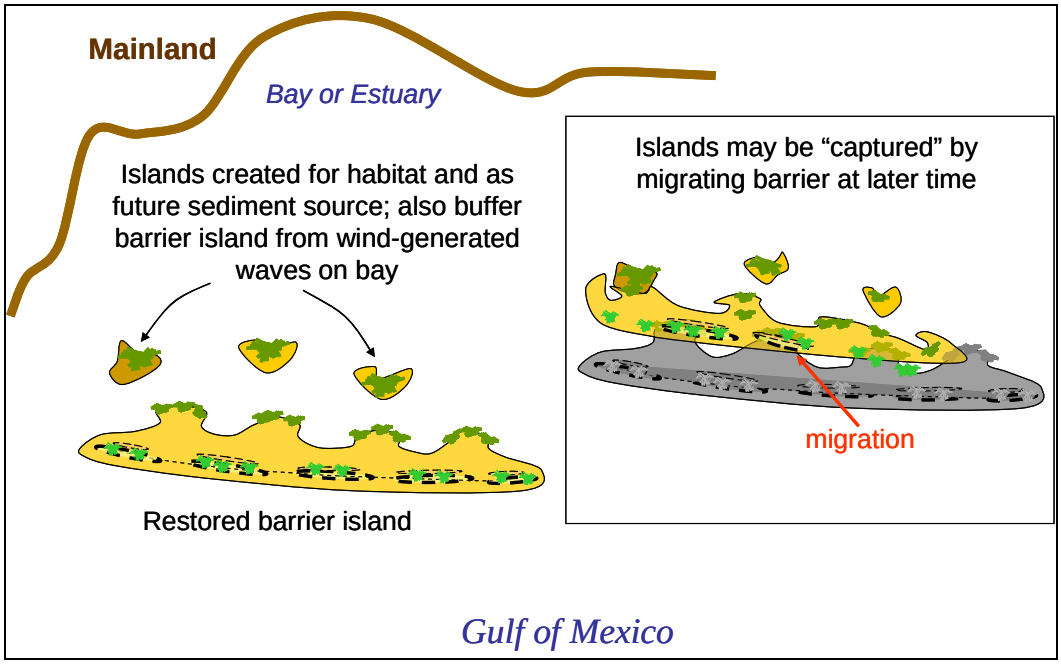

Figure 6. Regional design providing future sources of sediment for migrating barrier island.

Conclusions

In previous reviews of the literature (Schwartz 1973; Leatherman 1979, 1985), the dominant processes for barrier island migration were determined to be: (1) inlets, (2) overwash, and (3) eolian transport. Neocatastrophic events such as storms, although relatively short in duration, were suggested as the primary cause of long-term geomorphic change. Processes such as superconstruction (aggradation) of the barrier through eolian-induced deposition, shoal growth, longshore transport and spit formation, and local consolidation through self-loading of underlying substrate could be significant factors in morphologic evolution, depending on the local setting and processes.

For the NGOM, the relative significance of each process varies with location. Along the Eastern Region, a relatively abundant supply of littoral sediment both from a Pleistocene headland and the inner shelf, plus a stable substrate, creates a system that is much like those reviewed in the previous literature summaries. In this area, long-term morphologic change is similarly controlled by inlet processes, overwash, eolian transport, longshore transport, and vegetative cover. In the Central Region, a less plentiful supply of littoral sediment, a slightly consolidating substrate, and a dominant westward-directed longshore transport creates a system of five barrier islands that have, over historic time scales, migrated rapidly to the west while reducing their subaerial footprint and volume. In this region,

longshore transport is the dominant process of migration, followed by overwash, breaching, and existing inlets. Finally, along the Western Region, a low regional source of littoral sediment, a consolidating substrate, and increasing bay and inlet areas have created a system that is rapidly disintegrating. Low barrier elevations in this region result in overwash and breach formation having a greater contribution to morphologic evolution. Eolian transport does not occur as readily because low barrier elevations are wet during periods when wind speed exceeds the critical threshold for sediment motion. Sand that has overwashed the barrier may overlie a substrate that has not been previously loaded, thereby reducing the net subaerial beach due to consolidation. Common to all the regions is erosion of the bayshore during return flows from the bays to the Gulf after landfall of tropical cyclones and the post-frontal phases of winter storms when strong northerly winds occur.

Long-term modeling of barrier island morphologic response is required to evaluate the regional restoration concepts discussed herein (Figures 5 and 6). For the NGOM, these models should include pertinent processes including the propensity for both Gulf and bayshore erosion and overwash; the potential for consolidation of the underlying sediment as a function of loading, substrate characteristics, and time; erosion and eolian transport characteristics of vegetated and unvegetated clay, silt, organics, and sandy sediment; and the availability of littoral sediment to rebuild the island in the post-storm phase. The research discussed here develops a model that can be applied to understand the long-term stability of these islands, and how they can be maintained within the context of future rise in eustatic sea level and potential increase in storm frequency and intensities forecasted by the Intergovernmental Panel on Climate Change (2008).

3 Review: Barrier Island Modeling and Consolidation

Overview

In this section, selected conceptual and numerical models that calculate morphologic-scale characteristics and long-term (decades to centuries) evolution of barrier islands are reviewed. This summary is not intended to be all-encompassing, but is intended to highlight relationships and modeling studies pertinent to understanding long-term evolution and large-scale restoration of barrier islands in deltaic environments. As compared to models intended for predicting the evolution of mainland sand beaches, additional processes and phenomena that may be important for predicting barrier island evolution in deltaic settings are listed in Table 5.

In addition to modeling applications, studies that have examined and modeled consolidation of barrier islands in coastal regions are discussed. This review lays the foundation for development of the 2D MCO model and is intended to demonstrate the uniqueness of this study as compared with previous work.

Table 5. Processes of potential importance in modeling barrier island evolution in deltaic settings.

Washover sand into the bay and possible “recapture” of this sand at a later time as the island migrates.
Wave-induced erosion on the bay shore due to wind-generated waves on the bay (if bay fetch and wind speed are sufficient).
Inlet breaching from both ocean and bay side of island.
Potential for permanent inlet formation and loss of barrier sand to ebb and flood tidal deltas.
Multiple sediment types. - Typically, sand beach on ocean and fine sediment (silt and clay) marsh in back barrier; sand may be limited in thickness and overlie a core of fine sediment and organics.
Wave transformation over muddy seabed and fluid mud that may modify incoming waves.
Consolidation of the underlying substrate and potential for additional loading of the substrate through migration, and loading of back barrier marsh with washover deposits.

Previous studies

Modeling

Conceptual

The Bruun Rule (Bruun 1962) is the simplest model for long-term evolution of the shoreface. It predicts equilibrium shoreface retreat given the rate of relative sea level rise and the vertical and horizontal extents of the active profile. The relationship is formulated by equating the volume eroded by relative sea level rise to the sediment required to increase the elevation of the active profile, and the profile retreats parallel to itself. Dean and Maurmeyer (1983) modified the Bruun Rule for barrier islands (hereafter, "Barrier Bruun Rule"), including terms relating the active extent of the lagoon (or bay) in the vertical and horizontal dimensions.

$$R = S\frac{L_* + L_W + L_L}{\left(B_o + h_*\right) - \left(B_L + h_L\right)} \tag{1}$$

Recession of the shoreline is given by R, the rate of relative sea level rise is S, L_* is the width of the active ocean profile, L_w is the width of the barrier island, L_L is the width of the active lagoon (bay) profile, B_o and B_L are the berm heights on the ocean and lagoon, respectively, and h_* and h_L are the active depth of the ocean and lagoon profiles, respectively (Figure 7). Dean and Maurmeyer (1983) noted that if the active profiles on the ocean and bay are equal ($B_o + h_* = B_L + h_L$), there would be no potential for building up of the island during landward migration and the barrier island would narrow, essentially "drowning in place." Interestingly, the terms "drowning in place" and "island submergence" have been used to describe evolution of barrier islands and presence of sand shoals in Louisiana (McBride et al. 1995; Stone et al. 2004) as well as to explain submergence of barriers for the shelf offshore of Fire Island, New York (Sanders and Kumar 1975).

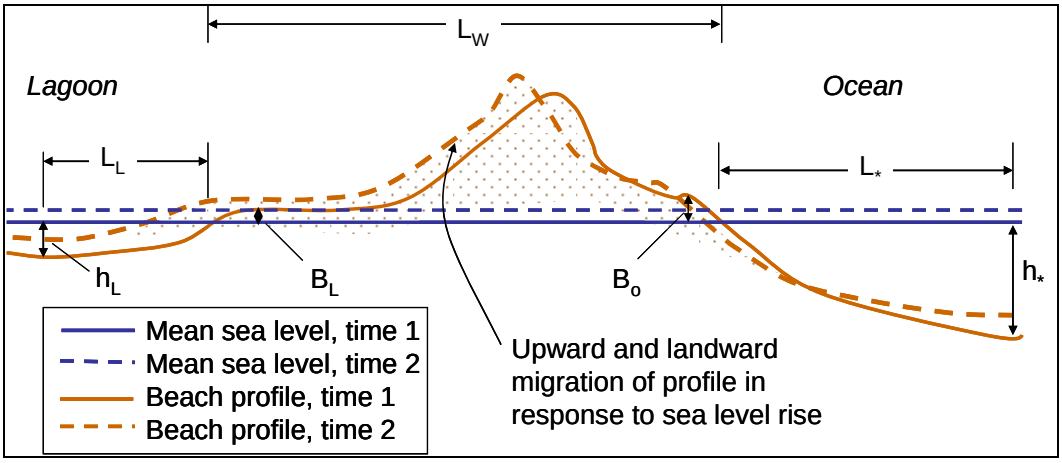

Figure 7. Bruun Rule modified for barrier island migration due to sea level rise (adapted from Dean and Maurmeyer 1983; Dean et al. 2002).

Maurmeyer and Dean (1982) applied the original form of the Bruun Rule and compared predictions to the Barrier Bruun Rule. They compared calculations at six barrier island sites along the Atlantic East Coast of the United States, from New Jersey to North Carolina, and found that the original Bruun Rule under-predicted retreat rates by 60 percent whereas the Barrier Bruun Rule estimated the average within 3 percent.

In application of the Bruun Rule to 37 locations along the barrier islands and headland beaches of Louisiana, a deltaic system that overlies a consolidating substrate, List et al. (1997) found no significant correlation between predicted and measured shoreline recession. The study applied the original Bruun Rule and modified it to account for loss of fine sediments as the beach eroded. The calculations under-predicted retreat by 72 and 58 percent of the observed change for analyses from 1880s through 1930s, and 1930s through 1980s, respectively. The authors discussed reasons for the lack of correlation, including: (1) massive redistribution of sediment alongshore from the nearshore and shoreface, which has resulted in regions of sediment surplus and deficit in the sediment budget; (2) rapid disintegration of wetlands which has created an inability for barriers to maintain their subaerial form as they retreat; and (3) loss of sand-sized sediment through formation of ebb and flood deltas, which have increased due to larger tidal prisms. The List et al. (1997) study illustrated that simple profile retreat modeled by the original Bruun rule accounting for loss of fine sediments did not apply to the Louisiana coast. However, inference from Maurmeyer and Dean's (1982) study suggests that application of the Barrier Bruun Rule may have improved correlation.

Based on shoreline position data spanning at least an 80-year period, McBride et al. (1995) characterized eight geomorphic response-types for barrier island systems for sites in the northern Gulf of Mexico and north-eastern Florida. The authors found that barrier islands in Louisiana were best characterized by landward rollover, retreat, and breakup. Landward rollover, in which overwash processes cause erosion and retreat of the ocean beach and accrete the bayside, was noted to initiate once the barrier island had reduced to a critical width such that washover deposits would reach the bay. Breakup of barrier islands occurred when the island narrowed and breached during storms. Inlets that formed did not close, but widened. Barrier island systems with a high rate of relative sea level rise, such as Louisiana, are dominated by landward-directed, cross-shore processes with longshore transport having secondary importance.

As described in the preceding chapter, Campbell (2005) developed a four-stage conceptual dynamic morphosedimentary model (DMSM) describing barrier island retreat for the mixed deltaic sediment barrier islands in Louisiana, and the model has been applied in conjunction with numerical models to design several nourishment projects. The DMSM accounts for retreat of the beach in response to relative sea level rise and release of silt from the barrier beach to the offshore.

The DMSM begins with an initial barrier with a thin sand layer over mixed deltaic sediment (sand, silt, and clay), backed by a wide marsh system (Stage 1). During storms, the Gulfside sand is eroded and marsh vegetation and deltaic sediment are exposed to wave attack (Stage 2); sand is released to the system as the mixed-sediment beach retreats (Stage 3). Sand released in Stage 3 eventually accumulates back on the beach; however, the marsh is much reduced in area (Stage 4) (Campbell 2005).

The DMSM lends two new insights into understanding of barrier island processes in deltaic settings. First, for several locations in Louisiana, a break in the slope of the beach profile was observed between 1.5-2.0 m depth, relative to MHW. Shallower than 1.5-2.0 m, the beach had an equilibrium profile shape, and seaward of this depth, the profile was linear with a 1V:400H slope. The DMSM estimates the depth of closure for sand transport at this depth, and silt that is eroded from the barrier island is assumed to be deposited offshore of this depth. It is not known whether this break in slope is observed in other mixed-sediment environments.

Secondly, the DMSM postulates that most of the barrier island retreat occurs after the storm has passed, during the time when the protective sand beach has not yet recovered and the barrier island marsh and fine sediment are exposed to wave action (Campbell et al. 2007). Some support for this hypothesis exists in subaerial island area change for Raccoon, Whiskey, Trinity, East, and East Timbalier Islands, LA, in the year following Hurricane Andrew (1992-1993). During this time, the island areas decreased as compared to post-storm measurements in 1992 (Penland et al. 2003a and b). However, it is not known whether this continued area change was due to loss of the protective sand beach as postulated by Campbell et al. (2007), changes to morphology of the islands due to the storm (e.g., lower island elevation would increase overwash), or natural evolution that would have occurred with or without the sand beach.

Campbell et al. (2005a) discussed two approaches for restoration with the DMSM. The first is a "stable design," in which the project is planned such that the island is maintained in a geographic location by eliminating frequent overwash and breaching. The second is "retreat design," which allows the island to migrate but maintains a constant island area. The difference in design for these two types of restoration enters into the dune elevation and the amount of fine sediment that is lost offshore over the project life.

The DMSM has been applied to develop sediment budgets which are then used in conjunction with other numerical models to design beach nourishment projects in Louisiana. Campbell et al. (2005b, 2006) discussed application to Holly Beach, West Grand Terre, and Shell Island; and Thomson et al. (2005, 2007) designed beach nourishment for Raccoon Island, East Grand Terre, and Chaland Headland. The volume required for the life of these projects was determined based on longshore transport rates into and out of the project area, overwash, erosion of the beach, and loss of fines offshore. For some of the projects, numerical modeling of longshore and cross-shore processes was conducted in conjunction with the sediment budget that had been formulated through application of the DMSM. For the Chaland Headland project (Thomson et al. 2007), sand was placed to build the Gulf side of the barrier beach, and silt was placed to create wetlands in the back barrier region. Consolidation of the back barrier marsh due to geologic subsidence, consolidation of the placed sediment, and the weight of additional sediment over the substrate was incorporated into the design. However, none of the beach nourishment

designs in Louisiana considered the potential for consolidation due to the additional loading of the beach itself, nor consolidation due to potential migration of the project onto a previously under-consolidated substrate.

Numerical

Decadal to Geologic-Scale Coastal Behavior Models. Several studies have modeled barrier island response to long-term changes in sea level rise and sediment supply over geologic time scales and large spatial extent. Cowell et al. (1995) developed a shoreface translation model and simulated barrier island transgression and recession on the Turncurry shelf, Sydney, Australia. This approach combined both heuristic and deterministic methods to predict evolution of a barrier island as it either: (1) migrated across the shoreface, (2) eroded and deposited offshore through rising sea level, or (3) evolved in an intermediate state between (1) and (2). The pre-existing substrate could be defined to be non-erosive, or comprised of sand or mud, and estuarine sediment deposition could be sand and mud. However, consolidation of estuarine sediments and the substrate as a function of washover deposits and migration of the barrier island were not included in the model.

Stolper et al. (2005) introduced a morphologic model called GEOMBEST for cross-shore evolution of barrier islands, the shoreface, and estuary over time scales of decades to centuries. The model incorporates sediment supply and availability represented by two grain size classes (mud and sand), relative sea level rise, and characterizes the subsurface stratigraphy. Morphologic evolution is calculated with sediment conservation principles in a manner similar to the Bruun Rule, with two differences. First, GEOMBEST represents portions of the subsurface with varying erodibility and retention characteristics, such as a less-erosive Pleistocene substrate, or mud which is rapidly eroded and lost from the system. Secondly, the model incorporates a time-lag in evolution as a function of depth, which characterizes long response times for the shelf. Stolper et al. (2005) simulations with GEOMBEST indicated that, as barrier islands migrated landward with rising sea level, the estuary behind the island filled in with fluvial and organic sediments thereby reducing accommodation space for migration of the barrier island. Infilling of the estuary was predicted to reduce island transgression rates, although the island narrowed and eventually became submerged. Shallow offshore slopes were associated with wide estuaries, and steep slopes with narrow or non-existent estuaries. Consolidation of the estuarine sediments due to autocompaction and migration of the barrier island was not considered.

Process-Based Modeling of Barrier Islands. Jiménez and Sánchez-Arcilla (2004) developed a model to calculate the decadal-scale evolution of a barrier spit along the Spanish Mediterranean coast. Shoreline response on the seaside and bayside shorelines was coupled with two sub-models. The open coast was forced with a morphological wave condition and local sand transport coefficient that produced representative decadal-scale longshore sand transport rates along the barrier spit. Bayshore accretion was triggered by overwash processes when the spit width was less than or equal to a critical value. Overwash transport rates were parameterized based on observed behavior of the barrier spit over 30 years. Thus, gradients in longshore sand transport rates on the seaside shoreline determined when the barrier spit eroded, reached a critical width, and initiated overwash processes to the bayside.

Alfageme and Cañizares (2005) applied the Delft3D wave, circulation, sediment transport, and morphology change model in evaluation of a design for the Whiskey Island, LA, West Flank barrier island restoration project. They simulated beach change due to four hurricanes and four tropical storms, intended to represent a 20-year project design life. Relative sea level rise was incorporated into the calculations with an increase in mean water level through time totaling 0.21 m over 20 years. Cold fronts, which occur approximately 30 times each year in the region, were not simulated and thus losses due to inlets and recession of the shoreline were likely under-predicted. Also, eolian transport, potential loss of wind-blown sand, and dune formation were not represented in the simulations. All simulations were conducted with a uniform 0.15-mm sand that was representative of the beach. Their results indicated that the center of the island was more stable than the flanks for both the with-project and without project simulations. Without the project, the flanks of the island experienced 120 m recession; with the project, the western flank migrated north 330 m and half of the back barrier marsh was covered with sand. The authors do not discuss whether the storms they modeled also simulated processes on the bayshore, i.e., storm surge in the bay and wind-generated wave erosion on the bayshore. Consolidation of the island due to additional loading of the project was not considered.

de Sonneville (2006) and Campbell et al. (2007) applied Delft3D to examine hypotheses of the DMSM. They found that, with conditions such that storm surge plus wave runup do not overtop an island with mixed sand and fine sediment, Delft3D calculations supported the differentiation of sand shoreward and finer sediment seaward of the break in slope (depth

of 2 m MHW). If the island is submerged during more severe storm events, all sand transport is directed onshore (onto back barrier or into the bay) via overwash processes. During typical (non-storm) wave conditions, sand transport occurs mainly in the surf zone while mud is transported and deposited offshore of the break in slope.

van Maren (2005) applied Delft3D to test hypotheses of barrier island formation and destruction at an actively prograding deltaic system, the Red River Delta in Vietnam. This deltaic system differs from the Mississippi River system in that there is an excess of sediment delivered to the nearshore system, and multiple barrier islands form in progressively seaward positions approximately every 100 years or so. These sandy deposits are approximately 10 m thick, spaced approximately 5 km apart in the cross-shore direction, and overlie a 40-50 m thick silt and clay layer. Thus, it is presumed that compaction of the silt and clay layers beneath the sand deposits would occur due to the weight of the sand deposits.

Through the numerical modeling, van Maren showed that onshore sediment transport due to asymmetry of intermediate height waves (2-3 m) was the mechanism that created nearshore bars which then migrated shoreward. This bar was considered to be the initial stages of barrier island formation. The mechanisms for erosion of the barrier islands were hypothesized to be river flooding and typhoons. In the modeling, two historical river flooding events did not sufficiently erode the barriers as has been observed in the field. Modeling of the typhoon event predicted landward migration of the barrier island. van Maren concluded that fluvial erosion was the main mechanism that opposed barrier island formation. Potential consolidation of the underlying substrate due to the sand loading was not considered.

Ellis and Stone (2006) modeled net longshore sand transport rates for the Gulf shoreline of Chandeleur Island, LA, using a wave-refraction model, WAVENG. Chandeleur Island is a transgressive barrier island system formed when the St. Bernard delta of the Mississippi River system was abandoned 2,000 years ago. Morphologic change of Chandeleur Island is dominated by overwash processes, although longshore and offshore transport also control evolution. The authors' calculations indicated a bi-directional net longshore sand transport system with a nodal zone in the center of the islands. From the calculated gradients in the net longshore transport system and implied volumetric flux to the southern portion of the Chandeleur Island, the authors concluded that this region should be

more stable than is observed. They discussed the potential for variable subsidence rates within the Chandeleur Island due to differences in the accommodation space above the Pleistocene platform. The authors speculated that thicker sequences of Holocene sediments in the southern portion of the Chandeleur Island may experience increased sediment compaction and subsidence as compared to the northern section of the islands, which may be a reason for the increased erosion in this region.

Consolidation

Overview

Compaction or consolidation can be a factor in coastal evolution if poorly-consolidated facies such as fine-grained sediment deposited by a river, or organic deposits that decay with time are subjected to additional weight. In the coastal environment, additional loading can occur with natural deposition of sediment, artificial placement of sediment, and construction of infrastructure. Primary consolidation occurs as fluid or gas that is trapped in the voids between the grains is expelled and the grains shift due to loading. Secondary consolidation continues indefinitely after the fluid and gas have been expelled as sediment grains deform (Wu 1966). The rate of consolidation decreases with time, but can increase with additional loading. Relative sea level change, the sum of eustatic sea level and local elevation change, is the net result.

Sediment has the potential to compress significantly under load due to factors such as reduction in void space, biochemical decay of organic materials, and grain shifting and breakage. Pore pressure increases if a load is applied to a saturated soil. For sands, the excess pore pressure is dissipated quickly due to their high permeability. However, clays, organic soils, and silts have much lower permeabilities; thus, the excess pressure dissipates much more slowly, and consolidation continues for a much longer time.

Consolidation of sediment occurs in three stages: (1) immediate settlement, which occurs as soon as the load is applied due to compression and solution of air in the voids (and, to a small degree, compression of trapped fluid and load transfer to the sediment); (2) primary consolidation, during which excess pore water pressure is dissipated; and (3) secondary consolidation or creep, which occurs after the excess pressure has been eliminated and continues indefinitely, at a decreasing rate due to shifting and

fracture of particles and breaking of inter-particle bonds (Sowers 1979) (Figure 8).

Coastal substrates that have the potential for significant consolidation include fine-grained sediment that has not been significantly loaded (e.g., clays and silts deposited by river systems), organic peaty sediment, and sediment with interlaying organic strata. Sediment loaded at an earlier time in its geologic history, e.g., due to glacial loading or construction of infrastructure, will rebound slightly once the load is removed. If reloaded with a greater weight, this sediment will continue the consolidation process.

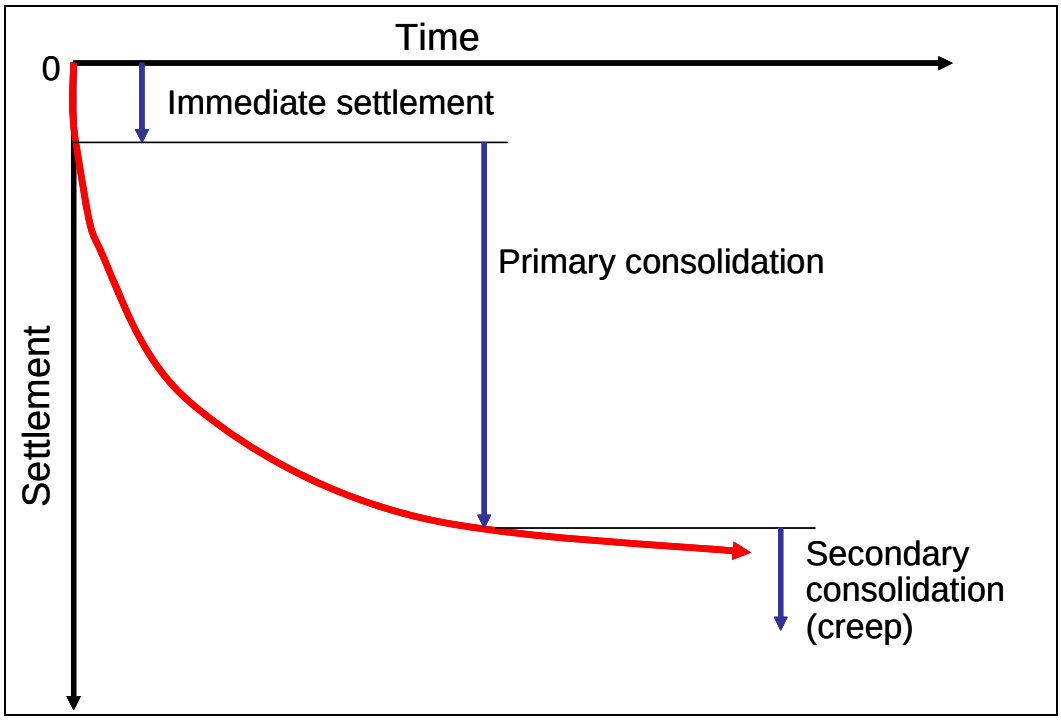

Figure 8. Definition of soil settlement and consolidation regimes.

Consolidation and barrier islands – a review

In this section, studies that have discussed geomorphologic evolution of coastal barrier islands, estuaries, bays, and lagoons due to differential loading of sediments and the resulting consolidation are reviewed. This review is intended to: (1) develop the state of understanding for this phenomenon, (2) establish an understanding for the magnitude and potential significance for observations, and (3) demonstrate that the subject of this technical report (modeling of consolidation due to loading by barrier islands through migration) is a unique topic.

Dillon (1970) and Newman and Munsart (1968) interpreted sediment core data in terms of the long-term migration of the barrier islands (Charleston-Green Hill barrier-lagoon, RI; Cedar and Parramore Island, VA). Outcroppings of lagoonal peat on the ocean side of the island, as well as lagoonal clay and silt beneath sand in the core data indicated that these islands had rolled over via washover processes as sea level increased elevation. Although these studies did not specifically discuss consolidation due loading by these barrier islands, they made the connection between the increase in eustatic sea level and island washover and migration. The importance of this finding to the present study is that barrier island migration may occur over potentially compressible lagoonal deposits of peat, clay, and silt, which could be a factor in future morphologic change of barrier islands with predicted rise in eustatic sea level.

Many studies have discussed compaction of peat deposits, either due to autocompaction (compaction due to self-weight) or compaction due to subsequent loading by estuarine sediments, in lagoons, estuaries, and deltaic settings (e.g., Bloom 1964; Kaye and Barghoorn 1964; Cahoon et al. 1995; Long et al. 2006; Meckel et al. 2007). Peat is much more compressible than other types of substrates such as sand, clay, silt, or mud. However, similar to sediment substrates, the magnitude of peat consolidation is related to the thickness of the deposit (Kuecher 1994; Meckel et al. 2007). For example, Bloom (1964) measured 13 to 44 percent compaction of a sedge-peat deposit due to loading by a 10 m deposit of estuarine mud in Clinton, Connecticut. Long et al. (2006) determined that rapid compaction was a primary mechanism driving coastal change for a coastal marsh in southeast England, United Kingdom, where the peat surface compacted at least 3 m due to loading by 4 m of intertidal mudflat and tidal channel sediments. Meckel et al. (2007) developed a compaction model for deltaic settings and concluded with a statement pertinent to this technical report: “high density, permeable sediments such as sand, at the surface (typically considered relatively stable) can be associated with high compaction rates, especially if they overlie thick peat deposits.”

Guber and Slingerland (1981) were the first to introduce the concept that back-barrier sediments can be compressed under loading by dredged material that is placed within the estuary or bay, or sediment overwashed (“washover” deposit) from a barrier island. Data from two dredged sediment disposal sites placed on the back marsh of Assateague Island, Maryland, indicated a linear relationship between the effective pressure (overburden) and subsidence of the marsh surface, with the older site

having greater subsidence due to the longer loading time. They also calculated that lateral plastic flow and diapirism (extrusion of sediment from the substrate such as "mudlumps" of the Mississippi River Delta system; Morgan 1951) are possible with loading by barrier island sands and tidal deltas, for cases in which the pore water pressure is the same order of magnitude as cohesion in the substrate (in units of kPa; Guber and Slingerland 1981).

Guber and Slingerland (1981) discussed three possible consequences of compaction and lateral flow of sediments in the vicinity of barrier islands:

1. Washover removes sand from the foreshore or dune system and, with settlement into a compressible marsh or bay subsurface, would induce more losses from the barrier island system rather than increasing elevation. Thus, the island would be susceptible to additional overwash in the same region and this additional overwash would increase migration and breakup of the island. Although eustatic sea level rise had been previously cited as the only mechanism for barrier island migration, Guber and Slingerland suggested that compaction may also be a factor in migration.
2. They speculated that the barrier island cross-section and resulting geomorphology may be influenced by the subsurface characteristics, especially if the subsurface were non-homogeneous. Variable retreat rates for barrier island systems might be related to subsurface characteristics (e.g., void ratio, permeability, yield criteria). Observations of washover fans on Assateague Island, Virginia and Maryland, showed lower elevations at the distal ends of the fan as evidenced by ponding as compared to the adjacent marsh surface which was at the mean water level. These fans also indicated that lateral flow of the subsurface sediments might have occurred, as evidenced by arcuate ridges paralleling the distal portions of the fans.
3. The potential for settlement must be known for characterization of the sediment budget of the barrier island system and washover fans. The authors presented a conceptual diagram illustrating the role of compaction in barrier island migration.

In a study of Virginia barrier islands, Gayes (1983) surveyed the barrier and beach profile, and took sediment cores across three consolidating barrier island systems, Assawoman, Metomkin, and Wallops Islands, VA. (Figures 9 through 13). These data show the compaction of clay and silt beneath the overlying sandy barrier island, which has occurred as the islands have migrated landward from 3.8 to 4.8 m/year. If consolidation of

the underlying substrate had not occurred, the sand-clay/silt interface would lie at approximately the zero MHW line. Void ratios (volume of voids divided by volume of solids) of the back-barrier sediment are greater than those of the clay and silt underlying the sandy barrier island, reinforcing the interpretation of consolidation due to the loading of the island. Based on the measurements and island migration rates, these barrier island systems have experienced consolidation between 0.1 and 3.5 m over 35 to 40 years. These data are discussed further and compared with the 2D MCO model in Chapter 4.

Kuecher (1994) studied the consolidation potential for sediment in the Mississippi River deltaic plain. He found values of the dimensionless compression index, C_c = 4.7 to 5 for peat and organic muck, 1 to 3 for prodelta mud, 0.86 for bay sediment, 0.123 for natural levee sands and silts, and 0.063 for point bar sands. Larger C_c values indicate a greater potential for consolidation. Kuecher concluded that the distribution and thickness of peaty marsh soils was a first-order cause of coastal land loss in Louisiana. In the region of the abandoned LaFourche Delta, thicker deltaic sediment correlated with the highest rates of land loss as compared to thinner deposits. Similarly, Penland and Ramsey (1990) found local rates of relative sea level rise related to the thickness of Holocene sediment for the Mississippi river delta and chenier plains. Kuecher discussed the consolidation associated with loading by barrier islands, and hypothesized that Pelto Bay and Big Pelto Bay north of the Isle Dernieres, evident as generally parallel to the Isle Dernieres barrier island chain in the 1853 shoreline map (Figure 14a), were initiated due to loading of the prodelta muds by the barrier island chain. After the settlement began, deposition of bay muds continued loading the underlying sediment. He conceptualized a cross-section of the underlying prodelta mud and barrier island, using available sediment core data from offshore of Trinity Island, the eastern-most barrier in the Isle Dernieres barrier chain (Figure 14b).

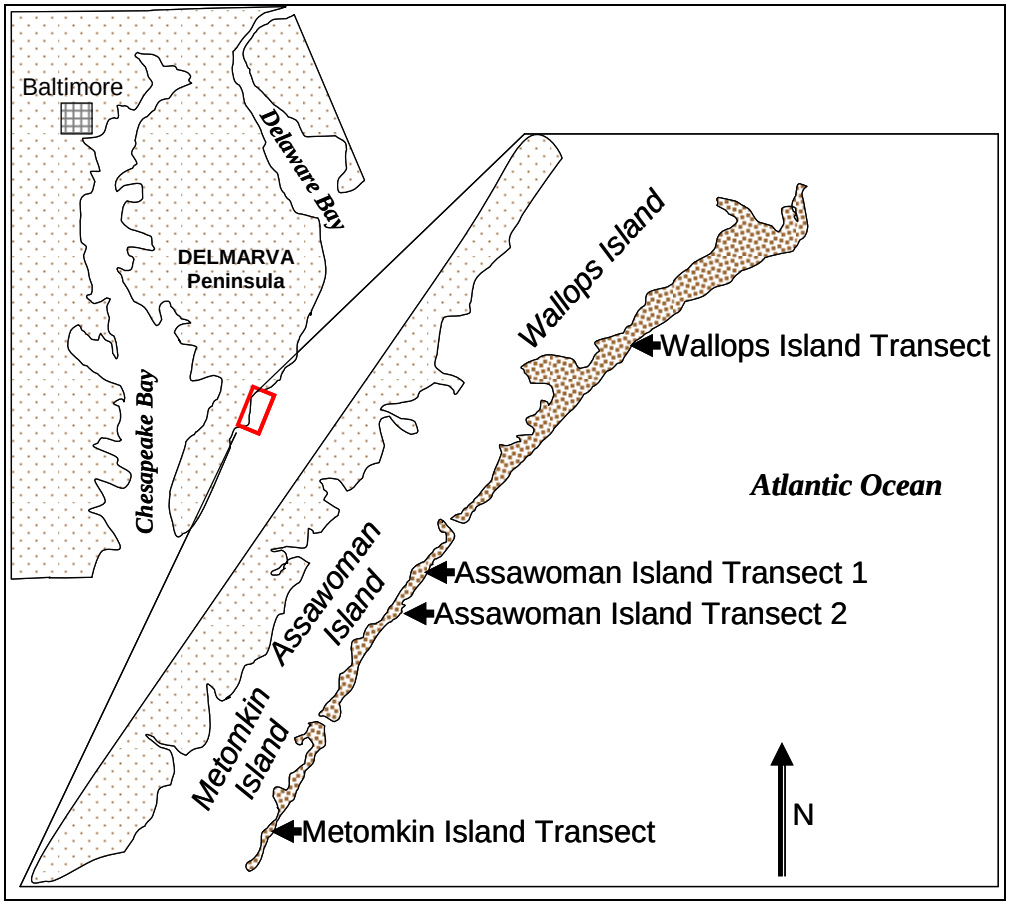

Figure 9. Location map for Virginia barrier island data (from Gayes 1983).

Roberts et al. (1994) linked consolidation of Holocene sediments in the Mississippi River deltaic system to the thickness of the deposits. In turn, the thickness of these deposits is correlated with the location of previous fluvial entrenchment by the Mississippi River system. Thus, with knowledge of the sediment type and former locations of fluvial entrenchment, Kuecher's (1994) and Roberts et al.'s (1994) work lend information with which to estimate potential future compaction of the substrate as a function of the magnitude of the loading.

In a review of first-level design models for barrier island beach nourishment with application to Louisiana, Dean (1997) noted that subsidence "is a potentially significant factor and must be considered in the response of the entire system." Dean discussed the additional consolidation incurred as the barrier islands continue retreating, stating that "upon retreat they load new uncompressed sediment, (and) subsidence occurs due to consolidation and the retreat process is thereby perpetuated."

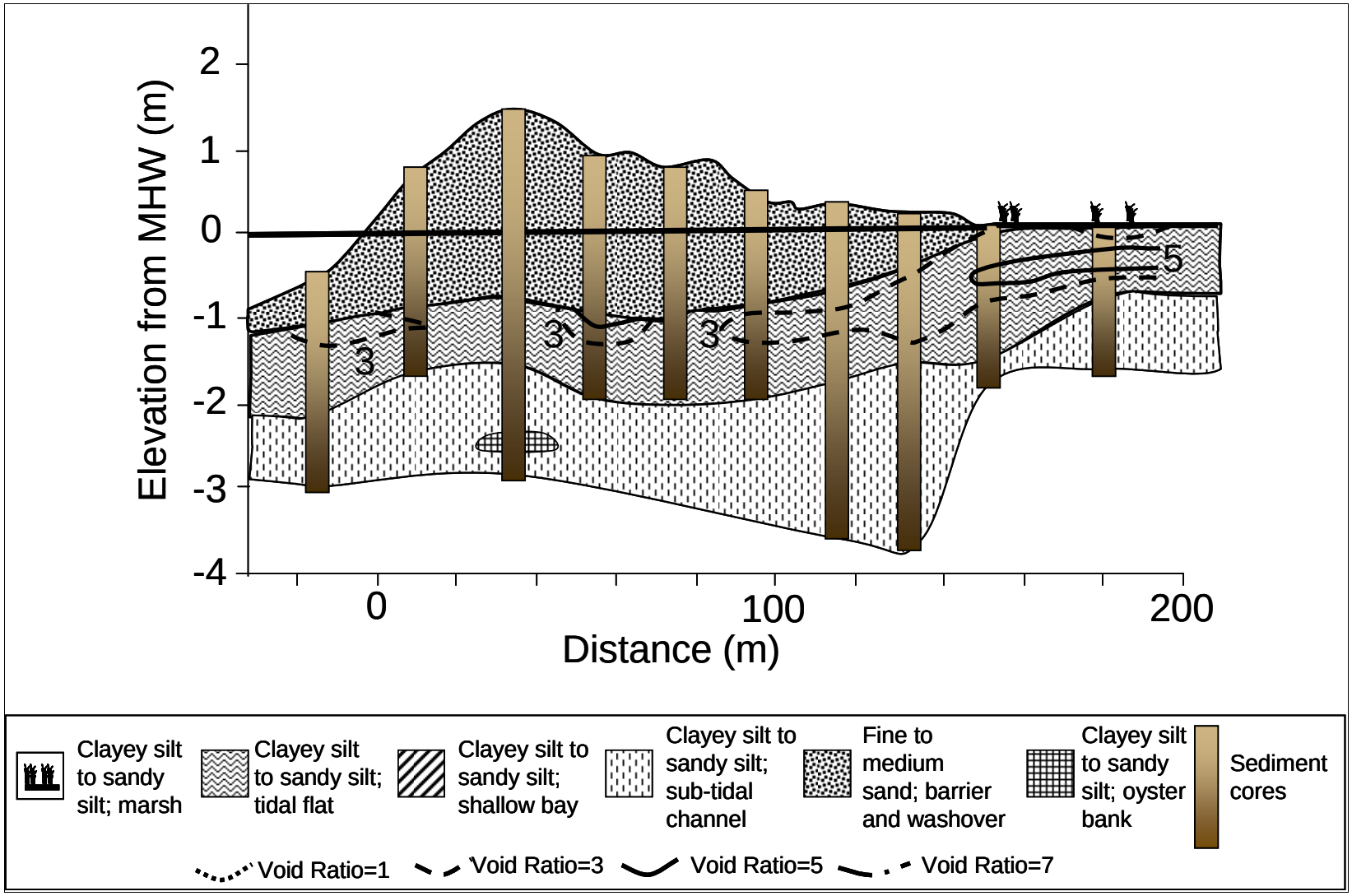

Figure 10. Assawoman Island, VA, Cross-Section #1 (adapted from Gayes 1983).

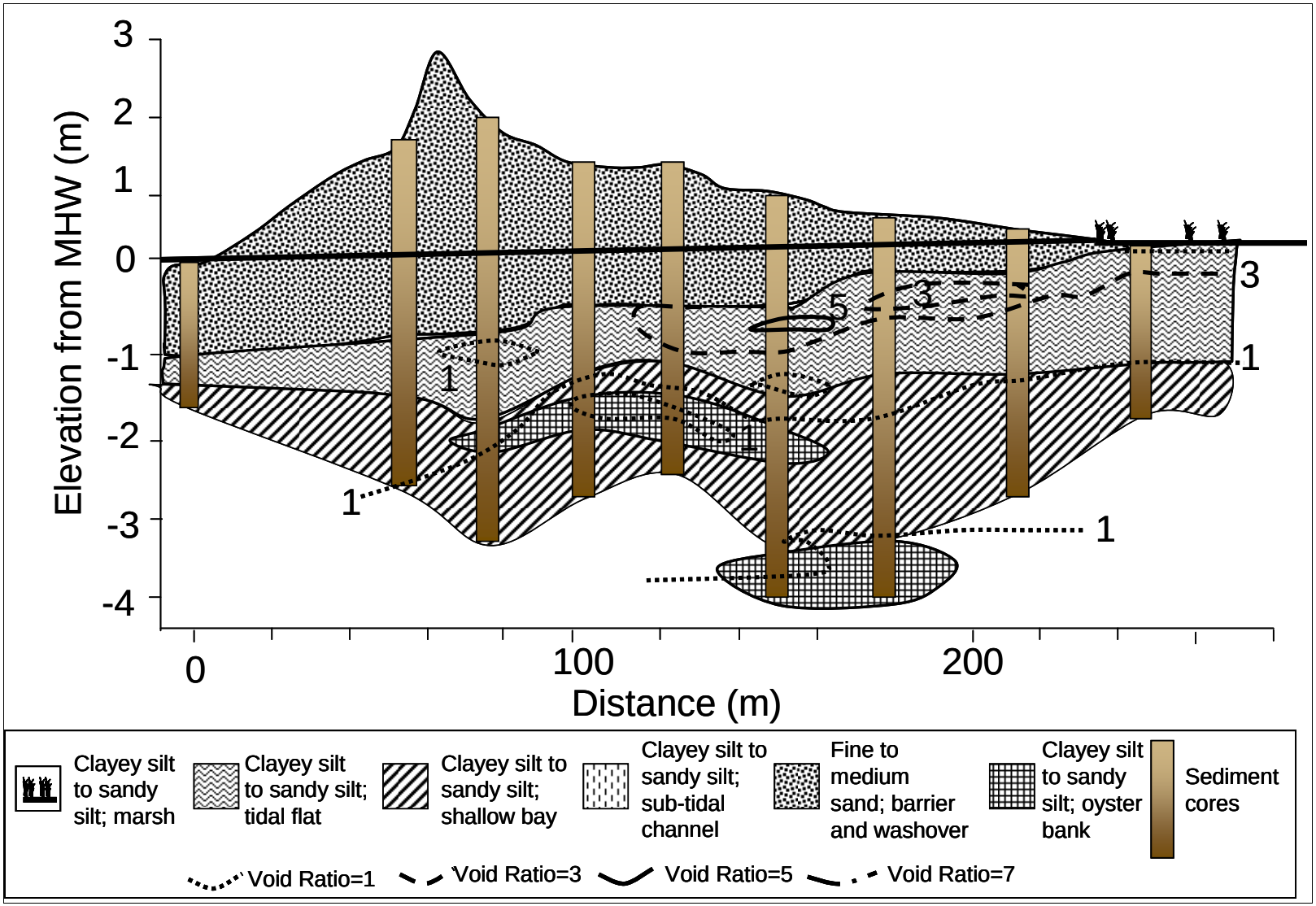

Figure 11. Assawoman Island, VA, Cross-Section #2 (adapted from Gayes 1983).

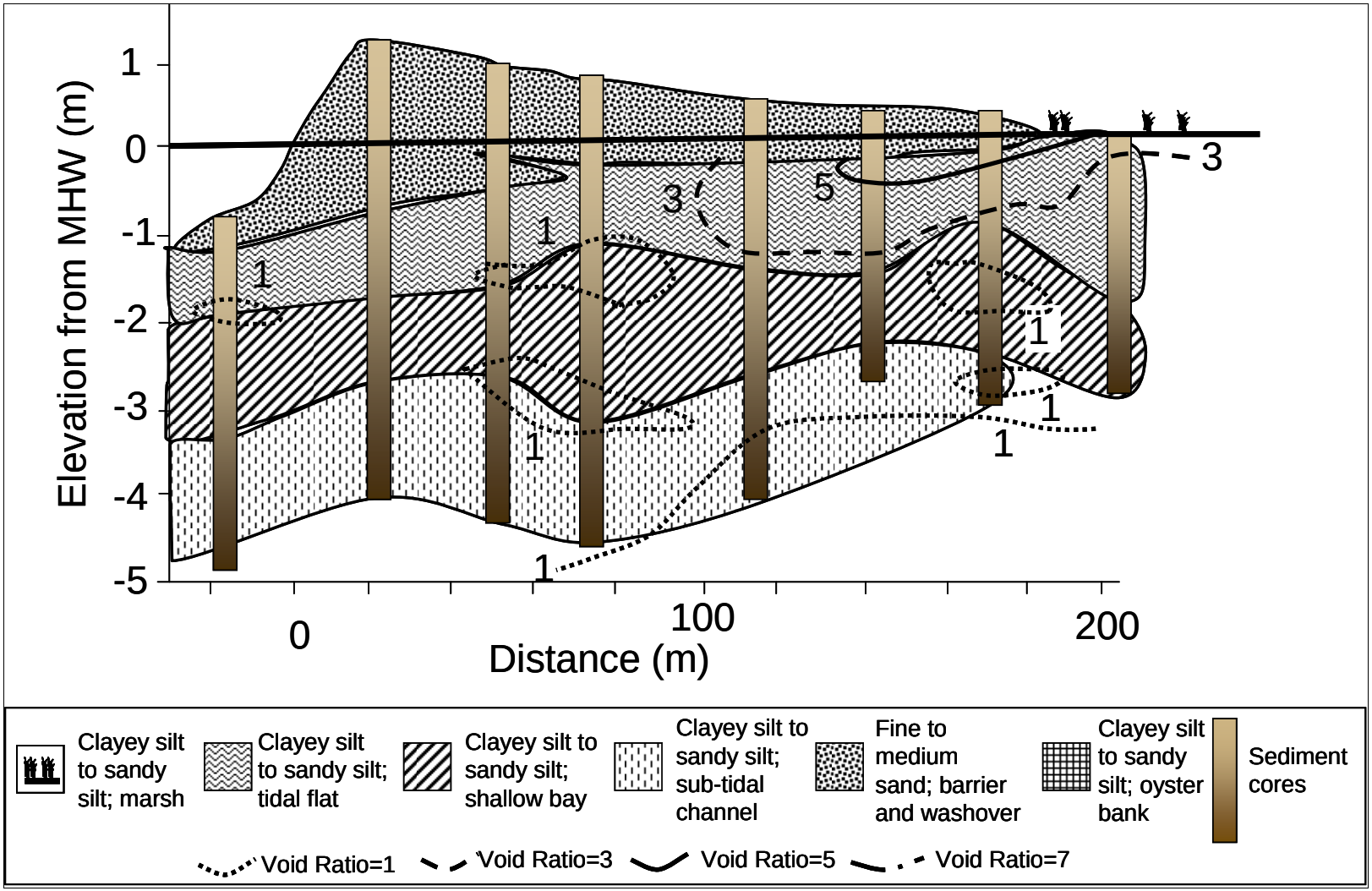

Figure 12. Metomkin Island, VA (adapted from Gayes 1983).

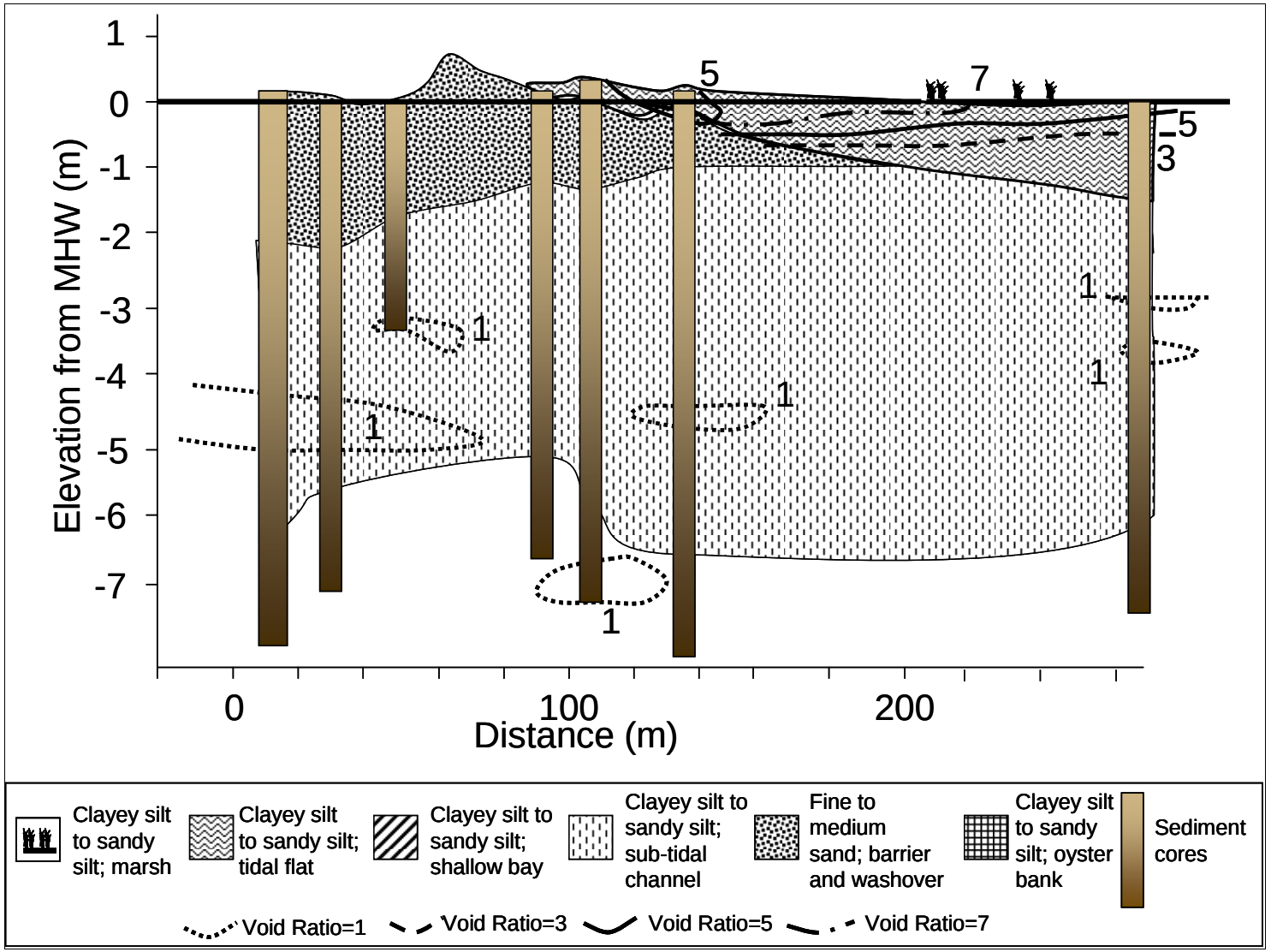

Figure 13. Wallops Island, VA (adapted from Gayes 1983).

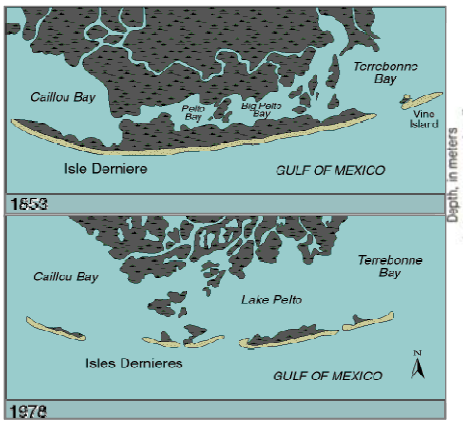

(a) Initiation of bay subsidence due to barrier loading? (hypothesis from Kuecher, 1994; figure from Penland and Boyd, 1981)

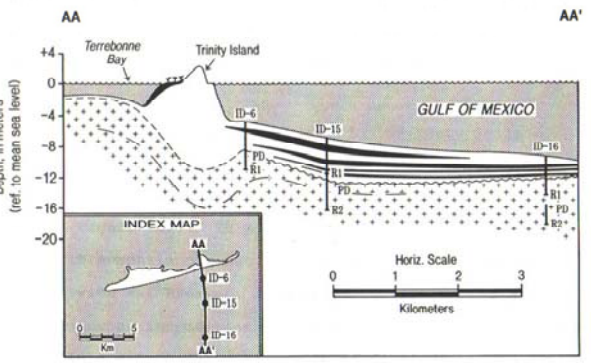

(b) Cross-section illustrating conceptual model for subsidence, Trinity Island, Louisiana (Kuecher, 1994)

Figure 14. Hypothesis about deformation of bay prodelta muds in Louisiana (Kuecher 1994).

Bourman et al. (2000) discussed rapid geomorphologic changes that have been observed at the River Murray Estuary, Australia due to eolian, riverine, tectonic, tidal, and wave processes, as well as changes in eustatic sea levels over the past 125,000 years and recent human activity. Of pertinence to this review is the observation that, as barrier islands fronting the River Murray Estuary have migrated landward over the past 3,000 years, they have exposed lagoonal markers (sediments, shells, tree stumps) on the ocean beaches. In addition, migrating dunes have differenttially loaded plastic mud in the lagoon resulting in an increase in height up to 10 m above present sea level. The authors discussed that differential loading of these lagoonal sediments was sufficient to explain their elevation, but that seismic events may have also played a role.

Conclusions

This chapter reviewed the state of knowledge for modeling barrier island morphologic change and discussed the potential role of consolidation in reference to barrier islands. The purpose of the review was to demonstrate that the topic of this technical report is unique and of potential significance for barrier islands overlying compressible substrates.

The review highlighted studies of barrier island evolution that have applied conceptual analyses and numerical modeling. Several of the numerical studies incorporated sand and mud fractions to represent various erosion and deposition regimes in the migration process. However, none of these studies considered the potential contribution of consolidation in the migration process and subsequent morphologic

change of the barrier island. In the review of consolidation literature, experiences in the United States as well as abroad demonstrated that loading of the substrate through barrier island migration can influence the resulting morphology change. In particular, a study by Guber and Slingerland (1981) discussed how subsurface characteristics can contribute to future morphology change of a barrier island system: the feedback between consolidation, barrier island elevation, and subsequent washover; the cross-section of the island as a function of subsurface characteristics and loading; and the apparent non-conservation of sediment because of compression of the substrate. None of the models that were reviewed is capable of calculating these processes. The 2D MCO developed in this research is unique because it links barrier island morphology change and migration to subsurface consolidation in a time-dependent manner. Model theory, development, sensitivity testing, and application are described in the next chapter.

4 Development of 2D Numerical Model

Purpose and scope

The 2D MCO model was developed in this research to investigate the role of consolidation on migration of sandy barrier islands that overlie compressible sediments. The model is intended to simulate processes typical of a low-energy deltaic setting such as in the Northern Gulf of Mexico, in which cross-shore morphology change and migration primarily occur during storms. A flowchart for the model is shown in Figure 15.

Initial conditions are defined by a sandy barrier island with a given cross-shore profile that overlies a sediment substrate of specified characteristics. The island evolves over years as a function of storm surge, wave height and period, and the rate of eustatic sea level change. Storm surge and wave height and period can be randomly generated about a user-specified mean, with storm intensity and the number of storms each year also varying randomly; or a specific data time series can be provided as input.

As shown in Figure 15, the 2D MCO model uses the wave conditions to calculate erosion, runup overwash, or inundation overwash depending on the storm conditions and relative elevation of the barrier island. If washover of the island occurs, the barrier migrates into the bay and consolidation occurs due to the existing and any new loading (if migration occurred onto partially-consolidated sediments). This chapter discusses the theory of the model, presents results of sensitivity testing, and compares model results with available data from three barrier islands in Virginia.

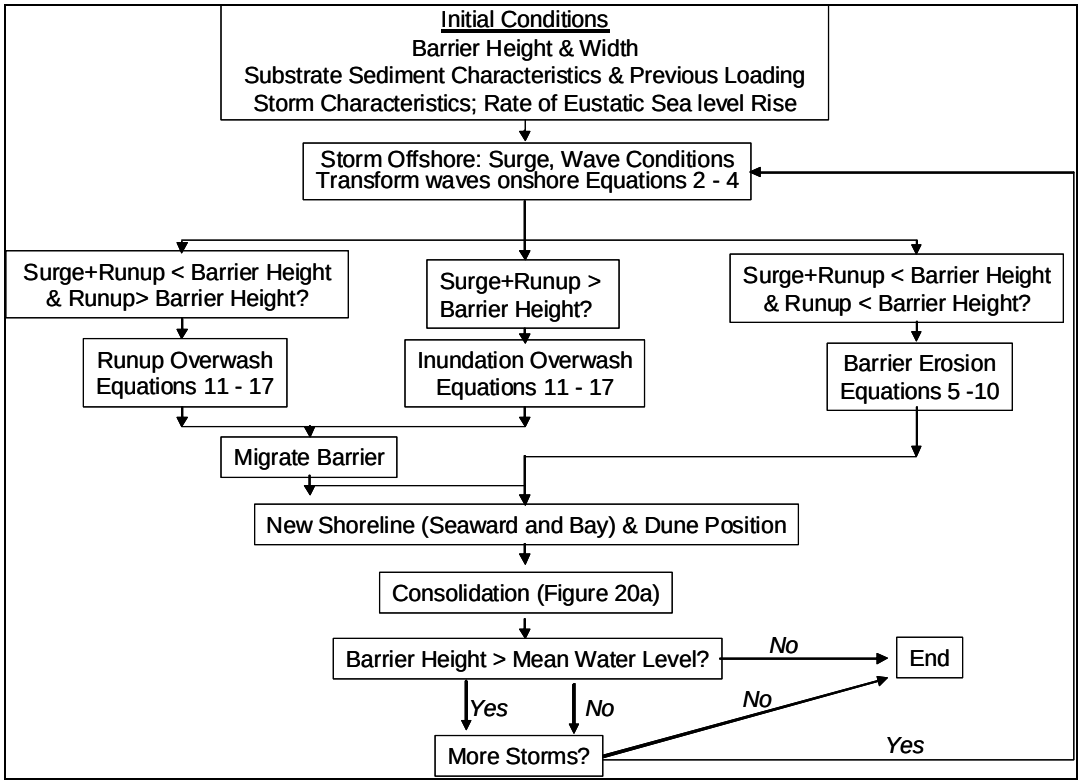

Figure 15. Flowchart for 2D MCO Model.

Theory

Wave transformation

In many deltaic settings, mud transported to the coast by the river system remains in the nearshore as a sub-aqueous mud layer that can be tens to hundreds of meters thick (e.g., Tubman and Suhayda 1976; Wells and Kemp 1986; Winterwerp et al. 2007). The mud has the capability to dissipate incoming waves and reduce wave height. A study by Tubman and Suhayda (1976) in East Bay, near the Mississippi River Delta, documented a decrease in wave height by 50 percent due to fluid mud over a 3.5-km distance. Also on the Louisiana coast, Sheremet and Stone (2003) compared wave measurements over a muddy seabed, near Atchafalaya Bay, to a site at a similar depth 150 km apart over a sandy seabed, offshore of the Isle Dernieres and Trinity barrier island systems. Sheremet and Stone found that the swell waves measured offshore of Atchafalaya Bay, the muddy environment, were attenuated by an order of magnitude as compared to the measurements in the sandy environment, although there was dissipation observed for the entire energy spectrum.

Because the focus of this study is not wave transformation through fluid mud, and because barrier island systems in Louisiana and Virginia are

best characterized with a sandy offshore bathymetry, 2D MCO is formulated herein with wave transformation calculations appropriate for a sandy seabed. Future improvements in the model could include advanced wave propagation over fluid mud, or 2D MCO could be coupled with an existing model that can represent these complex processes (e.g., Simulating Waves Nearshore Model (SWAN), Delft University of Technology 2009; Sheremet and Stone 2003). For site-specific applications to a coastal region with muddy bathymetry, this phenomenon should be included in the wave transformation process.

The 2D MCO model begins by transforming storm waves from deep to shallow water using a time series of wave height, period, and direction; or, the model can randomly generate wave and surge conditions from user-specified averages. Deep water waves are transformed from offshore measurements to breaking conditions using linear wave theory, in which time-dependent measurements of deep water wave height, $H_o(t)$, are related to wave height at breaking, $H_b(t)$, by (Dean and Dalyrmple 1984, p. 115).

$$H_b(t) = \left(\frac{\kappa}{g}\right)^{1/5} \left(\frac{H_o^2(t) C_o(t) \cos\theta_o(t)}{2}\right)^{2/5} \tag{2}$$

The breaking criterion is $\kappa = H_b(t)/d_b(t) = 0.78$, in which $d_b(t)$ is the depth at breaking, and the deepwater wave height and direction are given by $H_o(t)$ and $\theta_o(t)$, respectively. The deepwater wave speed is given by $C_o(t)$.

$$C_o(t) = \frac{L_o(t)}{T(t)} \tag{3}$$

where $T(t)$ is the wave period and $L_o(t)$ is the deep-water wave length equal to:

$$L_o(t) = \frac{gT(t)^2}{2\pi} \tag{4}$$

Erosion

Barrier island erosion and deposition offshore occur if the storm surge plus wave runup do not exceed the barrier island elevation (Figure 16a).

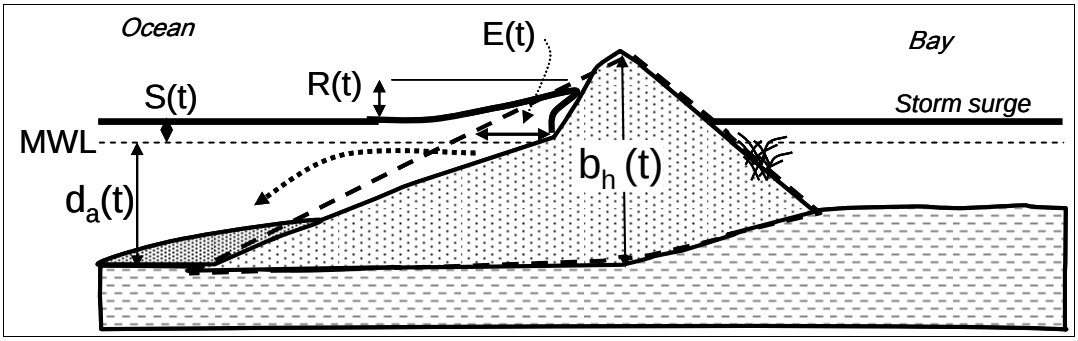

a. Erosion.

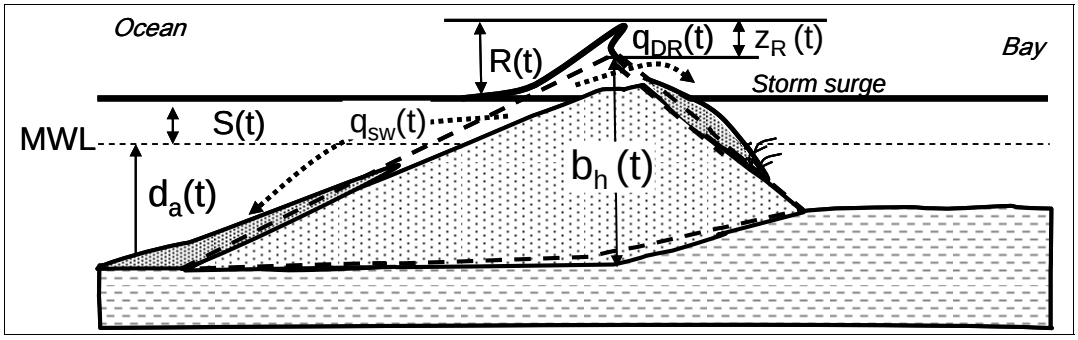

b. Runup overwash.

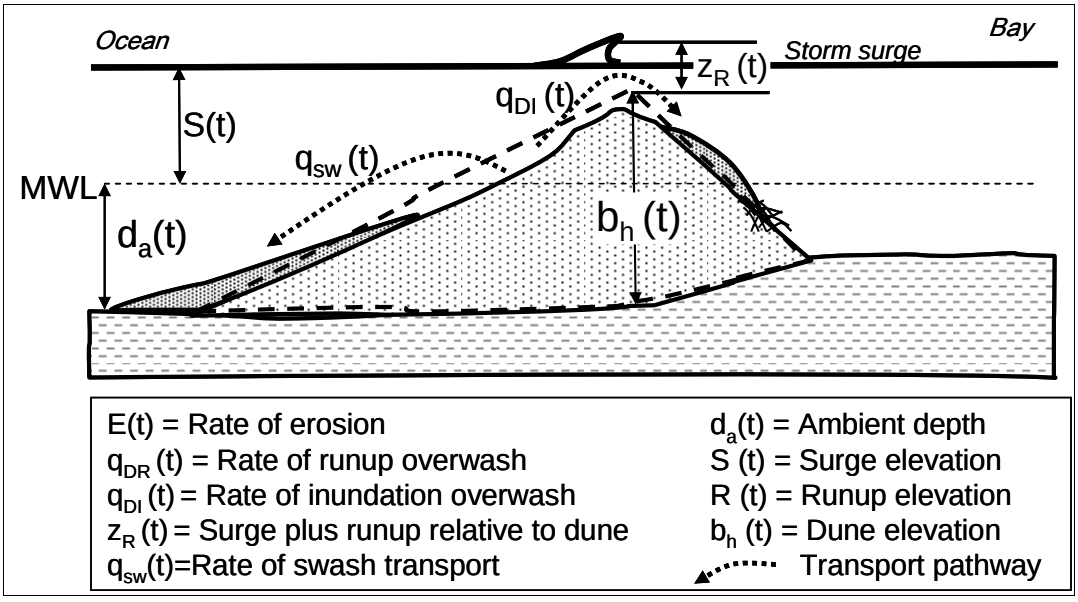

c. Inundation overwash.

Figure 16. Terminology for erosion and overwash calculations.

The time-dependent berm erosion, $E(t)$, is calculated using the Convolution Storm Erosion Method (Kriebel and Dean 1993).

$$E(t) = \frac{E_\infty}{2}\left\{1 - \frac{\beta_t^{\,2}}{1+\beta_t^{\,2}}\exp\left(-\frac{2\sigma t}{\beta_t}\right) - \frac{1}{1+\beta_t^{\,2}}\left[\cos 2\sigma t + \beta_t \sin 2\sigma t\right]\right\} \quad (5)$$

in which the maximum potential erosion retreat, E_∞, is given by:

$$E_\infty = \left(S(t) + 0.068 H_b(t)\right)\left(\frac{W_b(t)}{B + d_b(t)}\right) \quad (6)$$

The storm surge is $S(t)$, $W_b(t)$ is the width of the surf zone, and B is the berm elevation. In Equation 5, β_t is the ratio of the erosion time scale to the storm duration,

$$\beta_t = \frac{2\pi T_s}{T_D} \quad (7)$$

and $\sigma = \pi / T_D$, where T_D is the total storm duration. The characteristic erosion time scale of the system is given by,

$$T_s = 320\frac{H_b(t)^{1.5}}{g^{0.5}A^3}\left(1 + \frac{d_b(t)}{B} + \frac{\tan\beta(t) W_b(t)}{d_b(t)}\right)^{-1} \quad (8)$$

in which g is the acceleration due to gravity, and $\beta(t)$ is the beach slope. The width of the surf zone is calculated as:

$$W_b(t) = \left(\frac{d_b(t)}{A}\right)^{1.5} \quad (9)$$

in which A is the equilibrium beach profile parameter and can be related to median grain size or sand fall speed. The equilibrium beach profile concept was first developed by Bruun (1962) in 1954 (Komar 1998) based on beaches in Monterey Bay, California, and the exponential value confirmed by Dean (1977) in analysis of more than 500 beach profiles along the U.S. Atlantic and Gulf coasts and has since been applied to beaches around the world (e.g., Dean et al. 1993, Larson et al. 1999, Dean and Dalrymple 2002). The equilibrium beach profile relates the long-term

shape of the profile elevation of the beach profile, y, to distance offshore, x,

$$x = Ay^{2/3} \tag{10}$$

During an erosion event, the eroded sand is transported offshore and deposited, thereby decreasing depths offshore such that sediment volume is conserved. Avalanching of the profile is initiated if the slope is greater or equal to a user-specified avalanching angle with a default value of 30 deg.

Runup overwash and inundation overwash

Overwash is any wave uprush which passes over the "crown," or crest of the barrier beach (Leatherman 1979, p. 3). Of relevance to this study is the magnitude of the morphologic feature created by overwash and deposited on the bayside of the crest, called "washover," "washover deposit" or "washover fan" (Leatherman 1979, p. 2). The frequency and magnitude of overwash depend on long-term conditions, such as storm climatology, relative sea level rise, and sediment supply. Overwash and the resulting washover deposit are one of the mechanisms through which the barrier island migrates towards the bay (across shore). Two modes of overwash are simulated in the model: runup overwash and inundation overwash. Runup overwash occurs if the island is not submerged, and washover is caused by the uprushing wave bore. Inundation overwash occurs when the storm surge level and wave setup exceed the elevation of the barrier island crest, and the barrier island is submerged (Donnelly et al. 2009).

The overwash transport rate over the beach crest due to runup overwash per unit length of beach, $q_{DR}(t)$, can be described as (Donnelly et al. 2009).

$$q_{DR}(t) = 2K_R\sqrt{2g}\ {z_R}^{3/2}\sqrt{1-\frac{b_h(t)}{R(t)}} \quad \text{for} \quad 0 < z_R(t) \text{ and } S(t)+d_a(t) < b_h(t) \tag{11}$$

where K_R is a calibration coefficient that accounts for sediment concentration and properties of the wave bore, and $z_R(t)$ is the elevation of the runup, $R(t)$, relative to the dune crest elevation, $b_h(t)$ (Figure 16). For calculations herein, K_R was set equal to 0.005 as recommended by Donnelly et al. (2009).

The two-percent runup, $R_{u2\%}(t)$, is calculated as (Hughes 2004),

$$R_{u2\%}(t) = 4.4\left(S(t)+d_a(t)\right)\tan\beta(t)^{0.70}\left[\frac{M_F(t)}{\rho g\left(S(t)+d_a(t)\right)^2}\right]^{1/2} \quad \text{for } \frac{1}{30} \le \tan\beta(t) \le \frac{1}{5} \tag{12}$$

in which ρ is the density of water, and the maximum dimensionless depth-integrated wave momentum flux per unit width is:

$$\left[\frac{M_F(t)}{\rho g\left(S(t)+d_a(t)\right)^2}\right]_{\max} = A_0(t)\left[\frac{S(t)+d_a(t)}{gT_p(t)^2}\right]^{-A_1(t)}$$
$$\text{where} \quad A_0(t) = 0.6392\left(\frac{H_{mo}(t)}{S(t)+d_a(t)}\right)^{2.0256} \tag{13}$$
$$\text{and} \quad A_1(t) = 0.1804\left(\frac{H_{mo}(t)}{S(t)+d_a(t)}\right)^{-0.391}$$

The zeroth-moment deep water wave height is $H_{mo}(t)$, with associated peak period, $T_p(t)$. If wave height is randomly generated about a user-specified mean, 2D MCO calculates the peak wave period, $T_p(t)$, associated with $H_{mo}(t)$ using a relationship from Bretschneider (1966) based on hurricanes which has been modified for peak wave period.

$$T_p(t)(\text{sec}) = 2.13\sqrt{H_{mo}(t)(ft)} = 3.86\sqrt{H_{mo}(t)(m)} \tag{14}$$

The transport rate over the beach crest per unit width of beach due to inundation overwash, $q_{DI}(t)$, is given by (Donnelly et al. 2009) as:

$$q_{DI}(t) = 2K_I\sqrt{2g}\; z_R(t)^{3/2} + q_{DR}(t), \quad 0 < z_R(t) \text{ and } S(t)+d_a(t) \ge b_h(t) \tag{15}$$

in which K_I is an empirical coefficient, and $z_R(t)$ is as defined previously (Figure 15c). For calculations herein, K_I was set to 0.005 (Donnelly et al. 2009).

Transport in the swash zone is calculated as (Larson et al. 2004).

$$q_{sw}(t) = K_{sw}\; 2\sqrt{2g}\; R(t)^{3/2}\left(\tan\beta_{sw} - \tan\beta_{eq}\right) \tag{16}$$

where K_{sw} is an empirical coefficient, set equal to 0.0016 for calculations herein, β_{sw} is the local slope in the swash zone, and β_{eq} is the equilibrium slope calculated using equilibrium profile concepts,

$$\beta_{eq} = A\left(\frac{x_{dune}^{2/3} - x_{sw}^{2/3}}{x_{dune} - x_{sw}}\right) \tag{17}$$

Location of the dune and swash are given by x_{dune} and x_{sw}, respectively.

Consolidation

Terzaghi (1943) derived a relationship for primary consolidation, the process during which excess pore water pressure is dissipated from the particle matrix, based upon hydraulic principles. The assumptions for one-dimensional consolidation theory are: (1) a fully-saturated sediment system; (2) unidirectional flow of water; (3) one-dimensional compaction occurring in the opposite direction of flow; (4) a linear relationship between the change in sediment volume and the applied pressure (linear small-strain theory); and (5) validity of Darcy's Law, which states that the specific discharge (flow rate per area) through a porous medium is equal to the hydraulic gradient times the hydraulic conductivity (Yong and Warkentin 1966; Hornberger et al. 1998). For one-dimensional vertical flow, if the given loading p is less than the pre-consolidation loading p_c, then the maximum consolidation, z_c can be calculated as:

$$z_c = z_0\left(\frac{C_{c0}}{1+e_0}\log_{10}\frac{p}{p_0}\right) \quad if \;\; p < p_c \tag{18a}$$

where z_0 is the initial thickness of compressible sediment; C_{c0} is the compression index, determined experimentally from a consolidation test for $p < p_c$; e_0 is the initial void ratio, equal to the volume of voids divided by the volume of solids, and averaged over z_0; and p_0 is the initial loading on the sediment. If the given loading p is greater than or equal to p_c, the maximum consolidation is calculated as:

$$z_c = z_0\left(\frac{C_c}{1+e_0}\log_{10}\frac{p}{p_c}\right) \quad if \;\; p \geq p_c \tag{18b}$$

where Cc is the compression index for $p > p_c$, determined experimentally from a consolidation test. The parameter z_0 can be estimated from

sediment core data, regional depositional maps that represent the thickness of soft sediment, and high-resolution acoustic data at specific sites of interest with validation from sediment core data. In the formulations herein, the initial thickness of compressible sediment z0 is a constant for each simulation. However, future versions of the code could include a spatially-varying parameter as needed to represent site-specific stratigraphy. For the Mississippi River system, Kulp et al. (2002) analyzed data from more than 800 boreholes and mapped the topstratum lithosome, which represents fine-grained deposition in fluvial, deltaic, and shelf environments that overlies coarser-grained substratum. As first discussed by Frazier (1967), Kulp et al.'s data indicate that the thickness of topstratum sediment corresponds to the distribution of Holocene depocenters, with the maximum thickness approximately 120 m in vicinity of the modern Balize depocenter. Near the modern barrier islands, topstratum thickness ranges from approximately 10 to 30 m (Kulp et al. 2002, their Figure 7). Definitions for terms in Equations 18a and 18b are shown in Figure 17.

The value of the pre-consolidation stress can be estimated from Casagrande's consolidation test as illustrated in Figure 17b. To determine the pre-consolidation stress, the steps shown in Figure 17b are followed: (1) identify the point at the maximum radius of curvature, (2) draw a horizontal from that point, (3) draw a line tangent to that point, (4) draw a line bisecting (2) and (3); (5) draw a straight line from the over-consolidated portion of the curve, and finally determine the pre-consolidated loading by the intersection of (4) and (5). The magnitude of the pre-consolidation stress is decisive because it separates soils that are over-consolidated (i.e., these soils have experienced a greater load at some time in their past) from those that are under-consolidated (i.e., the present loading is the maximum that has occurred). Loading greater than the pre-consolidation stress will result in greater rates of consolidation than have previously occurred.

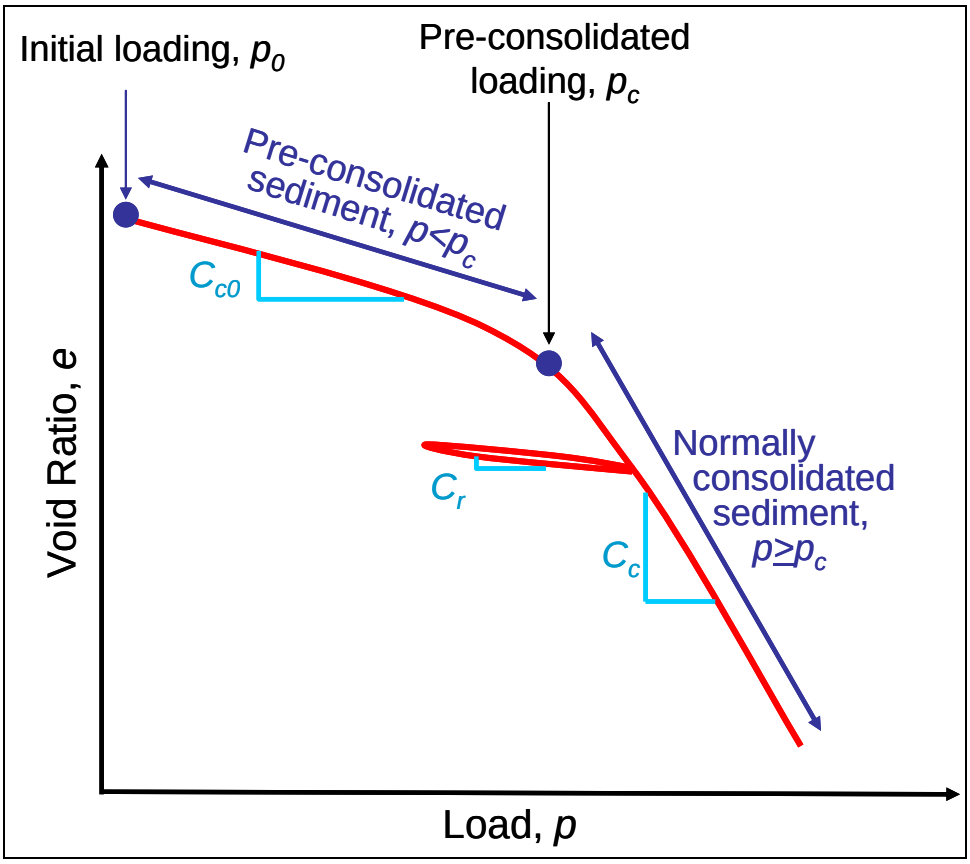

a. Definition of pre-consolidated and normally consolidated sediment.

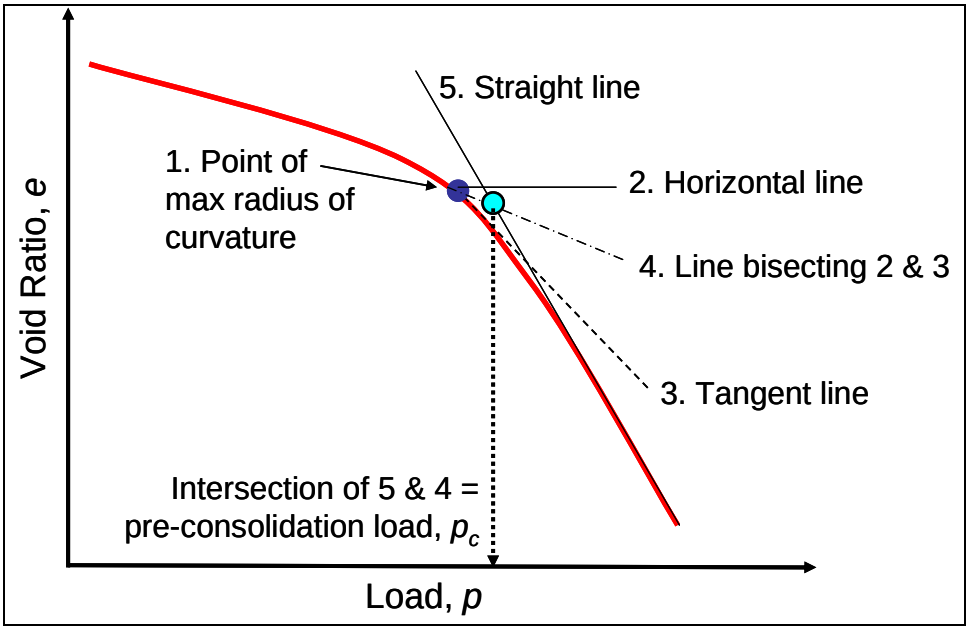

b. Determining pre-consolidation loading.

Figure 17. Parameters associated with consolidation testing.

Figure 18 shows results of a consolidation test conducted for a sediment sample at 12.5-13.1 m depth from Chaland Headland, a barrier island restoration project in Louisiana that was completed in January 2007. For the example shown in Figure 18, if the loading p is less than the pre-consolidation stress, p_0 = 660 kg/m2 and C_{c0} = 0.125 in Equation 18a. If p is greater than the pre-consolidation stress, then p_c =7,900 kg/m^2 and C_c = 0.4 in Equation 18b.

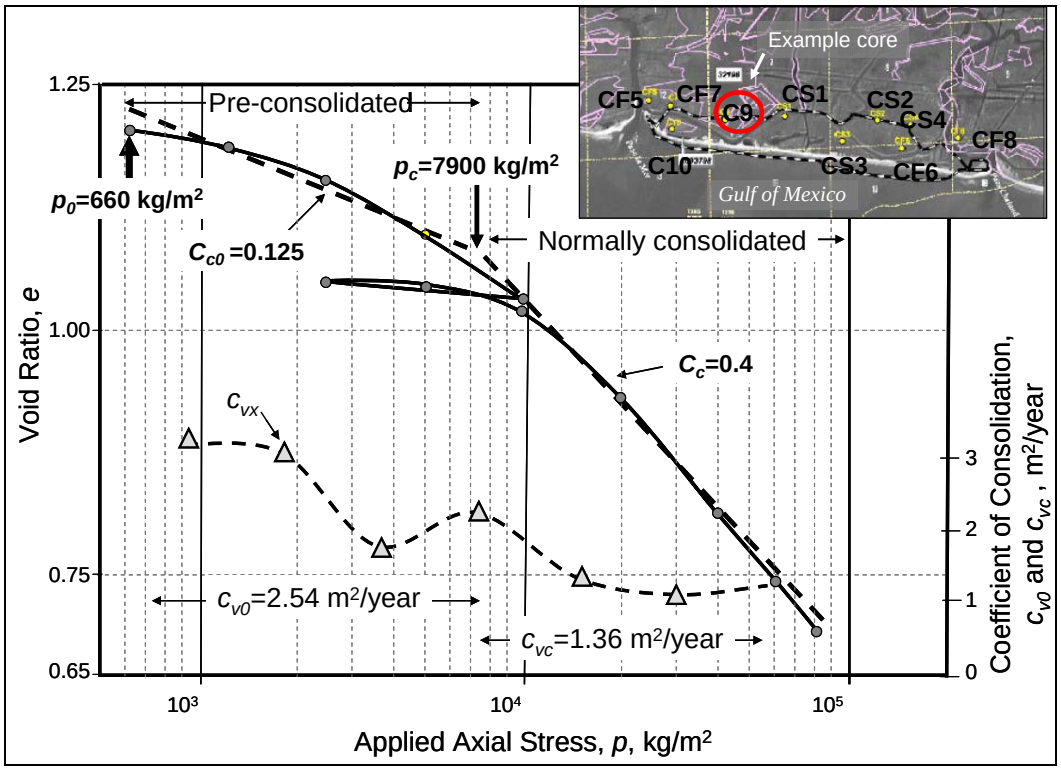

Figure 18. Example consolidation test from sediment sample taken at Chaland Headland, LA.

Terzaghi's (1943) time-dependent relationship for consolidation is:

$$\frac{\partial u}{\partial t} = c_{v0}\frac{\partial^2 u}{\partial z^2} \quad \text{if } p < p_c \tag{19a}$$

$$\frac{\partial u}{\partial t} = c_{vc}\frac{\partial^2 u}{\partial z^2} \quad \text{if } p \geq p_c \tag{19b}$$

where u is pore water pressure in excess of hydrostatic pressure, t is elapsed time, z is the vertical coordinate with the origin at the initial sediment surface, and c_{v0} and cvc represent a property of the compressible sediment called the coefficient of consolidation, which may vary

depending on whether the loading is less than or greater than the pre-consolidation stress (Figure 19).

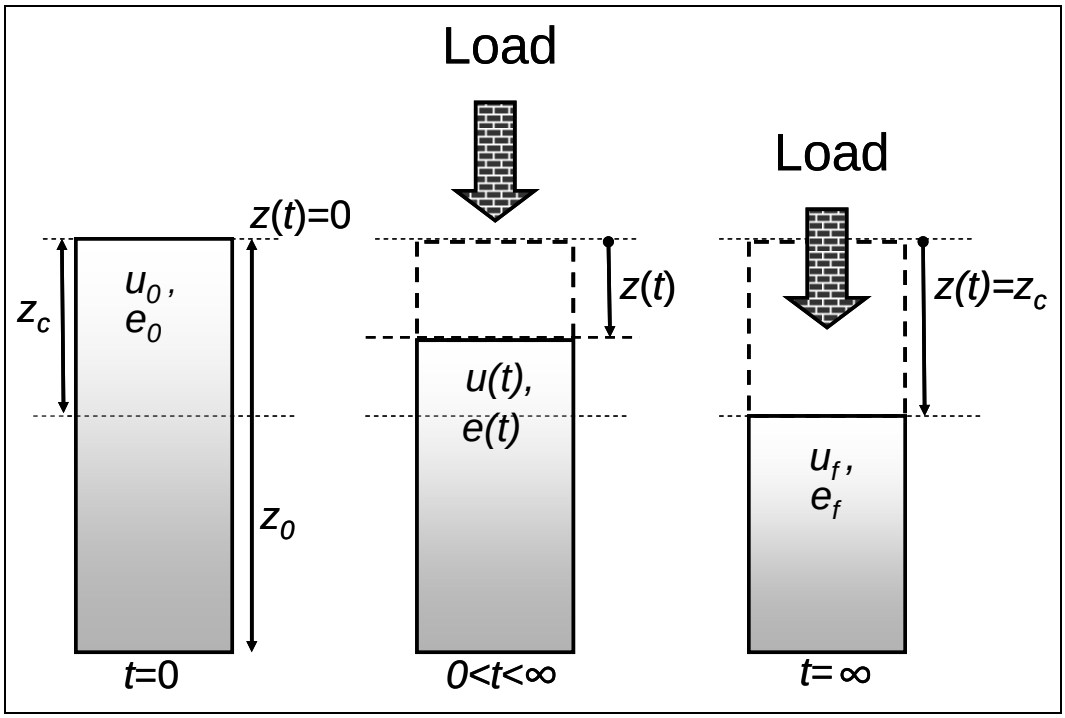

Figure 19. Definition sketch for consolidation relationship.

The proportion of the initial pore water pressure remaining at any time, $M(t)$, can be expressed as:

$$M(t) = \frac{1}{z_0}\int_0^{z_0} \frac{u}{u_0} dz = \frac{e(t) - e_f}{e_0 - e_f} \tag{20}$$

in which u_0 is the initial pore water pressure, $e(t)$ is the average void ratio at any time, and e_f is the final average void ratio corresponding to the consolidation test results for the portion of the curve less than or greater than the pre-consolidation stress. The variable $M(t)$ ranges from 1 and 0, at time t = 0 and infinity, respectively. The proportion of vertical consolidation that occurs at any time can also be expressed as:

$$z(t) = z_c(t)\left(\frac{e_0 - e(t)}{e_0 - e_f}\right) \tag{21}$$

Combining Equations 20 and 21 gives

$$z(t) = z_c(t)\left(1 - M(t)\right) \tag{22}$$

where $M(t)$ can be expressed as (Dean 2002, p. 119),

$$M(t) = 8\sum_{n=1}^{\infty} \frac{e^{-\left[(2n-1)\pi\right]^2 c_{v0} t / 4 z_0^2}}{(2n-1)^2 \pi^2} \text{ for } p < p_c$$
$$M(t) = 8\sum_{n=1}^{\infty} \frac{e^{-\left[(2n-1)\pi\right]^2 c_{vc} t / 4 z_0^2}}{(2n-1)^2 \pi^2} \text{ for } p \geq p_c \tag{23a, b}$$

and n is the index of the summation. In the numerical calculations, when the load changes from one time step to the next at a given location on the profile, an effective time, t_e, is back-calculated corresponding to the new load and previous total consolidation at that location. The effective time is then incremented by the time step and used in Equations 22, 23a, b to calculate consolidation at the next time step with the new load. Figure 20a shows a flowchart for the consolidation portion of the 2D MCO model in which the equations are represented as a function of each cell in the cross-shore, x (Figure 20b), and time, t.

The consolidation routine was evaluated with information presented by Blum et al. (2008) in which they discussed uplift and subsidence of the Mississippi River Delta over the past 30,000 years. Specific to this study, Blum et al. discuss the gradual deposition of approximately 40 m of deltaic sediment in the vicinity of New Orleans (90.5 deg longitude) from 11,500 to 4,000 years ago, and no additional deposition from 4,000 years ago to the present as the river's depocenter had moved further downstream. Blum et al.'s calculations with a three-dimensional visco-elastic consolidation model indicated that approximately 5.9 m surface deflection (the net of consolidation plus uplift) occurred over the past 10,000 years (see their Figures 3b and c, reproduced below in Figure 21b and c). As the river incised the Lower Mississippi River Valley with meltwater, the removal of sediment created an uplift of the surface from 30,000 to 9,500 years ago. This loading cycle (linear deposition of 40 m thickness from 11,500 to 4,000 years, then no deposition from 4,000 years to present) was programmed into the consolidation code with the same sediment-water density as discussed by Blum et al. (1,800 kg/m^3) and indicated a value of 6.7 m consolidation over the past 11,500 years (Figure 21). The value calculated by the consolidation routine developed herein is 15 percent

greater than Blum et al.'s results. However, Blum et al.'s value includes approximately 0.5 m occurred at the end of the uplift period. This comparison is considered validation of the consolidation routine.

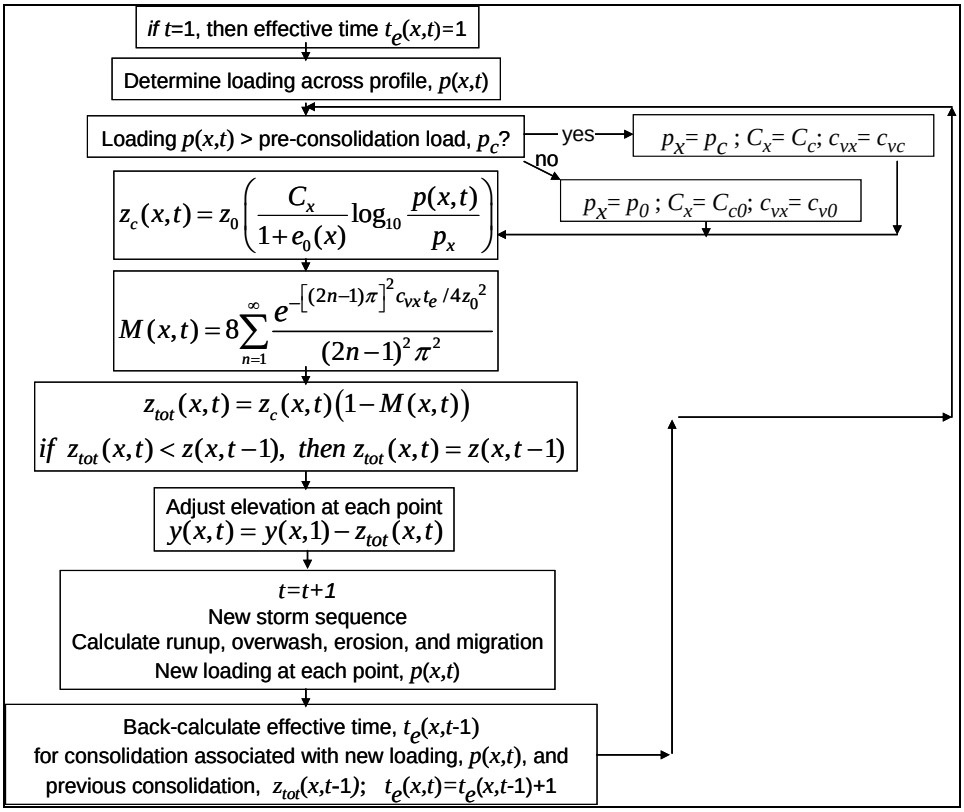

a. Flowchart.

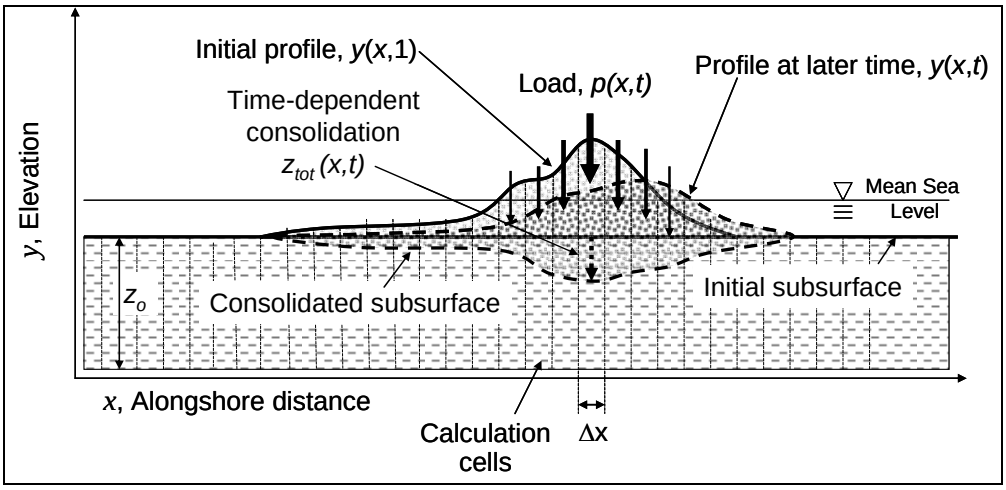

b. Definition of cells and variables.

Figure 20. 2D MCO consolidation routine.

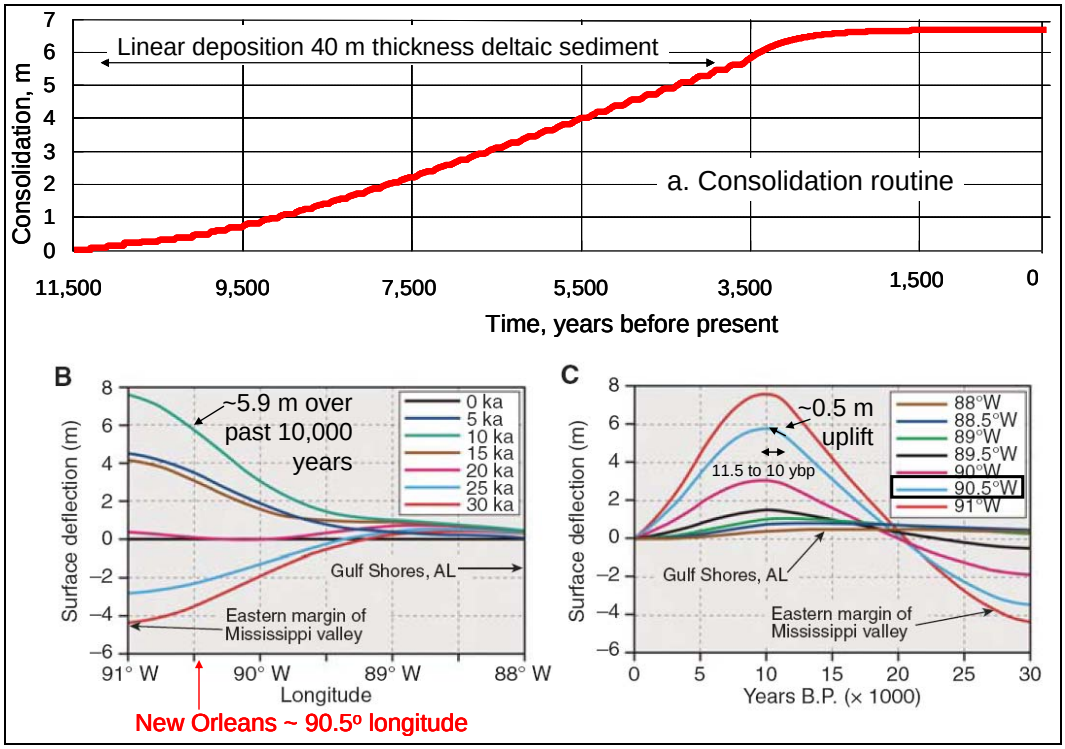

Figure 21. Comparison of consolidation routine (shown in (a)) to calculations from Blum et al. (2008) (reproduced in (b) and (c), their Figure 3b and c).

Bay processes

In the Northern Gulf of Mexico, tropical storms and cold front passage can create storm surge and waves on the bayshore of barrier islands if these islands front a bay or estuary of sufficient area (Stone et al. 2004; Georgiou et al. 2005). As a result, the island bayshore (composed of sand, clay, silt, and marsh vegetation) can be eroded. The storm surge on the bay occurs in the waning stages of the storm and thus is lower in magnitude; however, if it is sufficient, overwash back into the ocean (Gulf) can occur if the bay storm surge is greater than the island elevation (e.g., Kahn and Roberts 1982). The more typical case is for sediment eroded during storm passage to be eroded from the bay shoreline and lost from the island's littoral budget (Armbruster et al. 1995). The present version of 2D MCO presented herein does not include calculations for bay erosion, although these processes could be added.

Sensitivity analysis

Overview

Sensitivity analysis is the process of systematically changing model input parameters to evaluate the degree to which their variation changes model

calculations. For the 2D MCO, results from sensitivity calculations were evaluated with respect to whether they agreed with intuitive knowledge of processes and response, and whether the model calculations were greatly dependent on minor changes in one or more variables. The sensitivity analysis was conducted to develop a better understanding of 2D MCO operations as well as to build confidence in the calculations.

Ten sensitivity tests (called Analyses) encompassing 50 simulations were conducted for a barrier island with an initial triangular shape and local (ambient) depth equal to 0.5 m. Parameters that were varied were: (1) the magnitude of storm surge and offshore wave height and associated wave period; (2) maximum initial profile elevation; (3) initial island width; consolidation characteristics of the substrate, including (4) no consolidation and (5) variation in consolidation parameters; (6) rate of eustatic sea level rise; (7) tidal amplitude; (8) duration of the simulation; and (9) randomness of simulations for duration of 50 years. With the exception of 11 simulations (seven in Analysis 7, set for 100-year duration; and four in Analysis 9, with varying duration), all durations were set for 50 years although some input conditions resulted in the barrier island being below ambient depth and the simulation terminated prior to 50 years. Output parameters recorded were: dune migration distance, final dune elevation, volume of sediment sequestered due to consolidation, average storm water level (including surge, tide, ambient depth, relative sea level change, and runup elevation), volume eroded, volume of runup overwash, volume of inundation overwash, maximum thickness of consolidation, and duration of simulation. Details of these analyses are provided along with a Run ID number in Table 6. Figures 22 through 25 introduce model output; additional selected figures are shown in Appendix A.

The first figure in 2D MCO model output is a summary of the hydrodynamic and morphologic change that occurred during the entire simulation, as shown in Figure 22 for Analysis 2b with a dune of initial 4-m elevation, 2,500-m width, H_{mo} =1 m and S = 1 m, and other initial conditions as shown in Table 6. The top panel shows the total depth during the storm series for each year, including the ambient water depth, storm surge, tide, wave runup elevation, and relative sea level change. The second panel shows the time-variation of consolidation beneath the dune crest for each year of the simulation. For the simulation shown in Figure 22, the dune moved significantly after the 44th year and the consolidation shown beneath the dune crest decreased because the island

migrated onto less-consolidated sediment. The third and fourth panels show migration and elevation of the dune crest for each year of the simulation, respectively.

Figure 23 summarizes the erosion, runup overwash, and inundation overwash that occurred on the ocean (or gulf) side of the island. For the simulation shown in Figure 23, erosion (top panel) occurs with a decreasing magnitude as runup overwash (middle panel) and inundation overwash (lower panel) occur more frequently. The magnitude of erosion decreases with time as the island achieves an equilibrium profile condition.

Figure 24 summarizes response of the profile (top panel) and consolidated subsurface (bottom panel). The ambient and average storm depths are shown by dotted and solid horizontal blue lines, respectively, and the shape of the profile is shown at intermediate times during the simulation. As sand is eroded from the barrier island on the ocean (or gulf) side, it moves offshore and begins consolidation of the substrate, as observed by the consolidated subsurface that extends seaward of the island cross-section. The simulation shown here represents a newly-constructed island on a previously non-consolidated substrate; consolidation of the offshore portion of the profile would not occur if the island had previously migrated over that region. Additional sand from the island fills in the consolidated region. A similar process occurs on the bay side of the island: as barrier sand loads the substrate, additional sand is moved down slope from the island into the bay to fill in consolidated depressions. Therefore, the consolidated subsurface extends beyond the apparent barrier island footprint. In the lower panel of Figure 24, the elevation of the consolidated subsurface is shown for intermediate snapshots during the simulation. Because the island did not migrate during the first 37 years of the simulation, the bottom panel shows the island effectively sinking into the substrate up to 0.86 m during this time, similar to the “drowning in place” phenomenon that is observed in Louisiana. Once the island migrates after approximately 40 years, consolidation of subsurface sediment in the bay begins. The extent of the consolidated subsurface radiates outwards from the island with time.

Table 6. 2D MCO Sensitivity analysis with triangular Barrier Island[1].

Input Parameters								Calculations									
ID	H_{bar}, m	W_{bar}, m	H_{mo}, m	S, m	z_o, m	SL, mm/yr	η_a, m	Mig, m	H_{bar_f}, m	Vol_c, m^3	WL_{avg}, m	Vol_{er}, $m^3/m/yr$	Vol_{ow}, $m^3/m/yr$	Vol_{in}, $m^3/m/yr$	z_{max}, m	T_{max}, yr	Fig.
Analysis 1: Vary Storm Waves and Surge																	
1a	3	2500	0.5	0.5	10a	0	0	248/400	1.23/1.17	2526/2571	1.19/1.18	5.34/5.54	0	2.66/5.45	0.82/0.82	50	n/a
1b	3	2500	1	1	10a	0	0	3136	0.27	3193	1.74	3.03	0.003	78.1	0.79	36*	69-72
1c	3	2500	1.5	1	10a	0	0	2267	0.44	2960	1.85	1.77	0.014	79.7	0.79	34*	73-76
1d	3	2500	1.5	1.5	10a	0	0	3383	0.37	2906	2.43	1.07	0.026	263.1	0.67	17*	77-80
1e	3	2500	2	1.5	10a	0	0	3839	0.39	2917	2.70	0.45	0.133	307.9	0.65	15*	n/a
1f	3	2500	2	2	10a	0	0	3715/4074	0.44/0.26	2773/3134	3.11/2.72	1.00/0.47	0	469.9/410.5	0.60/0.62	11*/12*	n/a
Analysis 2: Vary Initial Dune Elevation with Consolidation																	
2a	2.5	2500	1	1	10a	0	0	3069	0.41	2427	2.00	1.47	0	205.8	0.63	15*	n/a
2b	3	2500	1	1	10a	0	0	2866	0.36	3063	1.79	2.86	0.05	83.2	0.78	34*	n/a
2c	4	2500	1	1	10a	0	0	3580	0.42	3835	2.07	8.10	0.018	83.8	0.86	46*	22-25
2d	5	2500	1	1	10a	0	0	366	2.20	3146	1.93	19.3	0	0	0.92	50	n/a
Analysis 3: Vary Initial Dune Elevation without Consolidation																	
3a	2.5	2500	1	1	0	0	0	541	1.87	0	1.73	4.48	0.03	12.6	0	50	n/a
3b	3	2500	1	1	0	0	0	372	2.26	0	1.94	8.04	0.0025	3.77	0	50	n/a
3c	4	2500	1	1	0	0	0	429	2.64	0	1.96	20.5	0	0	0	50	n/a
3d	5	2500	1	1	0	0	0	409	3.40	0	1.91	33.9	0	0	0	50	n/a

(Continued)

Table 6. 2D MCO Sensitivity analysis with triangular Barrier Island[1].

Input Parameters								Calculations									
ID	H_{bar}, m	W_{bar}, m	H_{mo}, m	S, m	z_o, m	SL, mm/yr	η_a, m	Mig, m	H_{bar_f}, m	Vol_c, m^3	WL_{avg}, m	Vol_{er}, $m^3/m/yr$	Vol_{ow}, $m^3/m/yr$	Vol_{in}, $m^3/m/yr$	z_{max}, m	T_{max},yr	Fig.
Analysis 4: Vary Initial Barrier Width with Consolidation																	
4a	4	1000	1	1	10a	0	0	1837	0.37	1462	2.13	9.96	0.14	107.0	0.74	21*	n/a
4b	4	1500	1	1	10a	0	0	3545	0.22	2412	2.24	10.2	0.18	139.4	0.79	26*	n/a
4c	4	2500	1	1	10a	0	0	3580	0.42	3835	2.07	8.10	0.018	83.8	0.86	46*	22-25
4d	4	3500	1	1	10a	0	0	500	1.91	3879	1.96	9.75	0.035	8.11	0.88	50	n/a
Analysis 5: Vary Initial Barrier Width without Consolidation																	
5a	4	1000	1	1	0	0	0	288	2.21	0	1.88	12.8	0.13	3.09	0	50	n/a
5b	4	1500	1	1	0	0	0	278	2.44	0	1.90	15.9	0	0	0	50	n/a
5c	4	2500	1	1	0	0	0	369	2.82	0	1.88	19.8	0	0	0	50	n/a
5d	4	3500	1	1	0	0	0	390	3.11	0	1.74	21.2	0	0	0	50	n/a
Analysis 6: Vary Consolidation Parameters																	
6a	4	2500	1	1	0	0	0	429	2.64	0	1.96	20.5	0	0	0	50	n/a
6b	4	2500	1	1	5a	0	0	428	2.24	1302	2.02	13.9	0.038	2.41	0.35	50	n/a
6c	4	2500	1	1	10a	0	0	3580	0.42	3835	2.07	8.10	0.018	83.8	0.86	46*	22-25
6d	4	2500	1	1	20a	0	0	1283	0.45	4499	2.03	7.87	0.075	78.4	1.37	18*	n/a
6e	4	2500	1	1	25a	0	0	879	0.02	4914	1.97	6.21	0.058	88.8	1.58	11*	n/a
6f	4	2500	1	1	5b	0	0	350	2.52	929	1.76	16.8	0	0	0.28	50	n/a
6g	4	2500	1	1	10b	0	0	388	2.13	1715	1.99	11.80	0.063	3.37	0.48	50	n/a
6h	4	2500	1	1	20b	0	0	1926	0.25	4250	2.01	5.72	0.03	64.7	1.00	33*	n/a
6i	4	2500	1	1	5c	0	0	403	2.26	1292	1.94	14.3	0.03	2.33	0.38	50	n/a
6j	4	2500	1	1	10c	0	0	2159	0.56	3742	1.84	7.14	0.02	55.0	0.90	50	n/a
6k	4	2500	1	1	20c	0	0	974	0.35	4820	1.96	6.81	0.015	60.98	1.58	16*	n/a

(Continued)

Table 6. 2D MCO Sensitivity analysis with triangular Barrier Island[1]. (Continued)

Input Parameters								Calculations									
ID	H_{bar}, m	W_{bar}, m	H_{mo}, m	S, m	z_o, m	SL, mm/yr	η_a, m	Mig, m	H_{bar_f}, m	Vol_c, m^3	WL_{avg}, m	Vol_{er}, $m^3/m/yr$	Vol_{ow}, $m^3/m/yr$	Vol_{in}, $m^3/m/yr$	z_{max}, m	T_{max}, yr	Fig.
Analysis 7: Vary Eustatic Sea Level Change Rate (100 yr simulation)																	
7a	4	2500	1	1	10a	0	0	2987	0.39	3877	1.94	7.89	0.027	70.1	0.86	50*	n/a
7b	4	2500	1	1	10a	2	0	2562	0.54	3770	1.97	6.94	0	66.3	0.86	50*	n/a
7c	4	2500	1	1	10a	2.4	0	2820	0.63	3694	1.86	7.72	0	69.0	0.88	53*	n/a
7d	4	2500	1	1	10a	10	0	3027	0.67	3561	2.09	6.70	0.068	95.9	0.88	44*	n/a
7e	4	2500	1	1	10a	20	0	1802	0.5	3049	2.25	6.89	0.047	69.4	0.88	42*	n/a
7f	4	2500	1	1	10a	30	0	1988	0.5	2848	2.29	6.51	0	112.0	0.87	33*	n/a
7g	4	2500	1	1	10a	40	0	1391	0.5	2579	2.33	6.30	0.0017	101.7	0.86	29*	n/a
Analysis 8: Vary Tidal Amplitude																	
8a	4	2500	1	1	10a	0	0	3580	0.42	3835	2.07	8.10	0.018	83.8	0.86	46*	22-25
8b	4	2500	1	1	10a	0	0.2	3763	0.34	3927	2.00	8.60	0.056	90.8	0.86	43*	n/a
8c	4	2500	1	1	10a	0	0.5	4255	0.34	3934	2.17	7.76	0.032	110.9	0.86	42*	n/a
8d	4	2500	1	1	10a	0	0.8	3152	0.45	3788	2.12	8.04	0.01	91.4	0.86	42*	n/a
8e	4	2500	1	1	10a	0	1	3749	0.48	3668	2.42	7.22	0	143.7	0.83	38*	n/a
Analysis 9: Vary Duration																	
9a	4	2500	1	1	10a	0	0	74	3.09	1407	1.81	20.3	0	0	0.63	10	n/a
9b	4	2500	1	1	10a	0	0	155	2.57	2001	1.92	17.0	0	0	0.77	20	n/a
9c	4	2500	1	1	10a	0	0	244	2.10	2471	2.01	12.8	0	4.07	0.83	30	n/a
9d	4	2500	1	1	10a	0	0	517	1.79	2746	1.93	10.0	0	21.9	0.85	40	n/a
9e	4	2500	1	1	10a	0	0	3580	0.42	3835	2.07	8.10	0.018	83.8	0.86	46*	22-25

(Continued)

Table 6. 2D MCO Sensitivity Analysis with Triangular Barrier Island[1] (Concluded).

Input Parameters								Calculations									
ID	H_{bar}, m	W_{bar}, m	H_{mo}, m	S, m	z_o, m	SL, mm/yr	η_a, m	Mig, m	H_{bar_f}, m	Vol_c, m^3	WL_{avg}, m	Vol_{er}, $m^3/m/yr$	Vol_{ow}, $m^3/m/yr$	Vol_{in}, $m^3/m/yr$	z_{max}, m	T_{max}, yr	Fig.
Analysis 10: Randomness of Results with Identical Setup for 50 yr Simulation																	
10a	4	2500	1	1	10a	0	0	3623	0.37	3870	2.09	8.46	0.02	88.3	0.85	44*	n/a
10b	4	2500	1	1	10a	0	0	3580	0.42	3835	2.07	8.10	0.018	83.8	0.86	46*	22-25
10c	4	2500	1	1	10a	0	0	4615	0.30	3987	2.11	9.11	0.028	125.0	0.85	38*	n/a
10d	4	2500	1	1	10a	0	0	3614	0.39	3875	1.99	8.13	0	74.9	0.86	47*	n/a

[1]All simulations conducted with ambient non-storm depth, d_a = 0.5 m (d_a = ambient depth).

Definition of Terminology:

H_{bar} = initial barrier height, W_{bar} = initial barrier width at base, H_{mo} = average deep-water storm wave height, S = average storm surge, z_o = thickness of actively consolidating sediment ("a" indicates $c_{v0} = c_{vc}$ = 2.5 m^2/yr (Virginia data), "b" indicates c_{v0} = 2.5 and c_{vc} = 1.4 m^2/yr (Louisiana data), "c" indicates $c_{v0} = c_{vc}$ = 5 m^2/yr (hypothetical values), SL = rate of eustatic sea level change, η_a = tide amplitude, Mig = total migration of dune crest, H_{bar_f} = final barrier height, Vol_c = volume consolidated, WL_{avg} = average storm water elevation, Vol_{er} = volume eroded, Vol_{ow} = volume runup overwash, z_{max} = maximum consolidation thickness at end of simulation, T_{max} = duration of simulation, Fig = figures associated with each simulation.

* = Barrier island below ambient depth; simulation terminated.

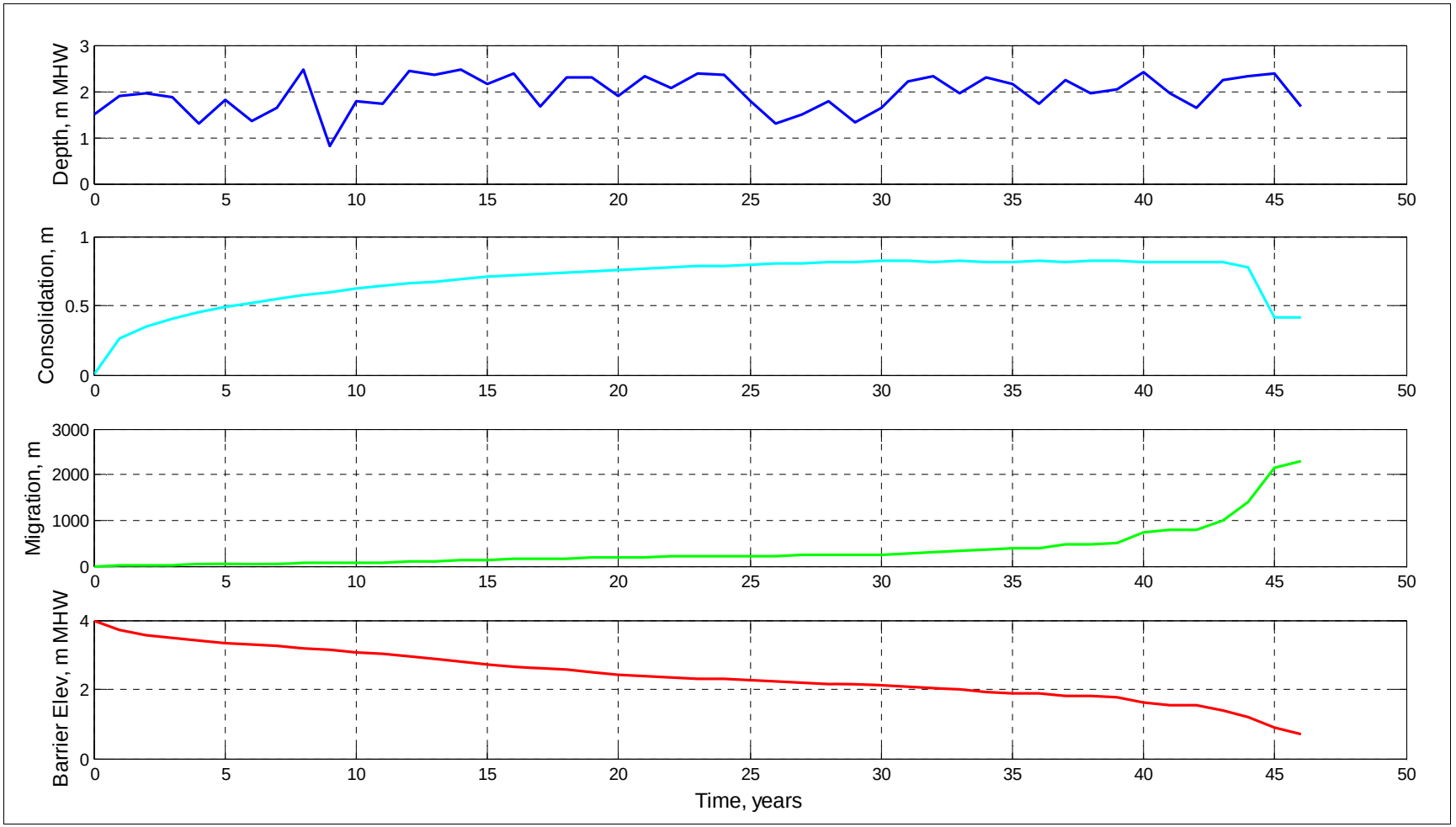

Figure 22. 2D MCO hydrodynamic and morphologic change summary (Table 6, Analysis 2c).

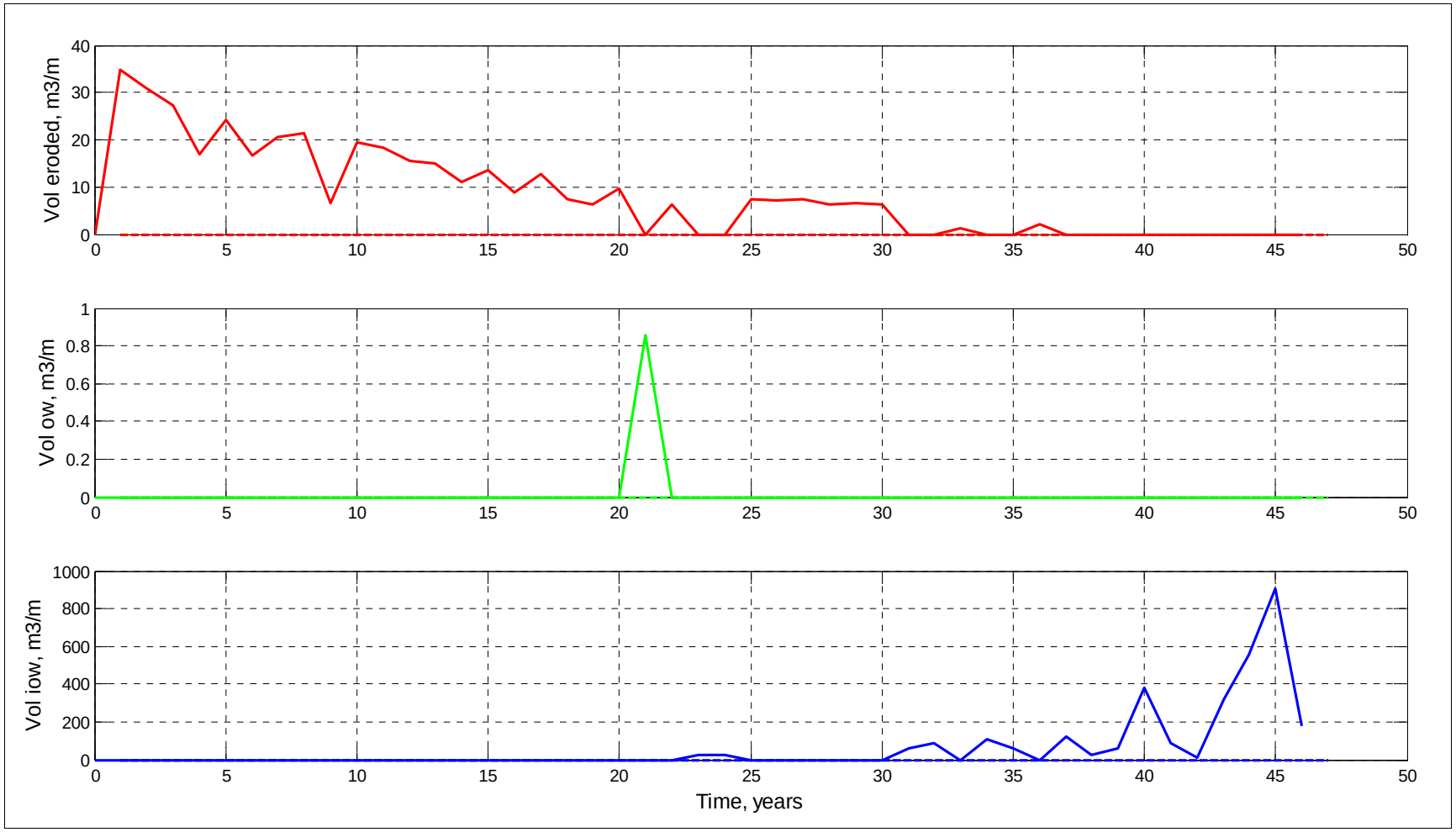

Figure 23. 2D MCO erosion and overwash summary (Table 6, Analysis 2c).

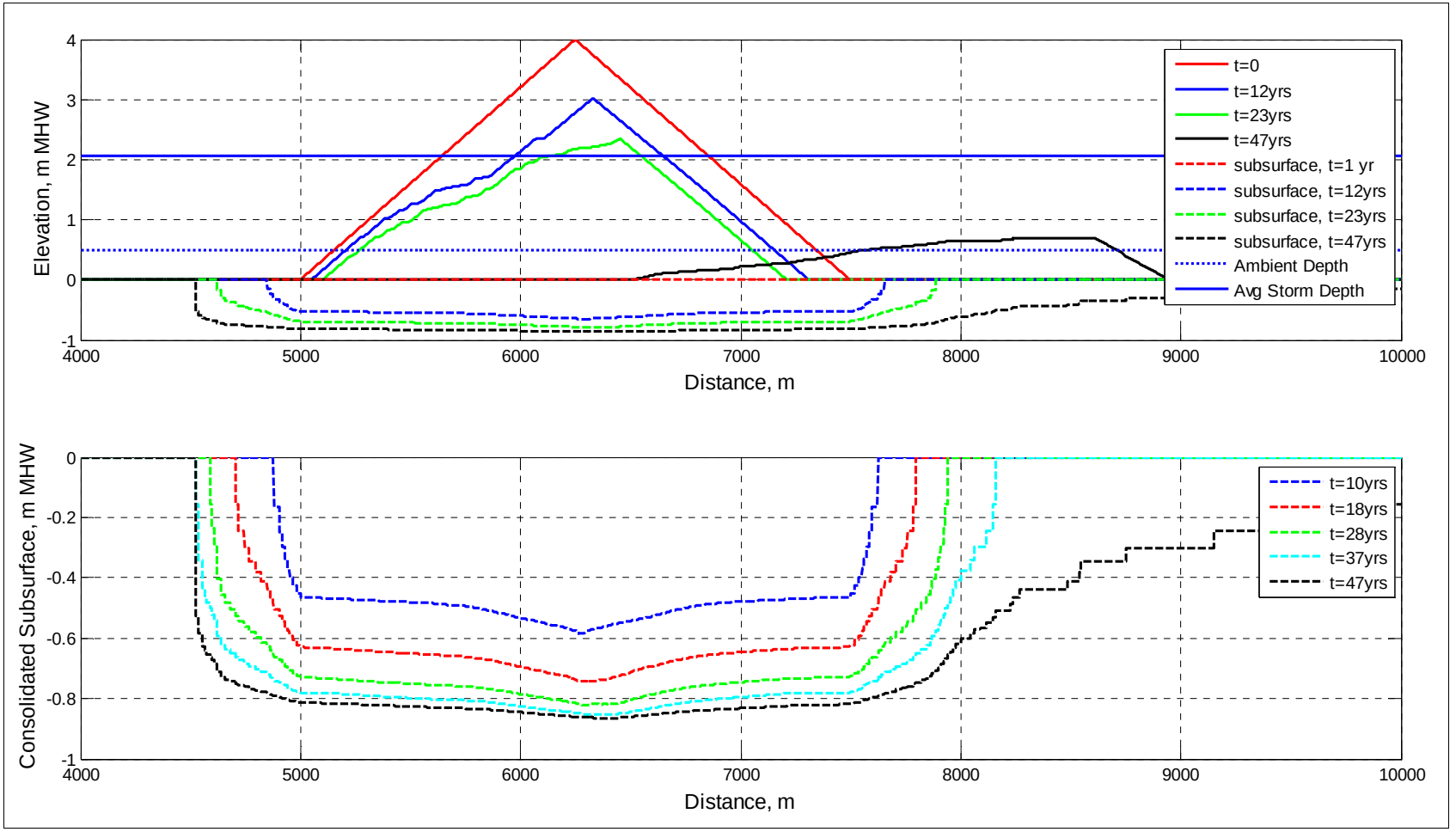

Figure 24. 2D MCO profile and consolidated subsurface (Table 6, Analysis 2c).

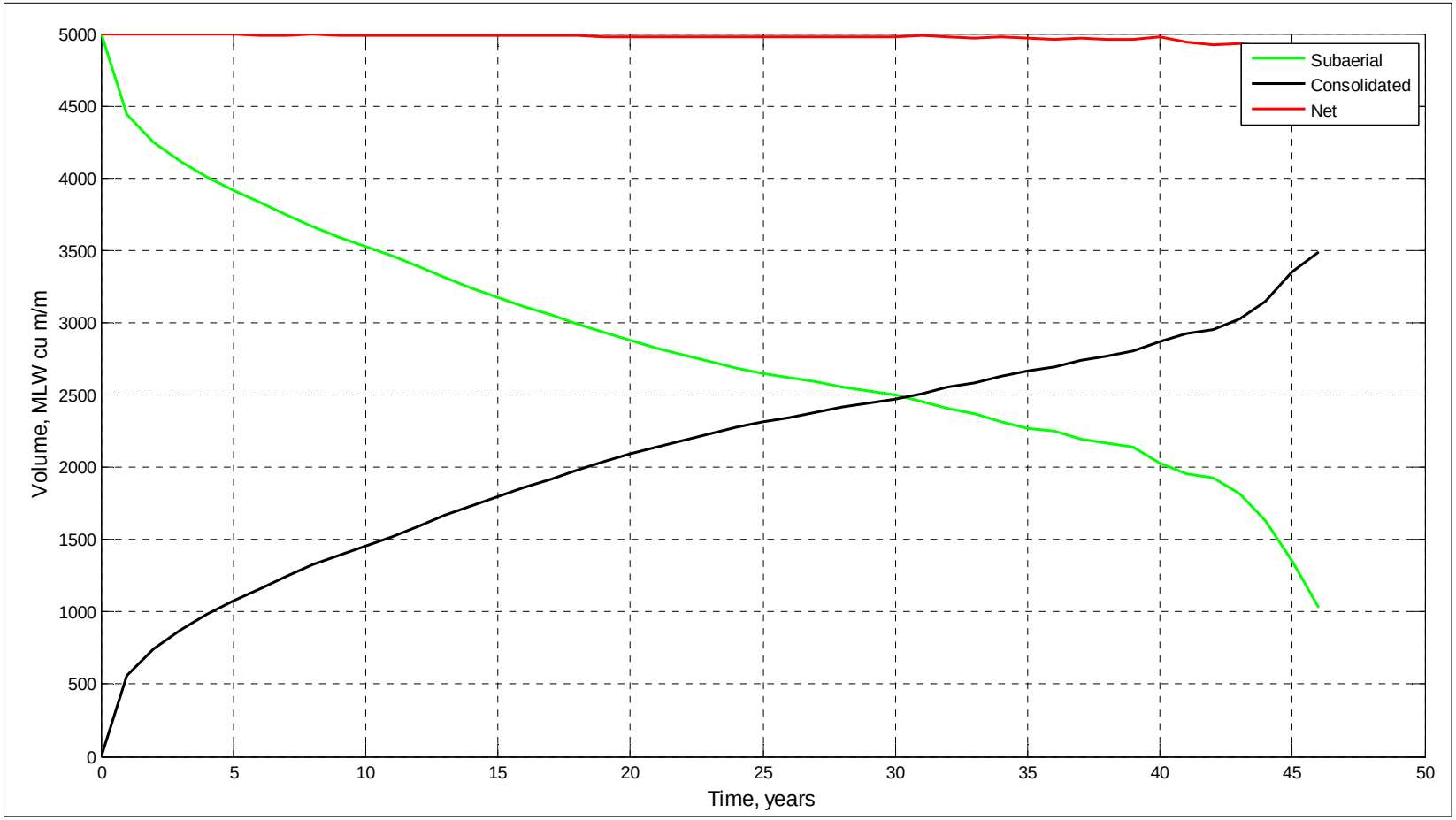

Figure 25. 2D MCO volume change summary (Table 6, Analysis 2c).

Analysis 2 varied the initial dune elevation from 3 to 5 m, with all other parameters held constant. Average storm wave height and surge were each 1 m for all simulations. Initial dune elevation was directly related to the maximum thickness of consolidation, z_{max}. This outcome is expected because a greater dune elevation results in a larger load on the substrate. Analysis 3 repeated these simulations for a non-consolidating substrate; this analysis is discussed in a following section.

Figure 25 shows the volume change summary from Analysis 2c (Table 6), summarizing the change in consolidated volume of sand, the volume of sand above the seabed, and the total sand volume, which is conserved through the simulation. This figure shows that approximately 3,500 m^3/m of barrier island sand was sequestered through the consolidation process, and an increase in the rate of consolidated sand can be observed at approximately year 44, when rapid migration occurred. Commensurate with this increase is a decrease in the volume of sand above the seabed. Additional selected output plots are shown in Appendix A and are not discussed in detail here.

Discussion

Analysis 1 varied the average value of deep-water wave height and surge during each simulation. Individual yearly storm parameters were randomly generated based on the mean value, with the resulting average water level at the island ranging from 1.2 to 3.1 m. As would be expected, storm intensity (as indicated by total water depth, equal to the sum of tide, surge, runup at the swash zone, initial (non-storm) depth, and relative sea level rise) was directly related to the magnitude of island migration and duration of the simulation, and indirectly related to the duration of the simulation (Figure 26). The larger values of migration occurred for simulations with inundation. Larger migration was also associated with a higher rate of Vol_c (volume per unit length of beach that was sequestered through consolidation) due to the movement of the island onto previously unconsolidated (or partially consolidated) bay sediments. The greatest wave height and surge simulation resulted in the island elevation at or below ambient depth after 11 years.

Analysis 2 varied the initial dune elevation from 3 to 5 m, with all other parameters held constant. Average storm wave height and surge were each 1 m for all simulations. Initial dune elevation was directly related to the maximum thickness of consolidation, z_{max}. This outcome is expected because a greater dune elevation results in a larger load on the substrate.

Analysis 3 repeated these simulations for a non-consolidating substrate; this analysis is discussed in a following section.

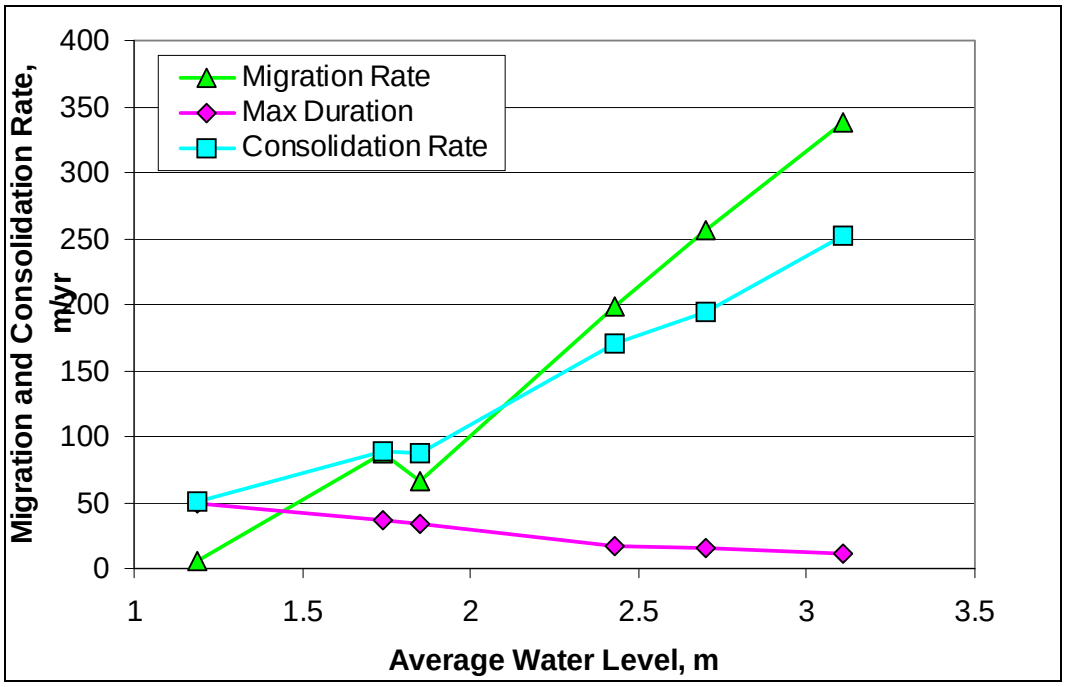

Figure 26. Sensitivity Analysis 1 (Table 6).

Analysis 4 varied initial island width from 1,000 to 3,500 m with the initial dune elevation at 4 m, for average deepwater storm waves and surge each equal to 1 m. Analysis 5 repeated Analysis 4 except for a stable substrate. In Analysis 4, the greatest migration occurred for the narrowest island, although that simulation terminated after 21 years because the island elevation eroded below ambient water depth. Larger island widths sequestered more sediment due to consolidation. The highest final dune elevation occurred for the widest island width. In Analysis 5, all simulations completed the full duration and the majority of morphologic change was due to erosion.

Analysis 6 varied consolidation parameters, both the thickness of compressible sediment (z_0) and the coefficients of consolidation (c_{v0} and c_{vc}, for loads less than and greater than pre-consolidation stress, respectively). All Analysis 6 simulations were conducted with an initial dune elevation of 4 m and 2,500 m width, and 1-m average storm wave height and surge. Four magnitudes of z_0 were evaluated: 5, 10, 20, and 25 m. Three sets of consolidation coefficients were applied: in Table 6, "a" indicates c_{v0} and c_{vc} = 2.5 m^2/year as measured by Gayes (1983) for the barrier islands evaluated in Virginia, "b" indicates c_{v0} = 2.5 and

c_{vc} = 1.4 m²/year as indicated by the Chaland Headland data (Figure 18), and "c" indicates c_{v0} and c_{vc} = 5 m²/year, hypothetical values to simulate extremely soft sediment.

Larger values of z_0 increase the magnitude of maximum consolidation (Figure 27). Analysis 6 calculations reflect this behavior, with the larger values of z_0 resulting in the greatest consolidation and decreased duration of the simulation. Smaller values of z_0 resulted in less consolidation and greater island elevations at the end of the simulation. For simulations varying the consolidation coefficients, greater values of these coefficients increased the volume of sediment that is sequestered through consolidation, which then reduced the final dune crest elevation. The first simulation in this series was conducted with no consolidation, and results in the greatest value of final dune crest equal to 2.6 m.

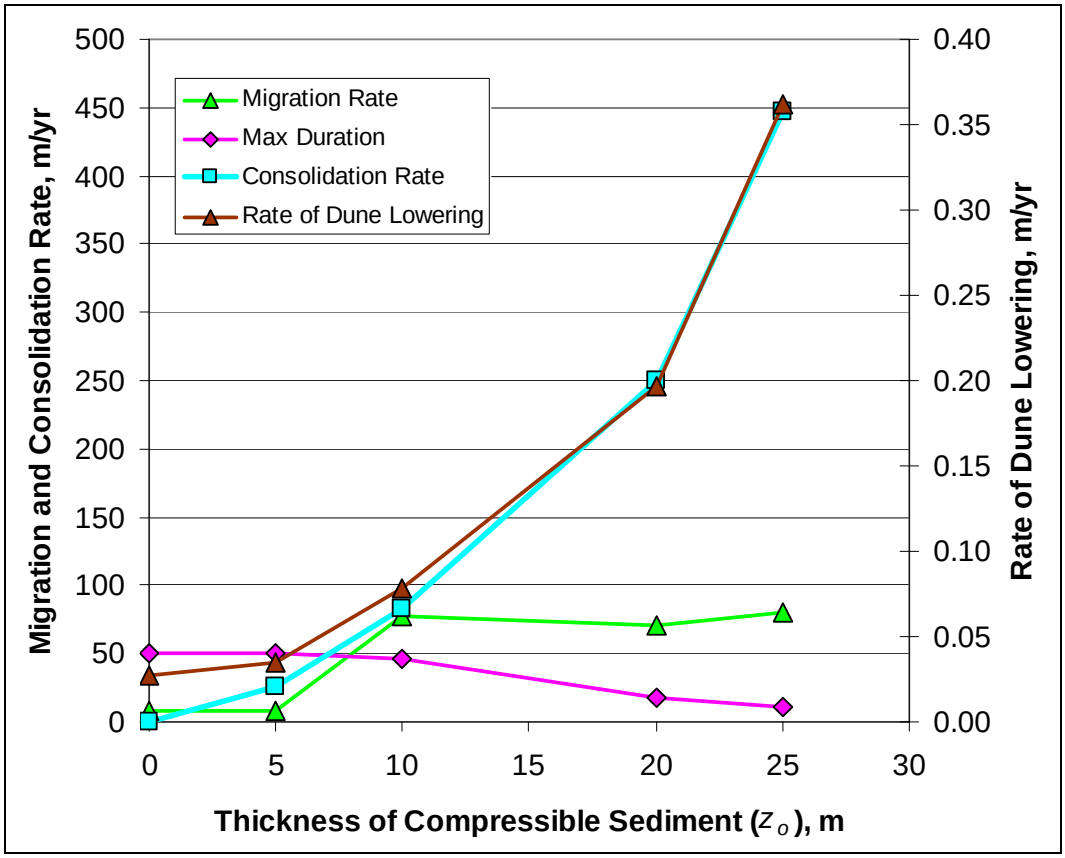

Figure 27. Sensitivity Analysis 6 (Table 6).

Analysis 7 varied the rate of eustatic sea level change, ranging from no change over the 100-year simulation period to a rise of 40 mm/year, approximately four times the sea level rise rate presently being experienced at Grand Isle, LA (9.24 mm/year, measured from 1947 to

2006, NOAA 2008a). Large rates of relative sea level rise were simulated to elucidate trends in the barrier island response and are not intended to represent present-day or imply future conditions. Figure 28 shows that higher rates of relative sea level rise reduced the life of the barrier island, and increased the rate of dune lowering and consolidation at greater values. The migration rate appears to be stable or decreasing, possibly due to the island being subsurface during some of the simulations as indicated by increasing values of inundation overwash for the higher two values (Table 6).

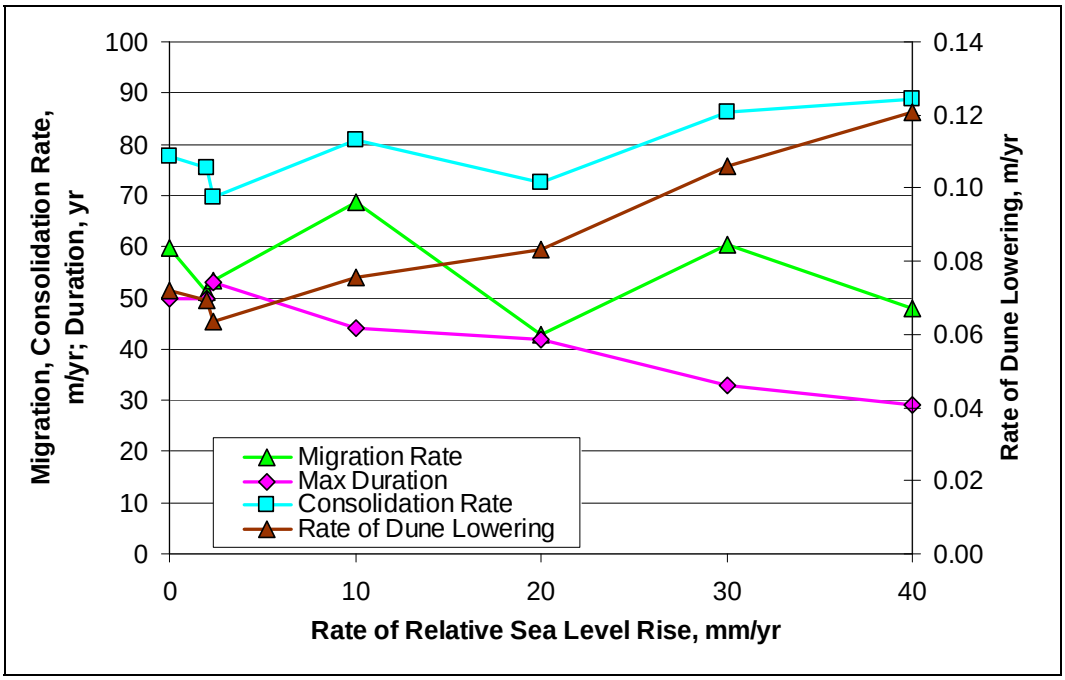

Figure 28. Sensitivity Analysis 7 (Table 6).

Analysis 8 included a tide factor that modified the mean water elevation at the time of the storm for each year of the simulation. Tidal elevations above the zero MHW datum were randomly generated up to the amplitude shown in Table 6 and added to the ambient depth at the time the storm occurred to represent high tide occurring at the time of the storm. Higher tides increased the inundation overwash and reduced the duration of each simulation.

Analysis 9 varied the duration of the simulation ranging from 10, 20, 30, 40, to 50 years. The 50-year simulation was terminated at 46 years because island elevation had eroded below the ambient depth. As would be expected, longer simulations resulted in lower final dune crest elevations,

greater migration distances, and a greater volume of consolidated sediment.

The final sensitivity analysis compared four simulations that were set to run for 50 years. All four of these simulations ended prior to the full duration of the run, ranging from 38 to 47 years, due to the island elevation eroding below ambient depth. A comparison of these simulations gives an indication of the variation associated with random generation of the wave height, associated period, and storm surge nature of 2D MCO results.

In summary, results of the sensitivity analyses with 2D MCO agreed with anticipated response of a barrier island as forced primarily by storms and cross-shore sediment transport processes. Applying the 2D MCO to predict past or future behavior of a barrier island system implies that storm-induced erosion, runup, and inundation overwash, as well as the potential for loading of the substrate and long-term consolidation, are the primary processes determining morphologic response. Other processes, such as a gradient in longshore transport, island vegetation and resistance to erosion, or inlet dynamics would be considered secondary processes (or accounted for with separate analyses) for an appropriate application of the 2D MCO. For many sites and limited applications, these assumptions are reasonable and the 2D MCO is expected to be applicable.

Comparison, calibration, and validation

Overview

The capability of 2D MCO to reproduce field measurements of consolidation and barrier island migration is evaluated in this section. Ideally, sufficient data would be available to calibrate and validate the model for a given site. “Calibration” is an iterative process of applying data as input to the model and comparing model calculations to measurements to determine unknown model parameters. “Validation” is the process of using those calibration parameters to reproduce another set of measurements made at a different time and preferably with considerably different forcing conditions. For field measurements discussed herein, sufficient data were not available for calibration and validation. In those cases, the term “comparison” is introduced to describe application of the model to measurements in which several unknowns were estimated. In these comparisons, the model input conditions were likely only one of many sets

that could be developed and executed in the model to adequately reproduce the measured response.

Data available for comparison included the profile cross-section and sediment core data for the locations in Virginia, as shown in Figures 9 to 12 (Gayes 1983). These data and their applications in the 2D MCO are discussed in the following sections.

Data from Virginia (Gayes 1983)

The Virginia data set included the profile cross-sections, sediment stratigraphy, and migration rate data for three sites as discussed by Gayes (1983), and as presented in Figures 9 to 12 and Appendix B. These measurements are discussed in more detail here as they were compared with simulations from the 2D MCO. They are summarized in Table 7. Note that data presented for Wallops Island (Figure 12) were not analyzed in detail by Gayes (1983) and were not applied for comparison herein because the site was considered to be disturbed. Infrastructure for NASA's Wallops Island Flight Center included a seawall constructed along the seaward boundary of the island, roads, and buildings. The island transect measured by Gayes (1983) was directed towards the bay from a road near the seawall. Also, the site appeared to have stopped migration due to accretion on the up-drift barrier island (development of Fishing Point Spit, southern Assateague Island) and did not exhibit a sand-bay sediment contact in the core data. The Wallops data are not discussed further herein.

The goals of model comparisons with the Virginia data were to test whether 2D MCO could reproduce the cross-shore shape and elevation of the profiles and magnitude and shape of the consolidated surface. Unknowns in this process were the initial profile shape, initial profile cross-sectional volume, storm wave and surge conditions during the simulation period, duration of simulation, the magnitude of z_o in the consolidation calculations (Equations 18, 20, and 23), and results from a Casagrande consolidation test of the subsurface or back barrier sediment cores (e_o, C_{c0},, C_c, p_0 and p_c in Equations 18a and 18b). Values of c_{v0} (assumed equal to c_{vc}) (Equations 19a, 19b, 23a, and 23b, see also the "a" values in Table 6) were available for Metomkin Island at two locations, and the average value of a back barrier sample equal to 2.5 m^2/year was applied for the Metomkin and Assawoman sites. In the absence of Casagrande consolidation test data, values for Chaland Headland (Figure 18) were adopted for the Virginia barrier islands.

Profiles on Assawoman Island and Metomkin Island exhibited a range in dune elevations (1.2 to 2.6 m MHW), maximum sand thicknesses below MHW (1.4 to 3.5 m), and cross-sectional volume of sand (200 to 340 m^3/m) (Table 7). All islands have marsh on the backbarrier, and the 2D MCO model was modified to allow the backbarrier marsh surface to maintain elevation with mean high water during the simulation period. Gayes discussed that the sites also have variability in relative sand supply (presumably through longshore transport processes) and back-barrier sediment sizes. Values of maximum consolidation when adjusted for island migration rates (3.8 to 4.8 m/year) and eustatic sea level rise (Gayes applied eustatic sea level rise equal to 1 mm/year) over a 40-year period are similar, ranging from 1 to 1.2 m. The mean, spring, and neap tidal ranges for Metomkin are 1.1, 1.3, and 0.85 m (Byrnes and Gingerich 1987).

Based on Gayes' description that overwash was "extensive" for the Metomkin site (at 1.2 m MHW dune elevation) and "infrequent" for the Assawoman sites (at 1.4 and 2.6 m MHW dune elevations), it is speculated that a dominant storm water level elevation (including surge, tide, and wave runup) was between 1.2 and 1.4 m MHW for this region of the coast. Byrnes and Gingerich (1987) measured subaerial profile elevations pre- and post-Hurricane Gloria (made landfall on 27 September 1985) at 10 transects along Metomkin Island. Several of their transect locations were along northern Metomkin Island and bracketed Gayes' site. The barrier island was overwashed during Hurricane Gloria with maximum elevations ranging from approximately 2.2 to 2.4 m mean low water (MLW) (1.1 to 1.3 m MHW). Based on water level measurements at two adjacent sites that documented 0.9 and 1.2 m storm surge elevations, Hurricane Gloria was estimated to have created approximately a 1 m storm surge elevation (no datum given) at the Metomkin sites and occurred at astronomically low tides (Byrnes and Gingerich 1987). Wave Information Study (WIS) data for sta 179[1], located in 18-m water depth at latitude 37.75 deg and longitude 75.33 deg , indicated that the mean H_{mo} = 0.9 m ± 0.6 m, with associated peak period T_p = 6 sec ± 2.8 sec. From these discussions and in the absence of other data, it is assumed that a reasonable value for total storm water elevation at the site ranges from 1.0 to 1.4 m MHW, with maximum deep-water significant wave height approximately 1.5 m.

[1] Wave Information Study Hindcast Data, http://frf.usace.army.mil/cgi-bin/wis/atl/atl_main.html, accessed April 30, 2008. Station 179 is in 18 m depth at latitude 37.75 deg and longitude 75.33 deg.

For comparison with 2D MCO, variations in storm surge, offshore wave height, and tidal elevation (randomly generated within the mean tide amplitude equals ±0.55 m) were applied to force the model over simulation periods equal to 40 (period evaluated by Gayes 1983), 100, and 150 years. Eustatic sea level rise was 2 mm/year (Douglas 1992; Peltier 1998) and the initial ambient offshore depth in absence of storms was zero relative to MSL (-0.65 m MHW). Ambient depth increased each year with eustatic sea level rise.

An trial-and-error process was applied in the modeling exercise, modifying the starting dune crest elevation, barrier island width, wave and surge conditions, duration of simulation, and thickness of compressible sediment z_o such that the measured profile cross-sections and cross-shore magnitude of consolidation were approximated after the simulation periods. The simulations are summarized in Table 8 and results are shown in Figures 29 through 34.

The 2D MCO model successfully reproduced the general subaerial shape of the profile and magnitude of the consolidated subsurface. Average water levels during the simulations ranged from 1.5 to 2.1 m MHW, including eustatic sea level rise, tide, storm surge, and wave runup that occurred during each simulation. These average storm water levels are greater than those indicated by the anecdotal data on surge elevations, which do not include wave runup. The consolidation process sequestered from 40 to 60 percent of the total sand volume over the simulation periods. As would be expected from the magnitude of sand that was sequestered through the consolidation process, the initial barrier island cross-sections required to "spin up" the model and develop the final cross-sections were much greater in volume than the measured cross-sections.

Table 7. Data from Virginia applied in comparison with 2D MCO (summarized from Gayes 1983).

Site	Dune Elevation (m, MHW)	Maximum Sand Thickness Below MHW (m)	Sand Volume (m^3/m)	Migration Rate (m/yr)	Relative Back-Barrier Sediment Size	Relative Frequency of Overwash	Relative Sand Supply	Maximum Consolidation due to Loading by Barrier Island Sand over 40 years* (m)
Assawoman 1 (Figure 9)	1.4	2.2	225	3.75	Finest; organic-rich	Infrequent	Greatest	1.1
Assawoman 2 (Figure 10)	2.6	3.5	343	4.05	Coarsest; greatest energy	Infrequent	Intermediate	1.0
Metomkin (Figure 11)	1.2	1.4	194	4.79	Medium	Extensive	Lowest	1.2
Wallops (Figure 12)	0.8	2.3	Disturbed site; not considered					

* Adjusted to remove sequestering of sand due to eustatic sea level rise = 1 mm/year (original value applied in calculation by Gayes 1983).

Table 8. Application of 2D MCO in comparison with Virginia Barrier Islands.[1]

Input Parameters					Calculations									
H_{bar}, m MHW	W_{bar}, m	H_{mo}, m	S, m MHW	z_o, m	Mig, m	H_{bar_f}, m MHW	Vol_c, m³ (%V)	WL_{avg}, m MHW	Vol_{er}, m³/m/yr	Vol_{ow}, m³/m/yr	Vol_{in}, m³/m/yr	z_{max_dune}, m MHW	T_{max}, yr	Fig.
Assawoman 1														
5	400	1.5	0.2	12a	77*	1.47	431 (56%)	1.80	4.15	0	0	1.13	40	
5.6	400	1.5	0.2	10a	148*	1.42	460 (50%)	1.51	3.06	0	0	1.05	100	
7	400	1.5	0.2	10a	208*	1.41	579 (48%)	1.60	3.51	0	0	1.09	150	29, 30
					Measurements									
					150*	1.4	–	–	–	–	–	1.1	40	
Assawoman 2														
5	400	1.5	0.2	13a	86*	2.48	473 (44%)	1.87	8.74	0	0	1.14	40	
7.6	400	1.5	0.2	9a	178*	2.42	577 (39%)	2.00	9.10	0	0	1.16	100	
9.6	400	1.5	0.2	9a	193*	2.38	704 (41%)	1.93	8.67	0.12	0	1.07	150	31, 32
					Measurements									
					162*	2.6	–	–	–	–	–	1.0	40	

(Continued)

Table 8. Application of 2D MCO in comparison with Virginia Barrier Islands[1] (Concluded).

Input Parameters					Calculations									
Hbar, m MHW	Wbar, m	Hmo, m	S, m MHW	zo, m	Mig, m	Hbar_f, m MHW	Volc, m3 (%V)	WLavg, m MHW	Voler, m3/m/yr	Volow, m3/m/yr	Volin, m3/m/yr	zmax_ dune, m MHW	Tmax, yr	Fig.
Metomkin														
4.9	400	1.5	0.2	13a	74*	1.27	461 (62%)	1.77	3.77	0	0	1.22	40	
7.6	400	1.5	0.35	11a	189 *	1.31	739 (56%)	1.80	7.56	0.22	0	1.28	100	
7.3	400	1.5	0.2	10a	208*	1.25	665 (52%)	2.12	4.75	0	0	1.16	150	33, 34
					Measurements									
					192*	1.2	–	–	–	–	–	1.2	40	

[1] All simulations conducted with ambient non-storm depth, d_a = 0.65 m (d_a = ambient depth).

Definition of Terminology:

H_{bar} = initial barrier height, W_{bar} = initial barrier width at base, H_{mo} = average deep-water storm wave height, S = average storm surge, z_o = thickness of actively consolidating sediment ("a" indicates c_{v0} =c_{vc} =2.5 m^2/yr, Virginia data), SL = eustatic sea level rise = 2 mm/yr, tide amplitude = 0.55 m, Mig = total migration of dune crest, H_{bar_f} = final barrier height, Vol_c = volume consolidated and percent of total volume, WL_{avg} = average storm water elevation, Vol_{er} = volume eroded, Vol_{ow} = volume runup overwash, z_{max_dune} = consolidation thickness beneath dune crest at end of simulation, T_{max} = duration of simulation, Fig. = figures associated with each simulation.

* = Direct comparison can not be made between measured and calculated migration rates, because calculations include initial adjustment of the profile and do not only represent movement of the island.

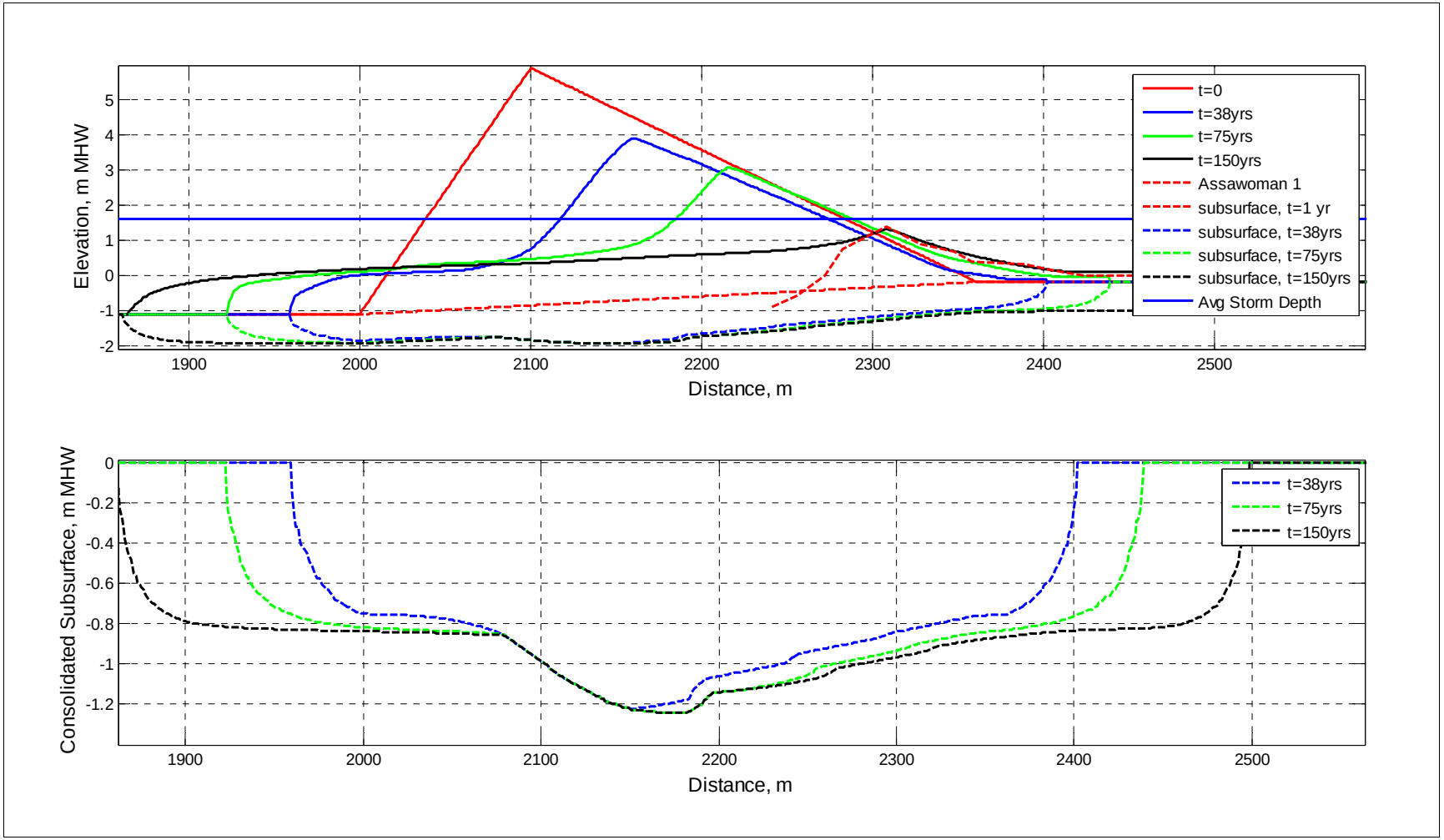

Figure 29. 2D MCO comparison with Assawoman 1, VA, for 150-year simulation: Evolution of profile (top) and consolidation magnitude (bottom).

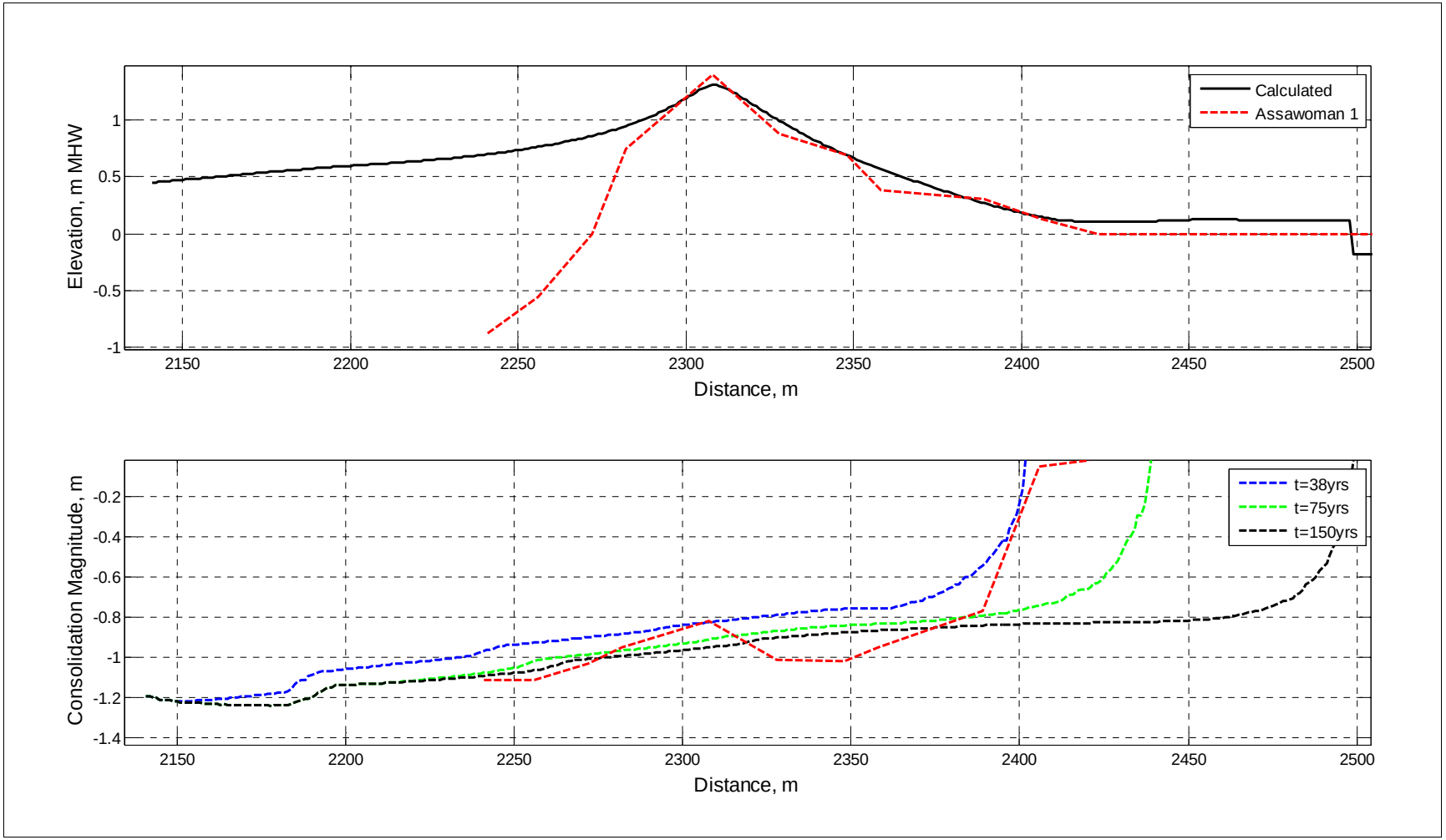

Figure 30. 2D MCO comparison with Assawoman 1, VA: Profiles (top) and consolidation magnitude (bottom) after 150 year simulation.

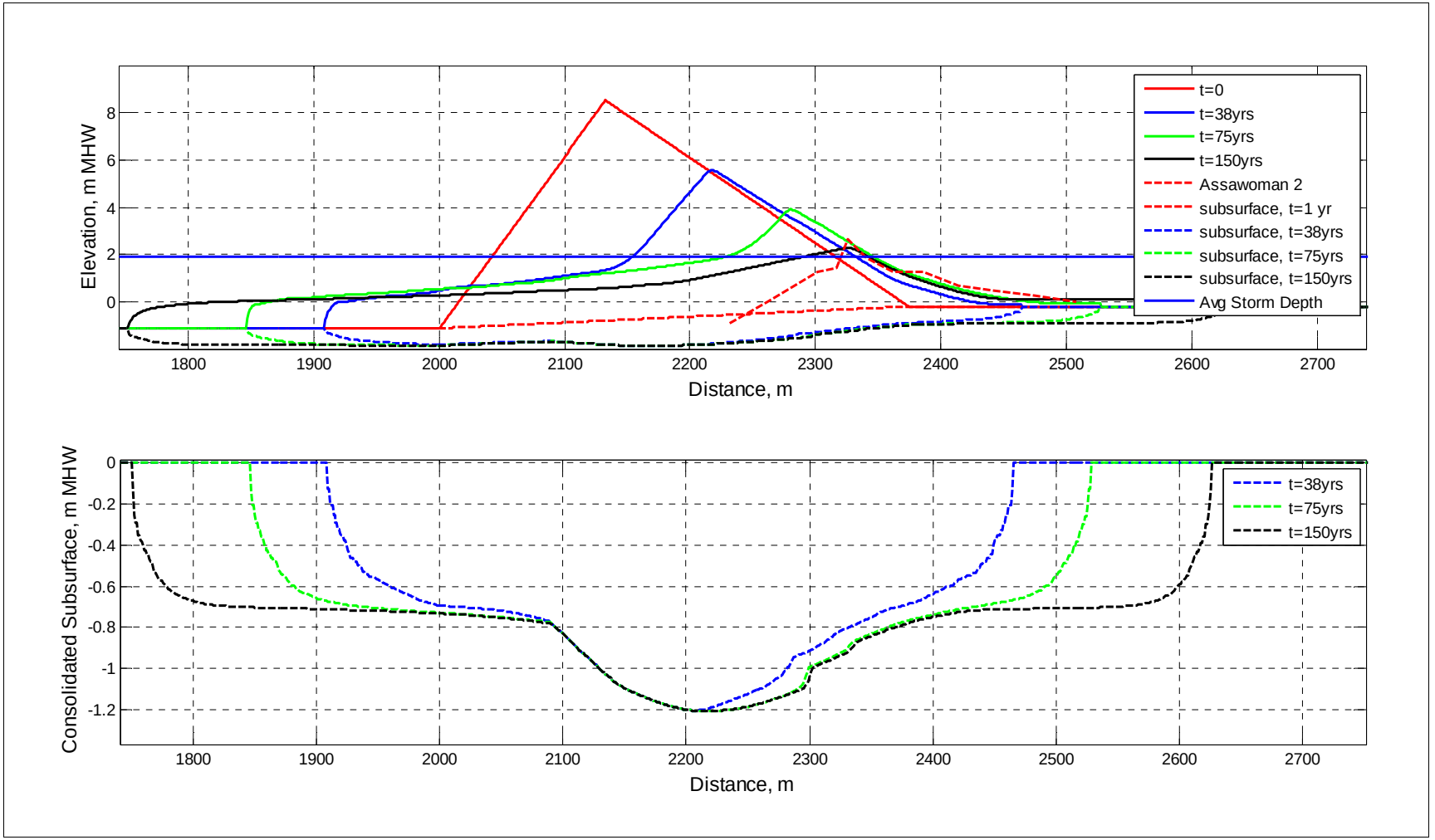

Figure 31. 2D MCO comparison with Assawoman 2, VA, for 150-year simulation: Evolution of profile (top) and consolidation magnitude (bottom).

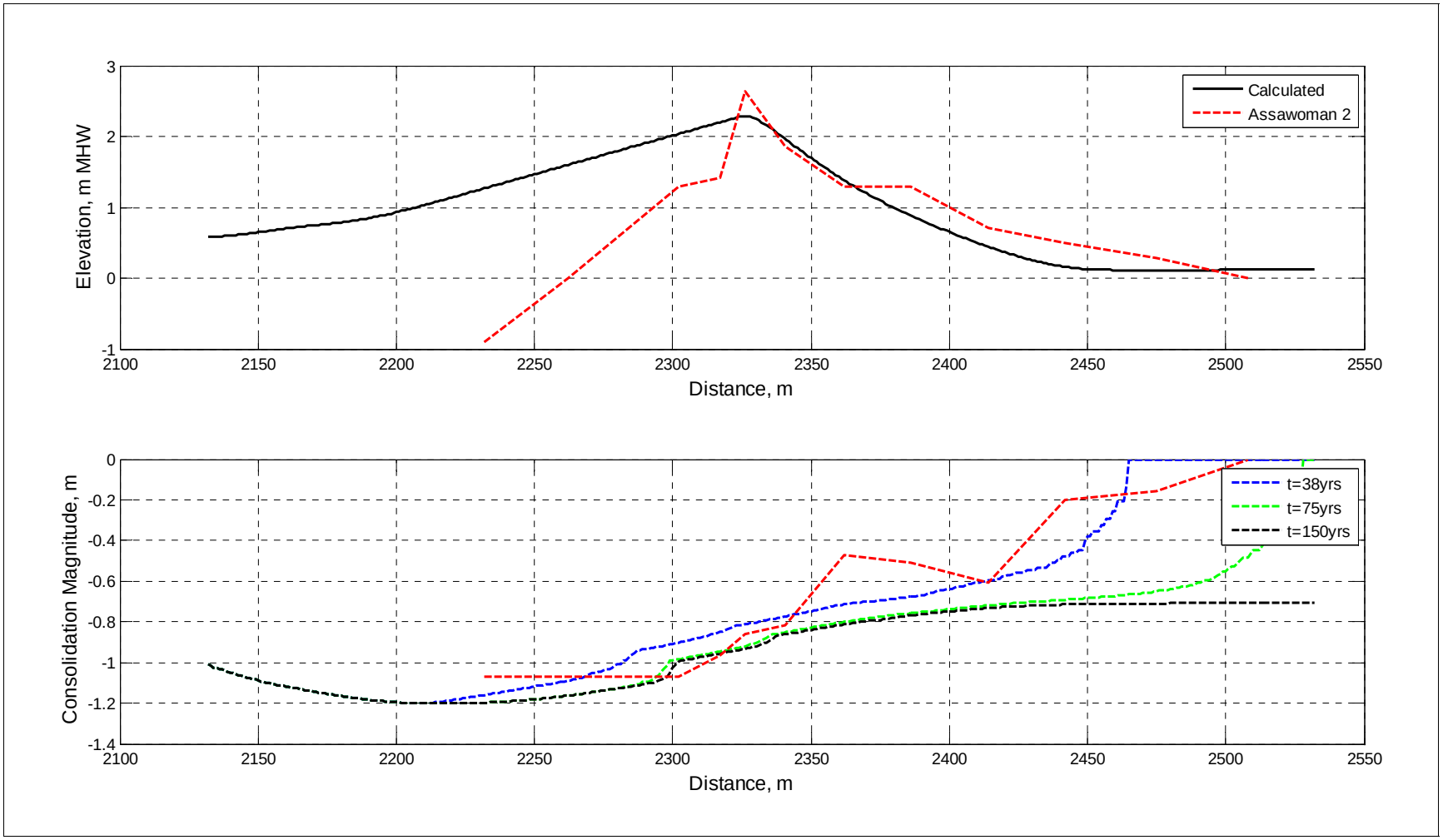

Figure 32. 2D MCO comparison with Assawoman 2, VA: Profiles (top) and consolidation magnitude (bottom) after 150 year simulation.

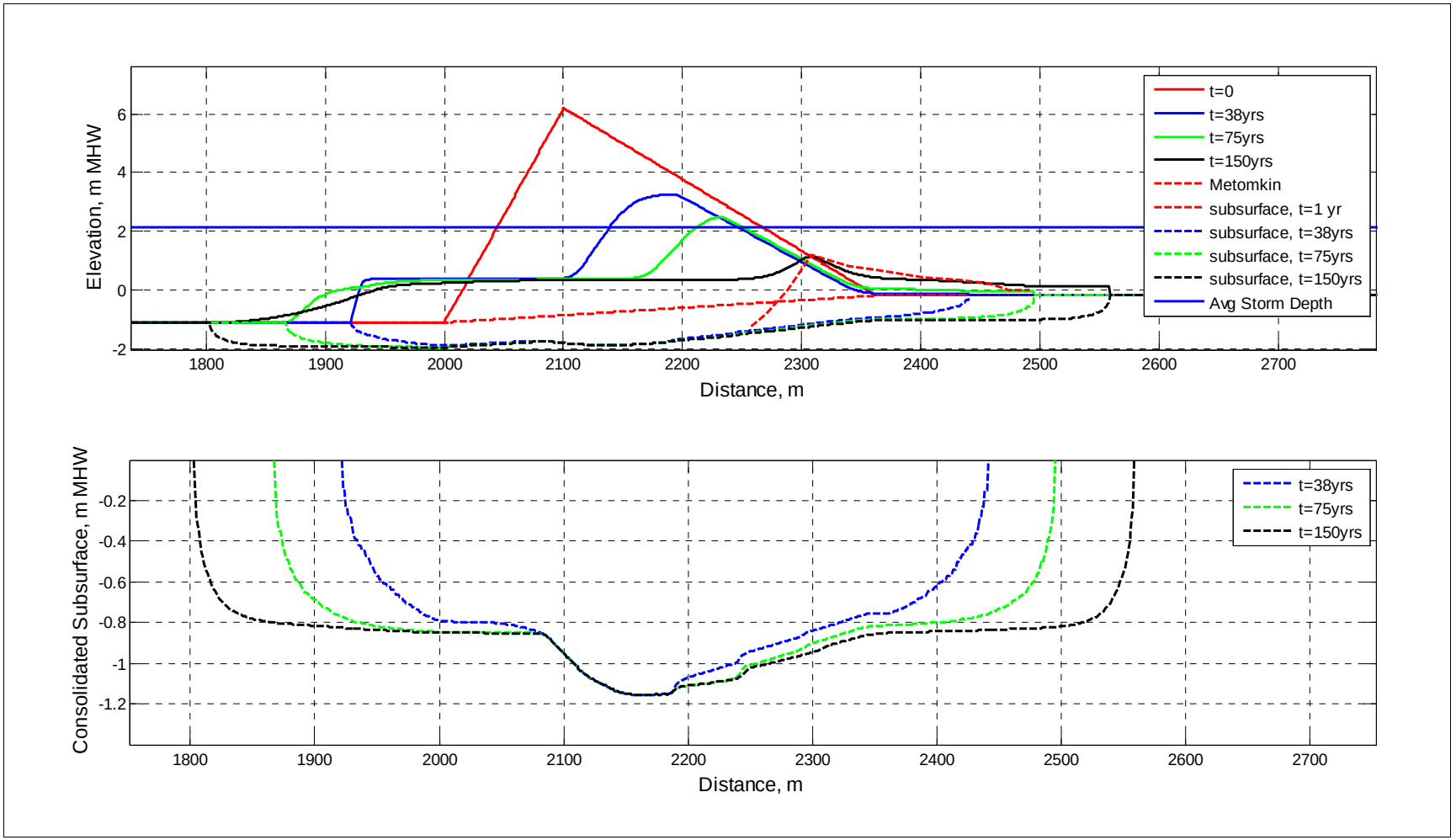

Figure 33. 2D MCO comparison with Metomkin, VA, for 150-year simulation: Evolution of profile (top) and consolidation magnitude (bottom).

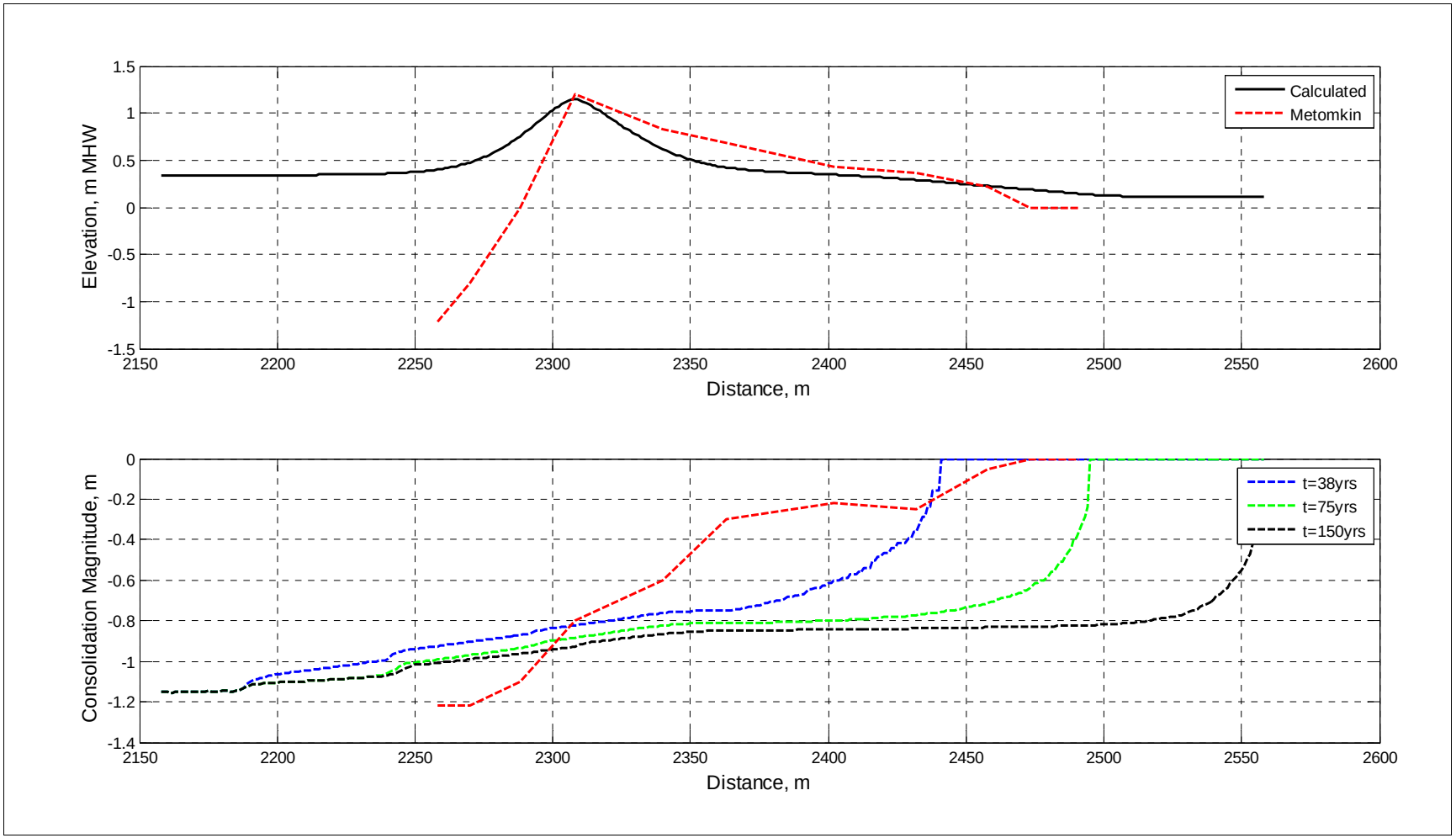

Figure 34. 2D MCO comparison with Metomkin, VA: Profiles (top) and consolidation magnitude (bottom) after 150 year simulation.

Implications of a consolidating substrate

To explore how consolidation modifies morphologic response of a barrier island, simulations were conducted with and without a consolidating substrate for dune crests ranging from 2.5 to 5 m elevation for 50 year durations. These simulations are Analyses 2 and 3 as listed in Table 6, and are compared in Figure 35.

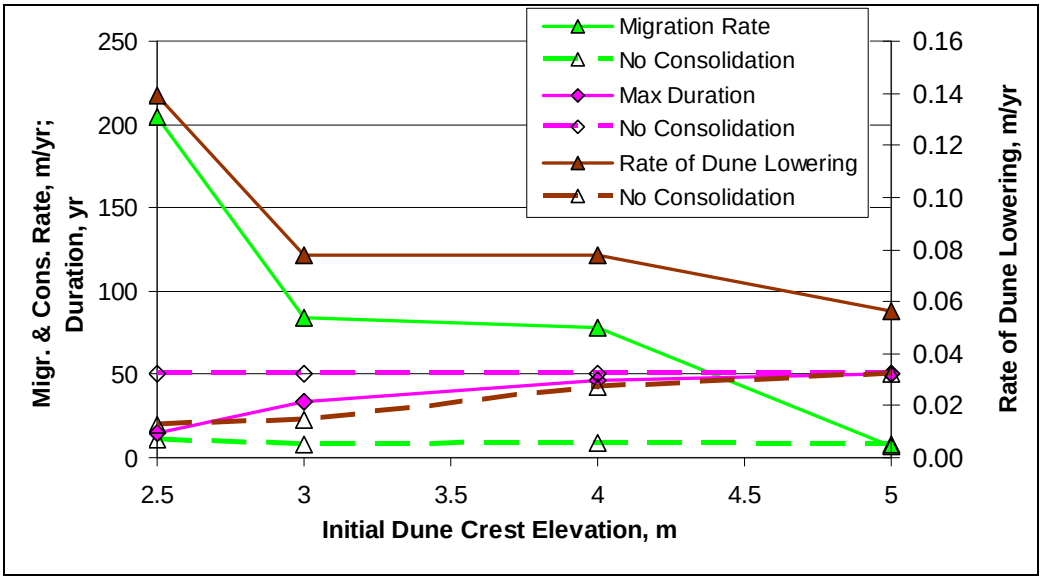

Figure 35. Comparison of consolidating and non-consolidating substrate (Sensitivity Analyses 2 and 3).

Figure 35 compares output for the consolidating and non-consolidating substrates, with the non-consolidating simulations indicated by dashed lines. All non-consolidating simulations completed the 50-year duration; however, simulations for the consolidating substrate with the lowest three dune elevations (2.5, 3.0, and 4.0 m) eroded below mean water level and these simulations were terminated prior to 50 years. Migration rates for the non-consolidating substrate were similar regardless of dune crest elevation, whereas the lower dune crest elevations for the consolidating simulations had greater migration rates which decreased as the dune increased elevation. The rate of migration for the 5-m dune crest was approximately the same for both the consolidating and non-consolidating substrates, indicating that there was sufficient sand volume in the system for the non-consolidating substrate to accommodate the consolidation process as well as remain relatively stable for the 50-year period.

For the consolidating substrate, the rate of dune lowering decreased with increasing initial dune crest elevation. Lowering of the dune crest is

initially rapid due to the consolidation process. For the 2.5, 3.0, and 4.0-m dune crests, the simulations terminated because the island submerged below ambient depth. Thus, these rates of dune lowering indicate a portion of the initial adjustment of the island through consolidation of the substrate. For the non-consolidating substrate, the rate of dune lowering increased slightly (from 0.01 to 0.03 m/year) as elevation increases. This increasing trend reveals another, less dominant, process in evolution of the island, which is the tendency for the sub-aerial island to be more stable when the relative elevation of the island to storm runup is small (z_R in Figure 16 and Equations 8 and 12). Once the island becomes sub-aqueous, the simulation terminates. If the dune crest elevations are sufficient to avoid significant overwash and inundation for the simulation period, migration rates do not vary as a function of substrate characteristics.

Conclusions

This chapter presented theoretical development, sensitivity analyses, and comparison of simulation results for the two-dimensional Migration, Consolidation, and Overwash (2D MCO) model developed herein. Sensitivity analyses with 2D MCO agreed with anticipated response of a barrier island as forced primarily by storms and cross-shore sediment transport processes. The 2D MCO model successfully reproduced the general shape and magnitude of profiles and the associated consolidated subsurface in a comparison of model results to data from Virginia, lending credence to the model calculations. An examination of how subsurface characteristics modify profile response indicated that barrier islands overlying a consolidating substrate are more likely to have: (a) reduced dune elevations due to the consolidation process, (b) overall volumetric adjustment of the profile to fill in compressed regions outside the immediate footprint of the island, and (c) increased overwash and migration when the dune reaches a critical elevation with respect to the total water elevation of the prevalent storm conditions.

Thus, 2D MCO has been shown to give reasonable results for cross-shore sand transport processes as well as consolidation behavior of the substrate as it is loaded by the barrier island. These calculations illustrated how the consolidation process modifies profile response through lowering of the dune elevation and increasing the propensity for overwash and migration. The next chapter examines some long-term processes that may occur during the non-storm period that can change the overall volumetric budget of the island.

5 Long-Term Processes in Barrier Island Evolution

Overview

The 2D Migration, Consolidation, and Overwash (2D MCO) model presented in Chapter 4 calculates storm-induced erosion and overwash and the resulting barrier island morphology change over time scales of years to centuries. The simplifying assumption in application of the 2D model is that long-term processes are relatively weak in modifying the barrier island cross-sectional profile during times without storms. However, the literature review in Chapter 2 as well as observations of barrier island response indicate that, for some locations and situations, post-storm and non-storm processes can alter the island cross-sectional and planform volume prior to the next storm. For these sites, long-term processes must be represented to properly calculate the morphologic response of the barrier island. The purpose of this chapter is to identify long-term processes that may occur in evolution of barrier island systems that overlie a compressible substrate, to discuss the theory behind each process, and characterize the magnitude of the process through data analysis or knowledge available in the literature.

Based on the literature review in Chapter 2, long-term processes necessary for characterizing long-term morphology change for barrier islands in the Northern Gulf of Mexico have been identified as:

1. A gradient in longshore sand transport (LST) that can provide a net source or sink of sand from the barrier island, create terminal spits, and migrate the island alongshore.
2. Post-storm recovery of the beach following a storm, via: (a) alongshore spit migration and attachment, and (b) bar migration onshore, welding to the beach, and berm formation.
3. Eolian or wind-blown sand transport and dune building for sites with a dry, sandy beach of sufficient width and elevation, and wind exceeding a threshold speed for a given sediment size on the beach.
4. Erosion of fine-grained silt, clay, and organic sediment during the immediate post-storm period, when barrier island sand has not yet returned to the beach and this sediment is exposed.

5. Long-term increase in bay area (through relative sea level rise, erosion of mainland, loss of wetlands on mainland) resulting in an increase in: (a) fetch distance, and therefore the potential for wind-induced erosion of the bay shoreline of the barrier island, and (b) tidal prism and adjacent inlet ebb and flood tidal delta volumes, thus increasing the amount of sand that is required from the adjacent barrier islands.

In the next section, each of these long-term processes is quantified at a level of detail consistent with the 2D MCO and developed in 2D MCO sub-modules to calculate potential response.

Theory and conceptual development of sub-modules

Gradient in longshore sand transport

A gradient in LST occurs if the source of sand transported into a specified region is either greater or less than the rate of alongshore sand transport leaving the region. A positive gradient in LST means that the transport rate into the area is less than the rate out of the area, resulting in a net loss or deficit of sand to the island segment being considered. A negative gradient in LST will result in the opposite: a gain or surplus of sand to the segment.

To calculate the gradient in LST, the active depth of the profile, D_A, is estimated as the sum of the berm crest elevation, h_{berm}, and depth of closure, D_c.

$$D_A = h_{berm} + D_c \tag{24}$$

The change in shoreline position due to LST, dx/dt_{LST}, is

$$\frac{dx}{dt_{LST}} = \frac{(Q_{in} - Q_{out})}{L_i D_A} \tag{25}$$

in which Q_{in} and Q_{out} are the net longshore sand transport rates into and out of the region considered, respectively, and L_i is the length of the shoreline segment considered (Figure 36). As an example, suppose Q_{in} - Q_{out} = -10,000 m^3/year, L_i = 1,000 m, and D_A = 4 m. Then dx/dt_{LST} = -10,000/(1,000 × 4) = -2.5 m/year, and the profile between the berm crest elevation and depth of closure recedes at this rate during the simulation.

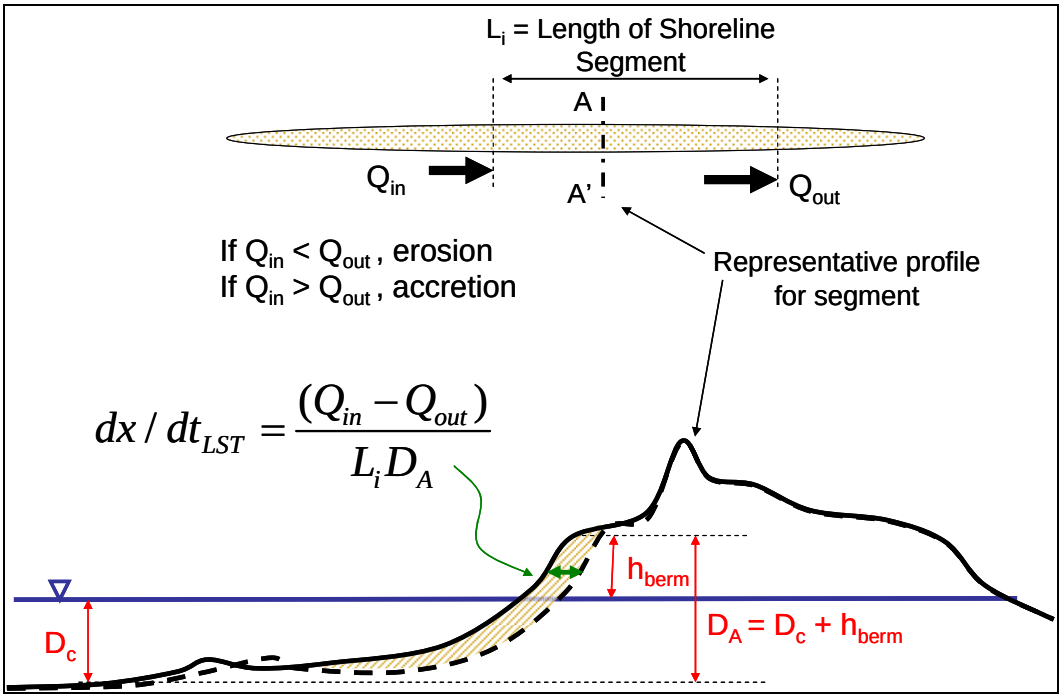

Figure 36. Definition of terms for incorporating a gradient in LST.

Post-storm recovery

During a storm, sediment can be eroded from the beach and transported seaward, as well as washed over the crest of the island and deposited on the backshore or into the bay. Sand that is eroded can be deposited offshore or transported alongshore. Fine sediment that is eroded can remain in suspension and be transported outside the littoral system of the island, and therefore be lost to its volumetric budget. These storm processes operate on time scales of hours to days. In contrast, recovery processes require weeks, years, or decades depending on the severity of the storm and constructive capability of the post-storm processes. Sand that is deposited offshore can form a bar and migrate onshore and eventually weld to the beach, thus returning to the barrier island system.

A conceptual Recovery Sub-Module was developed to describe a time-dependent sediment budget for the cross-shore profile following the storm, including any losses to the littoral budget through suspension of fines as well as the time-dependent onshore bar migration and welding to the beach. The volume of the subaerial barrier island can be described as:

$$V_i(t_o + t_s) = V_i(t_o) - V_{er}(t_s) \quad (26)$$

where V_i is the volume per unit width of the subaerial island, t_o is the time just prior to the storm, t_s is the storm duration, and V_{er} (t_s) is the volume eroded from the island during the storm. Assuming that a percentage of the volume eroded represented fine sediment that was suspended and lost from the littoral segment, the volume of sand deposited in the offshore bar, V_b (t_o + t_s), as a result of the storm can be represented by:

$$V_b\left(t_o + t_s\right) = \left(1 - p_f\right) V_{er}\left(t_s\right) \tag{27}$$

in which p_f is the percent of fine sediment in the eroded volume. During the post-storm recovery period, the time-dependent volume of bar welding to the subaerial beach, V_{bw} (t_o + t_s + t_w), is parameterized as:

$$V_{bw}\left(t_o + t_s + t_w\right) = V_b\left(t_o + t_s\right)\left(1 - e^{-k_1 t_w}\right) \tag{28}$$

where k_1 is an empirical coefficient governing the time of onshore migration of the bar, and t_w is the elapsed time since the storm ended. The form of this time-dependent relationship is shown in Figure 37a for V_b = 100 m^3/m, t_s = 0 year, and k_1 = 0.1, 0.05, and 0.01 $year^{-1}$. For this example, the volume in the offshore bar, V_b, was held constant as if replenished by another source of sand to illustrate the form of Equation 28. Figure 37b shows a similar simulation, except that the volume of the offshore bar is not replenished, and V_b decreases as sand is transported to the beach in the form of the welded bar.

As the bar welds to the shore, the width of the subaerial beach on the ocean side of the island, $W_o(t)$, increases. The width of the non-vegetated portion of the subaerial beach on the bay side of the island, $W_b(t)$, will increase in width (and may bury existing vegetation) if washover occurred during the storm. If the beach is vegetated or too narrow, the potential for eolian transport is reduced. For a narrow beach, any sand that is transported by the wind may blow over the island and into the bay or ocean.

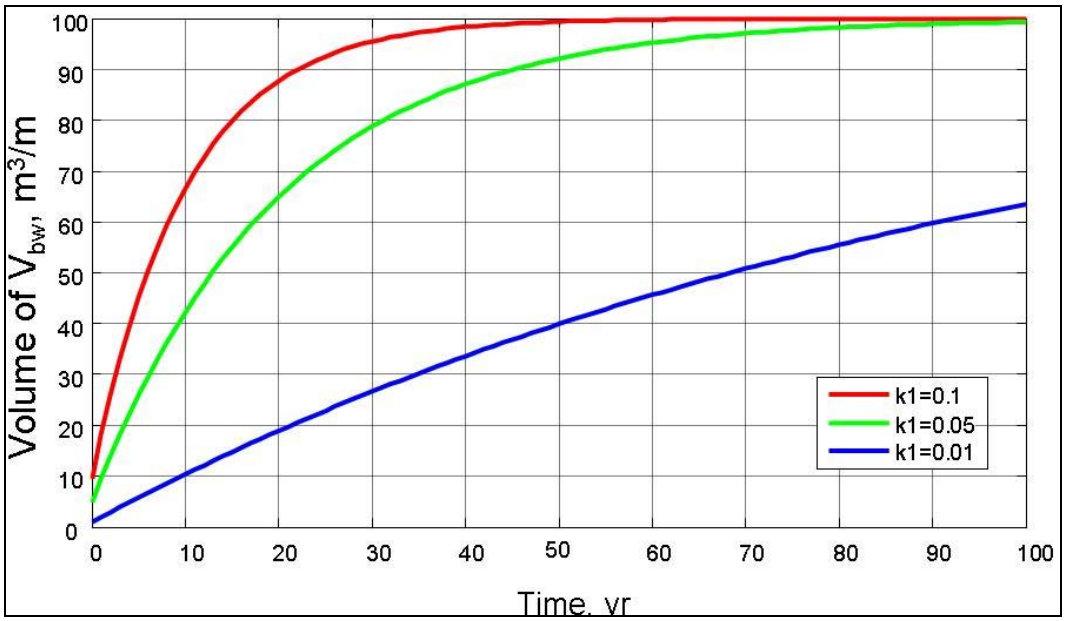

Volume of offshore bar, V_b, held constant.

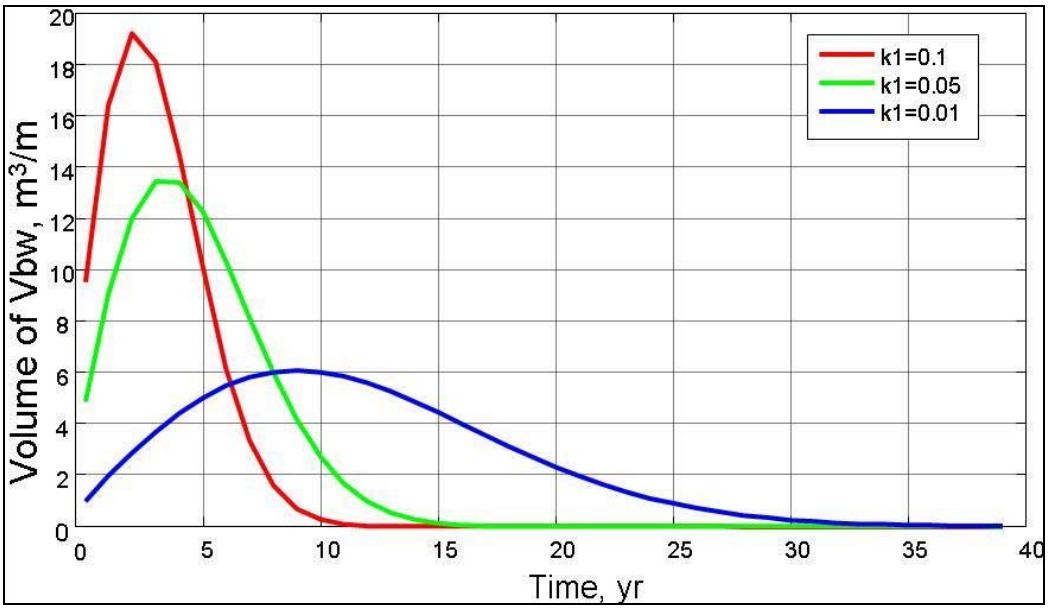

b. Volume of offshore bar, V_b, decreases as V_{bw} increases.

Figure 37. Plot of Equation 28 for initial V_b = 100 m^3/m and various k_1 values.

If the beach is saturated during the period when wind speed is sufficient for transport of sand, eolian transport cannot occur. The beach must increase elevation through overwash processes or the water level must decrease before sand can be mobilized by wind. In addition, the wind speed U_z, measured at elevation z, must exceed the threshold for initiation of motion, U_{zt}. Thus, the beach on the ocean and bay side of the island

must be of sufficient width, elevation, and have some minimum area without vegetation to initiate dune building. The minimum non-vegetated width necessary for wind-blown sand transport to occur and begin building a dune system is represented in the conceptual model both on the ocean and bay sides of the island by W_{wbs}. The wind-blown sand process is discussed in the following section. The conceptual model is illustrated in Figure 38.

Wind-blown (eolian) sand transport

The magnitude of wind-blown or eolian sand transport depends on characteristics of the sand available for transport (grain size, size distribution, moisture content, and degree of grain-to-grain packing), wind speed and vertical gradient of the wind at the beach surface, and local ground conditions such as topography, vegetation, and armoring of the beach (Hsu and Weggel 2002). The threshold wind speed for initiation of eolian sand transport, u_{*t}, can be calculated as:

$$u_{*_t} = A_t \sqrt{\frac{(\rho_s - \rho_a) g d_{50}}{\rho_a}} \tag{29}$$

where A_t is a dimensionless empirical coefficient found equal to 0.118, ρ_s is the mass density of sediment typically taken as 2.65 g/cm^3 for quartz sand, ρ_a is the mass density of air equal to 1.22 × 10^{-3} g/cm^3 at 18˚C, g is the acceleration due to gravity equal to 981 cm/sec^2, and d_{50} is the median diameter of the sand (cm). Representative median grain size for Isle Dernieres, LA, ranges from 0.16-0.19 mm or 0.016-0.019 cm (Dingler et al. 1992), which gives the threshold wind speed at the beach surface, u_{*t} = 21.7 to 23.7 cm/sec.

Wind speed data are typically obtained at or corrected to a standard elevation of 10 m above ground level (Hsu and Weggel 2002). The wind speed at any elevation, u_z, associated with the threshold speed at the beach can be determined as:

$$u_z = \frac{u_{*_t}}{\kappa} \ln\left(\frac{z_z}{z_r}\right) \tag{30}$$

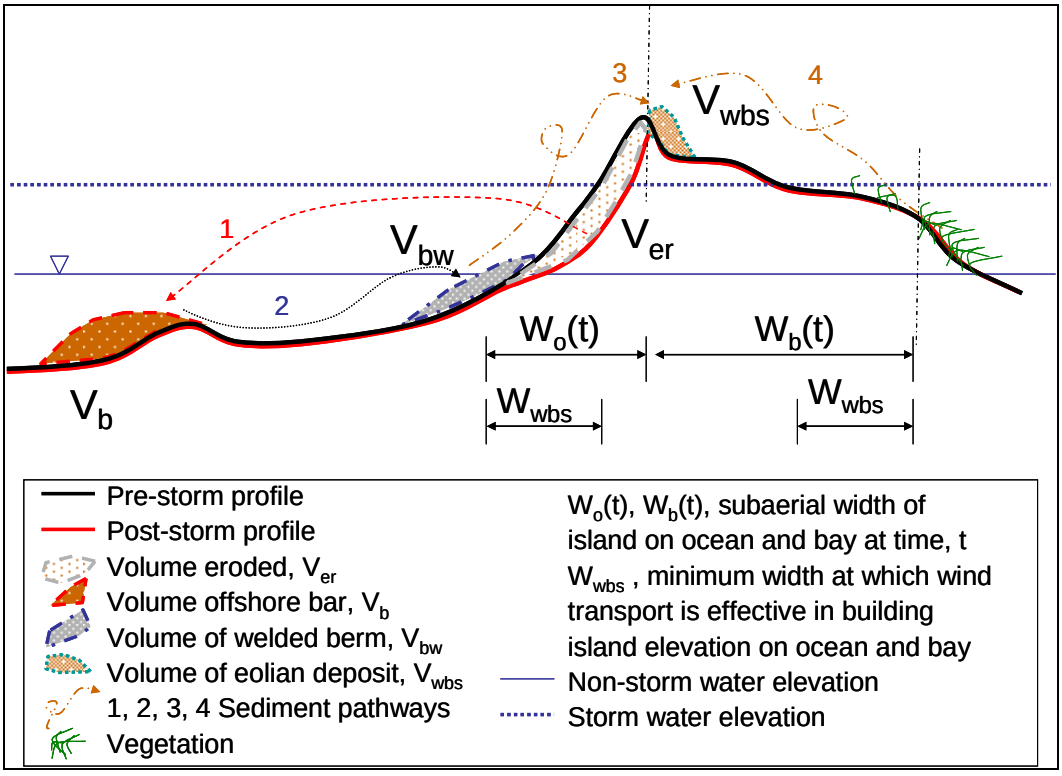

Figure 38. Recovery and eolian transport sub-modules.

where κ is von Karman's constant equal to 0.4, z_z is the elevation of the wind measurements, and z_r is the roughness length of the surface, which can be related to the median grain diameter (Namikas 2003) as:

$$z_r = \frac{2d_{50}}{30} \tag{31}$$

Applying Equations 30 and 31 for a dry beach with 0.16 mm median diameter sand and u_{*t} = 21.7 cm/sec, u_{10m} = 7.5 m/sec. Similar calculations with 0.19 mm diameter sand and u_{*t} = 23.7 cm/sec gives u_{10m} = 8.1 m/sec. Thus, wind speeds at the 10-m elevation that exceed approximately 7.5 - 8.1 m/sec are sufficient for eolian transport of sand on a dry beach with median grain size equal to 0.16-0.19 mm.

In two studies of eolian sand transport on Isles Dernieres, LA, Hsu and Blanchard (1991) and Dingler et al. (1992) measured eolian sand transport over an 18-month period and related the rate of eolian transport to the shear velocity at the beach as:

$$q_pot_{wbs} = 0.0243\left(10^{-4}\right)u_*^{\,3} \quad \text{g/(cm sec)} \tag{32}$$

where q_pot_{wbs} represents the fully-developed rate of eolian transport over an unvegetated beach.

In a series of laboratory wind tunnel experiments, Hotta (1984, p. 2.13) found that 10-12 m of unvegetated beach was necessary for the vertical distribution of eolian sand transport to become constant, or reach the fully-developed rate. Citing the *Shore Protection Manual* (1984), Hsu and Weggel (2002) recommended that a dune system designed for capture of eolian sand be set back at least 60 m on the beach (from the toe of the dune to the high water line) for full development of eolian transport. However, the original *Shore Protection Manual* (1984) reference to 60 m of beach width was in discussion of how far landward of the berm sand fencing should be constructed to avoid direct wave attack on the fence. In the notation introduced herein, we can define the minimum beach width necessary to achieve full eolian transport as:

$$\text{For an unvegetated beach, } W_{wbsb} = W_{wbso} \sim 12\,\text{m} \tag{33}$$

and we can estimate the actual wind blown sand transport rate, q_{wbs}, related to the minimum beach width as,

$$\text{if } W_o(t) < W_{wbso}, \quad q_{wbs} = \frac{W_o(t)\, q_pot_{wbs}}{W_{wbso}}$$

$$\text{or}$$

$$\text{if } W_b(t) < W_{wbsb}, \quad q_{wbs} = \frac{W_b(t)\, q_pot_{wbs}}{W_{wbsb}} \tag{34}$$

$$\text{else}$$

$$q_{wbs} = q_pot_{wbs}$$

Figure 39 shows an application of the eolian sand transport sub-module based on Equations 29 through 34 for a wind speed at 10 m elevation ranging from 2 to 30 m/sec, beach width that increases linearly from 11 to 25 m, and median grain size of 0.16 mm. For this example, the eolian sand transport rate is zero until the wind speed at the 10-m elevation exceeds approximately 7.5 m/sec in the fourth calculation.

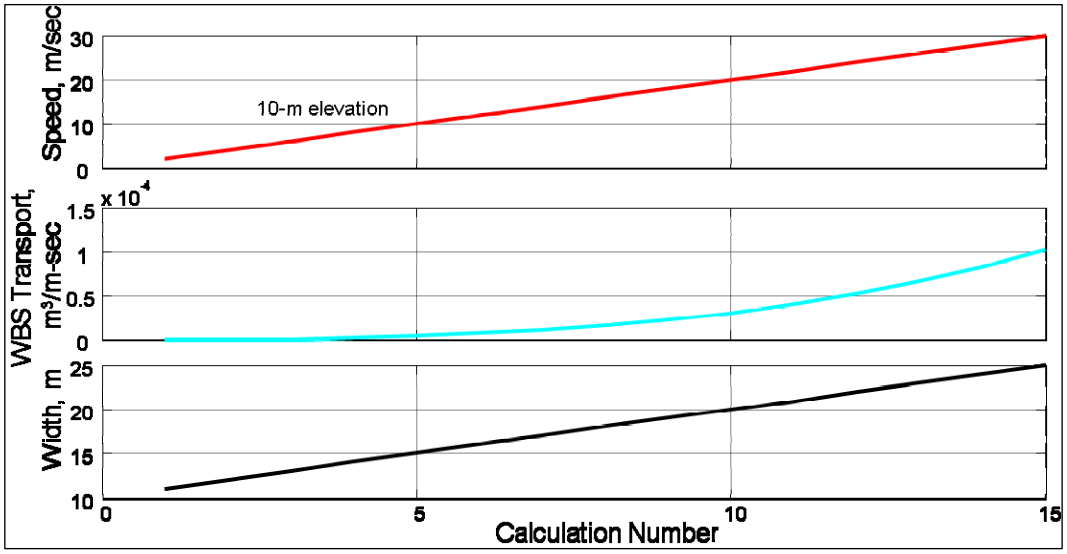

Figure 39. Example application of eolian transport sub-module.

Erosion of fine-grained sediment

Deltaic barrier islands are comprised of mixed sediments that were originally deposited by a river system and then sorted and reworked by marine processes. A typical stratigraphy for these islands includes a sandy beach face with thickness up to approximately 2-3 m, extending offshore from the wave breaking zone and onshore to the limit of recent overwash deposits (Dingler and Reiss 1989). Portions of the sandy beach exposed to energetic conditions may have a surface of shell hash, and the dunes may be vegetated. The bayside of a deltaic barrier island is usually a back-barrier marsh comprised of fine estuarine sediment that is deposited by tidal processes and during the post-frontal stage of storms. The underlying substrate of the entire island is a core of older deltaic deposits comprised of silt, clay, and mud. Figures 40a and b show two characterizations of stratigraphy for deltaic barrier islands in Louisiana. Figure 40c shows Stage 2 of Campbell's (2005) conceptual model of barrier island erosion illustrating a post-storm condition in which the sand has been eroded and the marsh and deltaic substrate are exposed to waves. Figures 41a and b show pre- and post-hurricane images from the Chandeleur Islands, LA, in which the protective sand beach was removed during the storm and the back-barrier marsh was exposed to waves during the period prior to beach recovery.

In this section, relationships to calculate the rate of erosion of fine-grained sediment, comprised of exposed marsh and mixed deltaic sediments, are presented. Erosion of fine-grained sediment and organics will occur after the protective sand veneer is removed and prior to any recovery of the

sand to the beach. In practice, coefficients in equations for erosion of cohesive sediment are determined based on laboratory testing of samples carefully extracted in-situ from the field site of interest, or based on field observations. Review of the literature indicates that no such analyses have been completed for fine-grained barrier island sediment such as defined herein.

The erosion rate of the fine-grained sediment, e_{fg}, can be expressed as:

$$\begin{aligned} e_{fg} &= k_{fg}\left(\tau_w - \tau_c\right) \quad \text{for } \tau_w > \tau_c \quad \left(kg/\mathrm{m}^2\,\mathrm{sec}\right) \\ e_{fg} &= 0 \quad \text{for } \tau_w \le \tau_c \end{aligned} \tag{35}$$

in which k_{fg} is an empirical erosion coefficient (kg/N-sec), τ_w is the maximum bed shear stress at the shoreface during a wave cycle, and τ_c is the critical shear bed stress required for initiation of erosion (N/m^2) (Whitehouse et al. 2000). Values for k_{fg} and τ_c are typically determined based on laboratory experiments or field observation. The maximum bed shear stress can be calculated as:

$$\tau_w = \frac{\rho_{sw} f_w U_{\max}^{\,2}}{2} \quad \left(\mathrm{N/m}^2\right) \tag{36}$$

where ρ_{sw} is the density of salt water equal to 1,025 kg/m^3, f_w is a bottom friction factor, and U_{max} is the maximum wave orbital velocity, calculated as (Demirbilek and Vincent 2002).

$$U_{\max} = \frac{gHT}{2L} \quad (\mathrm{m/sec}) \tag{37}$$

Local wave height, period, and length are given by H, T, and L, respectively. The friction factor varies depending on the Reynolds number associated with the wave breaking conditions, and is given here for rough turbulent flow assumed to be representative of the surf zone (Myrhaug et al. 2006).

$$f_w = c\left(\frac{A}{r_b}\right)^{-d} \tag{38}$$

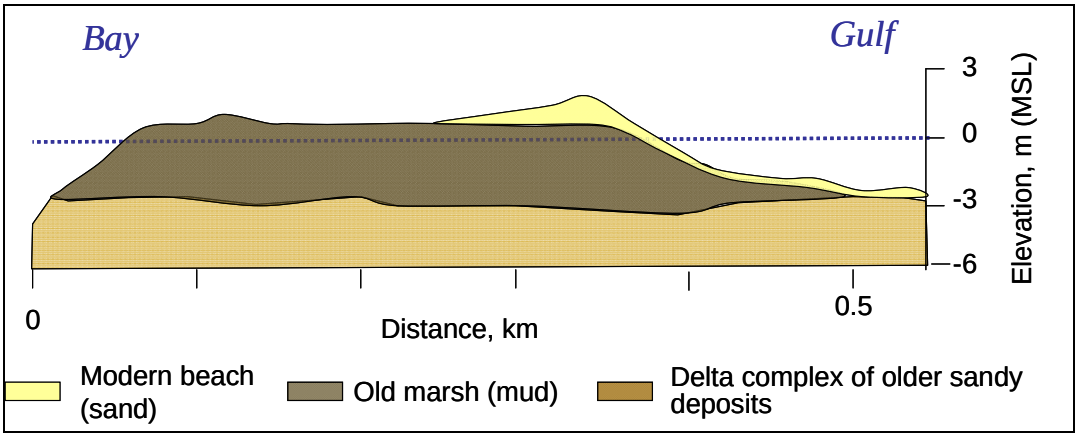

a. Based on Isle Dernieres, LA (adapted from Dingler and Reiss 1989).

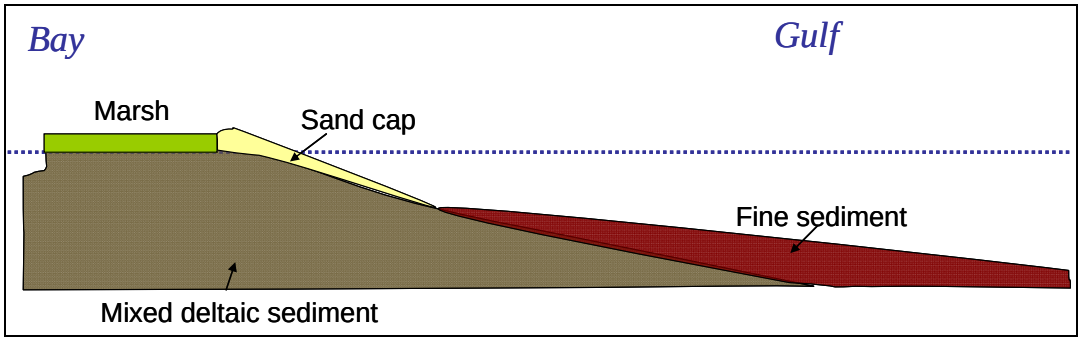

b. Pre-storm stratigraphy (adapted from Campbell 2005, Figure 6a).

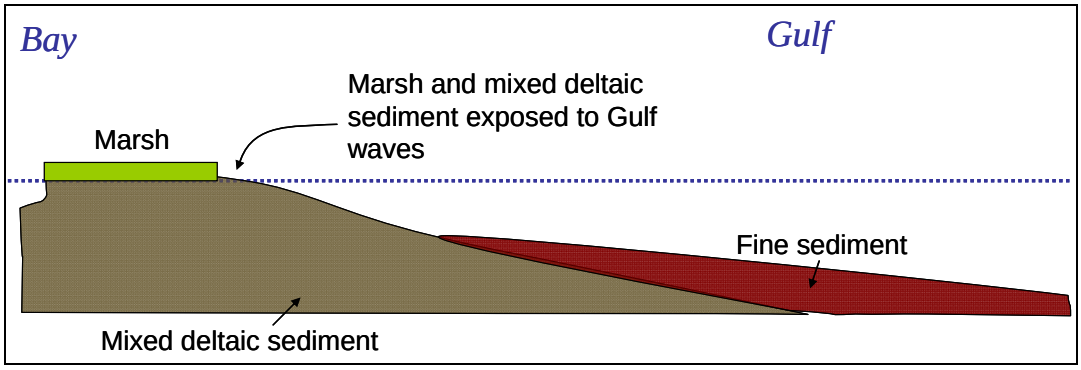

c. Immediately post-storm stratigraphy (adapted from Campbell 2005, Figure 6b).

Figure 40. Characterization of stratigraphy for deltaic barrier islands in Louisiana.

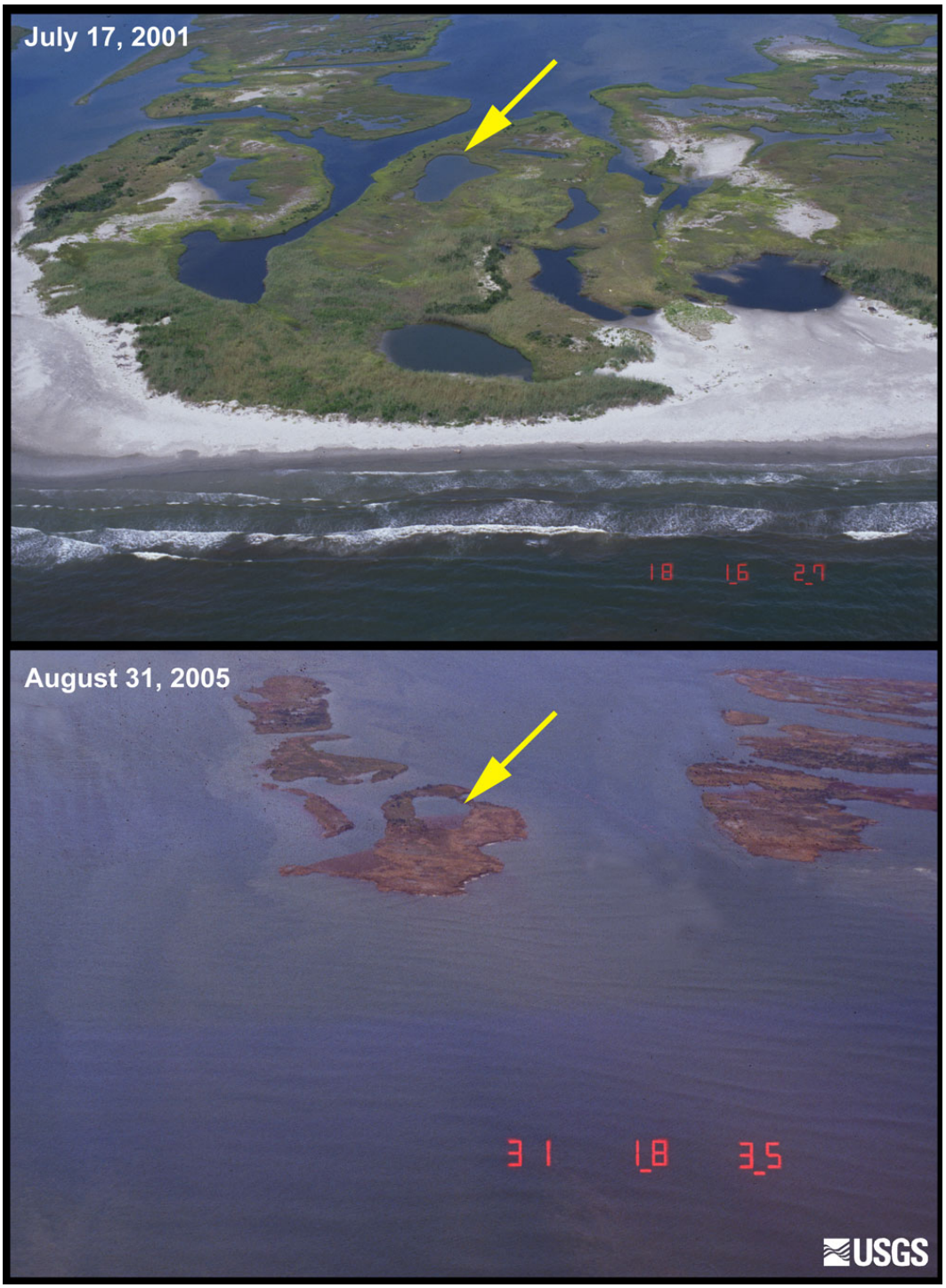

Figure 41. Pre-(top) and post-(bottom) Hurricane Katrina images of Chandeleur Islands, LA, showing removal of sand beach, followed by exposure and erosion of back-barrier marsh sediment (USGS 2007).

where A is the near-bed orbital wave amplitude equal to $U_{max}T$; r_b is the bed roughness equal to $d_{50}/12$, in which d_{50} is the median grain diameter; and the coefficients c and d depend on the ratio of A/r_b, taken here as $c = 0.112$ and $d = 0.25$ for representative mild surf-zone conditions and

sediment grain size d_{50} = 0.06 mm (coarse silt; finer sediment would result in the same coefficients). The volumetric change rate, q_{fg}, is calculated with an estimate of the thickness of fine-grained sediment exposed to wave action, z_{fg},

$$q_{fg} = \frac{e_{fg} z_{fg}}{\rho_{fg}} \quad \mathrm{m}^3/(\mathrm{m} \bullet \mathrm{sec}) \tag{39}$$

where ρ_{fg} is the specific weight of the fine-grained sediment, taken as 1,826 kg/m^3 for wet clay, silt, and mud. In practice, the amount of vegetation, extent of root mass within the fine-grained sediment and organics, and degree of compaction will significantly modify erosion and friction parameters. Thus, on-site validation or in-situ laboratory testing are required for accurate calculations. As discussed by Campbell (2005), the exposed back-barrier marsh can retreat rapidly in the post-storm period during which non-storm wave conditions occur.

Equations 35 through 39 were coded into a fine-grained sediment erosion sub-module. Figure 42 shows an example simulation with local wave heights ranging from 0.4 to 0.7 m (varying as a function of depth), and local depth ranging from 0.8 m to 1.4 m as a function of tide (bottom panel). Median grain size was 0.06 mm, thickness of exposed fine-grained sediment was 0.5 m, k_{fg} was 0.1 kg/N/sec, and the critical shear bed stress $\tau_c \sim 0$. For this example simulation, the total erosion over the 12-day period was 3 m^3/m (middle panel), and the erosion rate ranged from 2.5×10^{-6} to 3.5×10^{-6} m^3/m-sec (top panel).

Regional sources and sinks of sand

Decadal-scale morphologic evolution of barrier islands depends not only on local forcing processes, but also on regional sources and sinks as sediment is exchanged among the beaches, adjacent inlets, ebb and flood tidal deltas, estuaries, and bays. Morphologic properties of the barrier islands and tidal deltas are related to the tidal prism, waves, and water level including influence by storms and wind. Over long time scales, bays and estuaries tend to infill with sediment due to overwash from the ocean, fluvial deposition, and the increasing volume of flood tidal deltas.

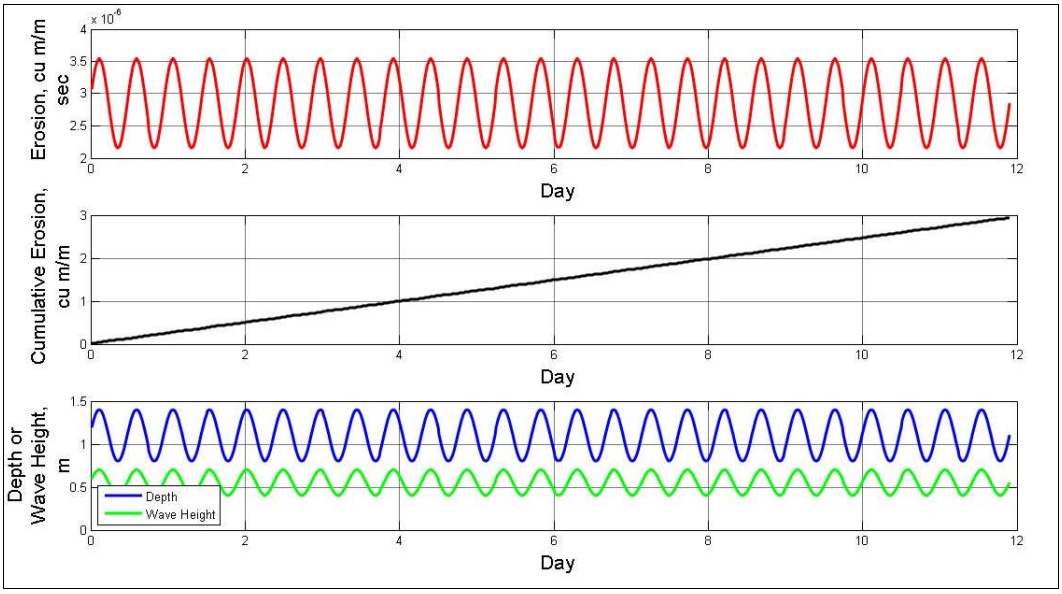

Figure 42. Example application of fine-grained sediment erosion sub-module.

However, some bay systems such as Barataria Bay, LA, are increasing in surface area because of regional subsidence, rapid increase in sea level, and wetland loss. For these types of systems, the increase in bay area has increased the tidal prism in the inlets, extended the ebb tidal deltas farther offshore, and increased the ebb tidal delta volume (List et al. 1997; FitzGerald et al. 2004). The response has been scouring of the tidal passes and an increased loss of sediment from the barrier islands. A decadal-scale Regional sub-module is developed to calculate the interdependency of regional sediment sources and sinks, ebb and flood delta volumes, bay tidal prism, and barrier island volume.

The sub-module adopts and extends concepts of the Inlet Reservoir Model (IRM) (Kraus 2000) to include time-dependent volumetric change on adjacent barrier islands and changes in bay area, tidal prism, inlet cross-sectional area, and ebb delta volume. The IRM is based on two assumptions: (1) conservation of sediment volume, or the sediment budget concept, by which the change in volume of a morphologic feature ΔV can be related to transport into and out of that feature, Q_{in} and Q_{out} over time duration Δt,

$$\Delta V = \left(Q_{in} - Q_{out}\right)\Delta t \tag{40}$$

and (2) the magnitude of Q_{out} is related to the volume of the feature, V, relative to its equilibrium volume V_{eq} (called the "Reservoir Model assumption") as:

$$Q_{out} = \frac{V}{V_{eq}} Q_{in} \tag{41}$$

The Regional sub-module developed describes a tidally dominated inlet in which the flood tidal delta is part of the total bay and represents a net loss (sink) to the littoral system.

Applying these concepts to the barrier island, inlet, and bay system represented in Figure 43, the volume in a morphologic feature, such as one of the bypassing bars, $B1$, can be numerically calculated as a function of time by combining Equation 40 and 41,

$$\Delta V_{B1} = \left(1 - \frac{V_{B1}(t)}{V_{B1eq}}\right) Q_2 \Delta t \tag{42}$$

in which $V_{B1}(t)$ represents the volume in Bypassing Bar 1 at time t, Q_2 is the transport into $B1$, and the equilibrium volume of $B1$ is denoted by V_{B1eq}. The change in volume ΔV_{B1} over the time interval Δt can be represented as:

$$V_{B1}(t) - V_{B1}(t - \Delta t) = \left(Q_2 - \frac{V_{B1}(t) - V_{B1}(t - \Delta t)}{2V_{B1eq}} Q_2\right) \Delta t \tag{43}$$

Combining terms (Kraus 2000), a stable numerical solution is obtained as,

$$V_{B1}(t) = \frac{1 - \beta_1}{1 + \beta_1} V_{B1}(t - \Delta t) + \frac{\bar{Q}_2(t) \Delta t}{1 + \beta_1} \tag{44}$$

where β_1 is a dimensionless coefficient related to the growth rate of the feature,

$$\beta_1 = \frac{\bar{Q}_2(t) \Delta t}{2V_{B1eq}} \tag{45}$$

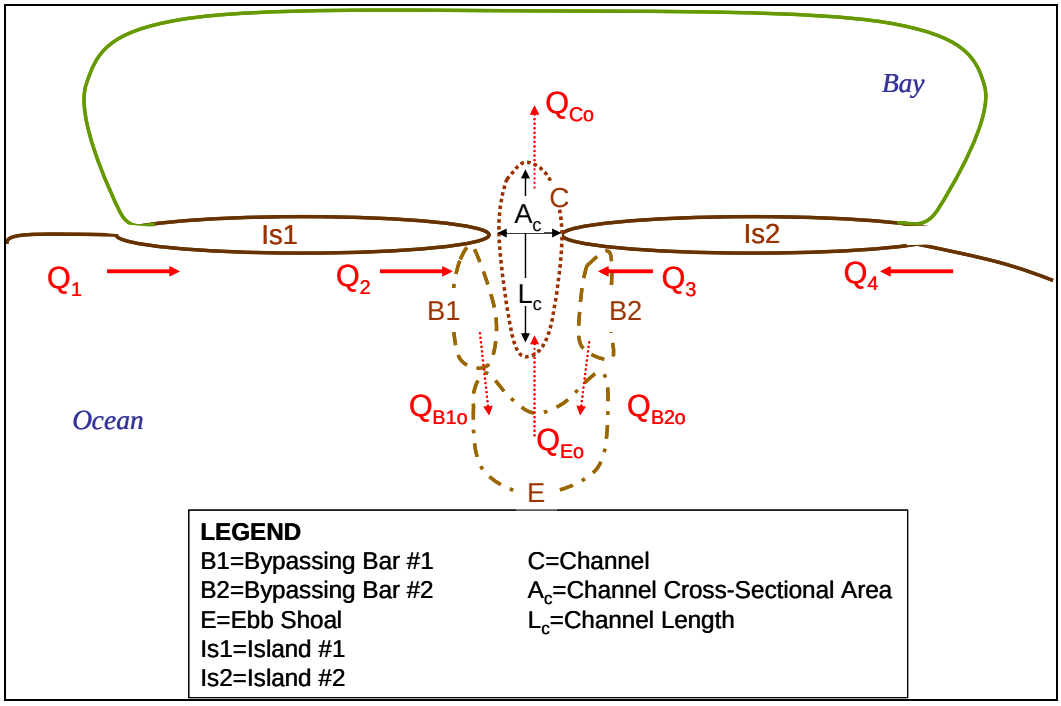

Figure 43. Terminology used in development of regional sources and sinks of sand sub-module.

The time-averaged transport rate into the morphologic feature $B1$ is $\bar{Q}_2(t)$.

$$\bar{Q}_2(t) = \frac{Q_2(t) + Q_2(t - \Delta t)}{2} \tag{46}$$

The transport rate out of $B1$ is given by:

$$Q_{B1o}(t) = \bar{Q}_2(t) - \left(\frac{V_{B1}(t) - V_{B1}(t - \Delta t)}{\Delta t} \right) \tag{47}$$

The equilibrium volume of the ebb delta is calculated as a function of tidal prism as given by Walton and Adams (1976),

$$V_{Ebb\ eq}(t) = C_1 P(t)^{n_1} \tag{48}$$

where C_1 and n_1 are empirical coefficients that depend on wave climate; for "mild wave exposure," C_1 = 5.9612 × 10^{-3} and n_1 = 1.24263, with $P(t)$ and $V_{Ebb\ eq}(t)$ in cubic meters. It is assumed that the total ebb volume $V_{Ebb\ eq}(t)$ represents the sum of the equilibrium volumes of the three inlet delta features shown in Figure 43,

$$V_{Ebb\,eq}(t) = \alpha_1 V_{B1eq}(t) + \alpha_2 V_{B2eq}(t) + \alpha_E V_{Eeq}(t) \tag{49}$$

where α_1, α_2, and α_E are user-defined coupling coefficients (Kraus 2000) such that $\alpha_1 + \alpha_2 + \alpha_E = 1$. The tidal prism is given by:

$$P(t) = 2A_{bay}(t)a_{bay} \tag{50a}$$

in which $A_{bay}(t)$ is area of the bay which can vary in time as,

$$A_{bay}(t) = A_{bay}(t - \Delta t)\left(1 + dA(t)\right) \tag{50b}$$

where $dA(t)$ is the annual change in bay area. In Equation 50a, the spring tidal amplitude in the bay a_{bay} is taken to be constant with the Barataria Bay situation in mind. The cross-sectional area of the channel, applied in the formulations as the equilibrium cross-sectional area for a given prism, $A_{Ceq}(t)$, increases or decreases as a function of decadal-scale change in spring tidal prism,

$$A_{Ceq}(t) = C_2 P(t)^{n_2} \tag{51}$$

where C_2 and n_2 are empirical coefficients, taken as $C_2 = 6.992 \times 10^{-4}$ and $n_2 = 0.86$ for Gulf Coast unjettied inlets, modified from Jarrett (1976) for metric units ($P(t)$ in cubic meters and $A_{Ceq}(t)$ in square meters).

The existing channel cross-section at any given time is $A_C(t)$. Channel volumes corresponding to $A_C(t)$ and $A_{Ceq}(t)$ are given by $V_C(t) = A_C(t)L_C$ and $V_{Ceq}(t) = A_{Ceq}(t)L_C$, respectively, where L_C is the length of the channel. If $A_C(t)$ becomes greater than $A_{Ceq}(t)$ because of a decrease in bay area or through dredging, then the channel is allowed to shoal at the next time step in the numerical model. For the shoaling calculation, if the transport rate exiting the ebb delta and entering the channel, $\bar{Q}_{Eo}(t)$ is less than required to fill the channel, then Equation 52 applies.

$$\begin{gathered} V_C(t) = V_C(t - \Delta t) + \bar{Q}_{Eo}(t)\Delta t \\ \text{for } A_C(t) > A_{Ceq}(t) \; and \; \bar{Q}_{Eo}(t)\Delta t \le V_C(t) - V_{Ceq}(t) \end{gathered} \tag{52}$$

If $\bar{Q}_{Eo}(t)$ is greater than required by the channel to achieve the equilibrium cross-section, then Equation 53 applies.

$$V_C(t) = V_C(t-\Delta t) + \bar{Q}_{Eo}(t)\Delta t - (V_C(t) - V_{Ceq}(t)) \quad \text{for } A_C(t) > A_{Ceq}(t) \text{ and } \bar{Q}_{Eo}(t)\Delta t > V_C(t) - V_{Ceq}(t) \tag{53}$$

If the existing channel cross-section $A_C(t) < A_{Ceq}(t)$, such as would occur with increasing bay area or channel infilling from longshore transport, an analytical approximation represents channel scour at the next time step,

$$V_C(t) = V_{Ceq}(t)\left(1 - e^{-t_{sc}/\tau_c}\right) + V_C(t-\Delta t)e^{-t_{sc}/\tau_c} \quad \text{for } A_C(t) \le A_{Ceq}(t) \tag{54}$$

where t_{sc} (years) is the elapsed time since scour of the channel was initiated, and τ_c (years) is a user-defined coefficient representing the time required for the channel to scour to equilibrium while $A_c(t) \le A_{Ceq}(t)$. The scour time counter t_{sc} is reset to zero if the channel later begins shoaling. For a resistant substrate, such as a gravel channel bed, τ_c would be large, whereas mobile sands or unconsolidated clays would have smaller values. Transport exiting the channel and depositing into a flood delta in the bay is given by:

$$Q_{Co}(t) = \bar{Q}_{Eo}(t) + \left(\frac{V_C(t) - V_C(t-\Delta t)}{\Delta t}\right) \tag{55}$$

Applying these principles, equations are developed for other inlet and barrier island morphologic features as shown in Table 9.

Sensitivity tests were performed to examine predictive properties of the Regional Sources and Sinks of Sand sub-module. Two such tests are presented here. The first illustrates how changing bay area modifies barrier island volume. Test 1 has initial parameters as follows: $V_{Is1} = V_{Is2}$ = 1.5 million m^3, A_{bay} = 50 million m^2, a_{bay} = 0.3 m, A_C = 10 m^2 (representing a new inlet), mean values of $Q_1 = Q_4$ = 50,000 m^3/year, and $Q_2 = Q_3$ = 70,000 m^3/year, Δt = 0.2 year, and τ_c = 10 year, indicating that the channel scour process requires 10 years to reach equilibrium. Annual longshore transport rates representative of the Louisiana coast were randomly generated about the mean values. Initial values of the channel cross-sectional area and ebb tidal deltas were near-zero, as would occur immediately after a breach in the barrier island.

Figure 44a shows the initial case with no change in bay area $dA(t) = 0$. The islands initially erode during formation of the ebb delta, but then begin to recover after approximately 80 years as the ebb delta bypasses to the islands. (Only one island is shown in the figures for simplicity; results for the islands are identical because forcing processes are symmetric). Figure 44b shows the same simulation except the bay area increased at 0.2 percent/year, such as would occur with long-term rise in sea level, loss of fringing wetlands, and erosion of mainland shores. As a result, the tidal prism and equilibrium ebb delta volume increase such that the islands disappear after approximately 70 years. Figure 44c shows results with a decrease in bay area of 0.2 percent/year, which would occur with anthropogenic infilling of the bay (Davis and Zarillo 2003) and riverine sediment deposition. As the tidal prism and equilibrium ebb delta volume decrease, the deltas bypass to the islands such that the islands begin to accrete after 55 years. The tidal inlet closes at 190 years as the channel fills with sand.

Sensitivity Test 2 extends the decreasing bay area case (shown in Figure 44c) to consider dredging of the channel at 5-year intervals if the channel depth becomes shallower than 5 m (Figure 45). Dredged sand from the channel is placed on the barrier islands at 5-year intervals in the simulations. Without dredging, the tidal inlet closes after 190 years. With dredging implemented every 5 years if the channel depth is shallower than 5 m, dredging commences after 40 years and dredged sand is placed on the adjacent islands. Each island benefits from placement of approximately 6 million m^3 of dredged sand over a 160-year period (approximately 37,500 m^3/year).

Table 9. Equations for regional sources and sinks of sand sub-module (Figure 43 for notation).

Bypassing Bar #1	
$V_{B1}(t)=\frac{1-\beta_1}{1+\beta_1}V_{B1}(t-\Delta t)+\frac{\bar{Q}_2(t)\Delta t}{1+\beta_1}$ $\beta_1=\frac{\bar{Q}_2(t)\Delta t}{2V_{B1eq}}$	$\bar{Q}_2(t)=\frac{Q_2(t)+Q_2(t-\Delta t)}{2}$ $Q_{B1o}(t)=\bar{Q}_2(t)-\left(\frac{V_{B1}(t)-V_{B1}(t-\Delta t)}{\Delta t}\right)$
Ebb Delta	
$V_{Ebb\,eq}(t)=C_1P(t)^{n_1}$; $V_{Ebb\,eq}(t)=\alpha_1V_{B1eq}(t)+\alpha_2V_{B2eq}(t)+\alpha_EV_{Eeq}(t)$; $V_E(t)=\frac{1-\beta_E}{1+\beta_E}V_E(t-\Delta t)+\frac{(\bar{Q}_{B1o}(t)+\bar{Q}_{B2o}(t))\Delta t}{1+\beta_E}$	$\beta_E=\frac{(\bar{Q}_{B1o}(t)+\bar{Q}_{B2o}(t))\Delta t}{2V_{Eeq}}$; $\bar{Q}_{B2o}(t)=\bar{Q}_3(t)-\left(\frac{V_{B2}(t)-V_{B2}(t-\Delta t)}{\Delta t}\right)$; $\bar{Q}_{Eo}(t)=(\bar{Q}_{B1o}(t)+\bar{Q}_{B2o}(t))-\left(\frac{V_E(t)-V_E(t-\Delta t)}{\Delta t}\right)$
Channel	
$P(t)=2A_{bay}(t)a_{bay}$; $A_{Ceq}(t)=C_2P(t)^{n_2}$ Shoaling $V_C(t)=V_C(t-\Delta t)+\bar{Q}_{Eo}(t)\Delta t$ for $\bar{Q}_{Eo}(t)\Delta t\le V_C(t)-V_{Ceq}(t)$	$V_C(t)=V_C(t-\Delta t)+\bar{Q}_{Eo}(t)\Delta t-\left(V_C(t)-V_{Ceq}(t)\right)$ for $\bar{Q}_{Eo}(t)\Delta t>V_C(t)-V_{Ceq}(t)$ Scouring $V_C(t)=\frac{V_C(t-\Delta t)+V_{Ceq}(t)(1-e^{-t_{sc}/\tau_C})}{2}$; $Q_{Co}(t)=\bar{Q}_{Eo}(t)+\left(\frac{V_C(t)-V_C(t-1)}{\Delta t}\right)$
Bay	
$A_{bay}(t)=A_{bay}(t-\Delta t)\left(1+dA(t)\right)$	
Island #1	
$V_{Is1}(t)=V_{Is1}(t-\Delta t)+\left(\bar{Q}_1(t)-\bar{Q}_2(t)\right)\Delta t$	$\bar{Q}_1(t)=\frac{Q_1(t)+Q_1(t-\Delta t)}{2}$
Bypassing Bar #2	
$V_{B2}(t)=\frac{1-\beta_2}{1+\beta_2}V_{B2}(t-\Delta t)+\frac{\bar{Q}_3(t)\Delta t}{1+\beta_2}$ $\beta_2=\frac{\bar{Q}_3(t)\Delta t}{2V_{B2eq}}$	$\bar{Q}_3(t)=\frac{Q_3(t)+Q_3(t-\Delta t)}{2}$ $\bar{Q}_{B2o}(t)=\bar{Q}_3(t)-\left(\frac{V_{B2}(t)-V_{B2}(t-\Delta t)}{\Delta t}\right)$
Island #2	
$V_{Is2}(t)=V_{Is2}(t-\Delta t)+\left(\bar{Q}_4(t)-\bar{Q}_3(t)\right)\Delta t$	$\bar{Q}_4(t)=\frac{Q_4(t)+Q_4(t-\Delta t)}{2}$

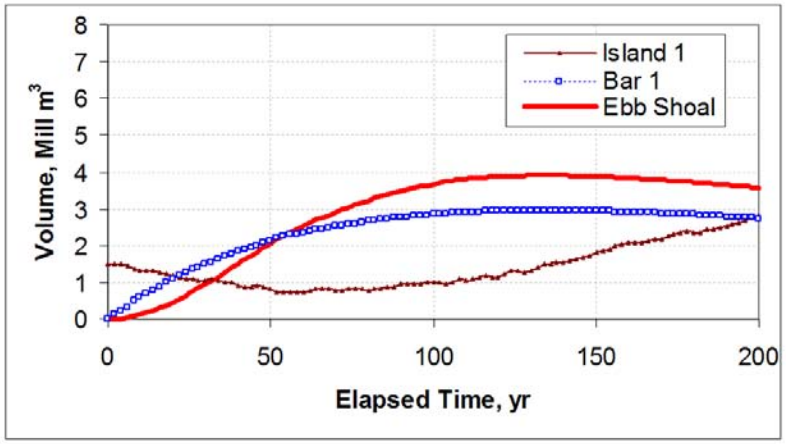

a. Bay area constant, $dA(t) = 0$.

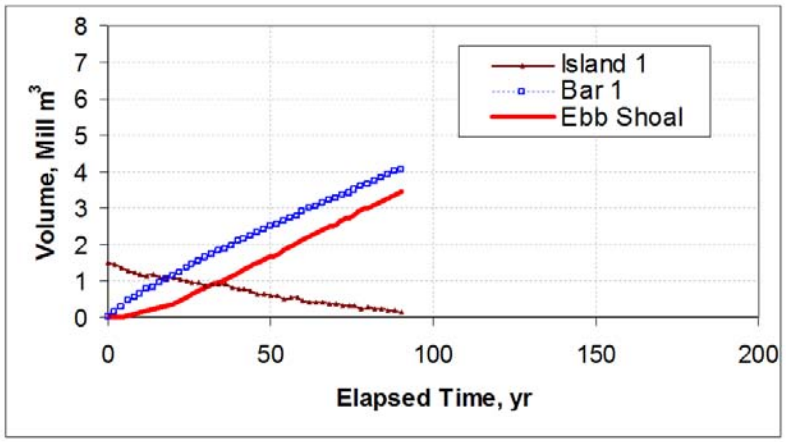

b. Bay area increase, $dA(t) = +0.02$ percent/year.

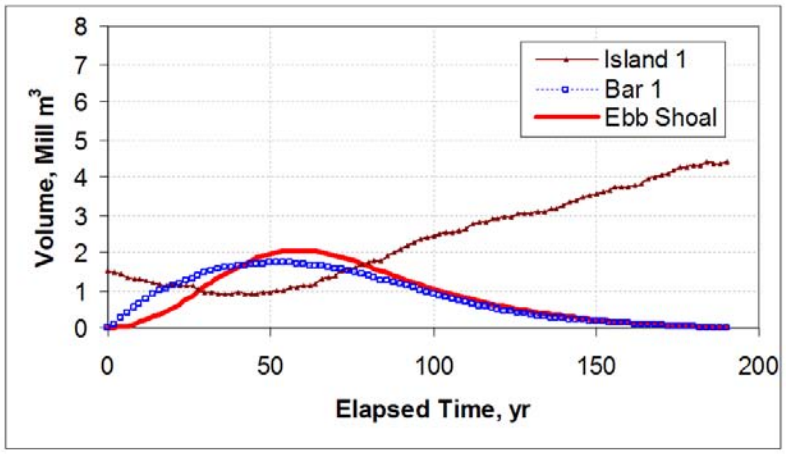

c. Bay area decrease, $dA(t) = -0.02$ percent/year.

Figure 44. Influence of bay area on barrier island and delta volumes (Test 1).

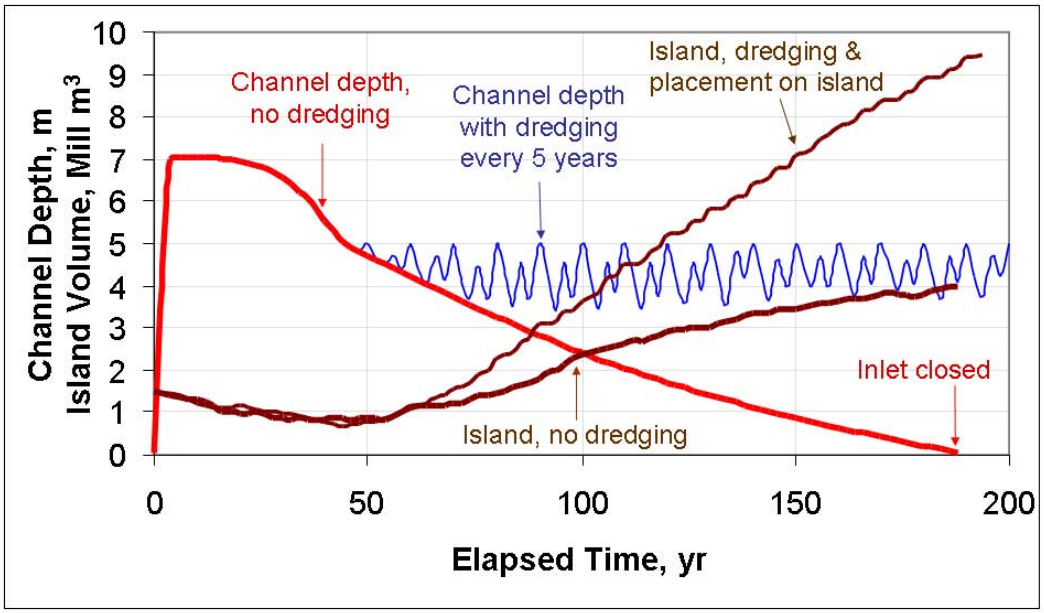

Figure 45. Infilling bay (area decreasing at 0.02 percent/year) with and without dredged channel and placement of dredged sand on adjacent islands (Test 2).

Data

Overview

Data for Louisiana barrier islands that document some of the long-term processes discussed herein have been discussed by Ritchie and Penland (1988) for the Caminada-Moreau Headland and Dingler and Reiss (1989, 1990, and 1995) for Trinity Island (Figure 46). The Caminada-Moreau data were available only as conceptual drawings as published by Ritchie and Penland (1988) and, therefore, were applied in a qualitative manner herein. Data for Trinity Island were originally published by Dingler and Reiss (1989, 1990, and 1995), and were reanalyzed (Dingler 2008). These data, together with process information from gage CSI-5 (Coastal Studies Institute 2008), provide information useful for testing the Eolian Transport and Fine-Grained Sediment Erosion sub-modules. Information from List et al. (1991) and FitzGerald et al. (2004) for Barataria Bay, LA, were applied to evaluate the Regional sub-module. Data are not available to document the recovery process, nor isolate the LST process in absence of other cross-shore and longshore processes. Thus, the LST and Recovery sub-modules cannot be unambiguously tested in a quantitative manner.

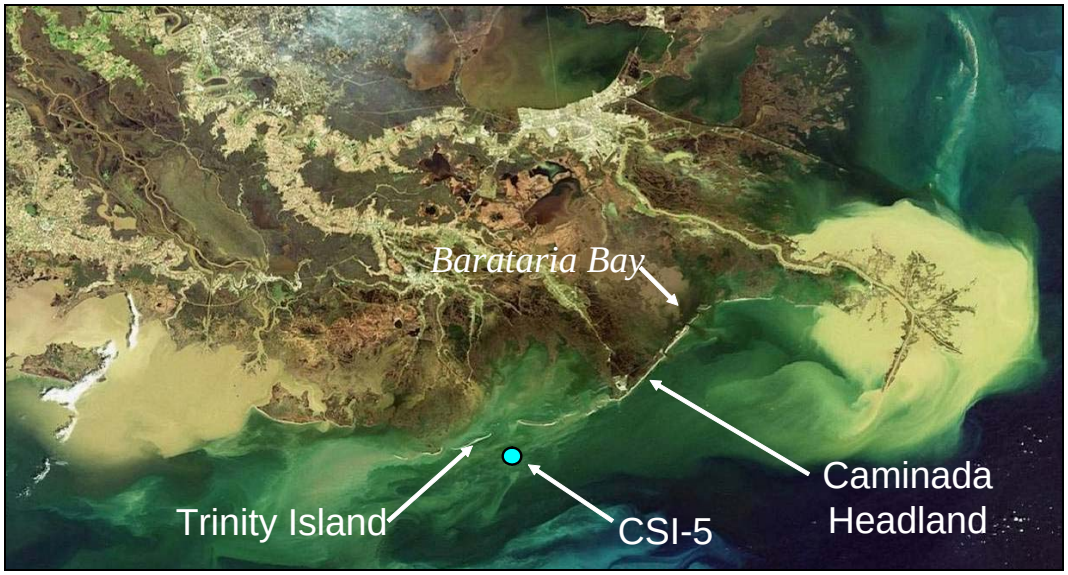

Figure 46. Location of data sets.

Eolian sand transport

As discussed by several authors (Muller and Stone 2001; Stone et al. 1997, 2004; Khalil 2008) and reviewed in Chapter 2, the highest percentage of wind speed exceeding the threshold for wind-blown (eolian) sand transport occur from the north-northeast for the northern Gulf of Mexico. The net result is that, for a barrier island with an east-west orientation, and a sufficient source of unvegetated dry sand, dune systems can accrete both towards the Gulf and Bay via eolian sand transport.

Figure 47 shows Profile H from Ritchie and Penland (1988, p. 116) illustrating rapid dune growth on Caminada Headland, LA, following Hurricane Bob, a Category 1 storm which made landfall at Grand Isle, LA, on 11 July 1979. Profile H was located Gulfward of the Cheniere Caminada, thus had a source of sand stored in the ridges landward of the beach. Dunes on other profiles in this region also accreted vertically, but none of them migrated towards the Gulf. Profile H had a net influx of sand from April to December 1980. Morphologic change of the dune from December 1980 to July 1981 indicates that eolian sand transport was the most likely process that eroded the dune on the north side of the profile and accreted it towards the Gulf. The result was dune migration towards the Gulf with the dune elevation approximately 2.4 m relative to MSL. The approximate volume change rate for the dune was a loss of 2 m^3/m (4 $m^3/m/year$) on the lagoon side and gain of 7 m^3/m (11 $m^3/m/year$) on the Gulf side, implying that eolian sand transport from the north (lagoon side of the profile) for the 7-month period was on the order of 4 $m^3/m/year$.

Accretion of the Gulf side may have also included berm welding, overwash, and eolian transport from the Gulf.

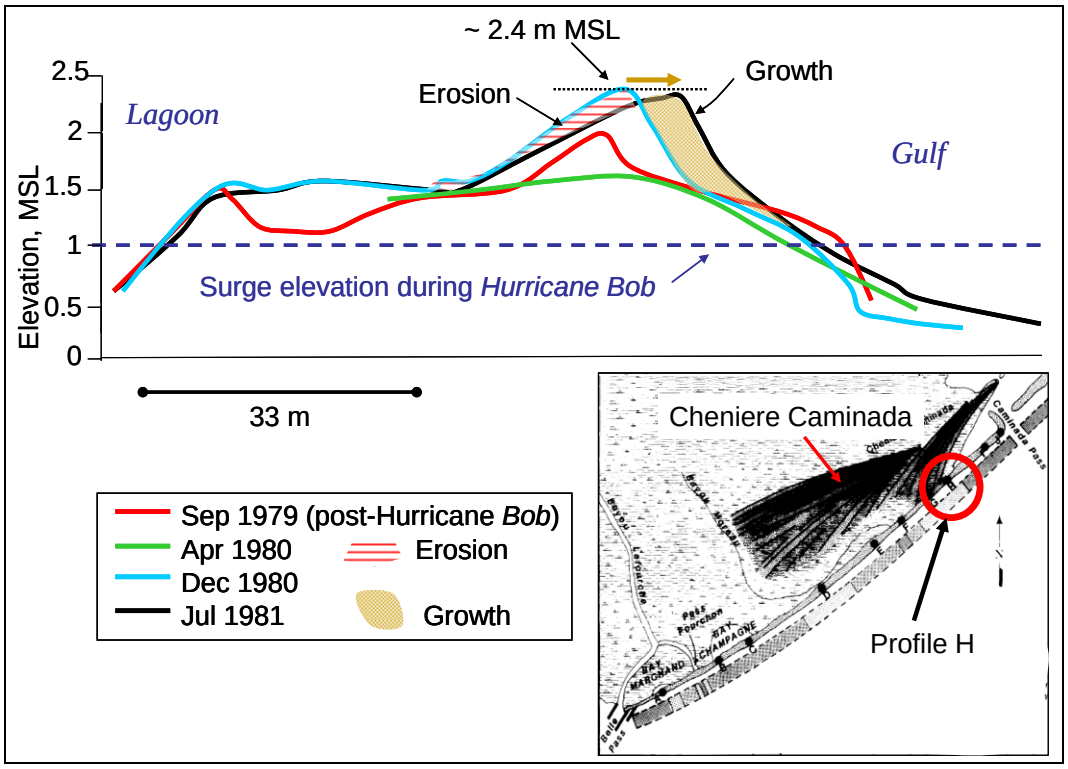

Figure 47. Example of rapid dune growth and migration gulfward (Profile H, adapted from Ritchie and Penland 1988, p. 116).

Figures 48 and 49 show the two profiles adjacent to Profile H. Both show dune growth, although Profile I maintained the same cross-shore location and most likely increased in volume through eolian transport from both the Gulf and Cheniere sides of the beach. Profile G moved landward and it is likely that some overwash processes occurred in addition to some eolian sand transport. The elevations of these dunes were 2.2 m and 1.9 m MSL, respectively. The accretion rate of Profile I dune was approximately 52 m^3/m over the 2.2-year period, or 19 $m^3/m/year$.

The last example from Caminada Headland is a 7.5-year data set of Profile J (Figure 50) showing destruction of the original dune system and reformation of a multiple dune system approximately 35 m landward. These profiles formed at elevations between 2.2 and 2.3 m MSL and were most likely formed through a combination of overwash and eolian sand transport processes.

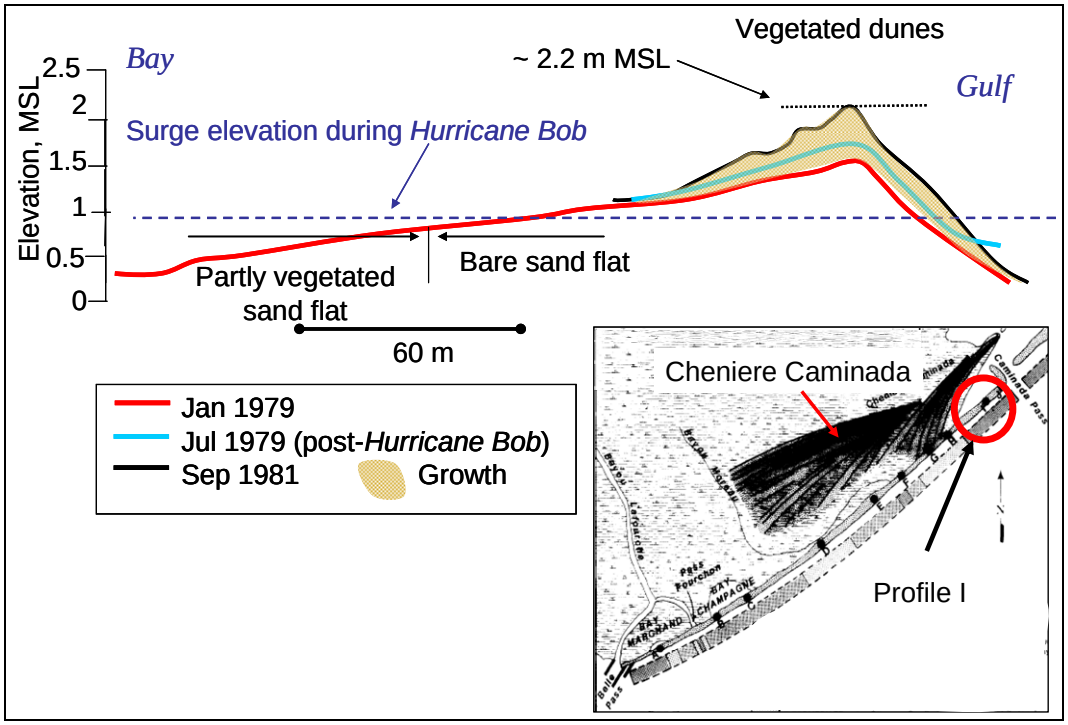

Figure 48. Example of continuously accreting dune ridge (Profile I, adapted from Ritchie and Penland 1988, p. 118).

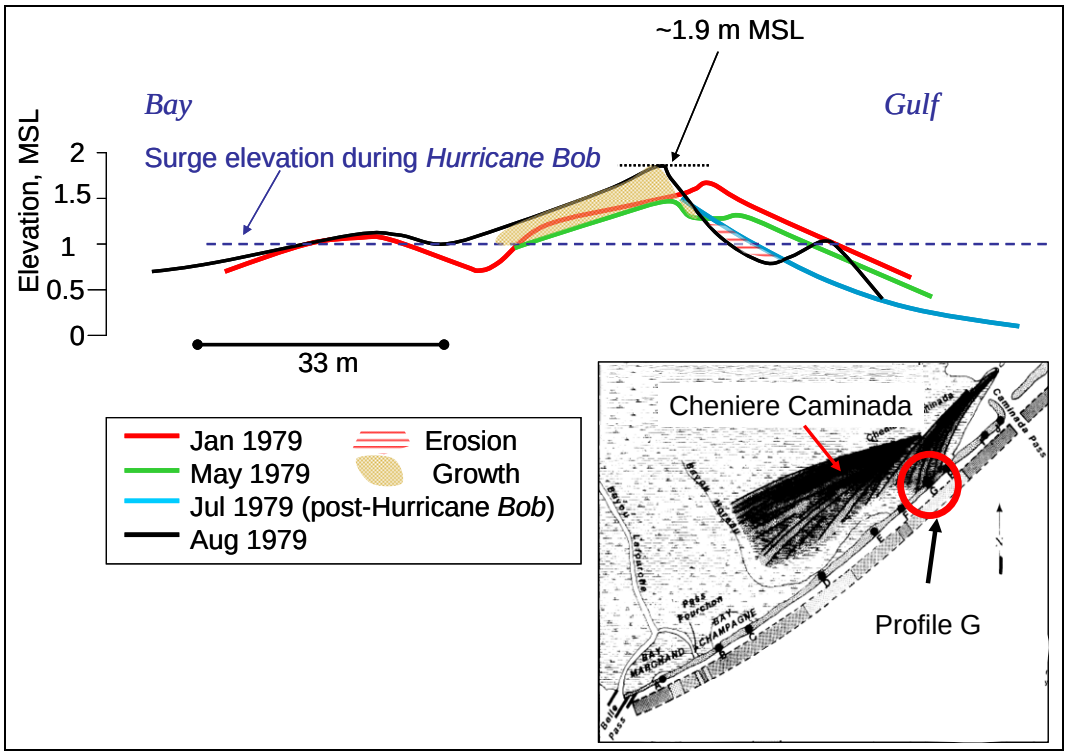

Figure 49. Retreating dune ridge (Profile G, adapted from Ritchie and Penland 1988, p. 115).

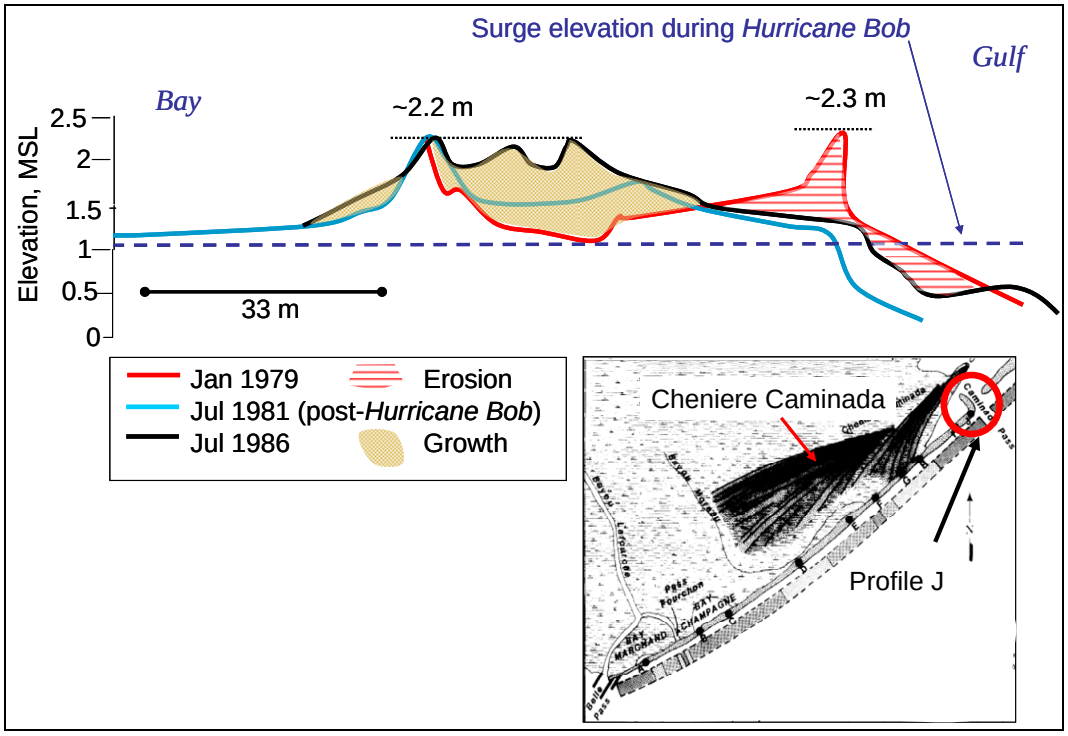

Figure 50. Dune erosion and recovery
(Profile J, adapted from Ritchie and Penland 1988, p. 119).

These data from Caminada Headland indicate that it is possible for dunes in Louisiana to reach 2.4 m elevation relative to MSL, given a sufficient source of unvegetated dry sand, wind speed exceeding the threshold (approximately 7.5 m/sec at 10 m elevation), and a sufficiently wide beach.

Dingler and Reiss (1989, 1990, and 1995; Dingler 2008) surveyed beach profiles on Trinity Island, part of the Isle Dernieres, over a 7-year period from September 1986 to November 1993 and took sediment cores documenting the sand-mud interface on the island in 1987. Volumetric change data are summarized in Table 10. These data show the nearly continuous recession of the island (Figure 51) through several storm seasons including Hurricanes Gilbert and Andrew, which made landfall on September 16, 1988, and August 25, 1992, respectively.

Table 10. Volumetric change for Trinity Island, LA (Dingler 2008).

Data from Dingler and Reiss (1991)	**Profile Date**					
	8/14/86	9/20/87	7/15/88	9/14/88	Hurricane Gilbert 9/16/88	9/28/88
Volume Above Zero (m^3/m)	451	382	341	347		330
Volume Below Zero and Above -1.25 m MSL (m^3/m)	51	73	51	48		74
Rate of Change Above Zero ($m^3/m/year$)		-75	-45	6.4	-19	
Rate of Change Below Zero and Above -1.25 m MSL ($m^3/m/year$)		24	-23	-3.3	28	
Total Rate of Change Above -1.25 MSL ($m^3/m/year$)		-51	-68	3.1	9	

Data from Dingler and Reiss (1995)	**Profile Date**					
	9/26/90	7/10/91	Hurricane Andrew 8/25/92 Surge: 2 m	9/1/92	11/8/92	11/12/93
Volume Above Zero (m^3/m)	114	118		39	33	21
Volume Below Zero and Above -2.1 m MSL (m^3/m)	445	315		378	370	-32
Rate of Change Above Zero ($m^3/m/yr$)		5.6	-478	-34	21	
Rate of Change Below Zero and Above -2.1 m MSL ($m^3/m/yr$)		-155	377	-51	-32	
Total Rate of Change Above -2.1 MSL ($m^3/m/yr$)		-150	-202	-85	-11	
Rate of Cohesive Sediment Erosion ($m^3/m/yr$)					-17	

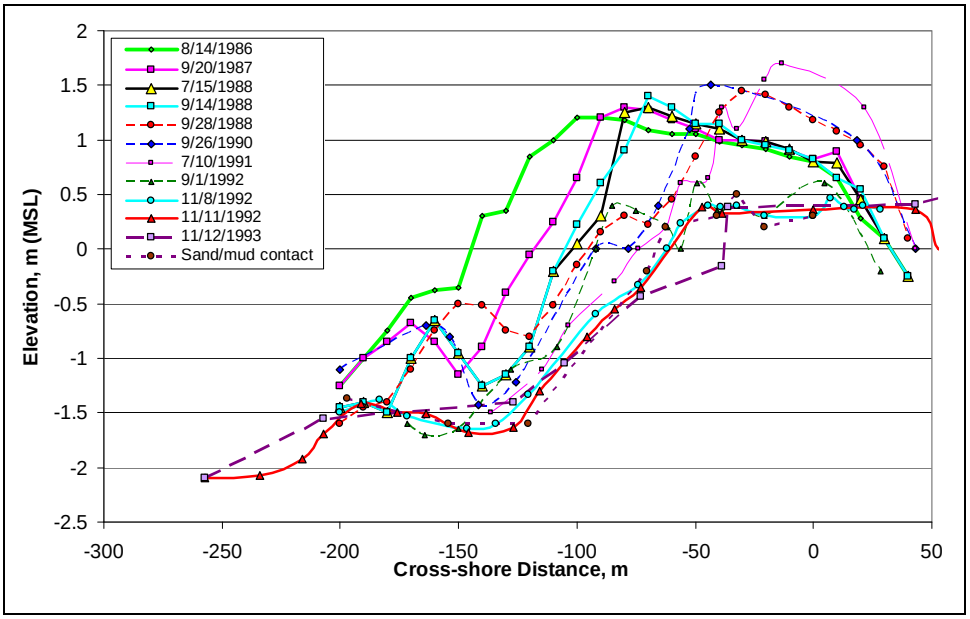

Figure 51. Beach profile data and sand-mud interface for Trinity Island, Isle Dernieres (adapted from Dingler and Reiss 1989, 1990, and 1995).

Figure 52 shows two of these profiles, from 28 September 1988 (post-Hurricane Gilbert), to September 1990, quantifying erosion of the berm at -2.2 $m^3/m/year$ and migration of the dune towards the Gulf, presumably through eolian sand transport, at 3.7 $m^3/m/year$. The sand-mud interface was not exposed during this 2-year period.

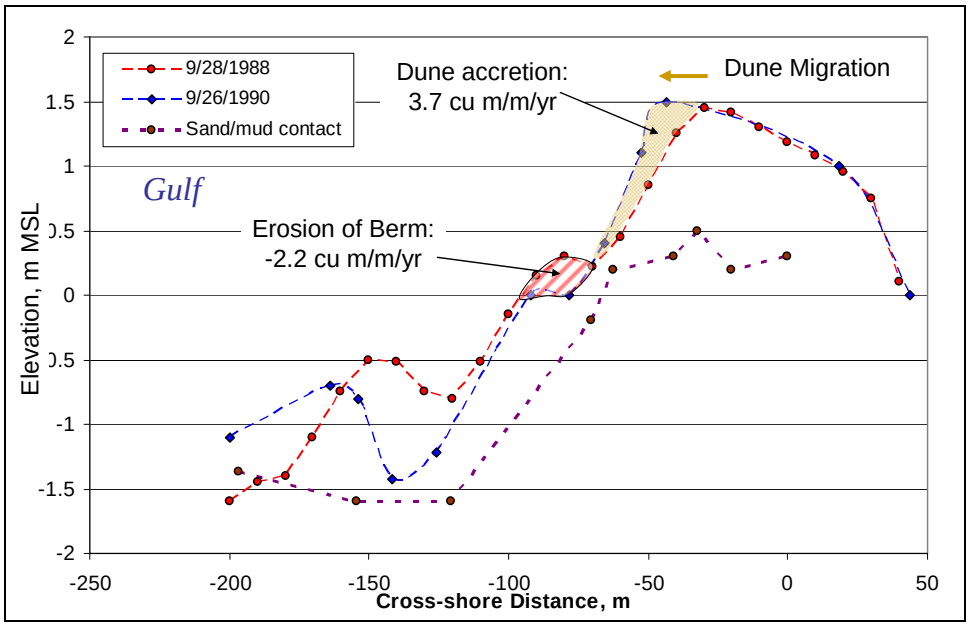

Figure 52. Profile evolution from September 1988 to September 1990 showing erosion of berm and dune migration towards gulf.

Thus, these data indicate that eolian sand transport can result in a net accretion of sand equal to approximately 4 m^3/m/year from the north. Wind data available from Coastal Studies Institute (CSI) gage CSI-5, located south of Terrebonne Bay were applied to evaluate the eolian sand transport sub-module. No process data were available for the time period corresponding to the profile measurements. Table 11 summarizes winds exceeding the threshold speed (Equations 30 and 31 give 7.8 m/sec at 18.72-m elevation for 0.16-mm sand) from 2001-2006 (all available years).

These data indicate that wind speed from the north exceeded that from the south in every year except 2001. North wind occurred more frequently than wind from the south.

Table 11. Summary of average wind speed exceeding threshold1, percent occurrence, sta CSI-52 (Coastal Studies Institute 2008), and results from eolian sand transport sub-module.

Date	Average Wind Speed and Standard Deviation (m/sec)		Percent Occurrence (%)		Potential Wind Blown Sand Transport as Calculated by Eolian Sand Sub-Module (1,000 $m^3/m/yr$)		
	From North	From South	North	South	North	South	Net (to the south)
2001	9.9 ± 1.6	9.7 ± 1.8	13.2	12.3	2.6	3.8	-1.2
2002	10.3 ± 2.1	9.6 ± 2.2	14.8	10.6	8.7	5.7	3.0
2003	10.2± 2.0	9.7 ± 1.9	12.7	10.4	6.1	3.5	2.5
2004	10.1 ± 1.8	9.5 ± 1.5	15.6	12.6	4.9	2.3	2.6
2005	10.3 ± 2.9	10.2 ± 3.2	17.0	7.7	17.2	10.3	7.0
2006	10.3 ± 2.0	9.9 ± 1.9	11.8	10.4	6.9	4.6	2.3
						AVERAGE ($m^3/m/yr$):	2.7 ± 2.6

[1]Threshold wind speed equals 7.8 m/sec for wind measured at 18.72 m elevation (Jose, 2008) and 0.16-mm sand.

[2]Located south of Terrebonne Bay, LA, Coordinates: -90°32', 29°3.2', in 6.3 m depth.

Applying the eolian sand transport sub-module with winds from each direction and assuming the beach width is not a limiting factor gives the potential eolian transport rate from each direction and each year (columns 6 and 7 in Table 11). Depending on the vegetation coverage, precipitation, and degree of inundation of the island, the eolian sand transport rate could be less than indicated for the north or south.

The average net eolian sand transport calculated with these data (column 8) was 2,700 m^3/m/year from the north to the south. This value is much greater than estimated from the profile data, which was

4 $m^3/m/year$. It is likely that the net eolian transport as measured from beach profile change is less than calculated with the Eolian Sand Transport sub-module because of storm surge and precipitation inundating the beach during periods of winds exceeding the threshold, vegetation which hinders transport, and sand that is transported by wind from the beach and deposited offshore. Therefore, an underestimate is to be expected.

Fine-grained sediment erosion

Figure 53 shows two profiles from the Trinity Island data set in which fine-grained sediment was exposed following Hurricane Andrew and eroded at a rate of 16.8 $m^3/m/year$ over the year between profile measurements. Local wave information was not available for this time period. Although minimal in coverage across the backbarrier, profile data indicate that it may have been a relatively calm year due to lack of evidence of washover deposition.

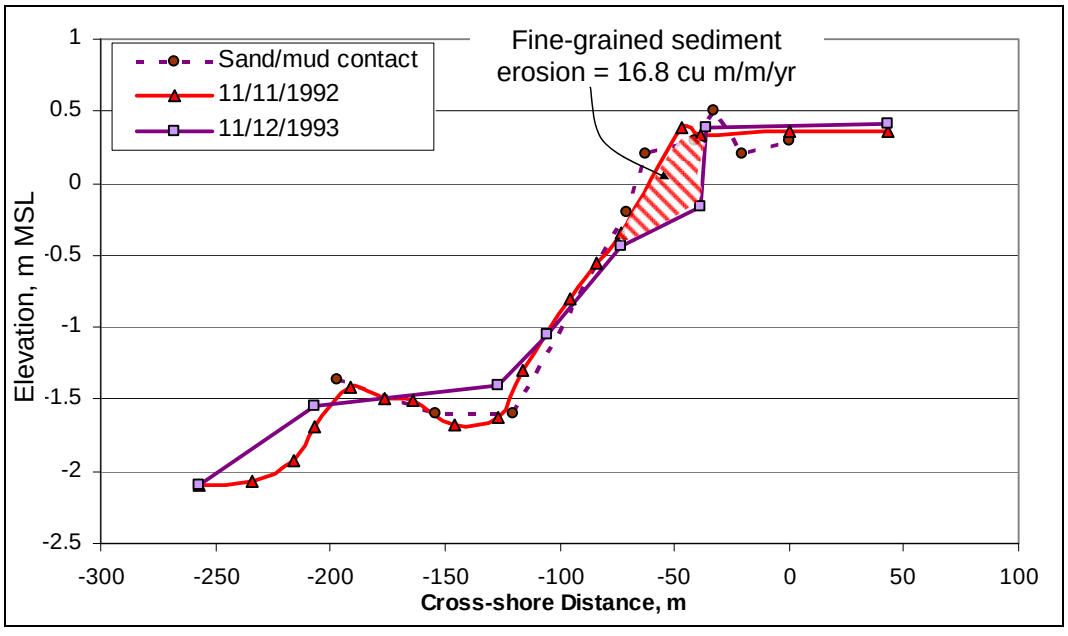

Figure 53. Erosion of fine-grained sediment from November 1992 to November 1993.

To evaluate the Fine-Grained Sediment Erosion sub-module with data from Trinity Island, wave height data from 2003 for sta CSI-5 were transformed from the measurement location (average depth of 6.7 m in 2003) to the local depth at the beach face (approximately 0.5 m MSL, Figure 53). The year 2003 was selected because it had only one Tropical Storm (*Bill* which had wind speeds of 50 knots (25.7 m/sec) and made landfall west of Isle Dernieres, NOAA (2008d)) and had few gaps in the data record. The Fine-Grained Sediment Erosion sub-module was

modified to calculate the erosion rate only if the water level was within the zone of fine-grained sediment (approximately between -0.4 and 0.4 m MSL, Figure 53); otherwise, erosion was set to zero.

Figure 54 presents results of the simulation, in which the erosion rate (top panel), cumulative erosion (middle panel), wave height and water level at the beach (bottom panel) are shown for the default coefficients as discussed previously (k_{fg} = 0.1 kg/N/sec), critical bed shear stress τ_c = 0, and thickness of fine-grained sediments z_{fg} = 0.8 m as indicated by the profile data (Figure 53). This simulation resulted in cumulative erosion for the year equal to 22.5 $m^3/m/year$, greater than the measured value of 16.8 $m^3/m/year$. If the empirical coefficient is reduced to k_{fg} = 0.075 kg/N/sec, the cumulative erosion equals 16.9 $m^3/m/year$, approximately equal to the measured value.

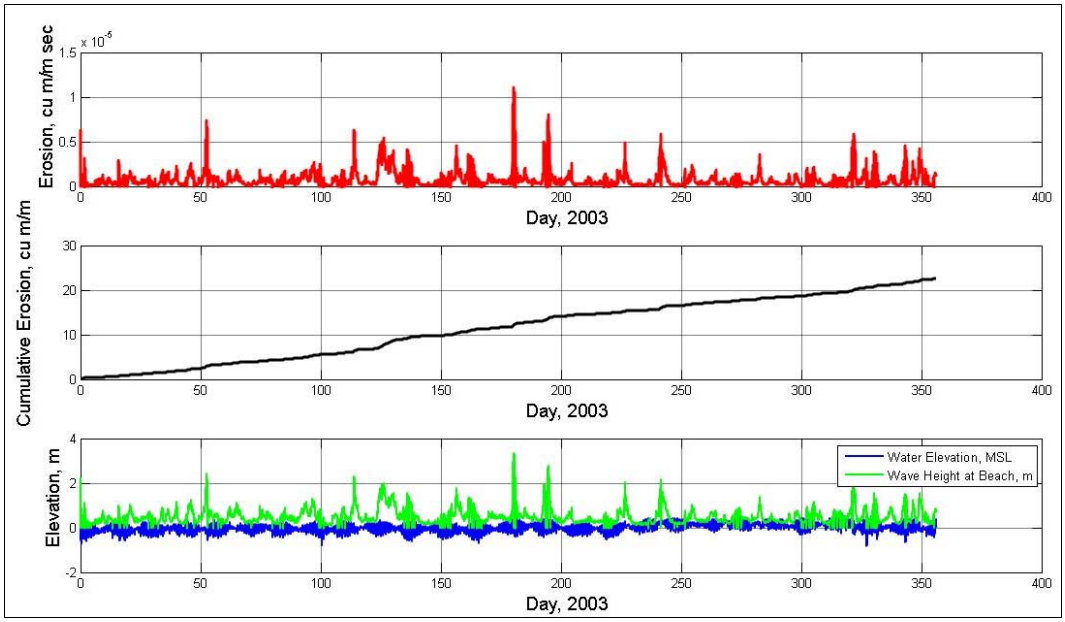

Figure 54. Application of fine-grained sediment erosion sub-module with wave information for 2003 from sta CSI-5.

Regional sources and sinks

The Regional sub-module was evaluated with data from the 1880s to 2000 for Barataria Bay, LA. Barataria Bay formed between distributaries of the Mississippi River system, the abandoned LaFourche delta to the west and the abandoned Plaquemines sub-delta and present-day Balize delta to the east. The bay is fronted by barrier islands that formed as the deltaic deposits were reworked by waves, storms, and wind and migrated towards the bay from both east and west. The present-day estuarine system is

microtidal (0.27 m tidal range), with mild wave climate (mean wave height 0.45 m), and protected by three barrier islands and four tidally-dominated passes (Figure 55). Because of an increase in relative sea level (9.24 mm/year, 1947-2006, Grand Isle; NOAA 2008a) and loss of wetlands, Barataria Bay has experienced an increase in area over the past 120 years, which has increased tidal prism and ultimately volume of ebb delta deposits (FitzGerald et al. 2004, 2007; Flocks et al. 2006; and others).

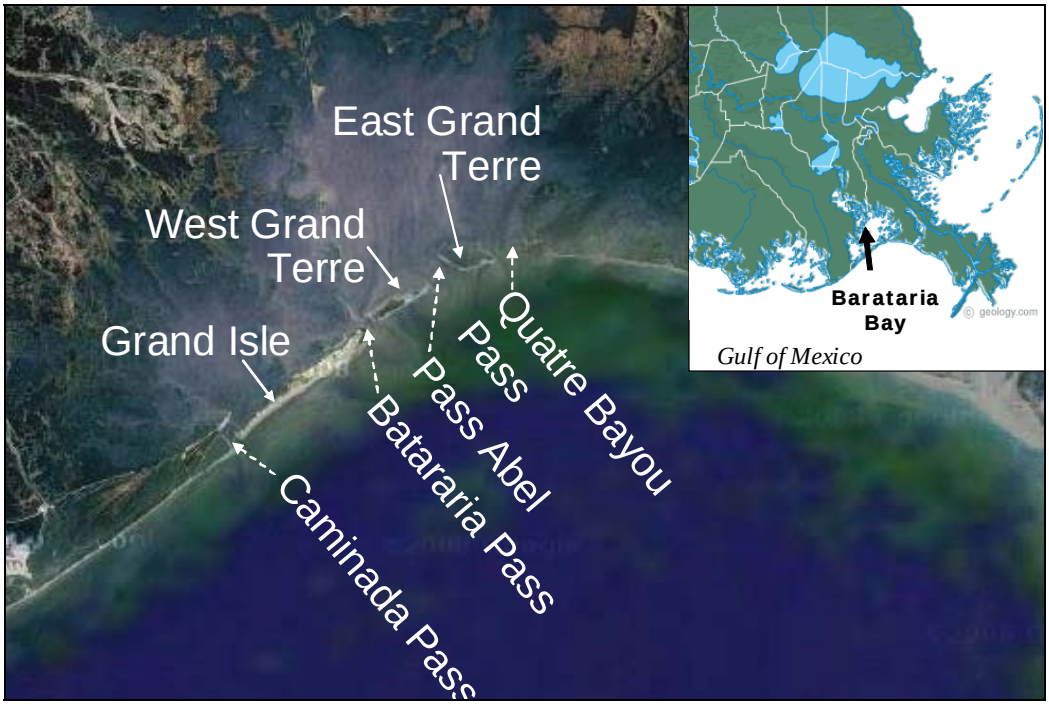

Figure 55. Location map for Barataria Bay, LA.

The Regional sub-module was applied to the Barataria Bay system with data from the 1880s representing the initial conditions and calculating for 158 years with a time step equal to 0.1 year. Coefficients in Equations 48 and 51 were modified to best represent historical evolution of the ebb tidal shoals and tidal passes (Figure 56). The total ebb shoal volumes (from List et al. 1991) and cross-sectional areas (from FitzGerald et al. 2007) for all the Barataria passes have historically been 37 and 45 percent greater, respectively, than would be indicated by Walton and Adams's (1976) and Jarrett's (1976) predictive equations. One reason for the larger values may be that site-specific characteristics increase the effectiveness of the tidal prism that scours the tidal passes and moves sediment to the ebb tidal shoals. For example, meteorological forcing during cold front passages significantly elevates bay water levels from 20-30 times per year (Georgiou et al. 2005). The larger tidal prism in the post-frontal phase would more

readily mobilize fine sediment, scour the tidal channels, and ultimately increase ebb shoal volumes and channel areas over those that are calculated with Walton and Adams' and Jarrett's relationships that were developed for a spring tidal prism.

Figure 57 shows calculations from the decadal-scale barrier island evolution model as compared to measurements. Tidal prism is proportioned through each tidal pass in relative proportion to the cross-sectional area of each pass.

To best represent measured cross-sectional inlet areas, the scour time coefficient was doubled after 50 years (from the initial value of τ_c = 20 years to τ_c = 40 years) for Caminada and Barataria Passes, which allowed more tidal prism to be captured by Pass Abel and Quatre Bayou Passes as is indicated by the measurements. This adjustment to the scour coefficient has justification in the partial stabilization of Caminada and Barataria Passes, which limited the cross-sectional expansion. Grand Isle, the island between Caminada and Barataria Passes, is the only permanently inhabited barrier island in Louisiana. It is likely that the islands began to be stabilized in the 1930s. A jetty was built at Barataria Pass in 1964 (Shamban and Moslow 1991), which further stabilized the cross-sectional area of Barataria Pass.

An increase in relative sea level equal to 9.24 mm/year was included in the calculations with a time-dependent loss of barrier island area and an increase in bay area, which averaged 1.3 percent/year from 1892 to 1989 (Levin 1993; Reed 1995). Longshore transport rates on the islands were based on information available in the literature, and ranged from 40,000 m^3/year (adjacent to Pass Abel) to 150,000 m^3/year (adjacent to Caminada Pass). Note that these calculations assume that all sediment eroded from the islands and channels represents sand, which is reasonable for islands and shoals in Louisiana with sediment that has been previously reworked by marine processes. However, it is likely that in situ deltaic deposits are mixed sand, silt, mud, and organics.

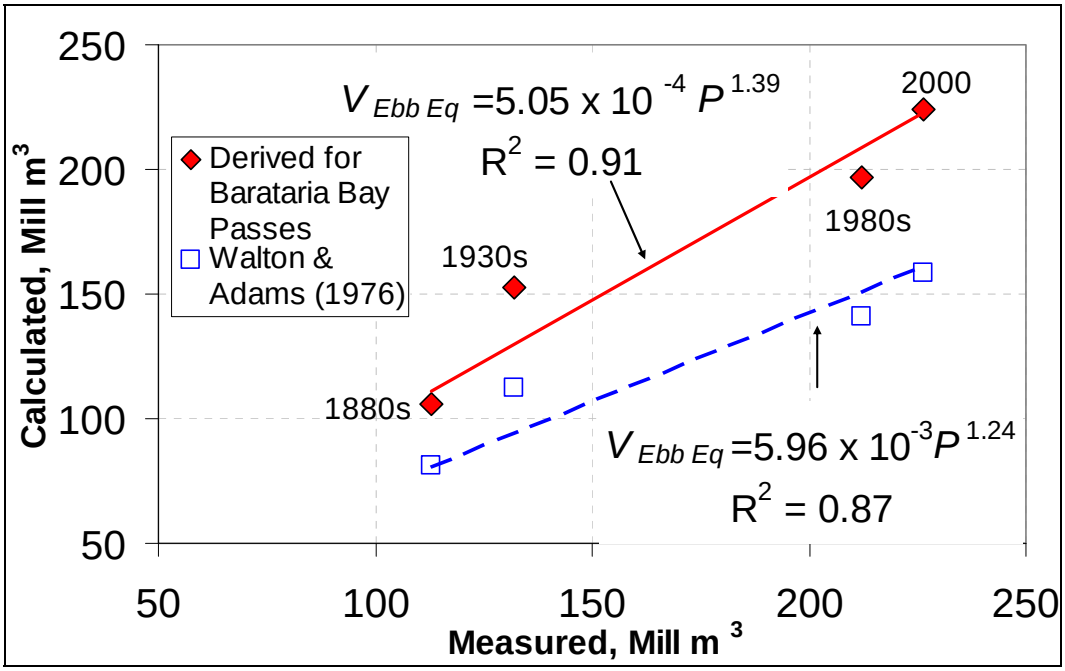

a. Equilibrium ebb delta volume (revised coefficients for Equation 48).

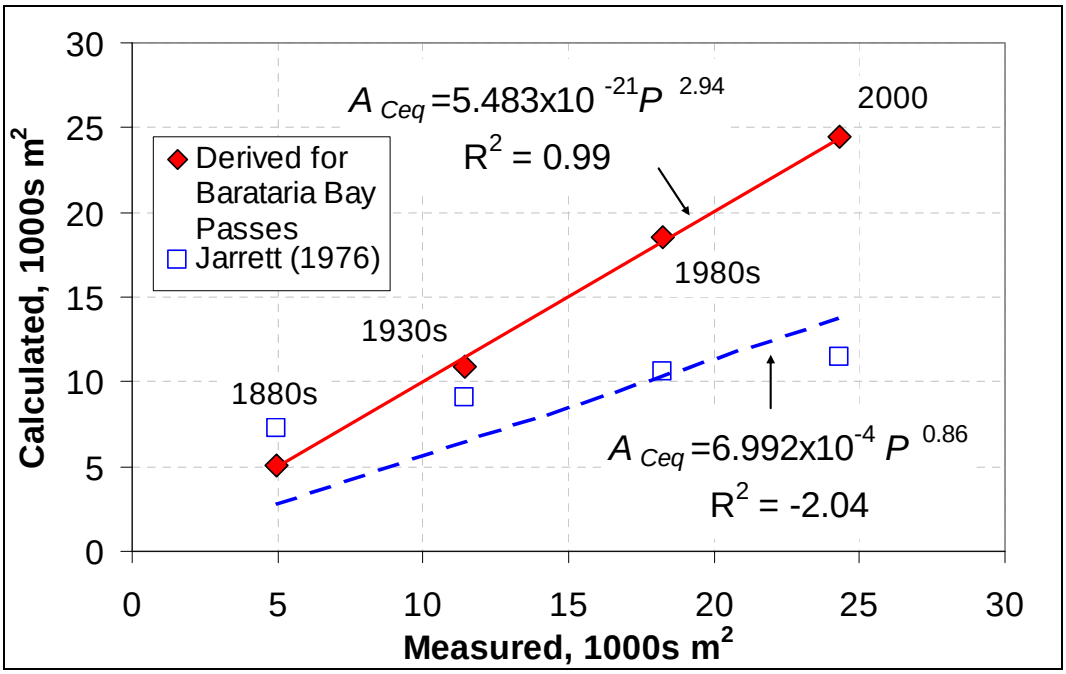

b. Equilibrium channel cross-sectional area (revised coefficients for Equation 51).

Figure 56. Coefficients for ebb delta volume and cross-sectional area relationships (Equations 48 and 51, respectively) derived for data from 1880s through 2000 for Barataria Bay Passes (ebb volumes from List et al. 1991, cross-sectional areas from FitzGerald et al. 2007).

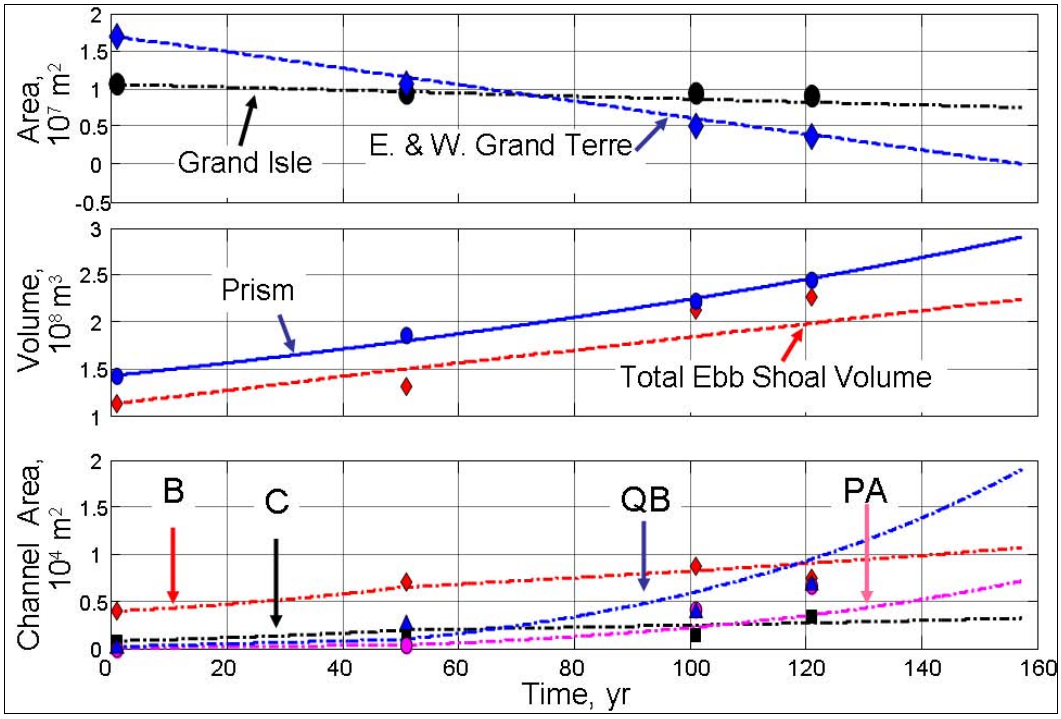

Figure 57. Comparison of regional sub-module with measurements, Barataria Bay, LA (B= Barataria, C = Caminada, QB = Quatre Bayou, PA = Pass Abel).

The calculations end after 158 years (year 2038), when the combined subaerial extent of East and West Grand Terre disappeared. Based on historical trends in shoreline position data, extrapolations by McBride and Byrnes (1997) indicated that the Grand Terre Islands would disappear by 2033 (data from 1884 to 1988).

Conclusions

This chapter quantified long-term processes that may modify the volumetric sediment budget of a barrier island system. The long-term processes considered were a gradient in longshore sand transport, post-storm recovery of the cross-shore profile, eolian sand transport and dune aggradation, erosion of fine-grained sediment after the protective sand veneer has eroded and prior to recovery, and changes to the regional sources and sinks. Two of these processes, post-storm recovery and eolian sand transport, are more likely where there is a surplus of sand in the littoral system, such as would occur after a restoration-scale renourishment project.

Sub-modules were developed for each of these long-term processes and evaluated in a qualitative manner. Sub-modules that could be tested with data were the Eolian Sand Transport, Fine-Grained Sediment Erosion, and

the Regional Sources and Sinks modules. These were evaluated and gave reasonable comparison with data available from the literature. The next chapter considers these long-term processes together with the 2D storm response in an assessment of the hypotheses proposed at the start of this research.

6 Evaluation of Hypotheses

Introduction

This chapter evaluates each of the three hypotheses introduced in Chapter 1 and develops recommendations based on results of these analyses. These hypotheses, reproduced below, concern morphology change of barrier islands that overlie a compressible substrate, such as deltaic mud or estuarine clay and silt, as compared to a more stable substrate such as sand, and how these islands can be preserved by infusion with sand from an external source. Sections 6.2 through 6.4 evaluate each hypothesis separately by means of the 2D MCO as presented Chapter 4, coupled with applicable long-term sub-modules as discussed in Chapter 5, and knowledge gained through the literature review presented in Chapters 2 and 3. Metrics are defined and applied to test the validity of each hypothesis, and the degree to which each hypothesis is met is discussed.

Section 6.5 integrates knowledge gained through this research and introduces the concept of functional restoration. Functional restoration is defined here as the minimum beach nourishment volume and cross-sectional design such that the island can perform as a wave break, storm surge buffer, and ocean boundary for the estuary, bay, and mainland over a specified time interval. The concluding section makes recommendations for functional restoration of barrier islands that overlie a compressible substrate.

Hypothesis 1

Overview

Hypothesis 1 is: "*Consolidation is a dominant process governing morphologic evolution and migration for barrier island systems overlying poorly-consolidated sediment*." Metrics introduced here to test this hypothesis are as follows:

1a. For barrier islands that overlie a compressible substrate (abbreviated as Barrier Island Compressible, BIC), the volume sequestered via consolidation through the migration process is a significant (arbitrarily defined here as >10 percent) portion of the

sand budget for the barrier island. A 10 percent change is considered an amount that is measurable.

1b. Morphology of BICs differs in elevation and width as compared to barrier islands overlying a stable substrate (abbreviated as Barrier Island Stable, BIS).

1c. With a sufficient source of sand to maintain subaerial elevation, migration rates are significantly greater for BIC as compared to BIS.

1d. Without a sufficient source of sand, the lifetime of BIC is reduced as compared to a BIS of comparable original dimensions.

Analysis

Metric 1a

Metric 1a tests whether the consolidated volume that is sequestered through the migration process is greater than 10 percent. Simulations presented in Table 6 for H_{bar} = 4 m, W_{bar} = 2,500 m, z_o = 10 m, and consolidation parameters "a" (c_{v0} = c_{vc} = 2.5 m^2/year) were evaluated to test Metric 1a. The average percentage and standard deviation of volume consolidated through the applicable simulations were calculated for all simulations and four subsets of these simulations. To form the subset analyses, the consolidated volume that occurred in an adjustment period (evaluated for 10, 20, 30, or 40 years) was subtracted from the total consolidated volume. These calculations are intended to account for initial adjustment of the profile; various durations are considered because duration required for initial adjustment is unknown. Table 12 and Figure 58 summarize this analysis.

Table 12. Evaluation of Metric 1a – volume sequestered through consolidation is greater than 10 percent of total barrier island volume*.

	All Simulations*	After 10 yr	After 20 yr	After 30 yr	After 40 yr
% Volume Consolidated	67.6 ± 14.6	41.4 ± 11.9	31.0 ± 10.0	23.8 ± 7.6	20.3 ± 4.5
Duration, yr	40.0 ± 10.2	41.4 ± 7.9	42.5 ± 6.4	43.9 ± 4.8	45.8 ± 3.4
Number of Data Points	22	21	20	18	14

* Evaluated for simulations listed in Table 6 for Hbar = 4 m, Wbar = 2,500 m, zo = 10 m, and consolidation parameters "a" (cv0 = cvc= 2.5 m2/yr).

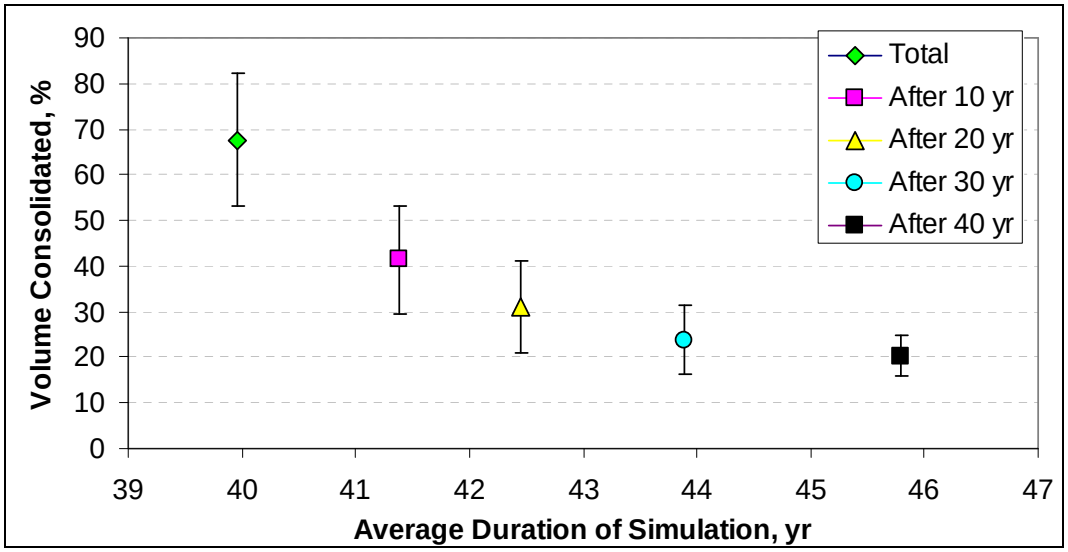

Figure 58. Percentage of total barrier island sand consolidated.

These results indicate that the volume of sand that is sequestered through the consolidation process can be as large as 68 percent for a barrier island overlying a poorly-consolidated substrate, such as would occur for new construction of a barrier island over a compressible substrate. If the initial adjustment of the island is subtracted from the total volume, the percent of sand sequestered through the consolidation process ranges from 20 to 46 percent, depending on the time estimated for the initial adjustment and the forcing parameters.

Data for Assawoman Island (two sites) and Metomkin Island, VA (Figures 10-12), were evaluated to determine the volume of sand that was below MHW, which represents sand that was removed from the subaerial barrier island volume through consolidation and eustatic sea level rise. The volume of sand below MHW due to eustatic sea level rise was calculated based on the island's migration rate, the duration of time the island existed at each sediment core, and the eustatic sea level rise rate (2 mm/year, Douglas 1992; Peltier 1998). Subtracting the eustatic sand volume from the sand volume below MHW gives the volume sequestered through the migration and consolidation process over approximately 40 years. These calculations are shown in Table 13 and indicate between 34-54 percent of the total island volume was sequestered through consolidation over the 40-year migration period.

Table 13. Evaluation of metric 1a for Virginia barrier islands.

Site and Figure	Total Sand Volume above Substrate, m^3/m	Volume of Sand Below MHW, m^3/m	Volume of Sand below MHW due to Eustatic SLR*, m^3/m	Net Volume below MHW due to Consolidation, m^3/m	% Consolidated
Assawoman 1, Figure 10	219	128	9	119	54%
Assawoman 2, Figure 11	363	138	15	123	34%
Metomkin, Figure 12	194	89	11	78	41%
				Average	43 ± 11%

* Eustatic sea level rise (SLR) = 2 mm/yr (Douglas 1992; Peltier 1998); island migration rates = 3.75 m/yr (Assawoman 1), 4.05 m/yr (Assawoman 2), and 4.8 m/yr (Metomkin).

In conclusion, Metric 1a is found to be valid: the volume sequestered through the consolidation process is at least 10 percent of the total volume change for a barrier island migrating over a compressible substrate. Based on 2D MCO applications with the substrate and forcing conditions considered here, this volume was approximately 20-46 percent of the total island volume. Data from three field sites in Virginia indicated an average of 43 ± 11 percent of the sand volume below MHW datum was sequestered through consolidation over a 40-year migration period.

Metric 1b

This metric evaluates whether the elevation and width of BICs differ from that of BISs. Data for Santa Rosa Island, FL, and West Ship Island, MS, presented by Stone et al. (2004) represent a relatively stable substrate (BIS). These sites are compared to islands overlying a compressible substrate, with data from Virginia (shown in Figures 10, 11, and 12) and Louisiana (Caminada-Moreau Headland, Figures 47 through 50, and Isle Dernieres, Figure 51). Table 14 lists the pertinent dimensions from each of these sites, all referenced to local MSL. Island width is not shown for some of the sites because the data do not cover the entire width of the island.

Table 14. Evaluation of Metric 1b.

Site	Figure	Maximum Elevation, m MSL	Width at MSL, m
BIS – Barrier Island Overlying Stable Substrate			
Santa Rosa Island, FL – 1995[1]	Stone et al. (2004, Fig. 7)	4.7, 1.9[2]	220, 250[2]
Santa Rosa Island, FL – 1998[1]	Stone et al. (2004, Fig. 9)	2.2, 2.0[3]	220, 200[3]
West Ship Island, FL – 1998[1]	Stone et al. (2004, Fig. 9)	3.1, 1.9[3]	--
Range		**1.9 – 4.7**	**200 - 250**
BIC – Barrier Island Overlying Compressible Substrate			
Assawoman 1, VA[4]	10	1.6	170
Assawoman 2, VA[4]	11	2.8	280
Metomkin, VA[4]	12	1.4	215
Caminada Headland, LA, Profile H	47	2.4	--
Caminada Headland, LA, Profile I	48	2.2	--
Caminada Headland, LA, Profile G	49	1.9	--
Caminada Headland, LA, Profile J	50	2.2-2.3	--
Trinity Island, LA	51	1.7	--
Range		**1.4 - 2.8**	**170 - 280**

[1] Adjusted from NGVD to MSL as MSL = NGVD-0.1m (Stone et al. 2004; Pensacola, FL, sta 8729840, NOAA 2008e).

[2] Pre- and post-Hurricane *Opal,* 4 October 1995.

[3] Pre- and post-Hurricane *Georges*, 26 September 1998.

[4] Adjusted from MHW to MSL as MSL = MHW + 0.24 m (Chincoteague NOAA sta 8630249, NOAA 2008f).

Although this analysis is limited to the available data sets, it lends insight into differences between morphology and behavior of BIC as compared to BIS. Elevations of BICs with sufficient sources of sand (e.g., Assawoman 1, Assawoman 2, Caminada Profiles H, I, and J; average elevation 2.3 m MSL) are comparable to the BIS sites (average pre-storm elevation 3.3 m MSL, average post-storm elevation 1.9 m MSL). Thus, a source of sand sufficient to offset losses to the island induced by consolidation of the substrate allows BIC to maintain elevations similar to BIS. However, BIC sites without a sufficient source of sand to replenish the volume retained through the consolidation process (Caminada Profile G, Metomkin, and Trinity Islands) have lower elevations (average 1.7 m MSL) than the BIS sites. Barrier islands overlying a compressible substrate have an additional loss to their sand budget, a decrease in volume due to the consolidation process, which is not a factor for the BIS sites. Based on the limited data, island widths appear comparable between BIS and BIC.

Thus, Metric 1b is found to be true for elevation if littoral sand is limited. Specifically, the availability of sand, either through longshore, onshore, eolian sand transport, or through mechanical placement controls the degree to which BIC can achieve elevations similar to BIS. Without the source of sand to replenish sediment sequestered through the consolidation process, BICs become lower in elevation than comparable BIS.

Metric 1c

Metric 1c tests whether the migration rates of BIC are greater than BIS, if a sufficient source of LST is available to provide sand for the island. To evaluate Metric 1c, the longshore sand transport (LST) sub-module was coupled with 2D MCO such that a sufficient source of sand replenished the barrier island through the migration process. Simulations were set for a 99-year duration with $H_{mo} = S = 1$ m, $H_{bar} = 4$ m, and $W_{bar} = 2{,}500$ m; for BIC, the thickness of compressible substrate was varied, $z_o = 10$, 15, and 20 m with consolidation parameters "a" ($c_{v0} = c_{vc} = 2.5$ m^2/year, Equation 19). Results of these simulations are summarized in Table 15.

Table 15. Evaluation of Metric 1c – migration rates of BIC are greater than migration of BIS if sufficient sand source is available.

Barrier Island Type	z_o, m	Net LST Source (m^3/m/yr)	Migration Rate, m/yr	Duration, yr
BIC	10	31.4	16.7	99
	15	47.5	63.6	60*
	20	72.6	57.3	43*
BIS	-	3.7	5.3	99

* All simulations were set for duration of 99 years; these runs terminated because maximum island elevation became sub-aqueous.

For BIC, net LST rates required to maintain the island through the migration process ranged from 31 to 73 m^3/m/year. This net LST rate was not sufficient to maintain the islands with $z_o = 15$ and 20 m for the full 99 years; simulations terminated after 60 and 43 years, respectively. With a stable substrate, the required net LST was reduced to 4 m^3/m/year for a 99-year simulation. Based on the results presented in Table 15, Metric 1c is valid, with migration rates for BIC ranging from 3 to 11 times greater than for a similar island over a stable (uncompressible) substrate.

Metric 1d

Metric 1d tests whether the lifetime of BIC is reduced as compared to BIS, in the absence of a sufficient sand source. Simulations to evaluate Metric 1d were discussed in Chapter 4 (Sensitivity Analyses 2 and 3, presented in Figure 35), and are summarized in Table 16. All BIC durations were less than those of BIS except for the largest barrier island (H_{bar} = 5 m, Sensitivity Analyses 2d and 3d). For these cases, the island provided a sufficient elevation to reduce washover as evidenced by similar migration rates for both BIC and BIS. Thus, Metric 1d is found to be valid except for BIC that are of sufficient elevation to reduce washover over the time periods of consideration.

Table 16. Evaluation of Metric 1d, lifetime of BIC is reduced as compared to BIS.

Sensitivity Analysis (Table 6)	H_{bar}, m	Duration, yr		Migration, m/yr	
		BIC	BIS	BIC	BIS
2a, 3a	2.5	15	50	205	10.8
2b, 3b	3	34	50	84	7.4
2c, 3c	4	46	50	78	8.6
2d, 3d	5	50	50	7.3	8.2

Hypothesis 2

Overview

The second hypothesis is: "Given similar forcing conditions, barrier islands overlying poorly consolidated sediment require a greater volume of sand, greater dune elevation, and greater width to maintain functioning as compared to islands over a non-compressible substrate." This hypothesis is evaluated with 2D MCO simulations over a 99-year period, although some simulations terminated prior to completing this duration because of complete submergence of the barrier island. Metrics with which to test this hypothesis are:

2a. The minimum volume required for restoration of BIC over a specified lifetime is greater than the minimum volume required to provide the same lifetime for BIS. Restated another way, given the same cross-sectional volume, the lifetime of BIC is less than BIS.

2b. The minimum elevation required to maintain functioning (elevation above MSL) of BIC over the specified lifetime is greater than the

minimum elevation required to provide the same functioning for BIS.

2c. The minimum width required to maintain functioning of BIC over the specified lifetime is greater than the minimum width required to provide the same lifetime for BIS.

Analysis

Metric 2a

Given the same nourishment volume, Metric 2a evaluates whether the lifetime (defined as the duration for which the maximum island elevation is above MSL) of BIC is less than BIS. To evaluate this metric, 15 simulations were conducted with 2D MCO with varying substrate characteristics (thickness of compressible substrate z_o = 0 (stable), 10, 15, and 20 m with consolidation parameters "a", $c_{v0} = c_{vc}$=2.5 m^2/year, Equation 19) and volume of initial beach nourishment varying up to 2,850 m^3/m. All simulations were set for a 99-year duration with $H_{mo} = S$ = 1 m, H_{bar} = 4 m, and W_{bar} = 2,500 m. Results of this test are shown in Figure 59.

Simulations for islands over a compressible substrate decreased in duration as compared to the stable substrate, with the exception of one simulation with a large initial fill volume (z_o = 10 m, initial fill volume = 2,550 m^3/m). Duration of the simulations decreased as the thickness of compressible sediment z_o increased, although the decrease in duration was not linear with increase in z_o. As would be expected, with an increase in the initial volume, the duration of the simulations also increased for the compressible substrate simulations. Metric 2a is valid with the exception for large fill volumes and less compressible substrate.

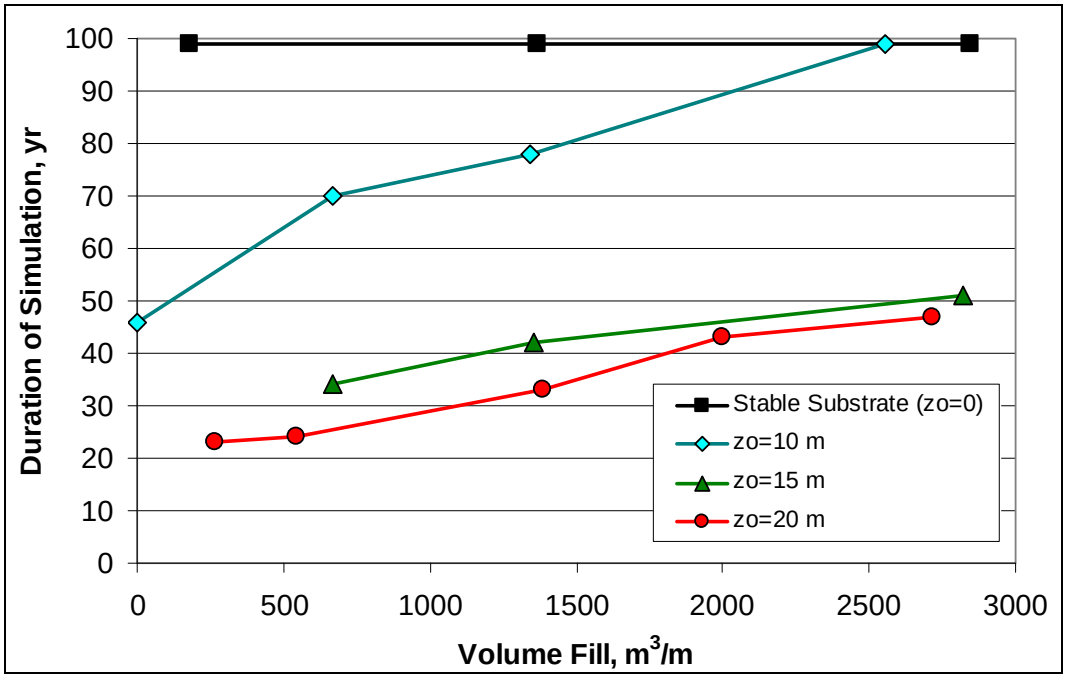

Figure 59. Lifetime of BIC compared to BIS as function of initial fill volume.

Metric 2b

Metric 2b tests whether the minimum elevation required for the barrier island to remain above MSL for a defined lifetime is greater for BIC as compared to BIS. To evaluate this metric, results from sensitivity analyses 2 and 3 (Table 6, see also Figure 45) were compared as shown in Figure 60. In these analyses, the initial dune crest was varied, H_{bar} = 2.5 to 5 m, with H_{mo} = S = 1 m, and W_{bar} = 2,500 m. The BIC was calculated with z_o = 10 m; larger z_o values would decrease the duration of the simulations.

All simulations were set for a 50-year period, but runs for the BIC with the initial dune crest elevation less than 5 m terminated due to the island eroding below MSL. Thus, Metric 2b is found to be valid for longer life-times. If the lifetime were defined to be 15 years, for example, the BIC would have the same lifetime as BIS for all initial dune crest elevations.

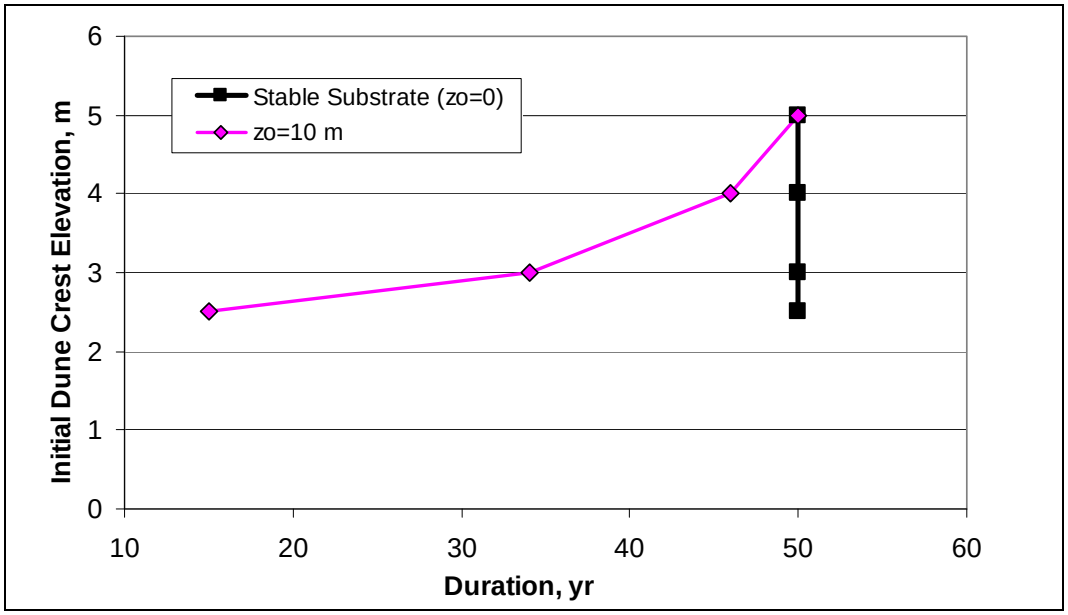

Figure 60. Duration of simulation as function of initial dune crest elevation and substrate.

Metric 2c

To evaluate Metric 2c, results from sensitivity analyses 4 and 5 (Table 6) were evaluated to determine the influence of barrier island width and substrate characteristics on duration. All simulations were set for a 50-year duration with $H_{mo} = S = 1$ m, $H_{bar} = 4$ m, and W_{bar} ranging from 1,000 to 3,500 m. Figure 61 shows how the duration of the simulation increases with increasing initial barrier island width for BIC with $z_o = 10$ m as compared to BIS. Using the same reasoning as discussed for Metric 2b, Metric 2c is valid for longer lifetimes.

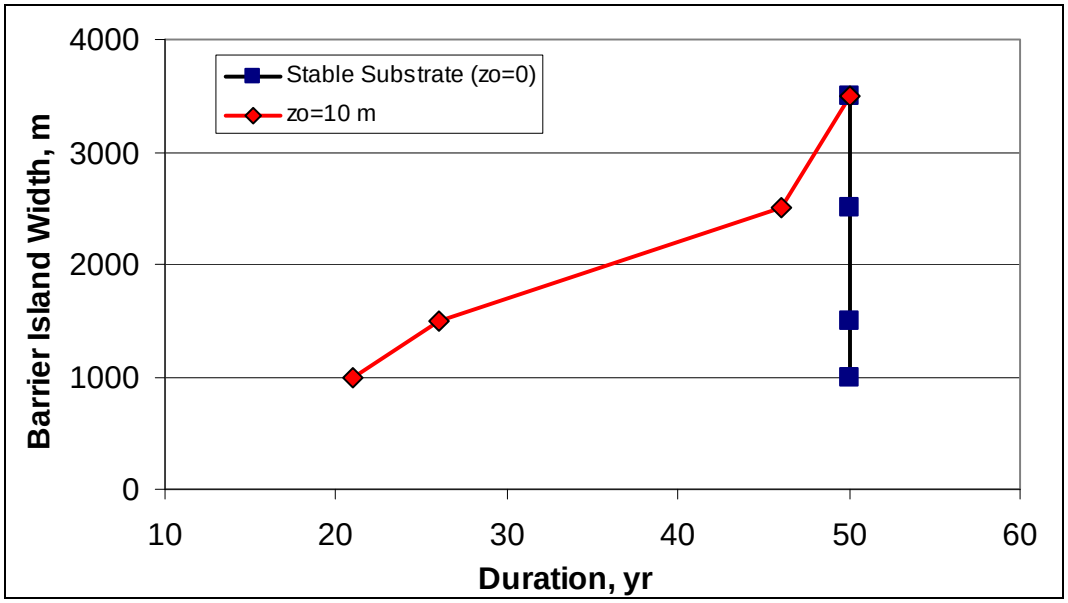

Figure 61. Influence of barrier island width on duration for BIC and BIS.

Hypothesis 3

Overview

The final hypothesis is: "To preserve barrier islands that overlie a compressible substrate, it is best to initially infuse a large volume of sand from an external source, rather than smaller quantities that are placed incrementally in time." Two restoration options were investigated to test this hypothesis. The restoration alternatives vary in the volume of initial placement and whether the island is replenished in subsequent years. The traditional method of beach fill design, termed the "Incremental" placement method here, represents large nourishment volume densities in the United States, of the order 250 m^3/m (Dean 2002, p. 23). These traditional nourishment projects are replenished on 2-, 5-, or 10-year intervals, or if the beach is severely eroded. The other method considered herein is a large-scale infusion of sand from an external source, on the order of 10 times the typical fill density, or 2,500 m^3/m, as the initial placement with little or no replenishment in subsequent years. This type of design is called the "Initial" placement method in the following sections. The Initial method has the advantage of only one cost for mobilization, construction, and demobilization. Disadvantages include a large initial cost and not having a scheduled renourishment that could be accelerated to repair an eroded island following a severe storm.

Thirty-three simulations were conducted with 2D MCO to evaluate the morphologic response as a function of volume of total beach nourishment

placed and substrate characteristics. All simulations were set to run for 99 years, but the simulations were terminated if the barrier island eroded below MSL. Incremental fills were placed at 10-year intervals, beginning at year 10; Initial fills were placed at year 10. All simulations were allowed to evolve over the first 10-year period to begin adjustment to the prevailing wave, surge, and substrate characteristics.

Four types of substrates were considered: a non-consolidating substrate, and three types of consolidating substrate characterized by the thicknesses of compressible sediments z_o = 10, 15, and 20 m. For the compressible substrate, values of $c_{v0} = c_{vc}$ =2.5 m^2/year and Casagrande test values for Chaland Headland (Figure 18) were applied (as in the comparison with the Virginia barrier island data). The initial dune crest elevations were 4 m, with 2,500 m width, and storm surge and wave height magnitudes averaged 1 m each. Beach nourishment volumes ranged from slightly lower than the typical fill density to greater than 10 times the typical density for the 99-year simulation period. The beach fill was uniformly distributed over the barrier island profile. Results of the simulations are shown in Table 17.

Table 17. Incremental method versus initial method of beach fill restoration – Hypothesis 3, application of 2D MCO.

Input Parameters						Calculations									
ID	H_{bar}, m	W_{bar}, m	dH, m	T_{pl}, yr	z_o, m ("a")	Mig, m	H_{bar_f} m	Vol_c, m^3	WL_{avg}, m	Vol_{er}, $m^3/m/yr$	Vol_{ow}, $m^3/m/yr$	Vol_{in}, $m^3/m/yr$	z_{max}, m	T_{max}, yr	Vol_ Fill, m^3/m
Analyses 11-14: Incremental Method, H_{mo} = S = 1 m, 10 yr adjustment prior to fill, fill every 10 years, 99 year duration															
Analysis 11: No consolidation															
11a	4	2500	0.01	10x9	0	526	2.45	0	1.87	15.3	0.0117	0	0	99	363
11b	4	2500	0.05	10x9	0	566	2.71	0	1.88	17.5	0	0	0	99	1778
11c	4	2500	0.075	10x9	0	544	2.99	0	1.81	18.8	0	0	0	99	2700
Analysis 12: z_o = 10 m															
12a	4	2500	0.01	10x4	10	3274	0.46	3901	2.03	8.3	0.065	81.4	0.87	46*	119
12b	4	2500	0.05	10x5	10	5873	0.31	5047	2.03	7.5	0.02	99	0.88	60*	818
12c	4	2500	0.075	10x8	10	7282	0.26	6159	1.98	6.31	0.044	86.1	0.89	83*	2400
12d	4	2500	0.085	10x9	10	1654	1.57	4707	1.99	5.72	0.0355	31.9	0.9	99	t3105
Analysis 13: z_o = 15 m															
13a	4	2500	0.01	10x3	15	2708	0.17	4762	1.9	8.17	0.042	91.4	1.24	30*	32
13b	4	2500	0.05	10x3	15	2269	0.38	4767	1.89	7.82	0	77.6	1.26	33*	435
13c	4	2500	0.2	10x3	15	2827	0.14	5203	1.98	7.71	0	81.2	1.3	36*	534
13d	4	2500	0.075	10x4	15	2742	0.21	5404	1.8	7.25	0	72.8	1.35	41*	886
13e	4	2500	0.1	10x4	15	2868	0.29	5574	1.8	7.21	0.017	75.1	1.37	43*	1217
13f	4	2500	0.12	10x4	15	2531	0.47	5978	1.82	6.39	0.0377	62.2	1.4	50*	1500
13g	4	2500	0.17	10x5	15	3813	0.42	7176	1.95	5.42	0.0023	75.2	1.46	60*	2852

(Continued)

Table 17. Incremental method versus initial method of beach fill restoration – Hypothesis 3, application of 2D MCO (Continued).

Input Parameters						Calculations									
ID	H_{bar}, m	W_{bar}, m	dH, m	T_{pl}, yr	z_o, m ("a")	Mig, m	H_{bar_f} m	Vol_c, m^3	WL_{avg}, m	Vol_{er}, $m^3/m/yr$	Vol_{ow}, $m^3/m/yr$	Vol_{in}, $m^3/m/yr$	z_{max}, m	T_{max}, yr	Vol_ Fill, m^3/m
Analyses 11-14: Incremental Method, H_{mo} = S = 1 m, 10 yr adjustment prior to fill, fill every 10 years, 99 year duration															
Analysis 14: z_o = 20 m															
14a	4	2500	0.05	10x2	20	1903	0.001	5274	1.93	6.34	0.044	83.3	1.47	23*	200
14b	4	2500	0.2	10x3	20	2271	0.24	6425	1.86	5.03	0.067	75.8	1.66	35*	1800
14c	4	2500	0.25	10x4	20	2465	0.25	7399	1.79	5.3	0	72.2	1.77	43*	3121
Analyses 15-18: Initial Fill, H_{mo} = S = 1 m, 10 yr adjustment prior to fill, 99 year duration															
Analysis 15: No consolidation															
15a	4	2500	0.25	10x1	0	562	2.51	0	1.92	16.8	0.0087	0	0	99	177
15b	4	2500	0.5	10x1	0	606	2.58	0	2.04	20.1	0	0	0	99	1365
15c	4	2500	1	10x1	0	663	2.94	0	2.08	27.5	0	0	0	99	2848
Analysis 16: z_o = 10 m															
16a	4	2500	0.1	10x1	10	3228	0.5	4089	2	7.92	0.01	70.5	0.87	54*	268
16b	4	2500	0.25	10x1	10	4270	0.45	4329	1.95	9.24	0	81.4	0.89	58*	678
16c	4	2500	0.5	10x1	10	5265	0.42	4945	2.1	0.65	0.062	85.7	0.9	67*	1391
16d	4	2500	1	10x1	10	2115	1.19	4853	2	11.2	0.0022	38	0.95	99	2833
Analysis 17: z_o = 15 m															
17a	4	2500	0.1	10x1	15	2091	0.3	4851	1.86	6.86	0.013	59.6	1.3	38*	265
17b	4	2500	0.2	10x1	15	2112	0.31	4862	2.01	8.88	0	82	1.26	33*	550
17c	4	2500	0.5	10x1	15	2066	0.3	5585	1.85	9.23	0	49.5	1.4	47*	1410
17d	4	2500	1	10x1	15	3073	0.2	7015	1.97	9.86	0.011	58.2	1.51	63*	2787

(Continued)

Table 17. Incremental method versus initial method of beach fill restoration – Hypothesis 3, application of 2D MCO (Concluded).

Input Parameters						Calculations									
ID	H_{bar}, m	W_{bar}, m	dH, m	T_{pl}, yr	z_o, m ("a")	Mig, m	H_{bar_f} m	Vol_c, m^3	WL_{avg}, m	Vol_{er}, $m^3/m/yr$	Vol_{ow}, $m^3/m/yr$	Vol_{in}, $m^3/m/yr$	z_{max}, m	T_{max}, yr	Vol_ Fill, m^3/m
Analyses 15-18: Initial Fill, H_{mo} = S = 1 m, 10 yr adjustment prior to fill, 99 year duration															
Analysis 18: z_o = 20 m															
18a	4	2500	0.1	10x1	20	1664	0.15	5082	1.98	5.68	0.07	74.8	1.47	23*	263
18b	4	2500	0.2	10x1	20	1740	0.16	5399	1.94	6.24	0.096	83.1	1.5	24*	546
18c	4	2500	0.25	10x1	20	2020	0.003	6268	2.01	5.58	0.02	60.7	1.65	33*	1387
18d	4	2500	0.75	10x1	20	1748	0.2	6584	1.88	6.8	0.01	44.2	1.8	43*	2000
18e	4	2500	1	10x1	20	1772	0.48	6950	1.86	7.94	0.0051	49.7	1.86	47*	2718

[1]All simulations conducted with ambient non-storm depth, d_a = 0.5 m (d_a = ambient depth), SL = rate of eustatic sea level change = 0, $\eta_{a\ a}$ = tidal amplitude = 0.

Definition of Terminology:

H_{mo} = average deep-water storm wave height, S = average storm surge, H_{bar} = initial barrier height, W_{bar} = initial barrier width at base, dH = initial or incremental elevation of beach fill placed over active profile, T_{pl} = years between placement intervals x number of placements, z_o = thickness of actively consolidating sediment ("a" indicates $c_{v0} = c_{vc}$ = 2.5 m^2/yr (Virginia data)), Mig = total migration of dune crest, H_{bar_f} = final barrier height, Vol_c = volume consolidated, WL_{avg} = average storm water elevation, Vol_{er} = volume eroded, Vol_{ow} = volume runup overwash, z_{max} = maximum consolidation thickness at end of simulation, T_{max} = duration of simulation, Vol_Fill = total volume of fill placed during each simulation.

* = Barrier island below MSL; simulation terminated.

Metrics to test this hypothesis are as follows:

3a. For BIC, the minimum volume to provide a defined level of protection (e.g., 20 year, 50 year) is less with the Initial Method of beach nourishment as compared to the Incremental Method.

3b. The Initial Method of placement provides more stability for BIC as compared to the Incremental Method of beach restoration. Stability of the island as evaluated here is defined in terms of a reduction in cross-shore migration rate, consolidation rate, and lowering of the maximum dune elevation (due to consolidation, erosion, and overwash processes).

3c. For the same lifetime, the total cost for an Initial restoration is less than the total cost of an Incremental restoration.

Analysis

Metric 3a

Metric 3a tests whether the Initial Method of fill placement provides more protection, through increased lifetime of the island, as compared to Incremental Method of placement. Figure 62 compares duration of the simulation for each type of fill and substrate evaluated. The non-consolidating substrate runs all completed the 99-year simulation duration, whereas all but one (2,650 m^3/m fill, z_o = 10 m) of the other simulations terminated prior to the 99-year duration. As expected, larger fill volumes increased the feasible lifetime for a simulation, regardless of the thickness of the consolidating substrate. However, there is no discernable trend for whether the Incremental Method or Initial Method provides longer duration; for the z_o = 15 m case, the Incremental Method results in slightly longer duration, whereas for the z_o = 20 m case, the Initial Method provides a longer simulation for larger fill volumes. As discussed in Chapter 4, data from Kulp et al. (2002, their Figure 7) indicated that z_o is a maximum of approximately 120 m in vicinity of the modern Mississippi River depocenter, and ranges from approximately 10 to 30 m in vicinity of the modern barrier islands. Thus, the values of z_o evaluated herein are likely representative of conditions in Louisiana. For many simulations, the two types of placement methods are similar in terms of longevity. Thus, Metric 3a does not hold true: both the Initial and Incremental Methods result in similar longevity for barrier islands regardless of substrate conditions.

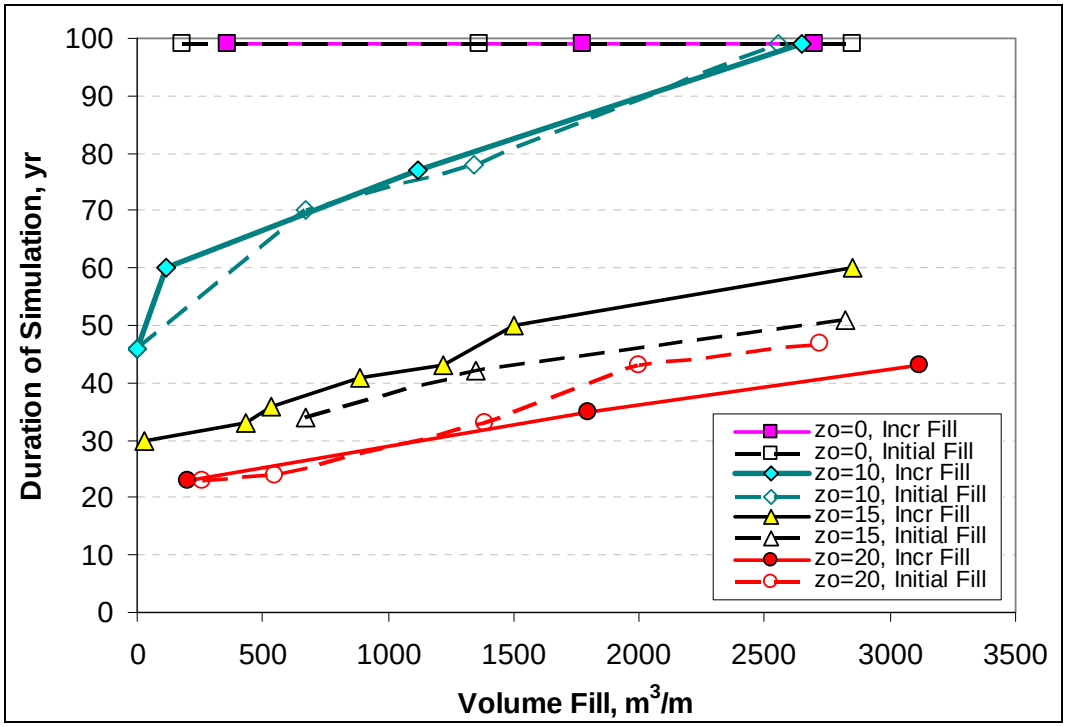

Figure 62. Duration of simulation as function of fill volumes, for incremental and initial methods of fill placement and various substrate characteristics.

Metric 3b

Metric 3b tests whether BICs are more stable with the Initial Method of fill placement as compared to the Incremental Method. Stability is evaluated in terms of the rate of cross-shore migration, consolidation, and dune lowering (due to consolidation, erosion, and overwash processes) as a function of the type of fill placement.

Figure 63 illustrates the difference in migration rates for the three different types of substrate as compared to a non-consolidating substrate, for total beach fill volumes ranging from near-zero to approximately 3,000 m^3/m. Note that, if Incremental fill simulations terminated because the barrier island was below MSL, then the fill volume only represents the quantity placed prior to termination.

The first observation from these simulations is that there is no difference in migration rates for the two methods of fill placement for a non-consolidating substrate. The migration rates for the two methods are similar and represent initial adjustment of the fill as indicated by the lack of runup and inundation overwash during the simulations (Table 12). The second observation is that, for different substrates, migration rates decrease for the Initial Method as compared to Incremental Method. The

decrease in migration rates ranges from approximately 5 to 20 m/year for the Initial fill placement method.

Figure 64 shows the consolidation rate for the various fill types, quantities, and substrate characteristics. As expected, an increase in the thickness of the compressible substrate, z_o, increases the rate of consolidation. However, two other observations are counter-intuitive at initial inspection, but can be understood if the migration process is considered. First, an increase in fill volume decreases the rate of consolidation, whereas it would be expected that larger volumes of beach fill would load the substrate and cause more consolidation. The decreasing trend is related to the decrease in migration with the larger fill volumes. As the island becomes more stable with larger fill volumes, the loading of bay sediments with washover sand is reduced and the magnitude of consolidation decreases. The second observation is that the Incremental Method results in slightly more consolidation than the Initial Method, also because of the migration process and new loading of the bay substrate.

Figure 65 shows the rate of dune lowering, representative of erosion, overwash, and consolidation, as a function of the fill volume and type of substrate. In general, the rate of dune lowering is similar for both placement methods, for all types of substrate. The difference between dune erosion for the Incremental and Initial Methods is greater for the largest z_o = 20 m, and larger fill volumes. This result is related to the migration and consolidation processes as described previously.

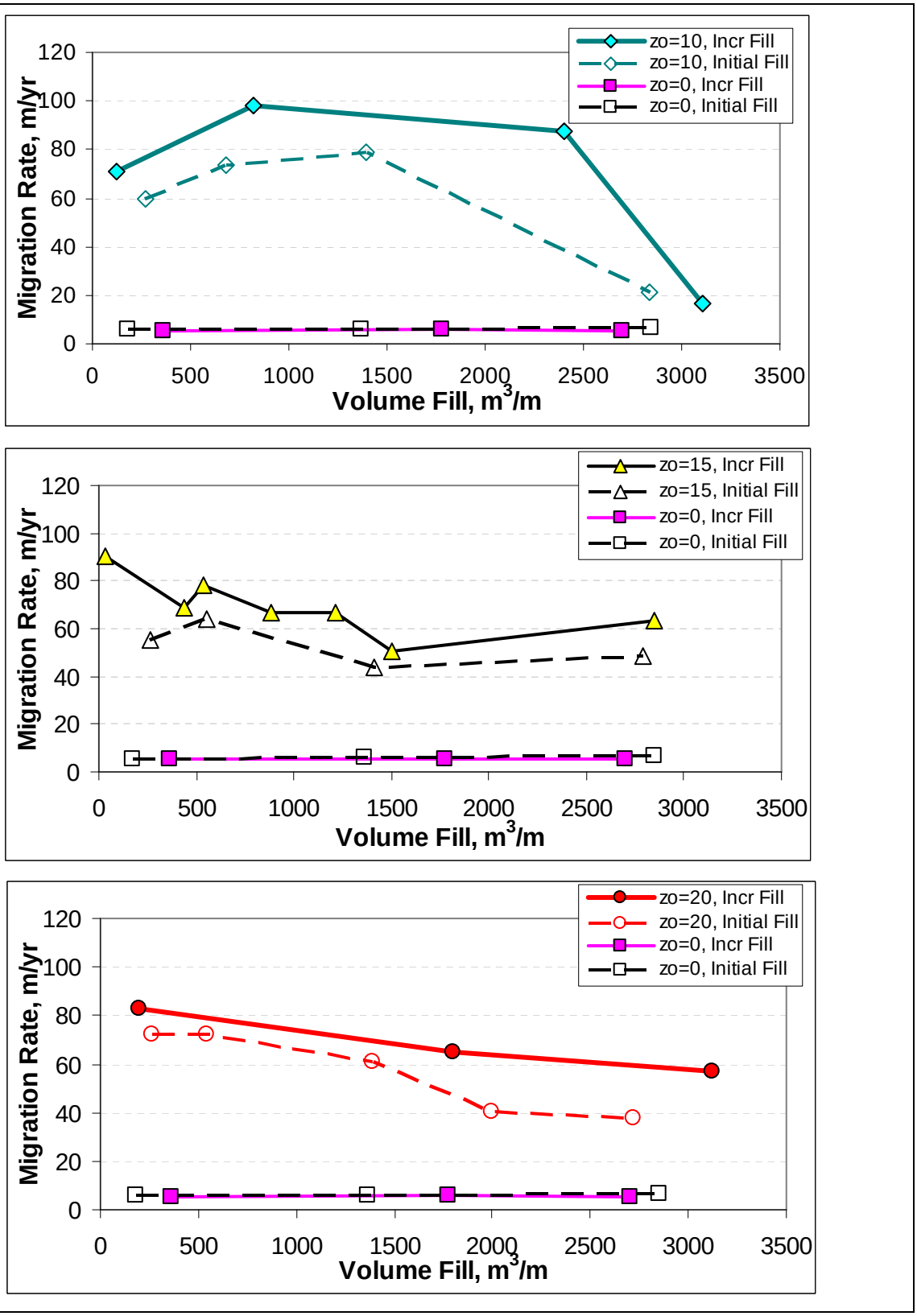

Figure 63. Migration rates as function of fill volumes, for incremental and initial methods of fill placement and various substrate characteristics.

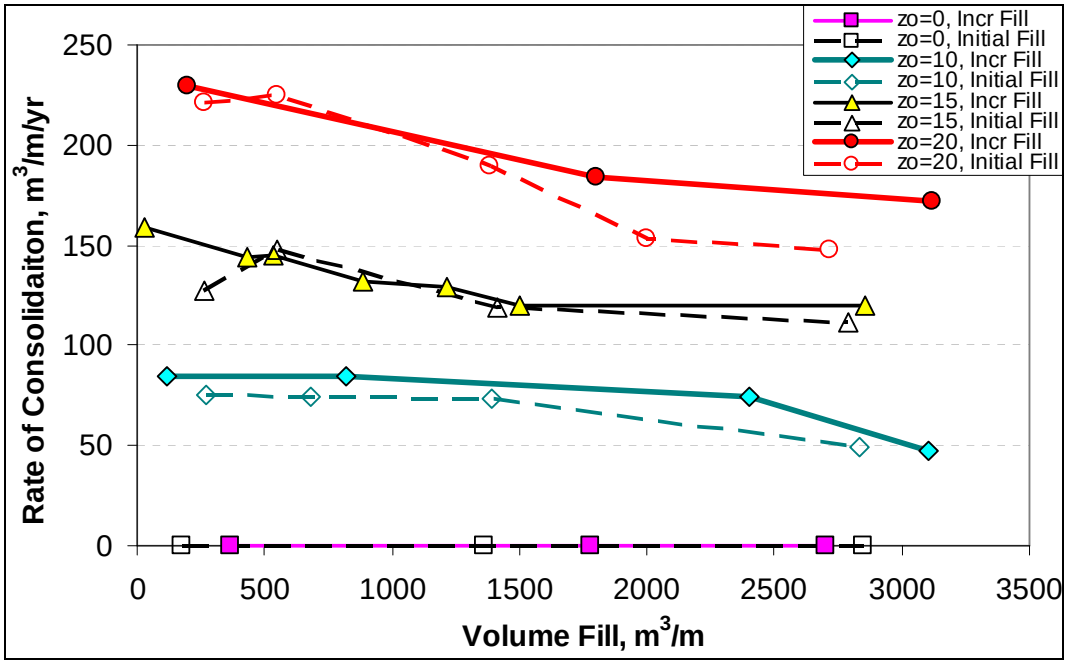

Figure 64. Consolidation rates as function of fill volumes, for incremental and initial methods of fill placement and various substrate characteristics.

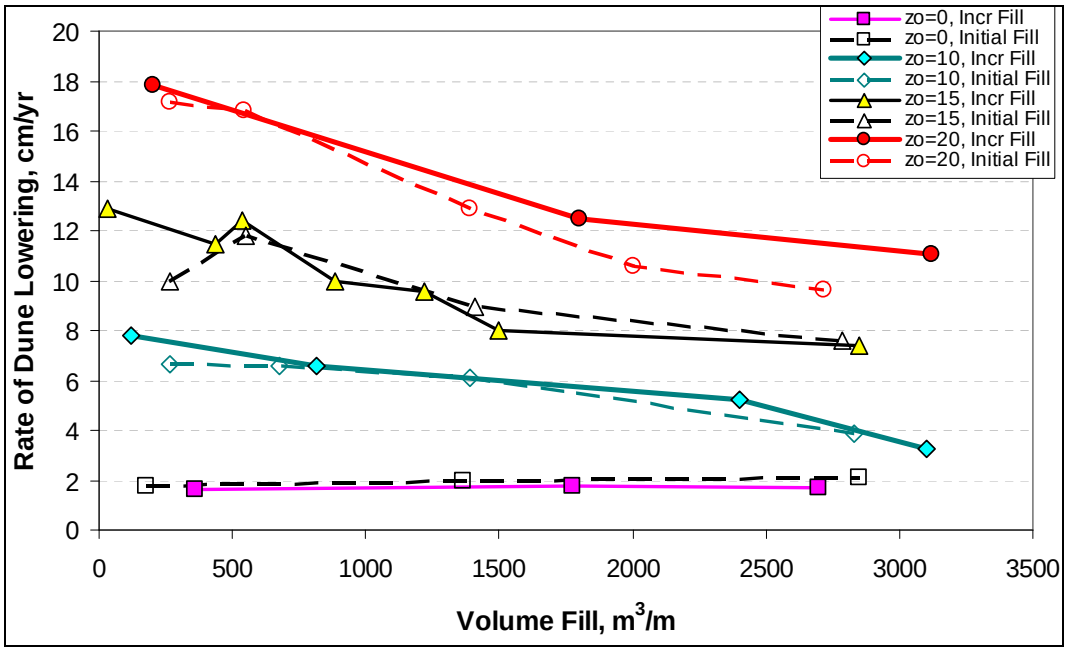

Figure 65. Rate of dune lowering (due to consolidation, erosion, and overwash processes) as function of fill volumes, for incremental and initial methods of fill placement and various substrate characteristics.

Summarizing Metric 3b tests for migration, consolidation, and dune lowering results in the following observations:

1. For a non-consolidating substrate, there was no discernable difference in migration, duration of the simulation, or rate of dune lowering between the two methods of placement.
2. For a consolidating substrate, migration rates decreased for the Initial Method as compared to Incremental Method, with a decrease in migration rates ranging from approximately 5 to 20 m/year. As a result of the decrease in migration rates, both the rates of consolidation and dune lowering were reduced for some Initial placement simulations as compared to similar values of Incremental fills. The reason for this is that greater migration rates result in washover sand that loads a previously non-loaded substrate, and thus more barrier island sand is sequestered through the consolidation process.

Thus, Metric 3b is valid as follows: as compared to the Incremental Method, the Initial Method decreased the cross-shore migration rate and consolidation rate for barrier islands overlying a compressible substrate. The Initial Method also decreased the rate of dune lowering (due to consolidation, erosion, and overwash) as compared to the Incremental Method for large thicknesses of compressible substrates and large fill volumes. Overall, considering cross-shore processes, the Initial Method reduces the subsequent migration of the island, which also reduces the new loading of bay sediment and sequestration of barrier island sand through consolidation. The reduction in the migration and consolidation processes for the Initial Method result increased stability or longevity of the island as compared to the Incremental Method of placement.

Metric 3c

Metric 3c compares the cost of Initial and Incremental restoration strategies, asserting that Initial placement cost less overall than Incremental restoration. To evaluate this metric, information from Coastal Planning and Engineering, Inc. (CP&E) (Thomson 2008) based on beach restoration projects in Louisiana was applied. CP&E constructed the Chaland Headland restoration project in Louisiana in 2006, and they have constructed and bid on many other projects in Louisiana and around the United States. Thus, their experience in estimating costs is pertinent to and reliable for evaluation of Metric 3c.

Table 18 shows total mobilization and demobilization and unit costs estimated by CP&E for a typical barrier island restoration project to be constructed in 2009 (Thomson 2008). These unit costs for pumping sand to the beach represent the lowest cost alternative; the unit cost for more

distant borrow sites evaluated by CP&E for a similar project ranged from \$19 to \$69/yd^3 (\$25 to \$90/m^3).

Table 18. Approximate costs for barrier island restoration projects in Louisiana (Thomson 2008)*.

Activity	Cost
Mobilization/Demobilization	\$3-\$4 Million
Pumping Sand to Beach	\$6-\$7/yd^3 (\$8-\$9/m^3)

* Assuming 4-6 miles (6.4-9.6 km) from borrow site to project and 7-ft (2.1-m) thickness of cut with cutterhead dredge.

To evaluate Metric 3c, costs listed in Table 18 were applied to a subset of simulations listed in Table 17 to compare Incremental and Initial restoration costs for simulations with similar durations. Based on these simulations, Incremental restoration would occur at 10-year intervals over multiple decades. To compare the total cost between Incremental and Initial nourishment projects, the costs incurred for future Incremental restoration projects were adjusted to present-day values. Two estimates were used in making these adjustments. First, the average inflation rate for a decadal period (the interval between each incremental renourishment) was calculated based on historical U.S. inflation from 1918 through 2008 (Financial Trend Forecasters 2008), and omitting the lowest and highest values. These calculations are shown in Table 19.

To calculate the cost associated with future Incremental nourishment, the average decadal inflation rate was applied,

$$FV\left(t(n)\right) = PV\left(t(n-1)\right)\left(1+Infl\right) \tag{56}$$

where FV is the future value at time t accounting for inflation, n is the number of the Incremental renourishment, PV is the previous value of the Incremental nourishment, and $Infl$ is the decadal rate of inflation. All future values were adjusted to a present-day (2009) equivalent value using an interest rate, ir = 5.75 percent/year as follows (Thomson 2008),

$$V(2009) = \frac{FV\left(t(n)\right)^{\left(t(n)-2009\right)}}{\left(1+ir\right)} \tag{57}$$

Table 19. Calculation of decadal-rate of inflation (Financial Trend Forecasters 2008).

Start Year	End Year	Average % Inflation Rate (for that decade)	
1998	2008	30.62	
1988	1998	39.67	
1978	1988	85.12	
1968	1978	83.82	
1958	1968	19.23	
1948	1958	20.68	
1938	1948	66.9	
1928	1938	-17.92 (deflation)	
1918	1928	23.57	
		All Data	Omitting Outliers
Average		39.08	40.64
Standard Deviation		33.89	25.18

in which V is the value evaluated in 2009, and time is in years. Then the total value of Incremental renourishment projects in 2009 dollars was calculated by summing up all renourishment costs. Pertinent information from these simulations is reproduced in Table 20 along with cost estimates, and Figure 66 shows the results graphically. Data in Table 20 correspond to average values shown in Figure 66a.

Table 20. Comparison of incremental and initial fill simulations: Total cost in 2009 dollars.

Type	ID	Vol Fill m3/m	No. Fill	Vol Fill Each Pl., m³/m	Date of Renourishment Project																						TOTAL $ Mill (2009)
					2009 Initial Mob	Demob	Sand	2019 Ren. #1 Mob	Demob	Sand	2029 Ren. #2 Mob	Demob	Sand	2039 Ren. #3 Mob	Demob	Sand	2049 Ren. #4 Mob	Demob	Sand	2059 Ren. #5 Mob	Demob	Sand	2069 Ren. #6 Mob	Demob	Sand	2079 Ren. #7 Mob	Demob	Sand	2089 Ren. #8 Mob	Demob	Sand	2099 Ren. #9 Mob	Demob	Sand	
z_o = 15 m; Duration 60 yr (Inc), 63 yr (Ini)																																	
Inc	13g	2852	5	570.4	3.5	38.8		4.9	54.5		6.9	76.7		9.7	107.8		13.7	1516		19.2	213.1		0	0		0	0		0	0		0	0		
2009 Value, $ Mill					3.5	38.8		2.8	31.2		2.3	25.1		1.8	20.2		1.5	16.2		1.2	13.0		0	0		0	0		0	0		0	0		157.4
Ini	17d	2787	1	2787	3.5	189.5		0	0		0	0		0	0		0	0		0	0		0	0		0	0		0	0		0	0		
2009 Value, $ Mill					3.5	189.5		0	0		0	0		0	0		0	0		0	0		0	0		0	0		0	0		0	0		193.0
zo = 20 m; Duration 23 yr (Inc), 23 yr (Ini-1), 24 yr (Ini-2)																																	
Inc	14a	3105	9	345	3.5	23.5		4.9	33.0		6.9	46.4		9.7	65.2		13.7	91.7		19.2	128.9		27.0	181.2		38.0	254.8		53.5	358.3		75.2	503.7		
2009 Value, $ Mill					3.5	23.5		2.8	18.9		2.3	15.2		1.8	12.2		1.5	9.8		1.2	7.9		0.94	6.3		0.76	5.1		0.61	4.1		0.49	3.3		122.0
Ini	16d	2833	1	2833	3.5	192.6		0	0		0	0		0	0		0	0		0	0		0	0		0	0		0	0		0	0		
2009 Value, $ Mill					3.5	192.6		0	0		0	0		0	0		0	0		0	0		0	0		0	0		0	0		0	0		196.1
z_o = 15 m; Duration 33 yr (Inc), 33 yr (Ini)																																	
Inc	13b	435	3	145	3.5	9.9		4.9	13.9		6.9	19.5		9.7	27.4		0	0		0	0		0	0		0	0		0	0		0	0		
2009 Value, $ Mill					3.5	9.9		2.8	7.9		2.3	6.4		1.8	5.1		0	0		0	0		0	0		0	0		0	0		0	0		39.7
Ini	17b	550	1	550	3.5	37.4		0	0		0	0		0	0		0	0		0	0		0	0		0	0		0	0		0	0		
2009 Value, $ Mill					3.5	37.4		0	0		0	0		0	0		0	0		0	0		0	0		0	0		0	0		0	0		40.9
z_o = 15 m; Duration 36 yr (Inc), 38 yr (Ini)																																	
Inc	13c	534	3	178	3.5	12.1		4.9	17.0		6.9	23.9		9.7	33.6		0	0		0	0		0	0		0	0		0	0		0	0		
2009 Value, $ Mill					3.5	12.1		2.8	9.7		2.3	7.8		1.8	6.3		0	0		0	0		0	0		0	0		0	0		0	0		46.3
Ini	17a	265	1	265	3.5	18.0		0	0		0	0		0	0		0	0		0	0		0	0		0	0		0	0		0	0		
					3.5	18.0		0	0		0	0		0	0		0	0		0	0		0	0		0	0		0	0		0	0		21.5
z_o = 15 m; Duration 50 yr (Inc), 47 yr (Ini)																																	
Inc	13f	1500	4	375	3.5	25.5		4.9	35.9		6.9	50.4		9.7	70.9		13.7	99.7		0	0		0	0		0	0		0	0		0	0		
2009 Value, $ Mill					3.5	25.5		2.8	20.5		2.26	16.5		1.8	13.3		1.5	10.7		0	0		0	0		0	0		0	0		0	0		98.2
Ini	17c	1410	1	1410	3.5	95.9		0	0		0	0		0	0		0	0		0	0		0	0		0	0		0	0		0	0		
2009 Value, $ Mill					3.5	95.9		0	0		0	0		0	0		0	0		0	0		0	0		0	0		0	0		0	0		99.4

(Continued)

Table 20. Comparison of Incremental and Initial Fill Simulations: Total Cost in 2009 Dollars (Concluded).

					Date of Renourishment Project																						
					2009		2019		2029		2039		2049		2059		2069		2079		2089		2099			
		Vol Fill	No.	Vol Fill Each Pl.,	Initial		Ren. #1		Ren. #2		Ren. #3		Ren. #4		Ren. #5		Ren. #6		Ren. #7		Ren. #8		Ren. #9		TOTAL	
Type	ID	m3/m	Fill	m³/m	Mob Demob	Sand	Mob Demob	Sand	Mob Demob	Sand	Mob Demob	Sand	Mob Demob	Sand	Mob Demob	Sand	Mob Demob	Sand	Mob Demob	Sand	Mob Demcb	Sand	Mob Demob	Sand	$ Mill (2009)	
z_o = 15 m; Duration 60 yr (Inc), 63 yr (Ini)																										
Inc	13g	2852	5	570.4	3.5	38.8	4.9	54.5	6.9	76.7	9.7	107.8	13.7	151.6	19.2	213.1	0	0	0	0	0	0	0	0		
2009 Value, $ Mill					3.5	38.8	2.8	31.2	2.3	25.1	1.8	20.2	1.5	16.2	1.2	13.0	0	0	0	0	0	0	0	0	157.4	
Ini	17d	2787	1	2787	3.5	189.5	0	0	0	0	0	0	0	0	0	0	0	0	0	0	0	0	0	0		
2009 Value, $ Mill					3.5	189.5	0	0	0	0	0	0	0	0	0	0	0	0	0	0	0	0	0	0	193.0	
zo = 20 m; Duration 23 yr (Inc), 23 yr (Ini-1), 24 yr (Ini-2)																										
Inc	14a	200	2	100	3.5	6.8	4.9	9.6	6.9	13.4	0	0	0	0	0	0	0	0	0	0	0	0	0	0		
2009 Value, $ Mill					3.5	6.8	2.8	5.5	2.3	4.4	0	0	0	0	0	0	0	0	0	0	0	0	0	0	25.2	
Ini-1	18a	263	1	263	3.5	17.9	0	0	0	0	0	0	0	0	0	0	0	0	0	0	0	0	0	0		
2009 Value, $ Mill					3.5	17.9	0	0	0	0	0	0	0	0	0	0	0	0	0	0	0	0	0	0	21.4	
Ini-2	18b	546	1	546	3.5	37.1	0	0	0	0	0	0	0	0	0	0	0	0	0	0	0	0	0	0		
2009 Value, $ Mill					3.5	37.1	0	0	0	0	0	0	0	0	0	0	0	0	0	0	0	0	0	0	40.6	
z_o = 20 m; Duration 35 yr (Inc), 33 yr (Ini)																										
Inc	14b	1800	3	600	3.5	40.8	4.9	57.4	6.9	80.7	9.7	113.4	0	0	0	0	0	0	0	0	0	0	0	0		
2009 Value, $ Mill					3.5	40.8	2.8	32.8	2.3	26.4	1.8	21.2	0	0	0	0	0	0	0	0	0	0	0	0	131.6	
Ini	18c	1387	1	1387	3.5	94.3	0	0	0	0	0	0	0	0	0	0	0	0	0	0	0	0	0	0		
2009 Value, $ Mill					3.5	94.3	0	0	0	0	0	0	0	0	0	0	0	0	0	0	0	0	0	0	97.8	
z_o = 20 m; Duration 43 yr (Inc), 43 yr (Ini)																										
Inc	14c	3121	4	780.25	3.5	53.1	4.9	74.6	6.9	104.9	9.7	147.5	13.7	207.3	0	0	0	0	0	0	0	0	0	0		
2009 Value, $ Mill					3.5	53.1	2.8	42.7	2.3	34.3	1.8	27.6	1.5	22.2	0	0	0	0	0	0	0	0	0	0	191.6	
Ini	18d	2000	1	2000	3.5	136.0	0	0	0	0	0	0	0	0	0	0	0	0	0	0	0	0	0	0		
2009 Value, $ Mill					3.5	136.0	0	0	0	0	0	0	0	0	0	0	0	0	0	0	0	0	0	0	139.5	

* Calculated with decadal-scale inflation rate *Infl* = 40.6% and interest rate *ir* = 5.75%, for 8-km length barrier island restoration, $8.50/m³ sand.

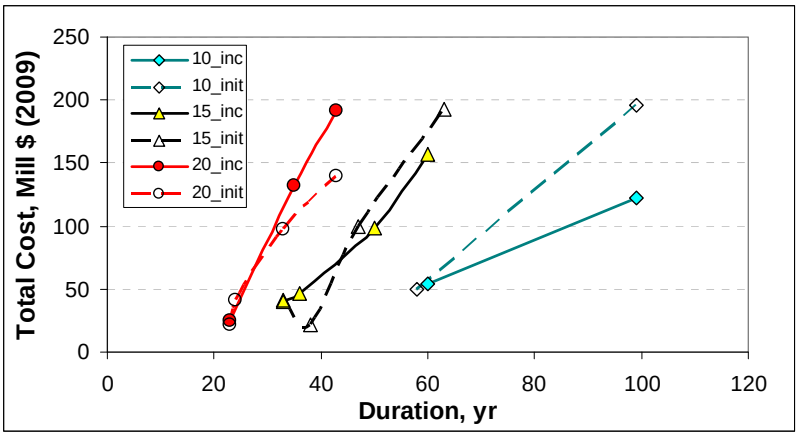

a. *Infl* = 40.6 percent (average) and *ir* = 5.75 percent.

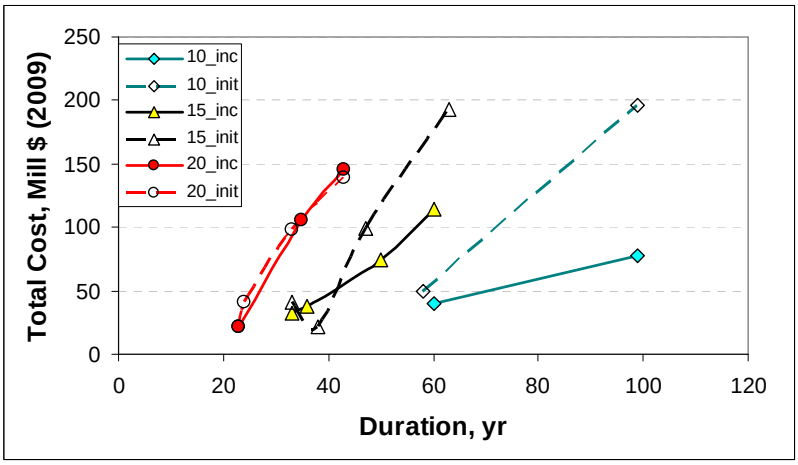

b. *Infl* = 15.5 percent (average minus one standard deviation) and *ir* = 5.75 percent.

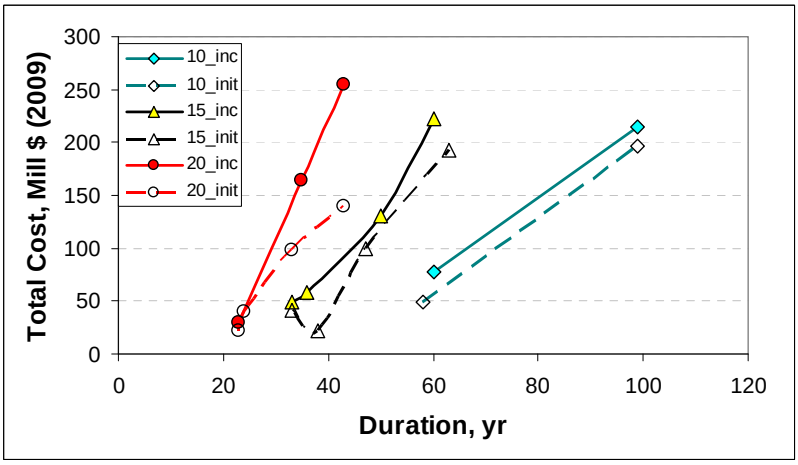

c. *Infl* = 65.8 percent (average plus one standard deviation) and *ir* = 5.75 percent.

Figure 66. Comparison of total cost for incremental and initial barrier island restoration projects, for various substrate conditions.

Implications for functional restoration in deltaic environments

Functional restoration is defined as the minimum beach nourishment volume and cross-sectional dimensions (elevation and width) such that a barrier island can perform as a wave break, storm surge buffer, and ocean boundary for an estuary, bay, and mainland over the project lifetime. Following this definition, a restored barrier island could migrate alongshore and cross-shore, and possibly overwash to some extent as long as it maintained functionality. As discussed in Chapter 2, overwash can be desirable from an ecological perspective, because it provides habitat for species that require fresh, unvegetated sand. However, extensive overwash can make the island vulnerable to future breaching and inlet formation, which inhibits functionality. Uninhabited islands with limited infrastructure such as nearly all the islands in Louisiana (except Grand Isle), most of the Mississippi Sound Islands (Petit Bois, Horn, East and West Ship Islands, Mississippi), and northern Assateague Island, Maryland, are examples of islands that function to protect an estuary and mainland coast, but which are allowed to migrate alongshore or cross-shore.

As discussed in Chapter 3, Campbell (2005) introduced the concepts of "stable design" and "retreat design" for coastal restoration of barrier islands in Louisiana. Campbell defined a stable design as one that maintained the barrier island in a geographic location by eliminating frequent overwash and breaching. Retreat design allowed the island to migrate, but maintained a constant island area. The difference between these two types of projects entered into the design of the dune crest elevation and percentage of fine sediment in the restoration volume. These two types of designs embody the concept of functional restoration.

The research discussed herein indicates that an initial large-scale infusion of sediment from an external source to stabilize the island is the most efficient type of functional restoration for deltaic and compressible substrates. A design to stabilize the island will minimize overwash and migration, thus reducing losses to the island sand budget that are incurred due to consolidation of the substrate. Barrier islands overlying a compressible substrate incur an additional volumetric loss due to the consolidation process as a function of the magnitude of loading applied to the substrate and duration of the loading. Because of this process, islands that migrate and overwash incur an additional loss due to consolidation, as compared to islands that are stable. The Initial Method of restoration provides volume sufficient to limit the migration process and is more effective at stabilizing an island as compared to the Incremental Method.

To best achieve a stable barrier island with ecological benefits, a design such as introduced in Chapter 2 (Figure 5b) and expanded below in Figures 67 and 68 would be most effective. This restoration includes careful design of vegetation which is planted at the time of initial construction to provide some stability prior to natural succession of native species. The conceptual design of the large-scale stable restoration has sufficient dimensions (width, elevation, and length) such that overwash of the island is rare and breaching does not occur in the central section during the project lifetime. The island width is great enough such that, if overwash occurs for an extreme storm, the washover sand is captured within the back-barrier marsh and maintained within the subaerial volume of the island. Ecological benefits such as washover deposits are realized in the spit features on the termini of the island. Primary and secondary dunes are of sufficient elevation to limit overwash during the majority of storms and provide a source of sand such that the underlying fine-grained sediment is not exposed during the project lifetime. Two rows of sand fences and native vegetation planted immediately after construction provide a means to capture eolian sand and reduce sub-aerial losses from the island. The island cross-section design would consider all coastal and meteorological forcing as well as the time-dependent consolidation of the substrate that is induced by additional loading and existing island weight over the project lifetime.

As discussed in Chapter 2 and shown in Figures 40, 67, and 68, some barrier islands in deltaic settings have a cross-section of mixed sediment, such as sand beach that overlays cohesive sediment which extends into a back marsh and bayshore. Stable restoration of deltaic barrier islands could mimic this natural setting with a cross-section of mixed sediment (Figure 68). This type of design could be achieved with a silt-clay mixture pumped from an external source to form the island core. Construction procedures to speed the dewatering and consolidation of the core could be employed prior to placement of sand over the surface, which would then provide a protective layer for the core. The sand layer should be of sufficient thickness so the core is not exposed during storms. This type of design would reduce the quantity of sand required for restoration, which can be of limited supply in deltaic settings. The fine sediment could extend into the back barrier to create a marsh area on the bayside of the island.

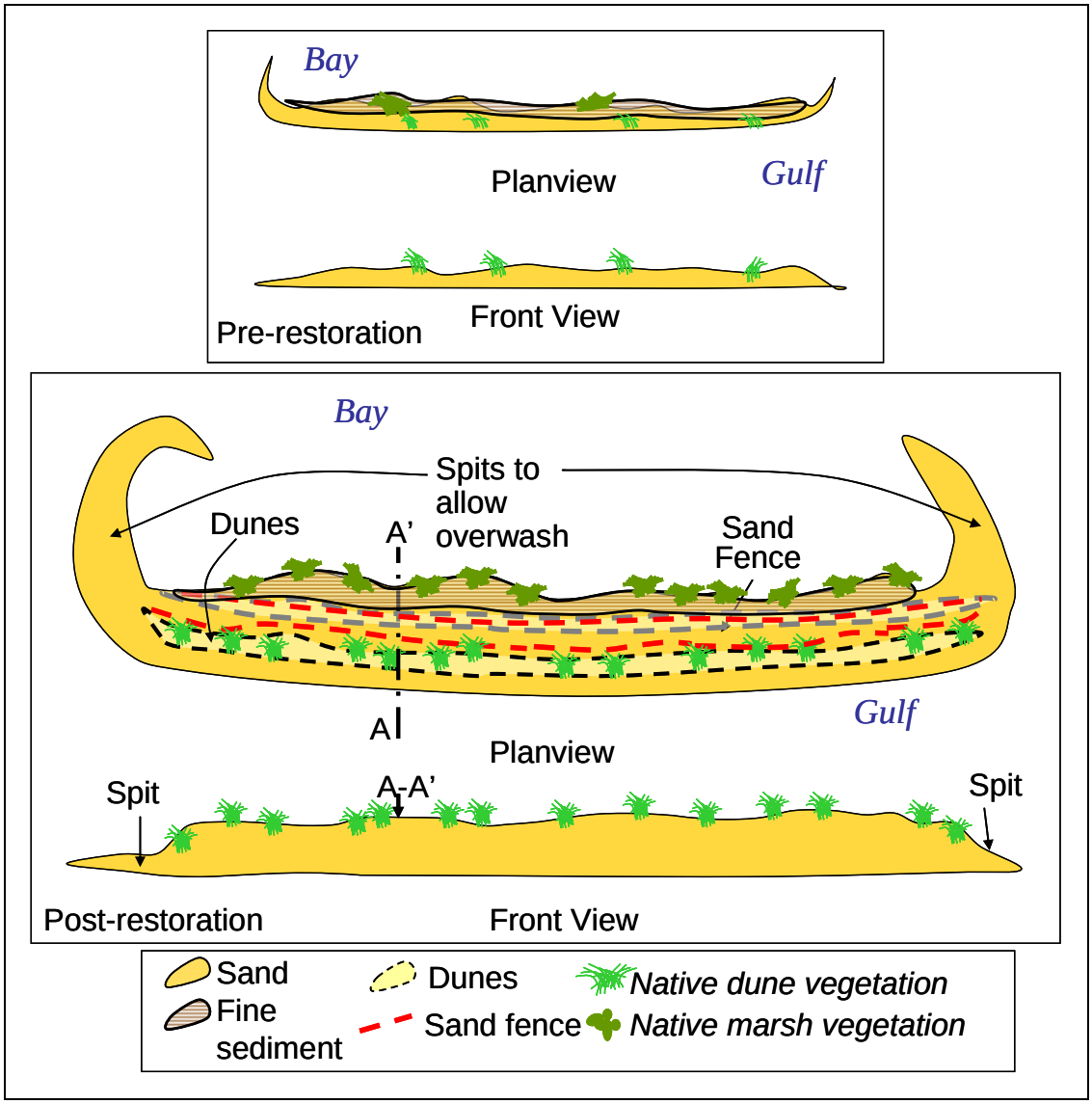

Figure 67. Conceptual design of large-scale stable restoration: Plan and front views.

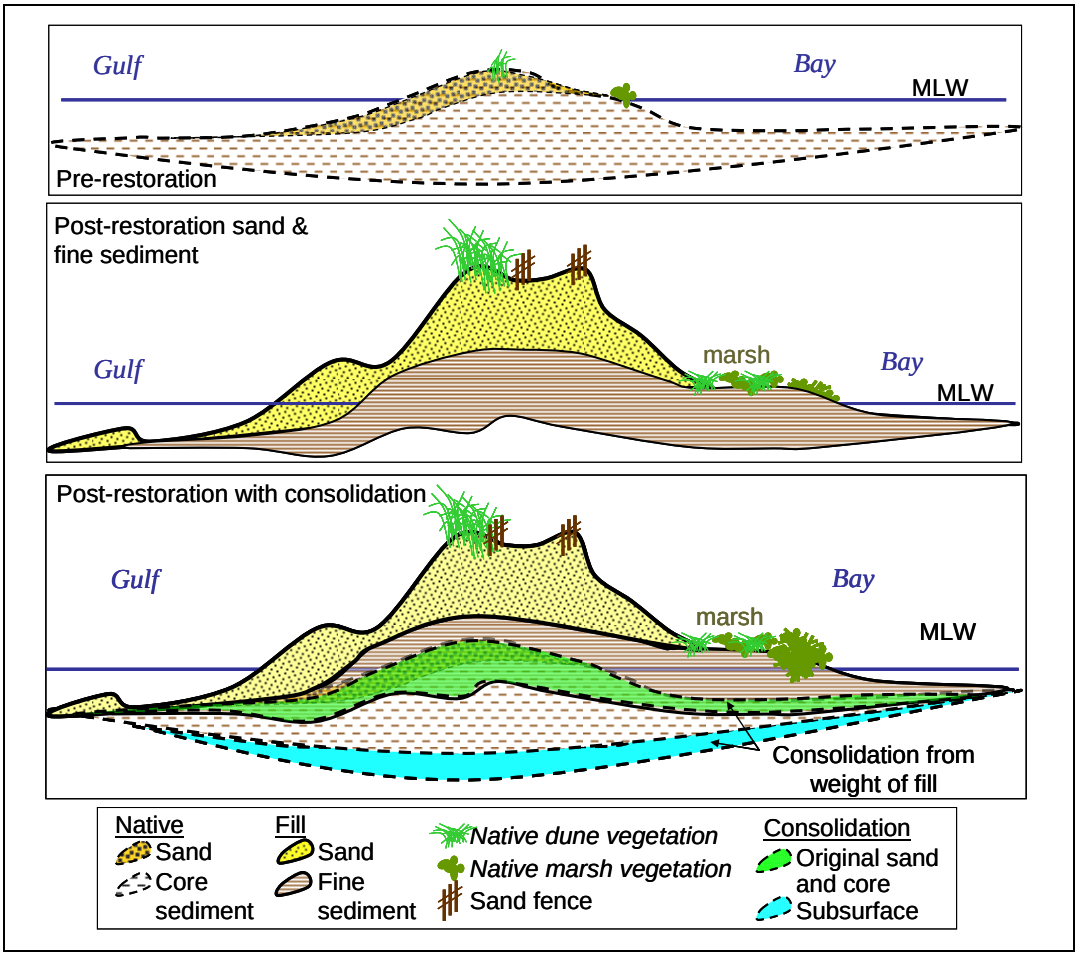

Figure 68. Conceptual design of large-scale stable restoration: Cross-sections.

Summary

This chapter evaluated three hypotheses that were introduced at the start of this research using 2D MCO, applicable sub-modules, knowledge gained through the literature review, and available field data. All hypotheses were valid, with some exceptions as noted in Table 21.

For a barrier island overlying a compressible substrate, general conclusions from this chapter were as follows: (1) consolidation of the underlying substrate due to the weight of a barrier island was found to be a dominant process governing morphologic evolution and migration; (2) as compared to barrier islands that overlie a stable substrate, islands overlying a compressible substrate required greater dune elevations, greater island widths, and larger sources of sand to avoid becoming sub-aqueous shoals; and (3) the best method to preserve islands that overlie a compressible substrate is to initially infuse a large volume of sand from an external source (“Initial Method”), rather than incrementally adding smaller volumes through time (“Incremental Method”).

Table 21. Summary of hypotheses and associated metrics.

Hypothesis and Metrics	Validity
1. Consolidation is a dominant process governing morphologic evolution & migration for barrier islands overlying poorly-consolidated sediment.	
1a. For BIC*, volume sequestered through consolidation process >10% total island sand budget.	Valid; 2D MCO = 20-46%; VA data 43 ± 11%
1b. Morphology (elevation, width) differs for BIC as compared to BIS.	Valid for elevation if a sufficient source of sand is unavailable to replenish quantity lost due to consolidation process; data coverage insufficient for width.
1c. With a sufficient source of sand, migration rates for BIC>BIS.	Valid; BIC migration = 3-11 × BIS migration.
1d. Without a sufficient source of sand, lifetime of BIC<BIS.	Valid, except for BIC of sufficient elevation to limit overwash.
2. Barrier islands overlying poorly-consolidated sediment require a greater volume of sand, greater dune elevation, and greater width to maintain functioning as compared to islands over a non-compressible substrate.	
2a. For same nourishment volume, BIC lifetime < BIS.	Valid except for large fill volumes.
2b. Minimum elevation for BIC to remain above depth > BIS.	Valid for longer project life (>15 yr).
2c. Minimum width for BIC to remain above depth > BIS.	Valid for longer project life (>15 yr).
3. To preserve barrier islands that overlie a compressible substrate, it is best to initially infuse a large volume of sand from an external source, rather than smaller quantities that are placed incrementally in time.	
3a. For a defined project life, minimum volume for Initial Method<Incremental Method.	Inconclusive.
3b. Initial Method provides more stability** for BIC as compared to Incremental Method.	Valid; migration rates decreased 5-20 m/yr, consolidation and erosion of dune reduced.
3c. Total cost of Initial Method < Incremental Method***.	Valid for more compressible substrates (>15 m thickness) such as in deltaic settings.

* BIC = Barrier Island over Compressible Substrate, BIS = Barrier Island over Stable Substrate.

** Stability defined as reducing cross-shore migration rate, consolidation rate, and loss of dune crest elevation.

*** Applying decadal-scale inflation rate = 15.5-40.6% and interest rate = 5.75%.

7 Conclusions

This research investigated and quantified the morphologic evolution of barrier islands that may migrate over an unconsolidated substrate. The study was accomplished through review of the literature, development of conceptual and 2D mathematical models, and analysis of data available from Louisiana and Virginia. No other pertinent data sets were found.

The 2D MCO model developed in this research represents barrier island morphologic change as a function of storm waves and water level, and the subsequent subsurface consolidation due to loading by the barrier island. The model calculates erosion, overwash, and washover caused by storms, and it can also represent additional loading as from infusion of sand from an external source. Time-dependent consolidation and morphologic evolution are calculated in response to the change in loading as the barrier island evolves over years to decades. Conclusions from this research are presented below.

Barrier islands overlying a consolidating substrate are more likely to have: (1) reduced dune elevations because of consolidation, (2) overall volumetric adjustment of the cross-shore profile to fill compressed regions outside the footprint of the island, and (3) increased overwash and migration after the dune reaches a critical elevation with respect to the total water elevation of the prevalent storm conditions. In effect, the consolidation process decreases the return period of the prevailing storm conditions. Numerical calculations with the model illustrated how consolidation modifies profile response through lowering of the dune elevation and increasing the potential for overwash and migration.

Three hypotheses were tested with the available data and models representing the governing processes. The hypotheses were found to be valid through examination of available data, model applications, and sensitivity analysis. For barrier islands that overlie a compressible substrate such as in a deltaic, bay, or estuarine setting, each hypothesis was examined as follows:

1. Consolidation under the weight of a barrier island was found to be a dominant process governing morphologic evolution and migration. The consolidation process was found to sequester between 20 and 40 percent

of barrier island sand, representing a significant loss to the barrier island sediment budget. If a sufficient source of sand was available to offset losses incurred during consolidation, the islands were predicted to maintain elevations similar to those islands migrating over more stable substrates, although the rate of migration was 3-11 times greater. Without a source of sand to replenish losses incurred during consolidation, the island drowned in place, eventually becoming a sub-aqueous shoal.

2. As compared to barrier islands that overlie a stable substrate, islands overlying a compressible substrate require greater dune elevations, greater island widths, and larger sources of sand to prevent being reduced to sub-aqueous shoals. Given a similar cross-section, islands overlying a compressible substrate became submerged more rapidly than comparable islands with a stable substrate.
3. The best method for preserving barrier islands that overlie a compressible substrate is to initially infuse a large volume of sand from an external source (called the "Initial Method"), rather than incrementally add smaller volumes through time ("Incremental Method"). Despite the additional consolidation that is incurred by the greater weight of the Initial infusion of sand, the larger volume reduces overwash and the consolidation that results as sand is washed over into the bay or estuary as happens with the Incremental Method. The Initial Method reduced total migration rate, consolidation, and erosion.

To conclude, this research was the first to quantify the volumetric loss to subaerial barrier islands through compaction of the underlying substrate, and to calculate how this subaerial loss in elevation then accelerates the morphologic evolution (erosion, overwash, and deposit of washover sand) and migration. The loss due to consolidation is a concern for islands with reduced sand sources to replenish the sand budget of the island, such as along coastal Louisiana, other deltaic settings, and those regions with soft bay or estuarine sediment or peat deposits. With a sufficient source of sand and constructive forcing processes, barrier islands experiencing compaction can rebuild vertically through eolian transport and overwash.

Large-scale restoration with an infusion of sand from an external location is a mechanical means of providing a source of sand to replenish compaction losses and restore the footprint of an eroding barrier island. Restoration of barrier islands can replace environmental habitat and maintain a dynamic coastal boundary for bays, estuaries, and mainland shores. The research presented herein has demonstrated that the Initial Method of restoration is the most favorable approach for barrier islands

overlying soft substrates, rather than the traditional (Incremental) method of restoration that has been conducted in the United States since the 1930s.

The 2D MCO and sub-modules developed herein show promise for improving understanding of natural and restored barrier islands. Additional data sets are required to further develop and expand models such as 2D MCO, understand the three-dimensional processes and response of these barrier island systems, and to apply these tools and knowledge to future restoration of barrier islands. Further research identified through this technical report is included in Appendix C. Briefly, four types of data collection and additional study have been delineated.

The first of these research areas concerns data collection and analysis of how the loading of natural and restored islands modifies the underlying substrate, both for clastic sediment and for organic deposits as a function of the static (in-place), overwash, and migration processes. Next, data are needed to quantify the rate of fine-grained sediment erosion under typical, storm (inundated), and with and without abrasive (sand) conditions. Coordinated laboratory and field studies are recommended for this purpose to understand microscale processes such as critical shear stresses under waves and current. The third area of research concerns analysis of historical data in conjunction with numerical modeling to understand and quantify the regional influence of bay area change and inlet evolution on the long-term evolution of barrier islands. Numerical study can investigate the benefit of creating or restoring bay islands with dredged sediment in protecting the bay shore of barrier islands from wind-generated waves on the bay. This numerical study may indicate a pilot field study is warranted, in which mechanical methods for rapid dewatering and consolidating the dredged sediment could be tested and evaluated. The final recommend-dation in Appendix C concerns integrating all the knowledge gained through these studies into advancing numerical modeling of barrier islands in deltaic and soft substrate settings.

Barrier islands provide a buffer for storm waves and surge and serve as a necessary boundary for estuaries and bays. They function to reduce storm impacts, provide habitat for static and migrating species, and maintain quiescent water and adjacent inlet functioning that are essential for life cycles of juvenile species. Barrier islands are increasingly being stressed with eustatic sea level rise, reduced sand sources, anthropogenic influences, and possible future increase in storm frequency and severity.

Islands overlying a soft substrate such as deltaic, bay, or estuarine sediment or peat deposits incur additional vertical losses because of compaction. Options for preservation of barrier islands with greatest storm and environmental benefits should be given priority in data collection, research, pilot studies, and restoration.

References

Alfageme, S., and R. Cañizares. 2005. Process-based morphological modeling of a restored barrier island: Whiskey Island, Louisiana, USA. *Proceedings 5th International Coastal Dynamics Conference*, American Society of Civil Engineers (ASCE). Barcelona, Spain, 11 p.

Allison, M. A. 1998. Geologic framework and environmental status of the Ganges-Brahmaputra Delta. *Journal of Coastal Research* 14(3):826-836.

Armbruster, C. K., G. W. Stone, and J. P. Xu. 1995. Episodic atmospheric forcing and bayside foreshore erosion: Santa Rosa Island, Florida. *Transactions, Gulf Coast Association of Geological Societies* Vol. XLV, 31-37.

Armon, J. W. 1979. Landward sediment transfers in a transgressive barrier island system, Canada. In: *Barrier Islands from the Gulf of St. Lawrence to the Gulf of Mexico*, S. P. Leatherman (ed.). New York, NY: Academic Press, 65-80.

Bartberger, C. E. 1976. Sediment sources and sedimentation rates, Chincoteague Bay, Maryland and Virginia. *Journal of Sedimentary Petrology* 46(2):326-336.

Berendsen, H. J. A. 1998. Birds-eye view of the Rhine-Meuse Delta (The Netherlands). *Journal of Coastal Research* 14(3):740-752.

Bloom, A.L. 1964. Peat accumulation and compaction in a Connecticut coastal marsh. *Journal of Sedimentary Petrology* 34(3):599-603.

Blum, M. D., J. H. Tomkin, A. Purcell, and R. R. Lancaster. 2008. Ups and downs of the Mississippi Delta. *Geology* 36(9):675-678. Boulder, CO: The Geological Society of America, Inc.

Bourman, R. P., C. V. Murray-Wallace, A. P. Belperio, and N. Harvey. 2000. Rapid coastal geomorphic change in the River Murray Estuary of Australia. *Marine Geology* 170:141-168.

Bretschneider, C. L. 1966. Wave generation by wind, deep and shallow water. In: *Estuary and Coastline Hydrodynamics*, A. T. Ippen (ed.). New York, NY: McGraw-Hill Book Company, Inc., p. 146.

Bruun, P. 1962. Sea level rise as a cause of shore erosion. *Journal of Waterways and Harbors Division* 88:117-130, ASCE.

Byrnes, M. R., and K. J. Gingerich. 1987. Cross-island profile response to Hurricane Gloria. In: *Coastal Sediments '87*, N. C. Kraus (ed.). New York, NY: New York, NY, ASCE, 1,486-1,502.

Byrnes, M. R., S. Griffee, and J. D. Rosati. 2009. Historical sediment budget for Mississippi Sound. Submitted to *Journal of Coastal Research* SI, in preparation.

Byrnes, M. R., R. A. McBride, S. Penland, M. W. Hiland, and K. A. Westphal. 1991. Historical changes in shoreline position long the Mississippi Sound barrier islands. *GCSSEPM Foundation Twelfth Annual Research Conference Program and Abstracts*, December 5, 43-55.

Cahoon, D. R., D. J. Reed, and J. W. Day, Jr. 1995. Estimating shallow subsidence in microtidal salt marshes of the southeastern United States: Kaye and Barghoorn revisited. *Marine Geology* 128:1-9.

Campbell, T. 2005. Development of a conceptual morphosedimentary model for design of coastal restoration projects along the Louisiana coast. *Journal of Coastal Research* SI 44:234-244.

Campbell, T., L. Benedet, and C. W. Finkl. 2005a. Regional strategies for coastal restoration along Louisiana barrier islands. *Journal of Coastal Research* SI 44:245-267.

Campbell, T., L. Benedet, and G. Thompson. 2005b. Design considerations for barrier island nourishments and coastal structures for coastal restoration in Louisiana. *Journal of Coastal Research* SI 44:186-202.

Campbell, T., B. de Sonneville, L. Benedet, D. J. R. Walstra, and C. W. Finkl. 2007. Investigation of morphosedimentary processes on a schematic Louisiana barrier island using process-based numerical modeling. *Proceedings, Coastal Sediments '07*, New Orleans, LA, ASCE, 671-684.

Campbell, T., G. Thomson, and L. Benedet. 2006. Design of the restoration of Shell Island, Louisiana, with application of a dynamic morphosedimentary model. *Proceedings, 30th International Conference on Coastal Engineering*, San Diego, CA, 3,862-3,872.

Cipriani, L., and G. W. Stone. 2001. Net longshore transport and textural changes in beach sediments along the Southwest Alabama and Mississippi barrier islands, USA. *Journal of Coastal Research* 17(2):443-458.

Coastal Planning and Engineering, Inc. 2007. Chaland Headland restoration (BA-38-2) CWPPRA project, project completion report. Prepared for Louisiana Department of Natural Resources and National Oceanic and Atmospheric Administration, 4,022 p.

Coastal Studies Institute. 2008. Wave-current-surge information for coastal Louisiana. Website accessed 5 July 2008, last updated 5 July 2008. http://wavcis.csi.lsu.edu/.

Coleman, J. M., H. H. Roberts, and G. W. Stone. 1998. Mississippi River Delta: An overview. *Journal of Coastal Research* 14(3):698-716.

Cowell, P. J., P. S. Roy, and R. A. Jones. 1995. Simulation of large-scale coastal change using a morphological behavior model. *Marine Geology* 126:45-61.

de Beaumont, L. E. 1845. Septieme lechón. In: *Lecons de geologie pratique*, P. Bertrand, (ed. and publisher), Paris, France, 221-252.

de Sonneville, B. 2006. *Morphodynamic modeling of a schematic barrier island*. MSc. Thesis. WL|Delft Hydraulics, Z3783.32, June.

Davis, R. A., Jr., and M. O. Hayes. 1984. What is a wave-dominated coast? *Marine Geology* 60:313-329.

Davis, R. A., and G. A. Zarillo. 2003. Human-induced changes in back-barrier environments as factors in tidal inlet instability with emphasis on Florida. Coastal and Hydraulics Laboratory Engineering Technical Note ERDC/CHL CHETN-IV-57, 18 p.

Dean, R. G. 2002. *Beach nourishment theory and practice, advanced series on ocean engineering*, Vol. 18. River Edge, NJ: World Scientific Press.

Dean, R. G. 1997. Models for barrier island restoration. *Journal of Coastal Research* 13(3), 694-703.

Dean, R. G. 1977. Equilibrium beach profiles: U.S. Atlantic and Gulf coasts. Ocean Engineering Report No. 12. Newark, DE: Department of Civil Engineering, University of Delaware.

Dean, R. G., and R. A. Dalrymple. 2002. *Coastal processes with engineering applications*. New York, NY: Cambridge University Press.

Dean, R. G., and R. A. Dalymple. 1984. *Water wave mechanics for engineers and scientists*. Englewood Cliffs, NJ: Prentice-Hall, Inc.

Dean, R. G., T. R. Healy, and A. P. Dommerholt. 1993. A "blind – folded" test of equilibrium beach profile concepts with New Zealand data. *Marine Geology* 109:253-266.

Dean, R. G., D. Kriebel, and T. Walton. 2002. Cross-shore sediment transport processes. In: *Coastal Engineering Manual*, Part 3, Chapter 3, David B. King, chairman, Engineer Manual EM 1110-2-1100. Washington, DC: U.S. Army Corps of Engineers.

Dean, R. G., and E. M. Maurmeyer. 1983. Models for beach profile response. In: *Handbook of Coastal Processes and Erosion*, P.D. Komar (ed.). Boca Raton, FL: CRC Press, 151-166.

Delft University of Technology. 2009. Surface WAter Nearshore model (SWAN). http://vlm089.citg.tudelft.nl/swan/index.htm, accessed 25 January 2009.

Demirbilek, Z., and C. L. Vincent. 2002. Water wave mechanics. In: *Coastal Engineering Manual*, Part II, Coastal Hydrodynamics Chapter II-1, Z. Demirbilek (chairman.), Engineer Manual EM 1110-2-1100. Washington, DC: U.S. Army Corps of Engineers, 121 p.

Dillon, W. P. 1970. Submergence effects on a Rhode Island barrier and lagoon and inferences on migration of barriers. *Journal of Geology* 78:94-106.

Dingler, J. R. 2008. Isle Dernieres centerline data. Excel spreadsheet, received September 2008.

Dingler, J. R., S. A. Hsu, and T. E. Reiss. 1992. Theoretical and measured aeolian sand transport on a barrier island, Louisiana, USA. *Sedimentology* 39:1,031-1,043.

Dingler, J. R., and T. E. Reiss. 1995. Beach erosion on Trinity Island, Louisiana, caused by Hurricane Andrew. *Journal of Coastal Research* SI 21:254-264.

Dingler, J. R., and T. E. Reiss. 1991. Processes controlling the retreat of the Isles Demieres, a Louisiana barrier island chain. *Proceedings Coastal Sediments '91*, ASCE, 1,111-1,121.

Dingler, J. R., and T. E. Reiss. 1990. Cold-front driven storm erosion and overwash in the central part of the Isles Dernieres, a Louisiana barrier-island arc. *Marine Geology* 91:195-206.

Dingler, J. R., and T. E. Reiss. 1989. Controls on the location of the sand/mud contact beneath a barrier island: Central Isles Dernieres, Louisiana. *Transactions, Thirty-Ninth Annual Meeting, Gulf Coast Association of Geological Societies*, 349-354.

Donnelly, C., M. Larson, and H. Hanson. 2009. A numerical model of coastal overwash. *Proceedings of the Institution of Civil Engineers, Maritime Engineering*. Lincolnshire, UK: Thomas Telford Publishers.

Douglas, B. C. 1992. Global sea level acceleration. *Journal of Geophysical Research* 97(C8):12,699-12,706.

Ellis, J., and G. W. Stone. 2006. Numerical simulation of net longshore sediment transport and granulometry of surficial sediments along Chandeleur Island, Louisiana, USA. *Marine Geology* 232:115-129.

Financial Trend Forecaster. 2008. InflationData.com website, published by Financial Trend Forecaster, last updated 13 October, 2008, accessed 13 October, 2008. http://inflationdata.com/inflation/Inflation_Rate/HistoricalInflation.aspx.

Fisher, J. J. 1968. Barrier island formation: discussion. *Geological Society of America Bulletin* 79:1,421-1,426.

Fisher, J. J., and E. J. Simpson. 1979. Washover and tidal sedimentation rates as environmental factors in development of a transgressive barrier shoreline, In: *Barrier Islands from the Gulf of St. Lawrence to the Gulf of Mexico*, S. P. Leatherman (ed.). New York, NY: Academic Press, 127-148.

FitzGerald, D. M. 1988. Shoreline erosional-depositional processes associated with tidal inlets. In: *Hydrodynamics and sediment dynamics of tidal inlets*, D. G. Aubrey and L. Weishar (eds.). Spring, Berlin, 186-225.

FitzGerald, D., M. Kulp, Z. Hughes, I. Georgiou, M. Miner, S. Penland, and N. Howes. 2007. Impacts of rising sea level to backbarrier wetlands, tidal inlets, and barrier islands: Barataria Coast, Louisiana. *Proceedings Coastal Sediments '07*, 13-17 May 2007, New Orleans, LA, 1,179-1,192.

FitzGerald, D. M., M. Kulp, S. Penland, J. Flocks, and J. Kindinger. 2004. Morphologic and stratigraphic evolution of muddy ebb-tidal deltas along a subsiding coast: Barataria Bay, Mississippi River delta. *Sedimentology* 51:1,157-1,178.

Flocks, J. G., N. F. Ferina, C. Dreher, J. L. Kindinger, D. M. FitzGerald, and M. A. Kulp. 2006. High-resolution stratigraphy of a Mississippi subdelta-lobe progradation in the Barataria Bight, North-Central Gulf of Mexico. *Journal of Sedimentary Research* 76:429-443.

Frazier, D. E. 1967. Recent deltaic deposits of the Mississippi River: their development and chronology. *Gulf Coast Association of Geological Societies Transactions* 27:287-315.

Gayes, P. T. 1983. *Primary consolidation and subsidence in transgressive barrier island systems*. MSc Thesis. State College, PA: Department of Geosciences, Pennsylvania State University.

Georgiou, I. Y., D. M. FitzGerald, and G. W. Stone, 2005. The impact of physical processes along the Louisiana coast. *Journal of Coastal Research* SI 44:72-89.

Gilbert, G. K., 1885. The topographic features of lake shores. U.S. Geological Survey 5th Annual Report, 87-88.

Guber, A. L., and R. Slingerland. 1981. Compaction and lateral flow as processes in barrier island and associated environments. In: *Field Guide to selected coastal geologic problems on the central Delmarva Peninsula, Eight Annual Assateague Shelf and Shore Workshop*. R. Slingerland, A. L. Guber, and H. W. Hanson, H. W (eds.). State College, PA: Pennsylvania State University, 14 p.

Hayes, M. O. 1979. Barrier island morphology as a function of wave and tide regime. In: *Barrier Islands from the Gulf of St. Lawrence to the Gulf of Mexico*, S. P. Leatherman (ed.). New York, NY: Academic Press, 1-29.

Hornberger, G. M., J. P. Raffensperger, P. L. Wiberg, and K. N. Eshleman. 1998. Elements of physical hydrology. Baltimore, MD: Johns Hopkins University Press, 302 p.

Hotta, S. 1984. *Wind blown sand on beaches*. PhD dissertation. Tokyo, Japan: Department of Civil Engineering, University of Tokyo.

Hoyt, J. H. 1967. Barrier island formation. *Geological Society of America Bulletin* 78(9):1,125-1,136.

Hsu, S. A., and B. W. Blanchard. 1991. Shear velocity and eolian sand transport on a barrier island. *Proceedings Coastal Sediments '91*, ASCE, 220-234.

Hsu, S. A., and J. R. Weggel. 2002. Wind-blown sediment transport. In: *Coastal Engineering Manual*, Part III, Coastal Sediment Processes Chapter III-4, David B. King (chairman), Engineer Manual EM 1110-2-1100. Washington, DC: U.S. Army Corps of Engineers, 78 p.

Hughes, S. A. 2004. Estimation of wave run-up on smooth, impermeable slopes using the wave momentum flux parameter. *Coastal Engineering* 51:1,085-1,104.

Interagency Performance Evaluation Team. 2006. The Storm. Draft final report of the Interagency Performance Evaluation Task Force, Vol IV. U.S. Army Corps of Engineers, 264 p., http://chl.erdc.usace.army.mil/Media/7/0/7/Vol-IV_The_Storm-maintext.pdf.

Intergovernmental Panel on Climate Change. 2008. Climate change 2007: The Fourth Assessment, Synthesis Report, http://www.ipcc.ch/pdf/assessment-report/ar4/syr/ar4_syr_spm.pdf, accessed 29 November 2008.

Jarrett, J. T. 1976. Tidal prism-inlet area relationships. General Investigations of Tidal Inlets GITI Report 3. Vicksburg, MS: U.S. Army Engineer Waterways Experiment Station.

Jiménez, J. A., and A. Sánchez-Arcilla. 2004. A long-term (decadal scale) evolution model for microtidal barrier systems. *Coastal Engineering* 51:749-764.

Johnson, D. W. 1919. *Shore processes and shoreline development*. New York, NY: John Wiley and Sons.

Jose, F. 2008. Personal communication, wind bird height at CSI-5, 10 July 2008.

Kahn, J. H., and H. H. Roberts. 1982. Variations in storm response along a microtidal transgressive barrier-island arc. *Journal of Sedimentary Geology* 33:129-146.

Kaye, C. A., and E. S. Barghoorn. 1964. Late Quaternary sea-level change and crustal rise at Boston, Massachusetts, with notes on the autocompaction of peat. *Geological Society of America Bulletin* 75:63-80.

Keim, B, R. A. Muller, and G. W. Stone. 2004. Spatial and temporal variability of coastal storms in the North Atlantic basin. In: *Storms and their Significance in Coastal Morpho-Sedimentary Dynamics*, G. W. Stone and J. D. Orford (eds.), and *Marine Geology* 210:7-15.

Khalil, S. M. 2008. The use of sand fences in barrier island restoration: Experience on the Louisiana coast. System-Wide Water Resources Program Technical Note ERDC TN-SWWRP-08-4. Vicksburg, MS: U.S. Army Engineer Research and Development Center, https://swwrp.usace.army.mil.

Kraus, N. C. 2000. Reservoir model of ebb-tidal shoal evolution and sand bypassing. *Journal of Waterways, Ports, Coasts, and Ocean Engineering* 126(3):305-313.

Kriebel, D. L., and R. G. Dean. 1993. Convolution method for time-dependent beach-profile response. *Journal of Waterway, Port, Coastal and Ocean Engineering* 119(2):204-227.

Komar, P. D. 1998. *Beach Processes and Sedimentation*. 2nd ed. Upper Saddle River, NJ: Prentice Hall.

Kuecher, G. J. 1994. *Geologic framework and consolidation settlement potential of the Lafourche Delta, topstratum valley fill sequence; implications for wetland loss in Terrebonne and Lafourche parishes, Louisiana*. Ph.D. Dissertation. Baton Rouge, LA: Louisiana State University, 248 p.

Kulp, M., P. Howell, A. Sandra, S. Penland, J. Kindinger, and W. S. Jeffress. 2002. Latest quaternary stratigraphic framework of the Mississippi River Delta Region. *Gulf Coast Association of Geological Societies Transaction* 52:573-582.

Larson, M., and N. C. Kraus. 1995. Prediction of cross-shore sediment transport at different spatial and temporal scales. *Marine Geology* 126:111-127.

Larson, M., N. C. Kraus, and R. A. Wise. 1999. Equilibrium beach profiles under breaking and non- breaking waves. *Coastal Engineering* 36:59-85.

Larson, M., S. Kubota, and L. Erikson. 2004. Swash-zone sediment transport and foreshore evolution: Field experiments and mathematical modeling. *Marine Geology* 212:61-79.

Leatherman, S. P. 1985. Barrier island migration: An annotated bibliography. *Public Administration Series: Bibliography*. Monticello, IL : Vance Bibliographies, 54 p.

Leatherman, S. P. (Ed.). 1979. *Barrier islands from the Gulf of St. Lawrence to the Gulf of Mexico*. New York, NY: Academic Press, 325 p.

Levin, D. R. 1993. Tidal inlet evolution in the Mississippi River Delta Plain. *Journal of Coastal Research* 9(2):462-480.

List, J. H., B. E. Jaffe, and A. H. Sallenger. 1991. Large-scale coastal evolution of Louisiana's barrier islands. *Proceedings Coastal Sediments '91*, ASCE, 1,532-1,546.

List, J. H., A. H. Sallenger, Jr., M. E. Hansen, and B. E. Jaffe. 1997. Accelerated relative sea-level rise and rapid coastal erosion: testing a causal relationship for the Louisiana barrier islands. *Marine Geology* 140:347-365.

Long, A. J., M. P. Waller, and P. Stupples. 2006. Driving mechanisms of coastal change: Peat compaction and the destruction of late Holocene coastal wetlands. *Marine Geology* 225:63-84.

Maurmeyer, E. M., and R. G. Dean. 1982. Sea-level rise and barrier island migration: an extension of the Bruun Rule to account for landward sediment transport. In: Abstracts of the *Northeastern-Southeastern Meeting* (March) Washington, DC: Geological Society of America.

McBride, R. A., and M. R. Byrnes. 1997. Regional variation in shore response along barrier island systems of the Mississippi River delta plain: Historical change and future prediction. *Journal of Coastal Research* 13(3):628-655.

McBride, R. A., M. R. Byrnes, and M. W. Hiland. 1995. Geomorphic response-type model for barrier coastlines: a regional perspective. *Marine Geology* 126:143-159.

McBride, R. A., S. Penland, M. Hiland, S. J. Williams, K. A. Westphal, B. Jaffe, and A. H. Sallenger, Jr. 1992. Louisiana barrier shoreline change analysis – 1853 to 1989: Methodology, database, and results. In: *Atlas of shoreline changes in Louisiana from 1853 to 1989*, S. J. Williams, S. Penland, and A. H. Sallenger (eds.). Reston, VA: U.S. Geological Survey.

McGee, W. J. 1890. Encroachments of the sea. In: *The Forum* 9, L. S. Metcalf (ed.), 437-449.

Meckel, T. A., U. S. Ten Brink, and S. J. Williams. 2007. Sediment compaction rates and subsidence in deltaic plains: Numerical constraints and stratigraphic influences. *Basin Research* 19:19-31.

Morgan, J. P. 1951. Genesis and paleontology of the Mississippi River mudlumps: Part I. Mudlumps of the Mississippi River. Louisiana Geologic Survey, Department of Conservation. *Geological Bulletin* 35, p. 57.

Moslow, T. F., and S. D. Heron. 1979. Quarternary evolution of Core Banks, North Carolina: Cape Lookout to New Drum Inlet. In: *Barrier Islands from the Gulf of St. Lawrence to the Gulf of Mexico,* S. P. Leatherman (ed.). New York, NY: Academic Press, 211-236.

Muller, R. A., and G. W. Stone. 2001. A climatology of tropical storms and hurricane strikes to enhance vulnerability prediction for the southeast U.S. coast. *Journal of Coastal Research* 17(4):949-956.

Myrhaug, D., L. E. Holmedal, and H. Rue. 2006. Erosion and deposition of mud beneath random waves. *Coastal Engineering* 53:793-797.

Namikas, S. L. 2003. Field measurement and numerical modeling of aeolian mass flux distributions on a sandy beach. *Sedimentology* 50:936-948.

National Oceanic and Atmospheric Administration (NOAA) Tides and Currents, Sea Levels Online. 2008a. Water level data for Grand Isle, Louisiana. http://tidesandcurrents.noaa. gov/ sltrends/sltrends_station.shtml?stnid= 8761724, last updated 5 August 2008, accessed 14 November 2008.

National Oceanic and Atmospheric Administration (NOAA) Tides and Currents, Sea Levels Online. 2008b. Water level data for Dauphin Island, Alabama, http://tidesandcurrents. noaa. gov/sltrends/sltrends_station.shtml?stnid =8735180, last updated 5 August 2008, accessed 29 November 2008.

National Oceanic and Atmospheric Administration (NOAA) Tides and Currents, Sea Levels Online. 2008c. Water level data for Pensacola, Florida, http://tidesandcurrents.noaa. gov/sltrends/sltrends_station.shtml?stnid= 8729840, last updated 5 August 2008, accessed 29 November 2008.

National Oceanic and Atmospheric Administration (NOAA), Coastal Services Center. 2008d. Historical hurricane tracks, Grand Isle, Louisiana, 2001-2006, http://maps.csc.noaa.gov/ hurricanes/viewer.html, last updated 15 May 2008, accessed 6 July 2008.

National Oceanic and Atmospheric Administration (NOAA), Tides and Currents, Bench Mark Data Sheets. 2008e. Bench mark data for Pensacola, Florida, http://tidesandcurrents.noaa.gov/data_menu.shtml?stn= 8729840%20Pensacola,%20FL&type=Bench%20Mark%20Data%20Sheets, last updated 23 November 2005, accessed 24 November 2008.

National Oceanic and Atmospheric Administration (NOAA), Tides and Currents, Bench Mark Data Sheets. 2008f. Bench mark data for Chincoteague, VA, http://tidesandcurrents. noaa.gov/data_menu.shtml?stn= 8630249 %20CHINCOTEAGUE,%20USCG%20STATION,%20VA&type=Bench%20Mark%20Data%20Sheets, last updated 23 November 2005, accessed 24 November 2008.

National Oceanic and Atmospheric Administration (NOAA). 2008g. Beach Nourishment: A Guide for Local Government Officials, Methods of Investigation to Identify Sources of Suitable Sand for Nourishment, http://www.csc.noaa.gov/ beachnourishment/html/geo/sand.htm, accessed 29 December 2008.

Newman, W. S., and C. A. Munsart. 1968. Holocene geology of the Wachapreague Lagoon, Eastern Shore Peninsula, Virginia. *Marine Geology* 6:81-105.

Nummedal, D., S. Penland, R. Gerdes, W. Schramm, J. Kahn, and H. Roberts. 1980. Geologic response to hurricane impact on low-profile Gulf coast barriers. *Transactions, Gulf Coast Association of Geological Societies*, Vol XXX, 183-195.

Oertel, G. F. 1979. Barrier island development during the Holocene recession, southeastern United States. In: *Barrier Islands from the Gulf of St. Lawrence to the Gulf of Mexico*, S. P. Leatherman (ed.). New York, NY: Academic Press, 273-290.

Otvos, E. G. 1985. Barrier platforms: Northern Gulf of Mexico. *Marine Geology* 63:285-305.

Otvos, E. G. 1981. Barrier island formation through nearshore aggradation – stratigraphic and field evidence. *Marine Geology* 43:195-243.

Otvos, E. G. 1979. Barrier island evolution and history of migration, north central Gulf Coast. In: *Barrier Islands from the Gulf of St. Lawrence to the Gulf of Mexico*, S.P. Leatherman (ed.). New York, NY: Academic Press, 291-319.

Otvos, E. G., Jr. 1970. Development and migration of barrier islands, Northern Gulf of Mexico. *Geological Society of America Bulletin* 81:241-246.

Peltier, W. R. 1998. Postglacial variations in the level of the sea: implications for climate dynamics and solid-earth geophysics. *Reviews of Geophysics* 36(4):603-689.

Penland, S., and R. Boyd. 1981. Shoreline changes on the Louisiana Coast. *Oceans 91,* 209-219.

Penland, S., R. Boyd, and J.R. Suter. 1988. Transgressive Depositional Systems of Mississippi Delta Plain: A Model for Barrier Shoreline and Shelf Sand Development. *Journal of Sedimentary Petrology* 58:932-949.

Penland, S., P. F. Connor, Jr., A. Beall, S. Fearnley, and S. J. Williams. 2005. Changes in Louisiana's shoreline: 1855-2002. *Journal of Coastal Research* SI 44:7-39.

Penland, S., and K. E. Ramsey. 1990. Relative sea-level rise in Louisiana and the Gulf of Mexico: 1908-1988. *Journal of Coastal Research* 6:323-342.

Penland, S., C. Zganjar, K. A. Westphal, P. Connor, A. Beall, J. List, and S. J. Williams. 2003a. Shoreline change posters of the Louisiana barrier islands: 1885-1996: Hurricane Andrew impact on the Isle Dernieres barrier island arc. U.S. Geological Survey Open-File Report 03-398, http://pubs.usgs.gov/ of/2003/ of03-398/.

Penland, S., C. Zganjar, K. A. Westphal, P. Connor, A. Beall, J. List, and S. J. Williams. 2003b. Shoreline change posters of the Louisiana barrier islands: 1885-1996: Hurricane Andrew impact on the Timbalier barrier island arc. U.S. Geological Survey Open-File Report 03-398, http://pubs.usgs.gov/of/2003/of03-398/.

Pepper, D. A., and G. W. Stone. 2004. Hydrodynamic and sedimentary responses to two contrasting winter storms on the inner shelf of the northern Gulf of Mexico. *Marine Geology* 210:43-62.

Peyronnin, C. A., Jr. 1962. Erosion of Isles Dernieres and Timbalier Islands. *Journal of Waterways and HarborsDivision* 8(WWI):57-69, ASCE.

Pierce, J. W. 1969. Sediment budget along a barrier island chain. *Sedimentary Geology* 3:5-16.

Reed, D. J. (Ed.). 1995. Status and rends of hydrologic modification, reduction in sediment availability, and habitat loss/modification in the Barataria-Terrebonne estuarine system. *Barataria-Terrebonne National Estuary Program Publication* No. 20. Thibodaus, LA: Barataria-Terrebonne National Estuary Program Office, Nicholls State University Campus.

Ritchie, W., and S. Penland. 1988. Rapid dune changes associated with overwash processes on the deltaic coast of South Louisiana. *Marine Geology* 81:97-122.

Roberts, H. H., A. Bailey, and G. J. Kuecher. 1994. Subsidence in the Mississippi River Delta – Important influences of valley filling by cyclic deposition, primary consolidation phenomena, and early diagenesis. *Transactions of the Gulf Coast Association of Geological Societies*, Vol. XLIV, 619-629.

Roberts, H. H., R. T. Beaubouef, N. D. Walker, G. W. Stone, S. Bentley, A. Sheremet, and I. van Heerden. 2003. Sand-rich bayhead deltas in Atchafalaya Bay (Louisiana): Winnowing by cold front forcing. *Proceedings Coastal Sediments '03*. Clearwater Beach, FL (CD-ROM).

Rosati, J. D., R. G. Dean, and G. W. Stone. 2009. A cross-shore model of barrier island migration over a compressible substrate. Submitted to *Marine Geology*, May 2009, in review.

Rosati, J. D., and N. C. Kraus. 2008. Model of barrier island evolution at decadal scale. *Proceedings, International Coastal Engineering Conference*. Hamburg, Germany: World Scientific Press, in press.

Rosati, J. D., and G. W. Stone. 2009. Geomorphologic evolution of barrier islands along the Northern Gulf of Mexico, USA, and implications for engineering design in barrier restoration. To appear, *Journal of Coastal Research* 25(1):8-22.

Rosati, J. D., and G. W. Stone. 2007. Critical width of barrier islands and implications for engineering design. *Proceedings Coastal Sediments 07*, ASCE, 1,988-2,001.

Rosati, J. D., R. G. Dean, N. C. Kraus, and G. W. Stone. 2007. Morphologic evolution of subsiding barrier island systems. *Proceedings 30th International Conference on Coastal Engineering*, J. Smith (ed.). San Diego, CA: World Scientific Press, 3,963-3,975.

Rosen, P. S. 1979. Eolian dynamics of a barrier island system. In: *Barrier islands from the Gulf of St. Lawrence to the Gulf of Mexico*, S. P. Leatherman (ed.). New York, NY: Academic Press, 81-98.

Sánchez-Arcilla, A., J. A. Jiménez, and H. I. Valdemoro. 1998. The Ebro Delta: Morphodynamics and vulnerability. *Journal of Coastal Research* 14(3):754-772.

Sanders, J. E., and N. Kumar. 1975. Evidence of shoreface retreat and in-place drowning during Holocene submergence of barriers, shelf off Fire Island, New York. *Geological Society of American Bulletin* 86, p. 65.

Schwartz, M. L. 1971. The multiple causality of barrier islands. *Journal of Geology* 78:94-106.

Schwartz, M. L. (Ed.). 1973. *Barrier islands*. Benchmark Papers in Geology. Stroudsburg, PA: Dowden, Hutchinson, and Ross, Inc., 451 p.

Shamban, A. J., and T. F. Moslow. 1991. Historical morphologic evolution and sedimentation at Barataria Pass, Louisiana. *Proceedings Coastal Sediments '91*, ASCE, 1,375-1,388.

Sheremet, A., and G. W. Stone. 2003. Wave dissipation due to heterogeneous sediments on the inner Louisiana shelf. *Proceedings Coastal Sediments '03*, Clearwater Beach, FL, CD-ROM.

Shore Protection Manual. 1984. 4th ed., 2 Vol, U.S. Army Engineer Waterways Experiment Station. Washington, DC: U.S. Government Printing Office.

Sowers, G. F. 1979. *Introductory Soil Mechanics and Foundations: Geotechnical Engineering*. 4th edition. New York, NY: Macmillian Publishing Co., Inc.

Stanley, D. J., and A. G. Warne. 1998. Nile Delta in its destruction phase. *Journal of Coastal Research* 14(3):794-825.

Stolper, D., J. H. List, and E. R. Thieler. 2005. Simulating the evolution of coastal morphology and stratigraphy with a new morphological-behaviour model (GEOMBEST). *Marine Geology* 218:17-36.

Stone, G. W., and C. Finkl. (Eds.). 1995. *Impacts of Hurricane Andrew on the coastal zones of Florida and Louisiana: 22-26 August 1992*. Fort Lauderdale, FL: Coastal Education and Research Foundation, 364 p.

Stone, G. W., J. M. Grymes, J. W. Dingler, and D. A. Pepper. 1997. Overview and significance of hurricanes on the Louisiana coast, USA. *Journal of Coastal Research* 13(3):656-669.

Stone, G. W., B. Liu, D. A. Pepper, and P. Wang. 2004. The importance of extratropical and tropical cyclones on the short-term evolution of barrier islands along the northern Gulf of Mexico, USA. *Marine Geology* 210:63-78.

Stone, G. W., and R. A. McBride. 1998. Louisiana barrier islands and their importance in wetland protection: Forecasting shoreline change and subsequent response of wave climate. *Journal of Coastal Research* 14(3):900-915.

Stone, G. W., and J. P. Morgan. 1993. Implications for a constant rate of relative sea-level rise during the last millennium along the northern Gulf of Mexico: Santa Rosa Island, Florida. *Shore and Beach* 61(4):24-27.

Stone, G. W., and J. D. Orford (Eds.). 2004. Storms and their significance in coastal morph-sedimentary dynamics. *Marine Geology* 210(1-4):1,368.

Stone, G. W., and F. W. Stapor. 1996. A nearshore sediment transport model for the Gulf of Mexico Coast, USA. *Journal of Coastal Research* 12 (3):786-792.

Stone, G. W., F. W. Stapor, J. P. May, and J. P. Morgan. 1992. Multiple sediment sources and a cellular, non-integrated, longshore drift system: Northwest Florida and southeast Alabama coast, USA. *Marine Geology* 105:141-154.

Stone, G. W., J. P. Xu, and X. Zhang. 1995. Estimation of the wave field during Hurricane Andrew and morphological change along the Louisiana coast. *Journal of Coastal Research* SI 21:234-253.

Terzaghi, K. 1943. *Theoretical soil mechanics*. New York, NY: John Wiley and Sons, 510 p.

Thomson, G. G. 2008. Personal communication, emails dated 19 and 22 September 2008, and spreadsheet titled "Construction Cost Estimate.xls" documenting economic cost analysis applied in Louisiana restoration projects.

Thomson, G. G., G. M. Grandy, and R. Sweeney. 2007. The challenges of restoring Louisiana barrier islands: From design through construction. *Proceedings Coastal Sediments '07*, New Orleans, LA: ASCE, 647-660.

Thomson, G. G., S. M. Khalil, and B. Tate. 2005. Sediment budgets as an aid for breakwater design: Raccoon Island case study. *Proceedings 14th Biennial Coastal Zone Conference*. New Orleans, LA, 17-21 July, NOAA/CSC/20518-CD, CD-ROM, 6 p.

Tubman, M. W., and J. N. Suhayda. 1976. Wave action and bottom movements in fine sediments. *Proceedings 15th International Conference on Coastal Engineering*. ASCE, 1,168–1,183.

URS, Inc. 2006. Hurricane Rita rapid response, Louisiana coastal and riverine high water mark collection. FEMA-1607-CR-LA, Contract No. EMW-2000-CO-0247, 79 p., http://www.fema.gov/pdf/hazard/flood/recoverydata/rita/rita_la_hwm_public.pdf.

U.S. Geological Survey. 2007. Coastal change and hazards: Hurricanes and extreme storms, Hurricane Katrina. http://coastal.er.usgs.gov/hurricanes/katrina/photo-comparisons/chandeleur.html, updated 10 October, 2007; accessed 15 June 2008.

van Maren, D.S. 2005. Barrier formation on an actively prograding delta system: The Red River Delta, Vietnam. *Marine Geology* 224:123-143.

Walton, T. L., Jr., and W. D. Adams. 1976. Capacity of inlet outer bars to store sand. In: *Proceedings 15th International Conference on Coastal Engineering* New York, NY: ASCE, 1,919-1,937.

Wells, J. T., and G. P. Kemp. 1986. Interaction of surface waves and cohesive sediments: Field observations and geologic significance. In: *Lecture Notes on Coastal and Estuarine Studies*, A. J. Mehta (ed.). *Estuarine Cohesive Sediment Dynamics* 14:43-65.

Whitehouse, R., R. Soulsby, W. Roberts, and H. Mitchener. 2000. *Dynamics of Estuarine Muds*. London, UK: Thomas Telford.

Winterwerp, J. C., R. F. de Graaff, J. Groeneweg, and A.P. Luijendijk. 2007. Modeling of wave damping at Guyana mud coast. *Coastal Engineering* 54:249-261.

Wu, T. H. 1966. *Soil Mechanics*. Chapter 5. Boston, MA: Allyn and Bacon, Inc., 91-117.

Xiqing, C. 1998. Changjian (Yangtze) River Delta, China. *Journal of Coastal Research* 14(3):838-858.

Yong, R. N., and B. P. Warkentin. 1966. *Introduction to Soil Behavior*. Chapter 8. New York, NY: Macmillan Company, 176-234.

Appendix A: Selected Figures From 2D MCO Sensitivity Analysis With Triangular Barrier Island

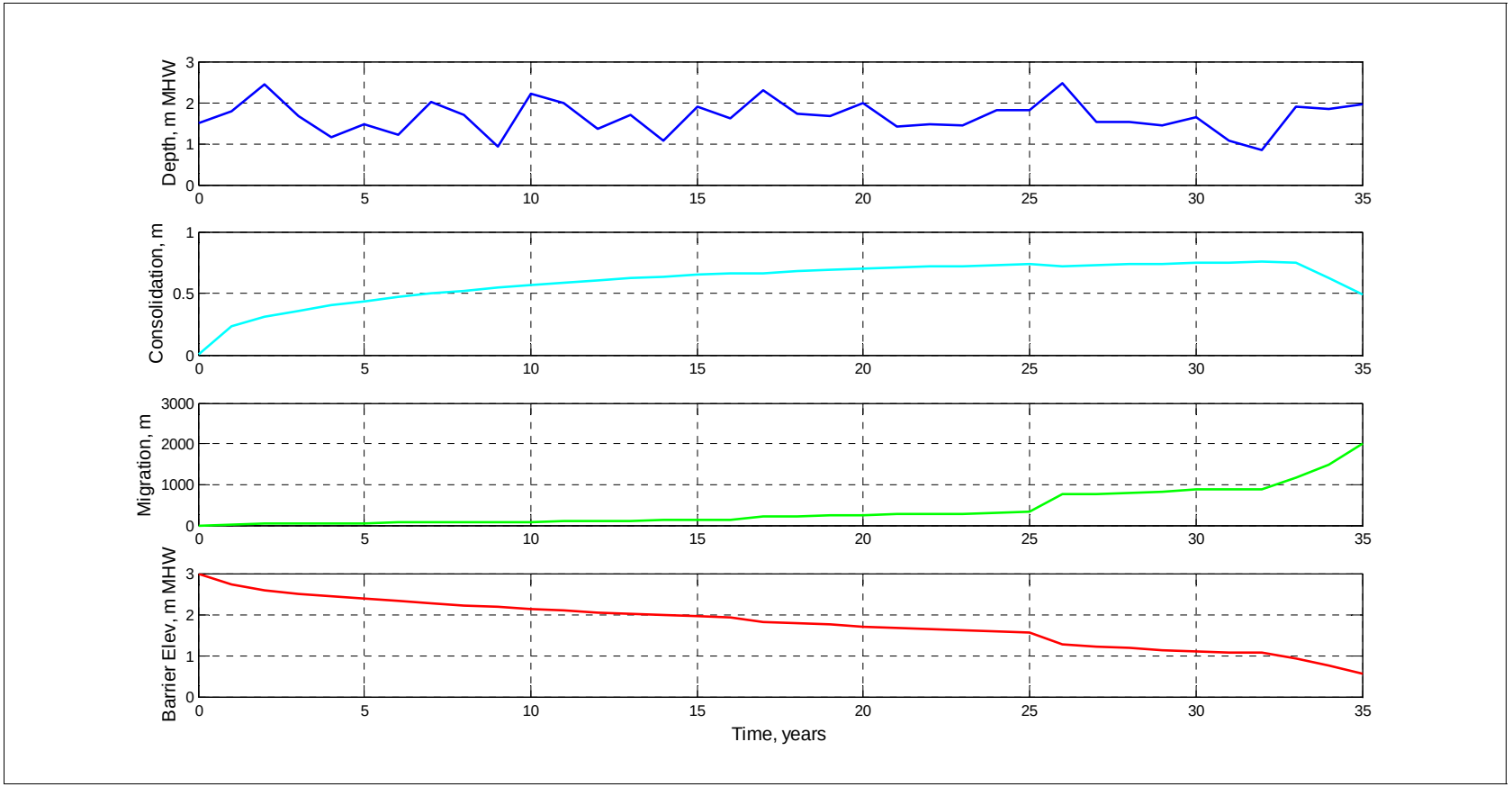

Figure 69. 2D MCO hydrodynamic and morphologic change summary (Table 6, Analysis 1b).

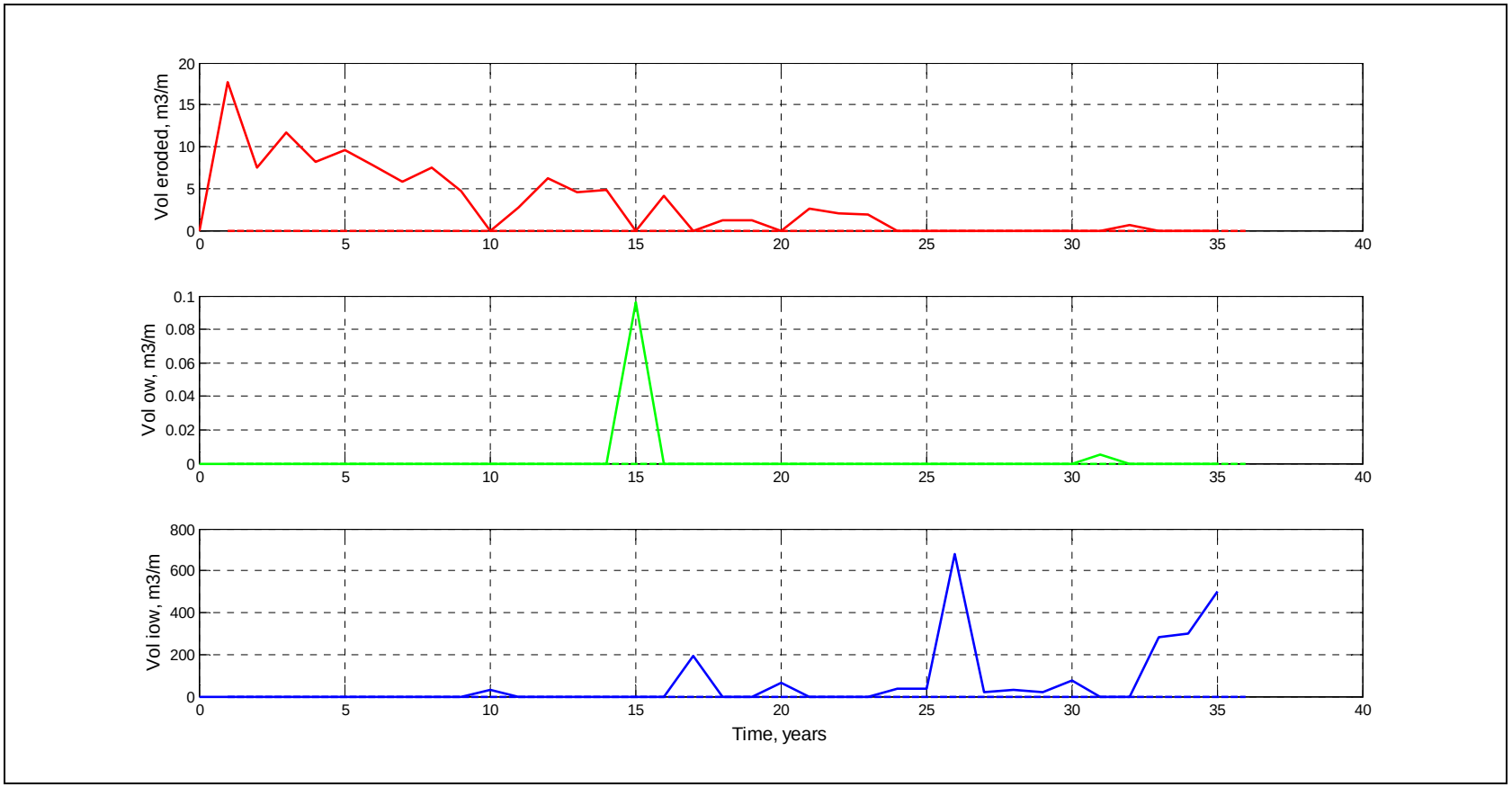

Figure 70. 2D MCO erosion and overwash summary (Table 6, Analysis 1b).

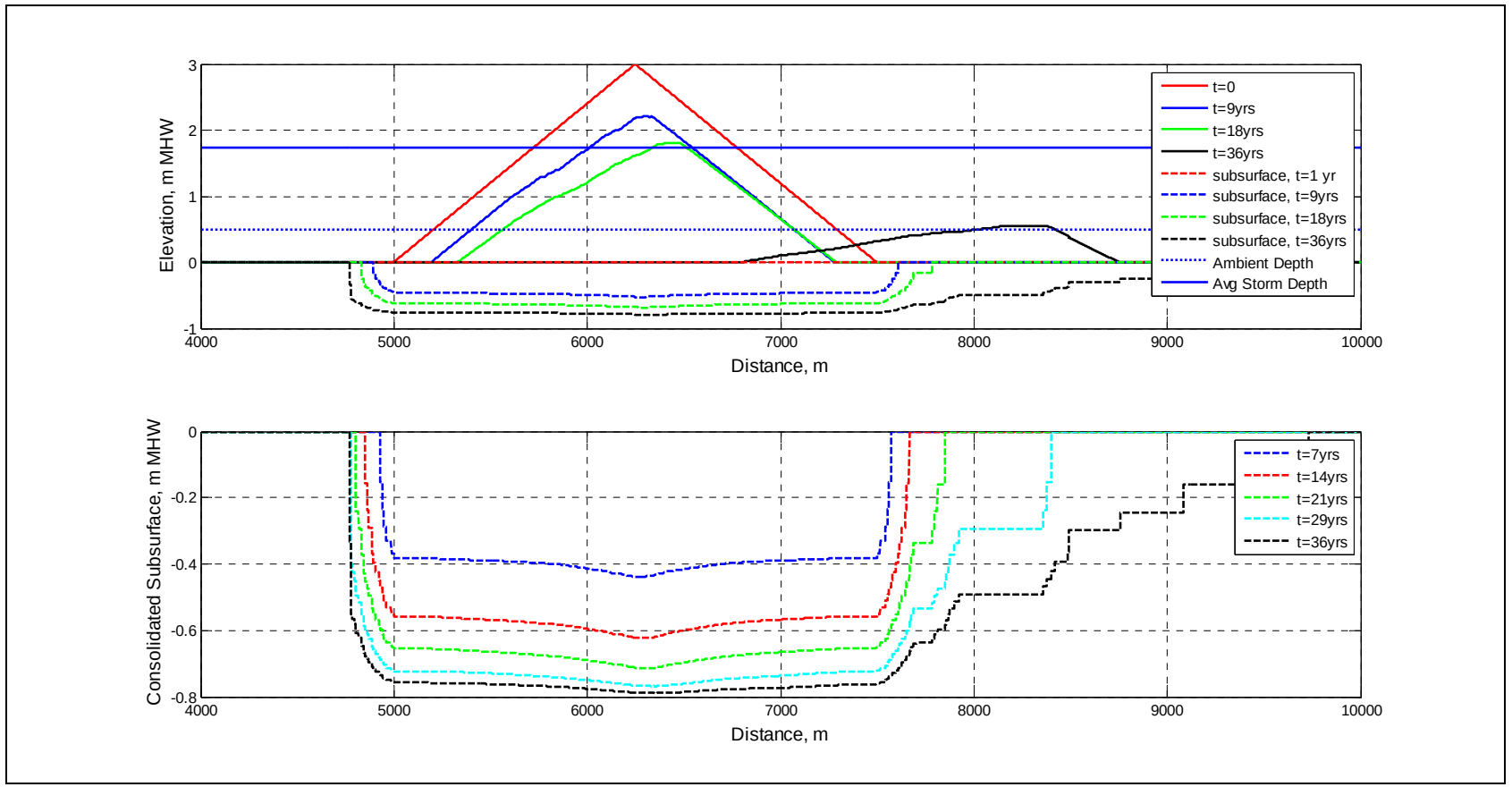

Figure 71. 2D MCO profile and consolidated subsurface (Table 6, Analysis 1b).

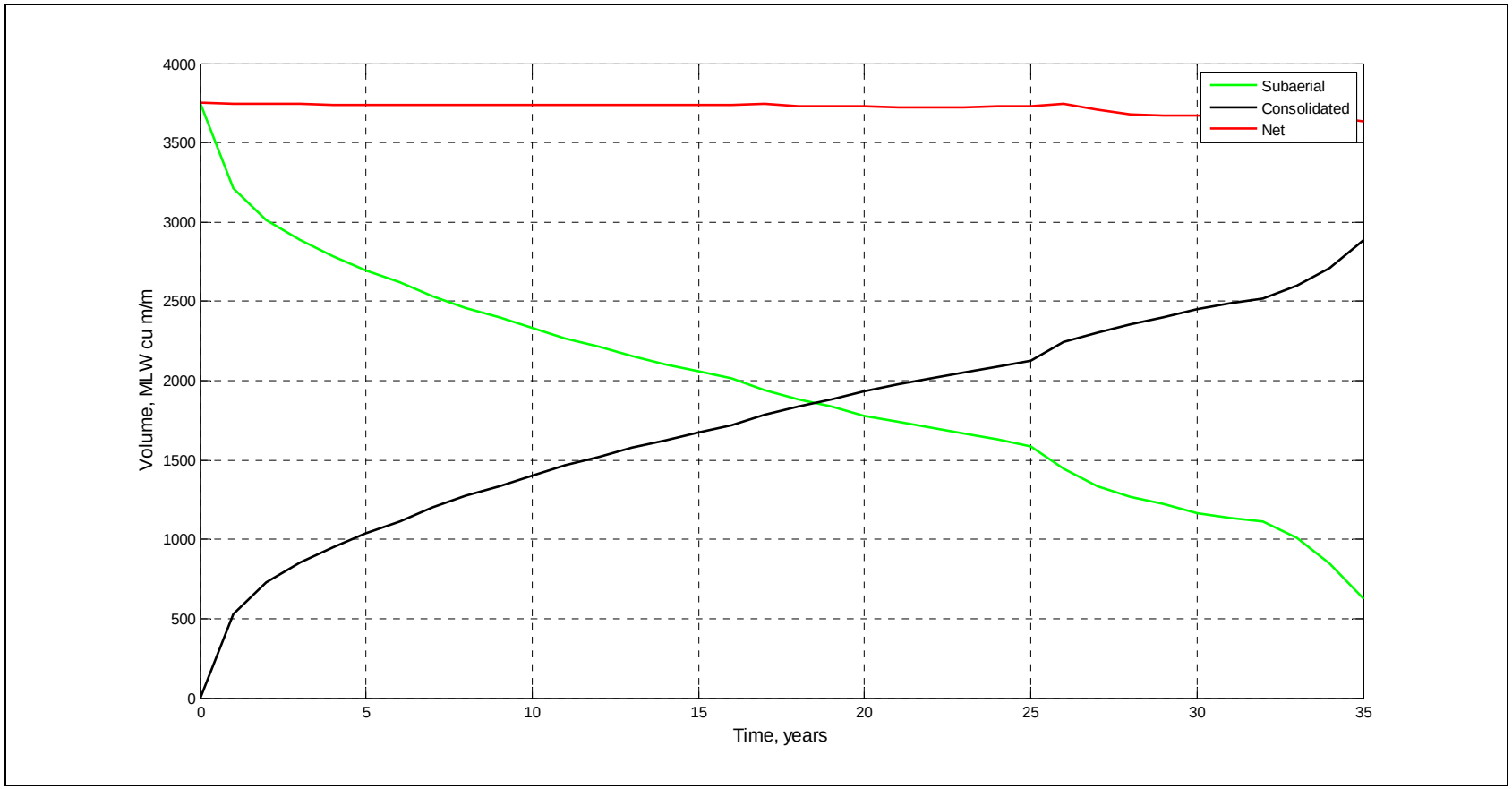

Figure 72. 2D MCO volume change summary (Table 6, Analysis 1b).

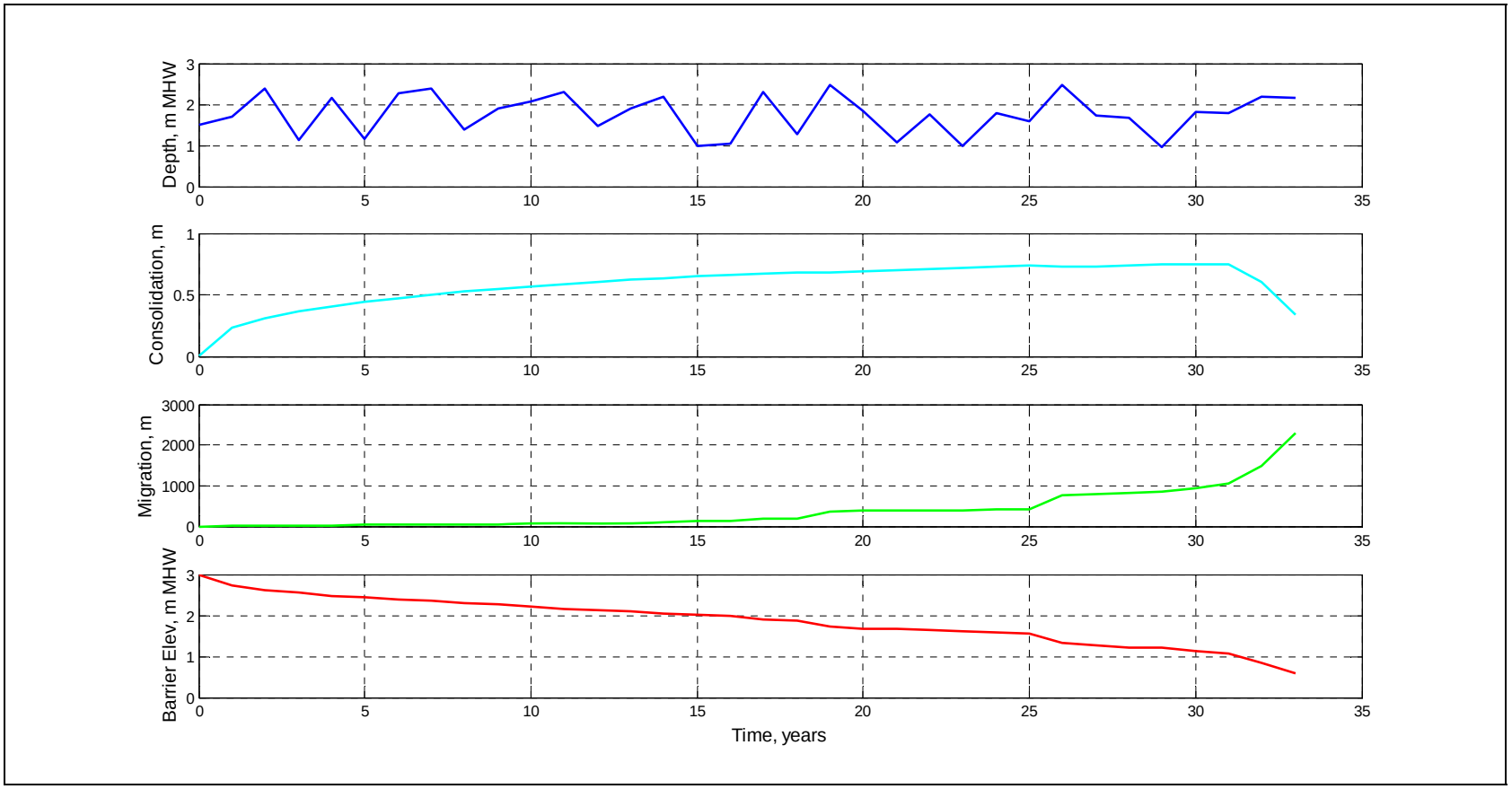

Figure 73. 2D MCO hydrodynamic and morphologic change summary (Table 6, Analysis 1c).

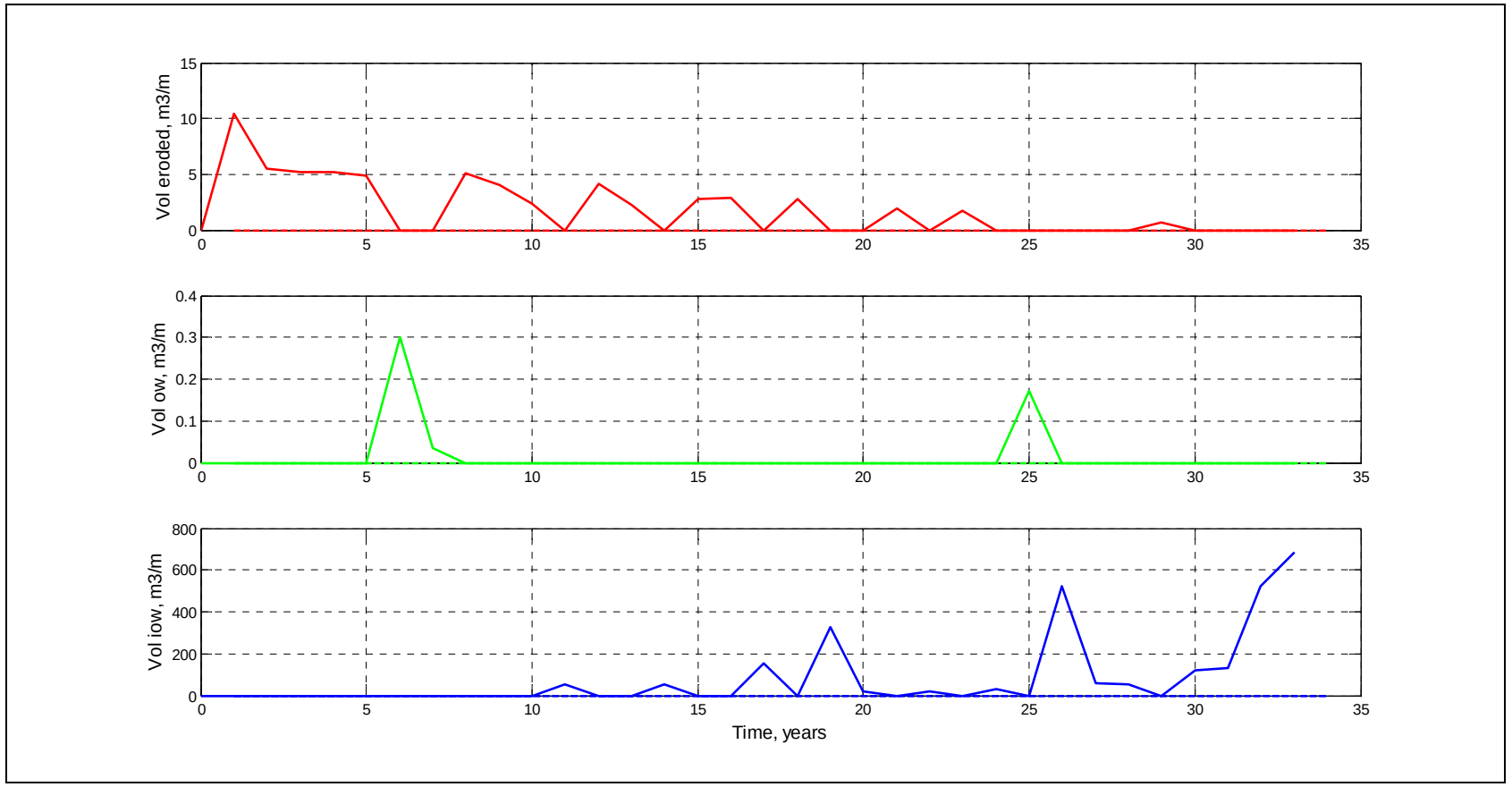

Figure 74. 2D MCO erosion and overwash summary (Table 6, Analysis 1c).

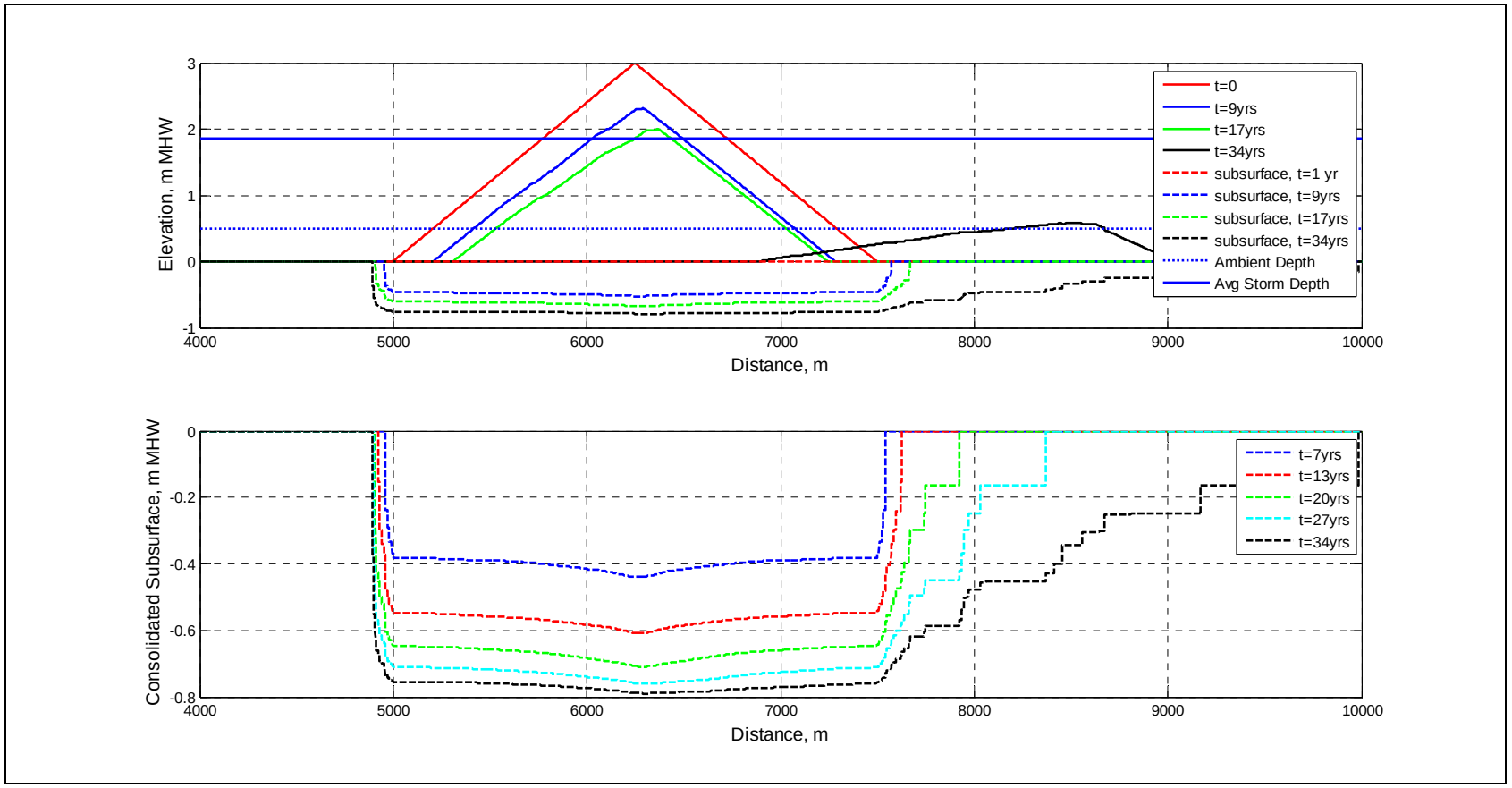

Figure 75. 2D MCO profile and consolidated subsurface (Table 6, Analysis 1c).

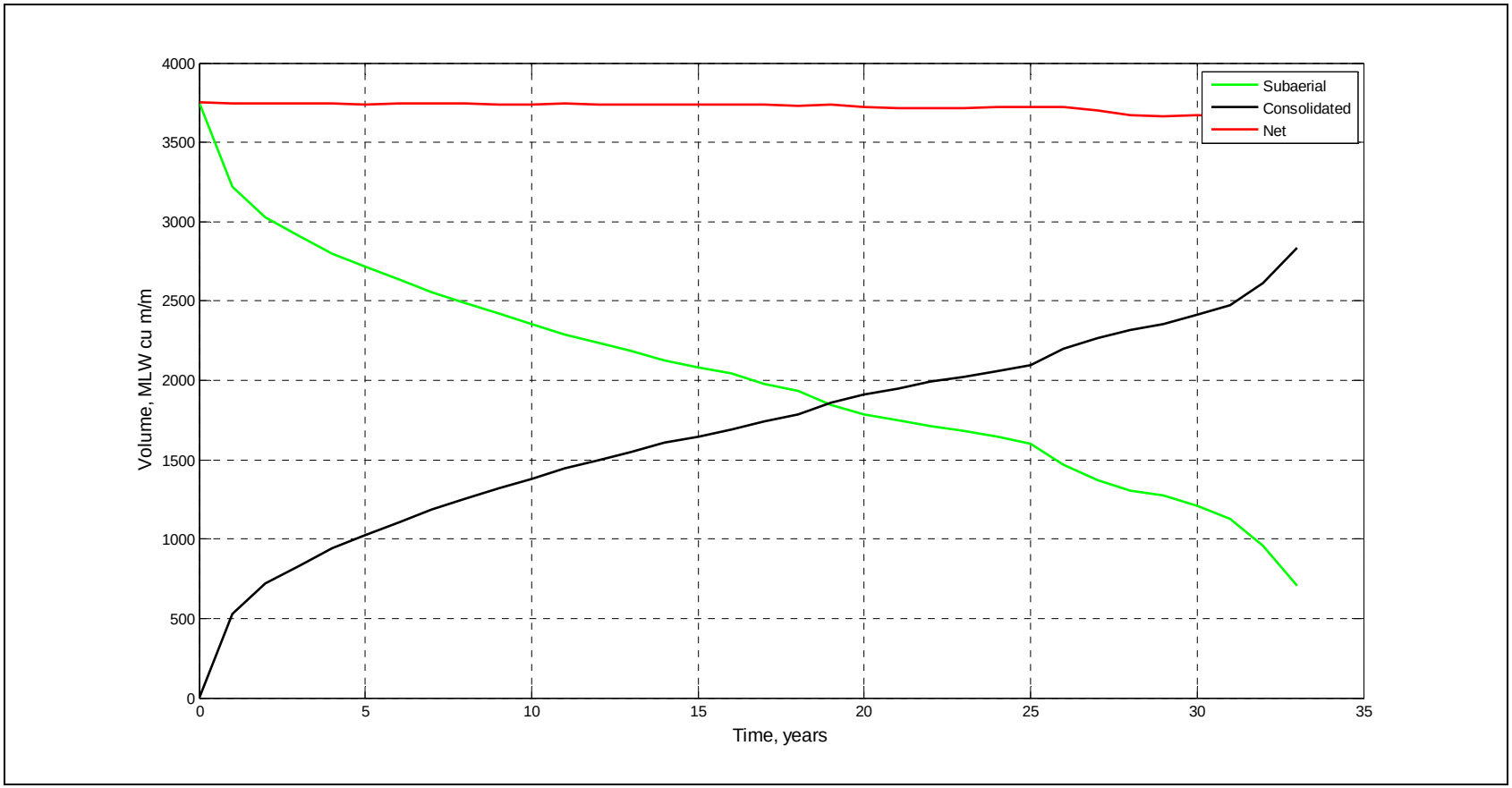

Figure 76. 2D MCO volume change summary (Table 6, Analysis 1c).

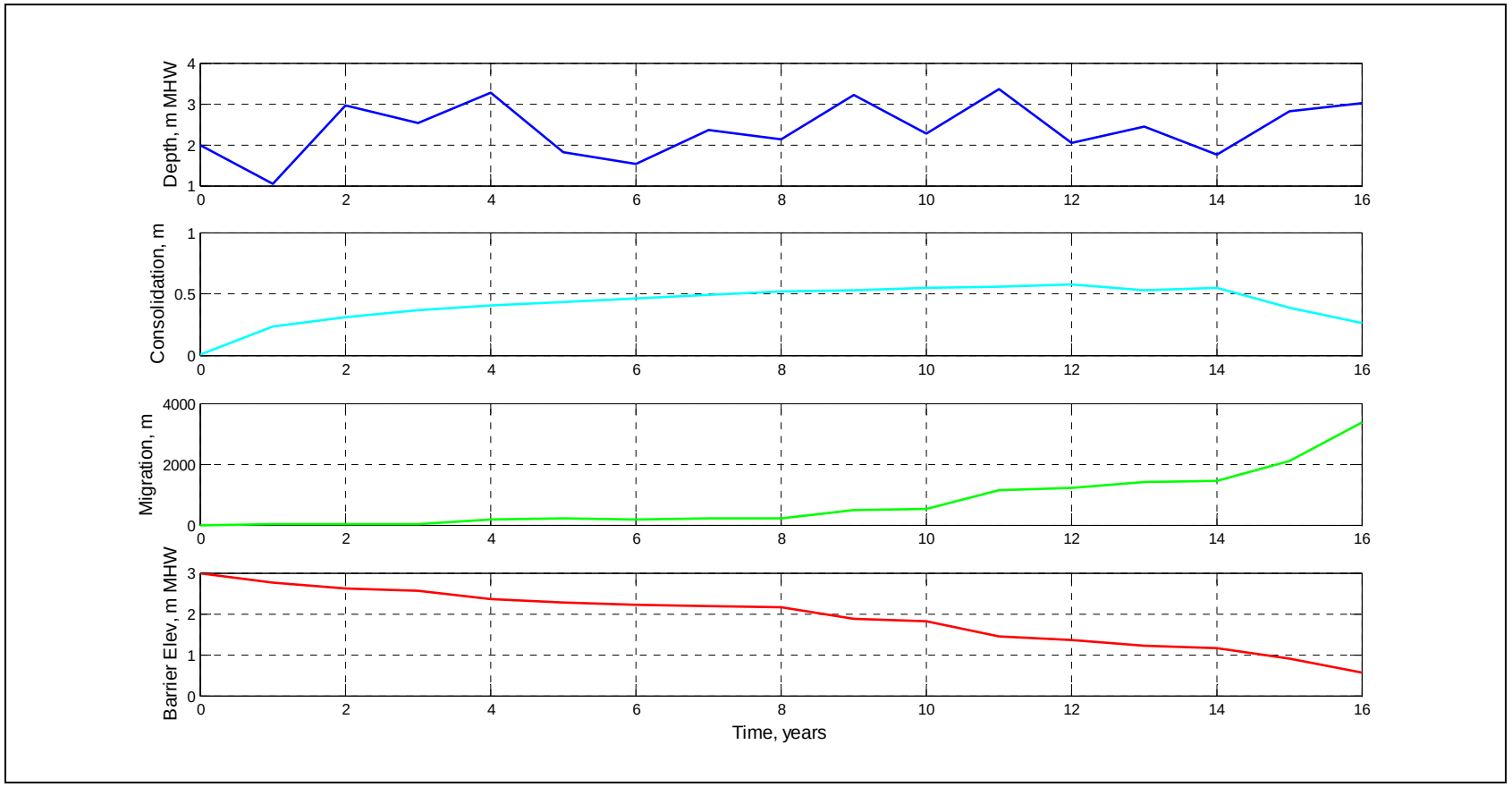

Figure 77. 2D MCO hydrodynamic and morphologic change summary (Table 6, Analysis 1d).

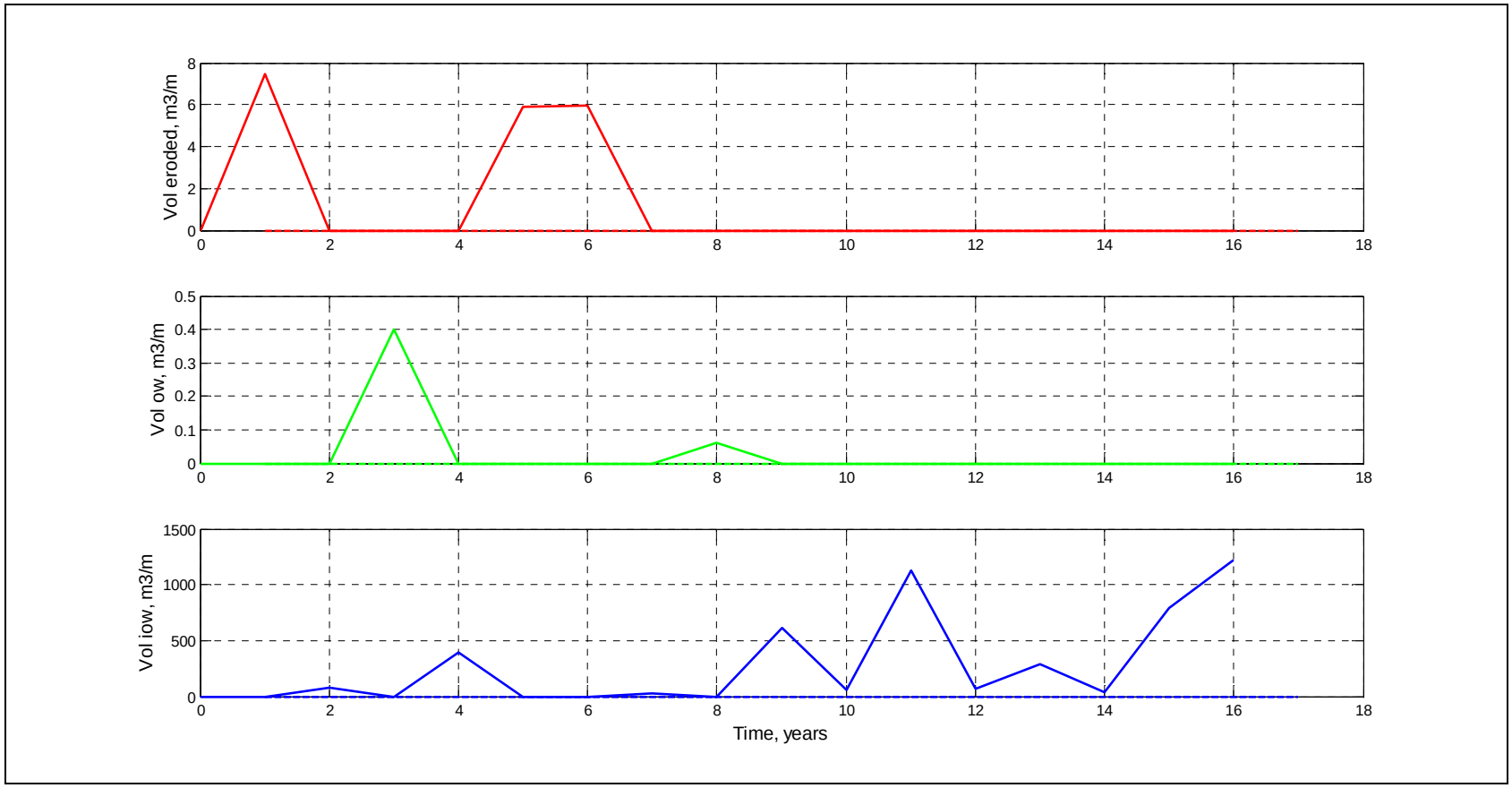

Figure 78. 2D MCO erosion and overwash summary (Table 6, Analysis 1d).

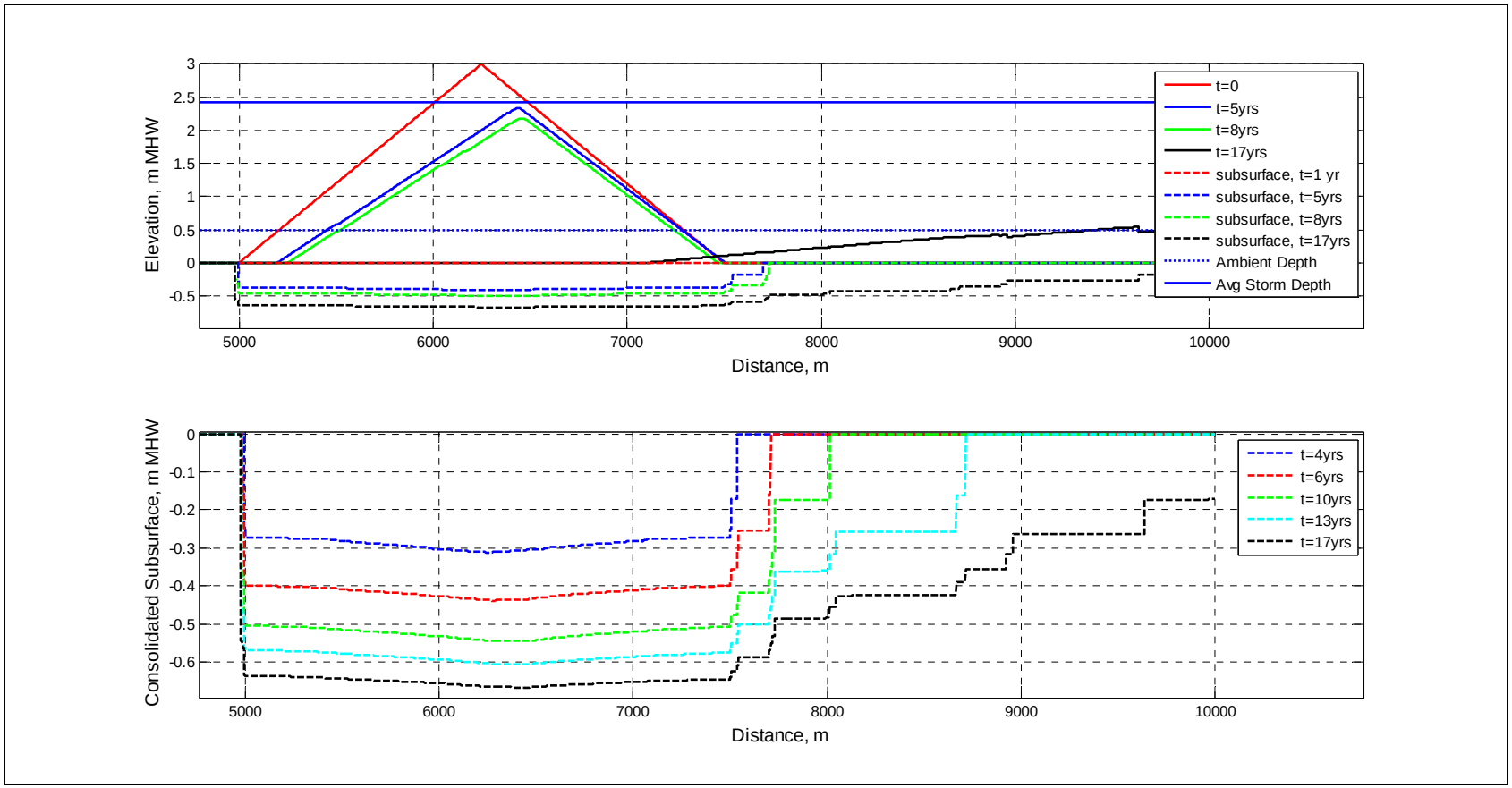

Figure 79. 2D MCO profile and consolidated subsurface (Table 6, Analysis 1d).

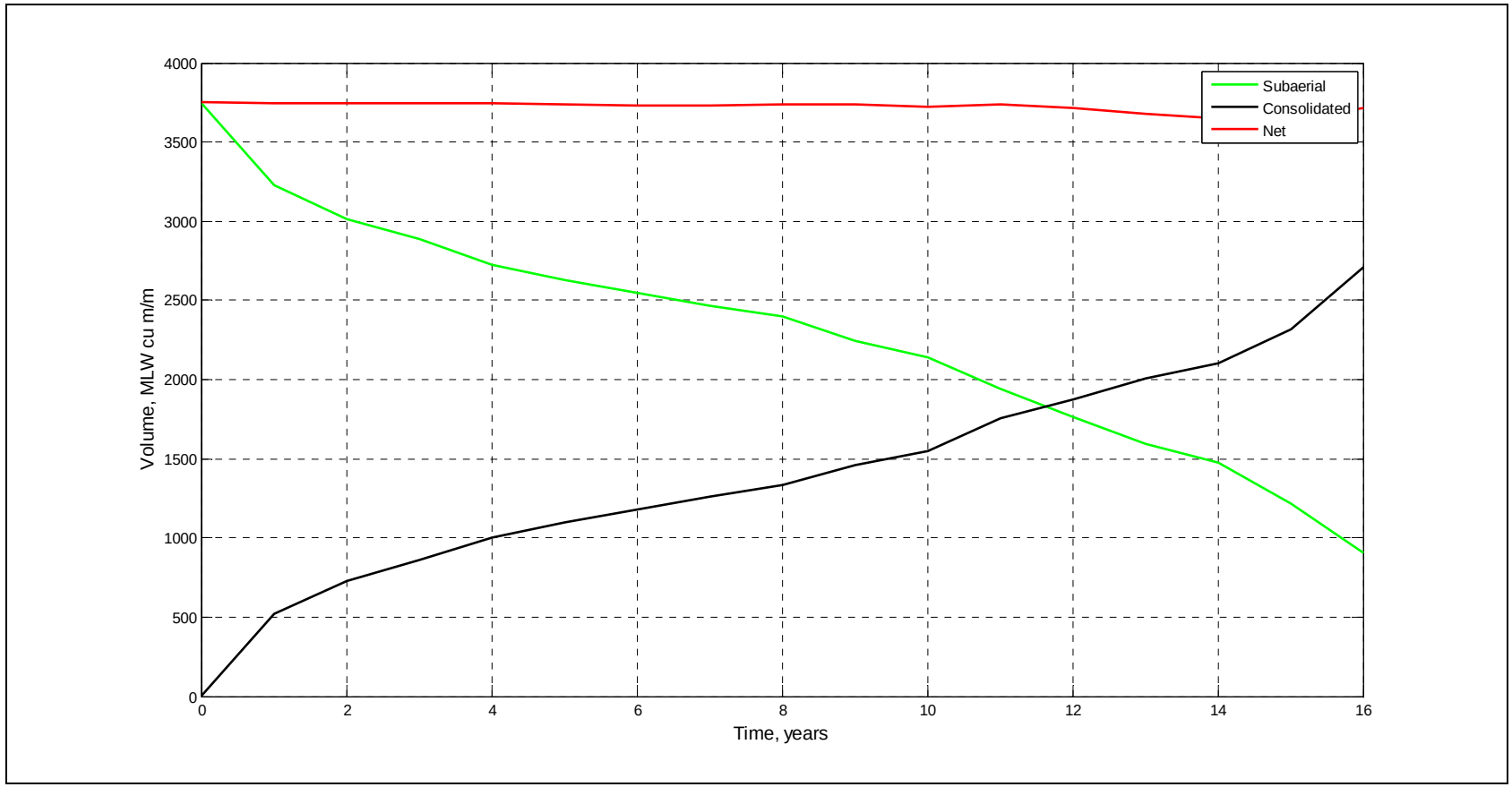

Figure 80. 2D MCO volume change summary (Table 6, Analysis 1d).

Appendix B: Barrier Island Consolidation Data From Virginia

Table 22. Elevation and facies data from Metomkin and Assawoman Islands, VA (digitized from Gayes 1983, his Figures 5, 6, and 7).

Core Number Elevation, m MHW; F = Facies[1]																			
Offshore		1		2		3		4		5		6		7		8		9	
Elev	F	Elev	F	Elev	F	Elev	F	Elev	F	Elev	F	Elev	F	Elev	F	Elev	F	Elev	F
Metomkin (Figure 12)																			
-0.82		1.2		0.90		0.67		0.41		0.26		0.16		-0.29		n/a		n/a	
	S		S		S		S		S		S		S		M				
-1.3		-0.80		-0.61		-0.35		-0.29		-0.27		-0.08		-2.0					
	T		M		M		M		M		M		M		T				
-1.9		-0.84		-0.74		-0.60		-0.49		-0.48		-0.33		-3.1	End				
	C		T		T		T		T		T		T						
-3.5		-1.3		-1.7		-1.3		-1.6		-1.7		-1.1							
	B		C		C		C		C		C		C						
-5.0	end	-2.9		-2.8		-3.4		-2.9		-2.5		-2.6							
			B		B		B		B		B		B						
		-4.1	end	-4.4	end	-4.7	end	-4.3	end	-2.9	end	-3.4	end						
Assawoman 1 (Figure 10)																			
0.56		0.73		1.5		0.97		0.77		0.44		0.32		0.24		0.08		0	
	S		S		S		S		S		S		S		S		M		M
-0.57		-0.89		-0.85		-0.97		-1.01		-0.93		-0.73		-0.36		-0.73		-0.89	
	M		M		M		M		M		M		M		M		T		B
-0.69		-1.0		-1.3		-1.2		-1.03		-1.2		-0.89		-0.57		-1.6		-1.8	end
	T		T		T		T		T		T		T		T		B		
-1.6		-1.7	end	-1.6		-1.9	end	-2.1	end	-2.1	end	-1.8		-1.6		-1.8	end		
	C				B								B		B				

(Continued)

Table 22. Elevation and facies data from Metomkin and Assawoman Islands, VA (digitized from Gayes 1983, his Figures 5, 6, and 7) (Concluded).

Core Number Elevation, m MHW; F = Facies[1]																			
Offshore		1		2		3		4		5		6		7		8		9	
Elev	F	Elev	F	Elev	F	Elev	F	Elev	F	Elev	F	Elev	F	Elev	F	Elev	F	Elev	F
Assawoman 1 (Figure 10)																			
-2.5	end			-2.3								-3.2	end	-3.7	end				
					O														
				-2.6															
					B														
				-2.9	end														
Assawoman 2 (Figure 11)																			
-0.08		0.15		0.18		0.13		0.12		0.09		0.14		0.03		0			
	S		S		S		S		S		S		S		S		M		
-11.2		0.24		-0.08		-0.05		-0.05		-0.06		-0.07		-0.02		-0.01			
	T		M		M		M		M		M		M		M		T		
-16.8	end	0.26		-0.10		-0.08		-0.09		-0.09		-0.10		-0.05		-0.12			
			T		T		T		T		T		T		T		C		
		0.31		-0.19		-0.14		-0.13		-0.14		-0.19		-0.14		-0.20	end		
			C		C		C		C		C		C		C				
		0.42	end	-0.20		-0.17		-0.14		-0.20		-0.38		-0.29	end				
					O		O		O		O		B						
				-0.22		-0.20		-0.22		-0.25		-0.48	end						
					T		T		T		C								
				-0.34	end	-0.28	end	-0.26	end	-0.36									
											B								
										-0.42	end								

[1] Facies description: M: Marsh, T: Tidal flat, C: Subtidal channel, B: Shallow bay, S: Sand, O: Oyster beds.

Appendix C: Data Needs and Recommendations for Future Research

Data needs to improve and validate barrier island evolution models and also to further basic understanding of morphologic change in deltaic settings were identified through this study. Although data collection and research studies can be expensive, coordination with other ongoing field monitoring programs, laboratory experiments, and numerical studies can make these recommendations viable. Because the time scale of the phenomenon is long, and three-dimensional (longshore, cross-shore, and vertical) properties must be considered, multi-agency approaches that cover a wide range of interests seems essential for success. Recommendations for field measurements are presented first, followed by potential historical, laboratory, and numerical modeling research studies.

1. For barrier islands in deltaic settings (or those that overlie a compressible substrate such as peat deposits or soft bay sediment), data are required to quantify the initial and long-term evolution of large-scale restoration projects. The temporal variation in consolidation of the substrate as a function of the weight of the overlying sediment can be used to validate models such as developed in this research. The time-dependent consolidation can be measured with settlement plates that are positioned on the surface of the pre-project island, which are then buried by the placed sediment. A series of settlement plates extending in a line from the ocean to bay located in the center of the project would provide the primary data set. Additional settlement plates at other locations in the project would supplement these data (Figure 81). These plates would have a rod of known length extending through the surface such that Geographic Positioning System coordinates of the top of the rods can be monitored through time. At locations adjacent to each settlement plate, another plate placed deeper into the substrate (as deep as feasible, ideally at least 10-20 m depth) will provide settlement information on how the substrate is compressed by the weight of the barrier island. Within the same region, but some distance away from the island, a separate set of settlement plates would be installed to serve as independent control for the island measurements and to document regional trends unrelated to the island. For the Chaland Headland restoration project, seven settlement plates were installed in 2007 at a cost of $1.9K/each (Coastal Planning and Engineering 2007). Other projects in Louisiana have estimated the cost of settlement plates at $3.5K/each (Thomson 2008).

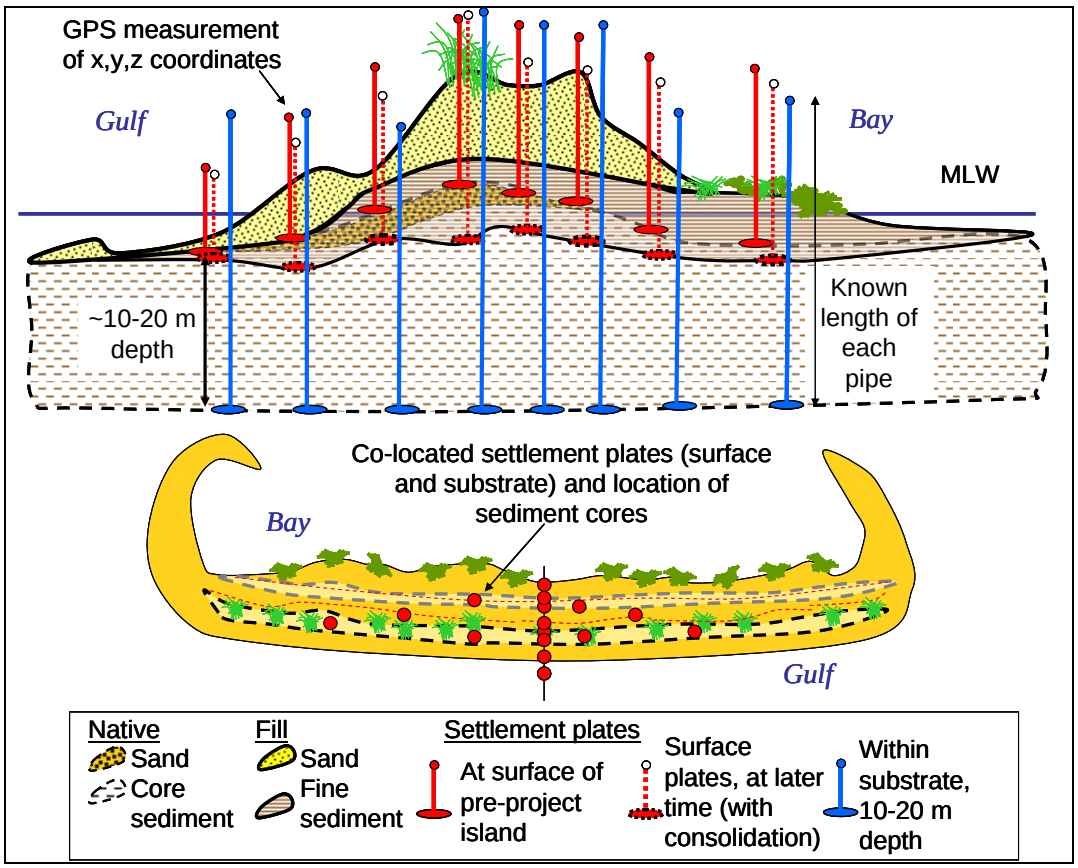

Figure 81. Example design for settlement plates and sediment cores.

2. For restored barrier islands, sediment cores at one or more transect extending across the island (ideally located in the vicinity of the settlement plates, if they have been installed) will provide information on the characteristics and thickness of the substrate as a function of location, applied loading, and duration of loading. Cores could be taken for the pre-project island, and 1, 2, 5, 10, and 20 years post-project. These data can be analyzed in conjunction with the settlement plates to determine characteristics of and changes in the stratigraphy of the restoration project and original (buried) island (Figure 81). A Casagrande consolidation test such as discussed in Chapter 4 (Figures 17 and 18) should be conducted for representative stratigraphy within the core (if sediment color or composition differs with depth) or at selected depths (e.g., 1, 5, and 10 m depth). Survey transects should be taken at the same time as the cores. The average cost of transects for the Chaland Headland, Louisiana restoration project was $630/transect (Thomson 2008). The cost for sediment cores includes mobilization and demobilization (from $10 to $20K) and $1.5K/core for a 6-m-length core and processing (splitting the core and sediment analysis) (NOAA 2008g).

3. Together with (1) and (2), measure overwash quantities, the magnitude of washover deposits, and how the washover sediment loads back-barrier marsh sediment as a function of time. Settlement plates can be positioned on the back-barrier marsh in areas vulnerable to overwash and allowed to be buried by washover sand through one or more storm seasons. In another area, a controlled experiment could be initiated with a known volume (weight) of sand placed over the back-barrier marsh, with settlement plates positioned as discussed in (1). These two deployments together with (1) would provide information on how back-barrier marsh responds to incremental increasing weight (as in the case of washover sand, which would presumably increase with time) as compared to a large weight of sand as in the controlled experiment. Differences (if any) would lead to better understanding of how large and small weights affect back-barrier marsh, and could be used to improve model calculations.

4. Pre-storm and multiple post-storm cross-shore profile surveys for a barrier island that overlies a compressible substrate will document post-storm recovery of the island, if any occurs. The post-storm profiles surveys would begin as soon as possible following the storm, and subsequent surveys to document recovery would be done at a relatively short interval thereafter (order of one or more weeks). The interval between subsequent data collection could lengthen in the post-storm period.

5. In a coordinated laboratory and field study, develop relationships for the erosion rate of fine-grained barrier island sediment as found in Louisiana. In situ samples of fine-grained sediment and organics from barrier islands could be placed in a wave flume with capability to vary wave height, period, and water depth through a range of values in controlled manner. Tests would be executed with full inundation and partial exposure of the sediment to determine which conditions are most erosive. Multiple samples are required to understand natural variability of the sediment, as well as reproducibility of the measurements. In a separate series of tests, sand would be added to the flume to determine how abrasive characteristics of sand increase the erosion rate. Wave heights near mild prototype conditions can be achieved with a flume in which waves with heights reaching 0.3 m, which will reduce laboratory scale effects yet simulate mild erosive conditions similar to those experienced in Louisiana.

   A field study of fine-grained barrier island sediment that has been exposed to wave action could be conducted in conjunction with the laboratory research. Weekly, bi-weekly, or monthly measurements of the beach

profile in the vicinity of the exposed sediment, as well as wave height, period, direction, and water level would be taken as part of this field monitoring. In Louisiana, there are existing WAVCIS (Wave-Current-Surge Information System) and NDBC (National Data Buoy Center) nearshore and offshore gages measuring wave, wind, and water level parameters, which would provide sufficient data for this type of field study. LiDAR (Light Detection and Ranging) data and controlled aerial photography at the site could be added onto ongoing data collection efforts at modest cost, and provide three-dimensional measurements of how the exposed fine-grained sediment erodes as compared to adjacent subaerial sand beaches. In a muddy deltaic system, a lack of water clarity would likely inhibit LiDAR bathymetric measurements. The fate of the eroded sediment – whether suspended and lost from the nearshore system, or deposited offshore of the wave breaking zone – could also be investigated through careful observation and monitoring. These measurements would lend insight into the processes and site conditions resulting in most rapid erosion of fine-grained clay, silt, and organics, develop relationships for numerically representing these processes, and help in designing future restoration projects.

6. In a numerical study, evaluate the benefit of creating dredged material islands in a bay or estuary to protect barrier islands from wind-generated waves on the open bay or estuary during periods of maximum winds with sufficient fetch (Figure 6). Questions to be addressed include: (a) how much wave energy the constructed islands buffer from the barrier island bay shore; (b) how much erosion of the constructed islands would be incurred during these wind-generated wave events, where the eroded sediment would be deposited (e.g., would it shoal in a nearby navigation channel or adversely affect water quality?), and the volume of sediment required to offset erosion and change in relative sea level to maintain the constructed islands; (c) how much consolidation of the artificial islands would occur due to placement over a poorly-consolidated bay substrate, as well as desiccation and consolidation of the dredged sediment itself; and (d) best location and planview design of the constructed islands to provide the greatest buffer to the barrier island bayshore. Placement of sediment in locations of former islands that have eroded or drowned would have the benefits of possibly increasing environmental acceptance of the restored island as well as a substrate that has already been partially consolidated from loading by the previous island. If the numerical simulations indicate that constructed islands are beneficial to the bay shore and a viable option, logistics for placement and retention of the dredge material would be

investigated (e.g., creating a sand foundation for fine sediment placement with sheet piling or hay bales as temporary dikes, employing means for rapid consolidation of the dredged sediment such as grids of dewatering pipes and vibrating rods). A pilot field study could be implemented to evaluate placement options and document wave buffering of the artificial islands. If the pilot study indicated the artificial islands were beneficial, an economic analysis of the costs and benefits associated with implementing creation of artificial islands as a regular part of dredging navigation channels would be required.

7. Investigate available data sets (history of delta lobe formation and evolution, bay sedimentation rates, rate of peat formation, available sediment cores) on the thickness of the compressible substrate in deltaic and soft substrate settings in areas with barrier island systems. Develop a geographic database documenting thickness of compressible sediment in the United States. Document long-term changes in elevation of barrier islands in selected regions to discern the magnitude of consolidation of the substrate due to the weight of the island versus other processes causing a decrease in elevation. High-resolution acoustic data at project sites can be validated with sediment core data to determine the initial thickness of compressible sediment z_0. These detailed measurements can be compared to the geographic database of compressible sediment thickness to determine uncertainty in the regional data.

8. As discussed in Chapter 5, the ebb shoals for the Barataria Bay passes have volumes larger than obtained with empirical relationships. There are several possible reasons for these larger volumes, and these hypotheses could be investigated with existing data and through numerical modeling.

    a. Numerically investigate the role of cold front and hurricane passage on the evolution of ebb shoals. It is possible that the post-storm tidal prism that is flushed from the bay may be sufficient to provide a long-term source of sediment to the ebb shoals. For the post-storm tidal prism to account for the difference in shoal volumes, it must be greater than the spring prism that is applied in the empirical relationships. A numerical study could be conducted with a circulation model using wind and water level measurements from a cold front and hurricane to calculate the post-storm prism in the tidal passes. These prisms then could be compared with empirical relationships to assess the validity of this hypothesis.

b. It is possible that the increase in relative sea level over the 120-year period of bathymetric measurements has resulted in an abandonment of a portion of the ebb tidal shoal volume. Therefore, only a portion of the ebb shoal is actively supported by the available spring tidal prism. This hypothesis could be evaluated by assessing the depth at which sediment of a given grain size would be deposited on the ebb shoal with the maximum spring tidal currents for each tidal pass as a function of tidal prism, which varies with bay area and cross-section of the tidal passes. As relative sea level has increased over the 120-year period in Barataria Bay, the tidal prism has changed due to increasing bay area and deepening of the tidal passes. The depth of closure for waves can also be calculated for typical and storm waves. If the maximum spring tidal depth of settlement is larger than the depth of closure for waves, it would represent an effective "depth of closure" for the ebb shoals. The total ebb shoal volume abandoned through the change in the ebb shoal depth of closure could be calculated and applied to assess the validity of this hypothesis.

9. Develop and validate a fully-coupled, multiple-sediment layer (e.g., sand layer overlying a cohesive core and deltaic substrate, seaward of a fine-grained bayshore sediment and organics) barrier island morphologic numerical model including processes such as implemented in 2D MCO and sub-modules. Include variability in the thickness of compressible sediment, z_o, as determined by sediment core and high-resolution acoustic data. Additional processes that could be added include barrier island breaching and inlet evolution, spit formation and migration, and growth of vegetation and capture of eolian sand. The fully-coupled barrier island model would have the capability to represent a sand layer overlying core sediment with fine-grained sediment and organics on the bayshore, erosion of the fine-grained sediment if exposed, and subsequent fate of the eroded sediment; variable thickness of the compressible substrate based on site-specific lithology; eolian sand transport, vegetation growth, placement of sand fences, and dune building; longshore sand transport and alongshore barrier island migration; barrier island erosion, overwash, and cross-shore migration; post-storm recovery; island breaching and possible inlet formation; wind-generated waves on the bayshore as a function of fetch and wind speed, and erosion of the bay shoreline; and how evolution of adjacent inlets and shoals affects the island.

Knowledge gained through study and mathematical modeling of coasts in deltaic settings can be applied to other, more stable substrates, to

understand how a potential future rapid increase in eustatic sea level could affect barrier island migration and longevity. For example, the increase in relative sea level for Grand Isle, LA, has been 9.24 mm/year from 1947 to 2008 (NOAA 2008a). In 10 years, coastal Louisiana has experienced an increase in relative sea level roughly equal to what is predicted to occur over the next 50 years with the present eustatic rate in sea level rise of approximately 2 mm/year (Douglas 1992; Peltier 1998). Lessons learned from historical analysis of the barrier islands, bays, and tidal passes in Louisiana and other deltaic settings, laboratory and field studies, as well as mathematical modeling of future evolution can be applied to more stable coastal regions as indicators of possible change over the next century.

REPORT DOCUMENTATION PAGE

Form Approved
OMB No. 0704-0188

Public reporting burden for this collection of information is estimated to average 1 hour per response, including the time for reviewing instructions, searching existing data sources, gathering and maintaining the data needed, and completing and reviewing this collection of information. Send comments regarding this burden estimate or any other aspect of this collection of information, including suggestions for reducing this burden to Department of Defense, Washington Headquarters Services, Directorate for Information Operations and Reports (0704-0188), 1215 Jefferson Davis Highway, Suite 1204, Arlington, VA 22202-4302. Respondents should be aware that notwithstanding any other provision of law, no person shall be subject to any penalty for failing to comply with a collection of information if it does not display a currently valid OMB control number. **PLEASE DO NOT RETURN YOUR FORM TO THE ABOVE ADDRESS.**

1. REPORT DATE *(DD-MM-YYYY)*	**2. REPORT TYPE**	**3. DATES COVERED** *(From - To)*
September 2009	Final report	

4. TITLE AND SUBTITLE

Barrier Island Migration Over a Consolidating Substrate

5a. CONTRACT NUMBER

5b. GRANT NUMBER

5c. PROGRAM ELEMENT NUMBER

6. AUTHOR(S)

Julie Dean Rosati

5d. PROJECT NUMBER

5e. TASK NUMBER

5f. WORK UNIT NUMBER

7. PERFORMING ORGANIZATION NAME(S) AND ADDRESS(ES)

U.S. Army Engineer Research and Development Center
Coastal and Hydraulics Laboratory
3909 Halls Ferry Road
Vicksburg, MS 39180-6199

8. PERFORMING ORGANIZATION REPORT NUMBER

ERDC/CHL TR-09-8

9. SPONSORING / MONITORING AGENCY NAME(S) AND ADDRESS(ES)

U.S. Army Engineer Research and Development Center
Coastal and Hydraulics Laboratory
3909 Halls Ferry Road
Vicksburg, MS 39180-6199

10. SPONSOR/MONITOR'S ACRONYM(S)

11. SPONSOR/MONITOR'S REPORT NUMBER(S)

12. DISTRIBUTION / AVAILABILITY STATEMENT

Approved for public release; distribution is unlimited

13. SUPPLEMENTARY NOTES

14. ABSTRACT

Barrier islands that overlie a compressible substrate load and consolidate the underlying subsurface. Through time, the elevation and aerial extent of these islands are reduced, making them more susceptible to inundation and overwash. Sand washed over the island and onto back-barrier marsh or into the bay or estuary begins the consolidation process on a previously non-loaded substrate, with time-dependent consolidation a function of the magnitude of the load, duration of load, and characteristics of the substrate. The result is an increase in the overwash, migration, breaching, and segmentation of these islands.

This research determined the degree to which consolidation affects the evolution of barrier island systems overlying a poorly-consolidated substrate, both for natural islands and those that have been restored with an infusion of sand from an external source. A two-dimensional (cross-shore) mathematical model was developed, tested with field data, and then applied to evaluate how a compressible substrate modifies long-term barrier island evolution. The model spans time durations of years to decades and represents cross-shore evolution of a sandy barrier island due to erosion, runup, overwash, migration, and time-dependent consolidation of the underlying substrate due to loading by the island.

(Continued)

15. SUBJECT TERMS		
Barrier island	Numerical modeling	Consolidation
Migration	Storm response	Beach Nourishment
	Deltaic coasts	Beach fill

16. SECURITY CLASSIFICATION OF:			**17. LIMITATION OF ABSTRACT**	**18. NUMBER OF PAGES**	**19a. NAME OF RESPONSIBLE PERSON**
a. REPORT	**b. ABSTRACT**	**c. THIS PAGE**			**19b. TELEPHONE NUMBER** *(include area code)*
UNCLASSIFIED	UNCLASSIFIED	UNCLASSIFIED		218	

Abstract (Continued)

The implications of two strategies for restoring these islands (a one-time “Initial” large-scale infusion of sand from an external source versus traditional “Incremental” beach nourishment and subsequent smaller maintenance volumes) were tested.

Barrier islands overlying a compressible substrate are more likely to have reduced dune elevations due to consolidation, incur overall volumetric adjustment of the profile to fill in compressed regions outside the immediate footprint of the island, and experience increased overwash and migration when the dune reaches a critical elevation with respect to the prevalent storm conditions. Initial large-scale infusion of sand from an external source decreased the cross-shore migration rate, consolidation rate, and rate of dune lowering for barrier islands overlying a compressible substrate as compared to the Incremental restoration. The reduction in the migration and consolidation processes for the Initial Method resulted in more stability of the island as compared to the Incremental Method.